Morpho-functional study of the paired fins of the extant coelacanth Latimeria : Considerations on the terrestrialization process of vertebrates

Rohan Mansuit

MUSÉUM NATIONAL D'HISTOIRE NATURELLE

École Doctorale 227
Sciences de la Nature et de l'Homme : évolution et écologie

Année 2020

N ° attribué par la bibliothèque
|_|_|_|_|_|_|_|_|_|_|_|_|_|

THÈSE

pour obtenir le grade de

DOCTEUR DU MUSÉUM NATIONAL D'HISTOIRE NATURELLE

Spécialité : Anatomie fonctionnelle

présentée et soutenue publiquement par

Rohan MANSUIT

Le 12 Novembre 2020

Étude morpho-fonctionnelle des nageoires paires du cœlacanthe actuel *Latimeria* - Considérations sur les modalités de la terrestrialisation des vertébrés

sous la direction de :
Gaël CLEMENT, Professeur, CR2P UMR7207 MNHN-CNRS-SU, Directeur
Marc HERBIN, Maitre de conférences, MECADEV UMR7179 MNHN-CNRS-SU, Encadrant

devant le jury :
Catherine BOISVERT, Senior Research Fellow, Curtin University, Australia, Rapporteure
Dominique ADRIAENS, Professor, Ghent University, Ghent, Belgium, Rapporteur
Per Erik AHLBERG, Professeur, Uppsala Universitet, Uppsala, Sweden, Examinateur
Anne-Claire FABRE, Postdoctoral Researcher, University of Zurich, Switzerland, Examinatrice
Anthony HERREL, Directeur de recherche, MNHN, Paris, France, Examinateur

"*For the less even as for the greater there is some deed that he may accomplish but once only; and in that deed his heart shall rest make again*"
J.R.R. Tolkien - *The Silmarillion*

"*Pour les plus humbles comme pour les plus grands il est une œuvre qu'il ne leur est donné d'accomplir qu'une fois, et dans cette œuvre leur cœur se met tout entier.*"
J.R.R. Tolkien - *Le Silmarillion*

REMERCIEMENTS

Ici s'ouvre une nouvelle page, sur cette thèse tout d'abord, qui je l'espère sera agréable à lire. Et puis sur une nouvelle aventure et de nouvelles expériences qui vont continuer à jalonner ma vie. Qui aurait pensé, il y a déjà 3 ans, que je finirais ce manuscrit dans un rush final plein de stress. Certainement pas moi, qui pensais à l'époque être capable de m'organiser correctement pour tout finir dans les temps, de façon tranquille. Naïf que j'étais !! Cette thèse de doctorat s'est bien chargée de m'apprendre que rien ne se passe jamais comme prévu, qu'il arrive toujours quelque chose qui vient te déranger dans ton travail lorsque tout va pour le mieux. Et au final, l'avance qu'on prend disparait. Mais je m'égare, comme je l'ai dit, cette page est le début pour moi d'un nouveau chapitre dans ma vie, mais il s'agit aussi de la première page par laquelle on commence à lire une thèse. Et il est temps pour moi de passer aux remerciements, pour toutes ces personnes qui m'ont accompagnées, de près ou de loin, durant ces 3 années.

Mes premiers remerciements vous sont bien sûr dédiés, Gaël Clément et Marc Herbin, vous qui m'avaient accepté, encadré et encouragé quand nécessaire pour mener à bien ce projet. Gaël, lors d'une de nos premières discussions quand j'étais encore un petit stagiaire de Master, tu as été le premier à m'avoir avoué que tout paléontologue avait un jour cassé, ou cassera, un fossile. Tu ne peux imaginer à quel point cela m'a rassuré, moi qui suis un éternel maladroit (je pense que tout le monde peut en témoigner). Marc, comme tu peux le constater, cette symphonie inachevée qu'est la thèse s'achève quand même. Tes remarques, tes encouragements et tes félicitations, à chaque fois spontanés, m'ont permis de surmonter ce maudit syndrome de l'imposteur, durant mes nombreuses périodes de stress et de doutes sur mon travail.

Outre mes deux directeurs, il me faut aussi remercier Anthony Herrel, toi qui a grandement collaboré à cette thèse et qui m'a aidé pour les manips et dissections. Sans toi, je ne sais pas si j'aurais pu faire un tel travail. Comme pour de nombreux étudiants, tu as toujours été présent pour répondre à mes questions et à me conseiller, tout comme pour corriger mon anglais quelque peu... aléatoire dirons nous.
Je vous remercie également tous les trois pour m'avoir proposé de participer à une mission de conservation sur ce petit archipel appelé Comores. J'en profite par la même pour remercier Agnès Iatzoura, photographe de cette mission, ainsi que Ibrahim Mohamed Toihir qui nous a si

bien accueilli sur place et sans qui la mission n'aurait pas eu lieu d'être.

I am grateful to Catherine Boisvert, Dominique Adriaens, Per Erik Ahlberg, Anne-Claire Fabre and Anthony Herrel for accepting to review the manuscript and to be members of my thesis jury. It is a pleasure and an honor.
I thanks Per Erik Ahlberg to accept to welcome me during my PhD in its lab at Uppsala, where I was able to present my project and to work in collaboration with Sophie Sanchez on the bone micro-structure of *Laugia groenlandica*. I also thanks all the members of the lab for their warm welcome and Vincent Dupret that accepted to host me.

Je tiens à remercier toutes les personnes qui m'ont permis d'acquérir toutes les données nécessaires pour ce travail de thèse: Paul Tafforeau à l'ESRF, Marta Bellato et Patricia Wils de la plateforme AST-RX du MNHN, pour les acquisitions des données tomographiques; Florent Goussard pour son aide lors de la segmentation des nageoires (et pour les échanges au boken lors des séances de Kenjutsu). I am also grateful to Bent Lindow (Copenhagen) to welcome me in the collections of the Natural History Museum of Denmark when I was looking for specimens of *Laugia groenlandica*.

Je remercie le Labex BCDiv qui a financé les frais de recherche de cette thèse, et Anne-Cécile Haussonne, sans qui j'aurais été perdu au niveau administratif.

Je tiens également à remercier non pas LE, mais LES deux laboratoires qui m'ont accueilli pour faire cette thèse: le CR2P et MECADEV, et toutes les personnes en faisant parti. Je remercie nos deux directrices d'UMR, Sylvie Crasquin et Fabienne Aujard pour m'avoir permis de mener à bien cette thèse dans les meilleures conditions. Il me faut également remercier l'ensemble de l'équipe FUNEVOL pour l'accueil chaleureux au sein de l'équipe. Les repas à la cantine à 11h30 où se mélangent chercheurs, post-doc, doctorants et stagiaires ont été l'occasion d'échanger sur de nombreux sujets, plus ou moins sérieux, et d'essayer de monter des projets de recherches plus ou moins loufoques: baculum, les constructions des wombats, dents de sabres... Si les repas étaient expédiés en 4ème vitesse (merci Alex ;)), la pause café était quand même là pour rattraper le coup.

Merci également tant à Maxime Labat que le "Pint of Science" pour m'avoir permis par deux fois déjà de participer à des évènements de vulgarisation scientifique, au combien importante

de nos jours pour transmettre de façon ludique la science et nos recherches.

Auré, Thibault koala, Churros et Rémi, les "paleux" même si au final un seul en fait vraiment. Merci pour tous ces bons moment en votre compagnie, les repas-dobble, les escape-games, et j'en passe.

Mes pensées vont aussi à mes co-bureaux: ceux d'abord qui ont commencé en même temps que moi: Maxime, Fanny (oui tu es comptée dedans, même si tu as commencé un an avant), Rémi et Christophe, ces Gravibones partis trop tôt (du bureau), et Colline. Je sais que mes éternelles maladresses étaient pour vous source d'amusement... à tel point que vous vous êtes même mis à les compter. Vous avez également réussi à me supporter lorsque je "vivais" les musiques tout en travaillant, spécialement lorsque j'écoutais ce chef d'œuvre qu'est la musique d'Howard Shore. Comme les sud-ouestistes diront toujours chocolatine (d'ailleurs mon correcteur automatique ne connait pas ce mot), mes expressions mosellanes resteront toujours là, même si "une borne, ça se ferme". Tant pis, malgré tous vos efforts, on ira toujours manger *entre midi*, il n'y a rien à faire.
Et puis bien sur à ceux qui sont arrivés plus tardivement pour leur thèse, mais déjà présent pour leurs stages: Ana notre psychomotricienne, Romain, Cyril, Laurie, Julie, Priscilla et Camille, la relève dans le bureau et dans l'équipe est assurée. Ca va être à vous maintenant d'animer les réunions d'équipes et bien sûr de lancer le très sacré "appel cantine".

Il me faut également remercier toutes ces personnes qui m'ont accompagnées, de prés ou de loin, durant ces trois années de thèse, et qui m'ont permis de me détendre et de souffler. L'USI et l'escalade tout d'abord, l'ambiance familiale durant nos séances. Et bien sûr notre petit groupe escalade + week-end jeux : Marty, Jojo, Rémi, Marie, Jess, Mélo, Clément et le petit Obiwen. Merci pour tous ces fous rires, ces TITRES à n'en plus finir, le camping, les repas chez les uns et les autres pour nos séances/ week-ends jeux de sociétés.

Mes chers investigateurs, nos différentes aventures ont commencé simplement par la présentation de l'univers loftcraftien par Louis dans ce lieu peu commun qu'est le Makay. Depuis nous nous enfonçons un peu plus à chaque fois dans l'horreur, à la recherche des terribles secrets qui façonnent notre monde. Puisque ma santé mentale n'a pas vacillé avec la thèse, il a fallu que je joue avec elle en votre compagnie, allant toujours plus loin aux confins de la réalité, depuis l'Amérique jusqu'au Moyen-Orient, en passant par Londres et Lyon, avec quelques

détours dans le Monde des Rêves et la rencontre de peuples étranges. Il est parfois difficile pour moi de savoir qui je suis: Rohan, Hector, Stefan, ou encore quelqu'un d'autre. Un jour peut être auront nous l'honneur de croiser notre Saigneur à tous, Celui qui rêve et attend au fond de la mer, et alors nous entonnerons d'une seule voix "Ph'nglui mglw'nafh Cthulhu R'lyeh wgah'nagl fhtagn !!". Mais toutes nos aventures ne seraient rien sans notre MJ au top de sa forme, capable de s'adapter à toutes nos lubies, jusqu'à carrément inventer un scénario original, j'ai nommé Louis. Promis, un jour nous saurons écouter tes avertissements, mais que veux-tu, nous sommes beaucoup trop curieux, lorsqu'il y a la porte d'un temple à ouvrir, ou des escaliers à descendre. Je ne me suis toujours pas remis de cette expérience à Bryn Celli Ddu, et pour moi qui travaille sur un animal marin, toute cette eau de mer est bien problématique.

Daf, Soso, Poyou, notre amitié est toujours présente depuis de toutes ces années, et il est difficile de mettre des mots sur tout ce qui nous lie, tellement de choses sont à dire, et seront dites et partagées pour les nombreuses années à venir.

Corinne et Gildas, la marraine et le tonton, et Paul, le filleul-cousin, je vous remercie également, vous qui m'accueillez régulièrement chez vous pour des repas d'où je repars à chaque fois avec un petit tup' pour le lendemain soir, et qui m'avaient accueilli à Prat-Bihan avec plaisir. Marie et Louise, les couz' parisiennes, quand on est ensemble, on reste de vrais gamins, même Paul peut parfois être plus mature que nous, mais c'est ce qui est génial justement.

Enfin il me faut remercier enfin ma famille. Les frères d'abord: le Max, Lolo et Guillaume (aka Doudou, oui ca te suit même dans ma thèse), les gars, les gros, et encore tant de mots doux (ou pas) qu'on a pu utiliser pour se parler, et qu'on utilise toujours, au grand désespoir de maman. Mais ça nous fait rire, donc c'est le principal. Sans vous tout aurait été différent et je n'en serais certainement pas là aujourd'hui. Lolo, quand on était piot, le paléontologue de la famille c'était toi. On va dire que je t'ai piqué ton rêve :)
Et bien sûr à vous, Papa et Maman, je vous remercie du fond du cœur. Je sais que vous m'avez toujours soutenu et encouragés dans mes choix, et tant les coups de pieds au derrière lorsque c'était nécessaire que vos encouragements ont forgé la personne que je suis aujourd'hui.

Contents

RÉSUMÉ **1**

INTRODUCTION **9**

1 - General context 11

2 - The paired fins of *Latimeria chalumnae* and objectives of the thesis 22

MATERIAL AND METHODS **34**

1 - Material 36

2 - Methods 39

CHAPTER I: Development of the paired fins of the African coelacanth *Latimeria chalumnae* **50**

Context of the Chapter I 52

CHAPTER Ia: Development and growth of the pectoral girdle and fin skeleton in the extant coelacanth *Latimeria chalumnae* 56

CHAPTER Ib: Development and growth of the pelvic fin in the extant coelacanth *Latimeria chalumnae* 99

CHAPTER II: Revision of the muscular anatomy of the paired fins of the living coelacanth *Latimeria chalumnae* **138**

Context of the Chapter II 140

Revision of the muscular anatomy of the paired fins of the living coelacanth *Latimeria chalumnae* 144

CHAPTER III: Evolution of the functional muscular anatomy of pectoral and pelvic appendages across the water-to-land transition **240**

Context of the Chapter III 242

Evolution of the functional muscular anatomy of pectoral and pelvic appendages across the water-to-land transition 244

CHAPTER IV: General conclusions and perspectives **294**

RÉSUMÉ ÉTENDU

Parmi les ostéichthyens, les sarcoptérygiens (vertébrés à membres charnus) sont caractérisés par la présence de nageoires ou de pattes musculeuses à insertion mono-basale. Ce groupe est représenté aujourd'hui par trois clades: les cœlacanthes, les dipneustes et les tétrapodes. Alors que les deux premiers clades sont des animaux de type « poisson », inféodés au milieu aquatique, les tétrapodes sont pour la plupart terrestre, et leur histoire évolutive est marquée par le processus de terrestrialisation, associé à un passage de nageoires charnues à des pattes munies de doigts permettant de se déplacer hors de l'eau. Les cœlacanthes sont uniquement représentés de nos jours par le genre *Latimeria* et par deux espèces, le cœlacanthe africain *Latimeria chalumnae*, présent dans le Canal du Mozambique et le cœlacanthe indonésien *L. menadoensis*, présent au large de Sulawesi en Indonésie et en Nouvelle-Guinée. Bien que peu diversifié aujourd'hui, le groupe des cœlacanthes (Actinistia) témoigne d'une longue histoire évolutive puisqu'il est connu dans le registre fossile dès le Dévonien inférieur, il y a plus de 400 millions d'années. Le groupe des cœlacanthes est aujourd'hui considéré comme étant le groupe-frère du clade Dipneuste + Tétrapode et est, de ce fait, considéré comme étant d'un intérêt majeur pour la compréhension des conditions de la terrestrialisation (communément appelée « sortie des eaux ») des vertébrés. Bien que phylogénétiquement plus éloigné des tétrapodes que le groupe des dipneustes, il possède des nageoires pédonculées formées par un court axe métaptérigien, similaire à celui des premiers tétrapodomorphes, et le cœlacanthe est donc souvent considéré comme un bon modèle pour étudier la terrestrialisation des vertébrés. Si son anatomie a été décrite de façon exhaustive dans la célèbre monographie rédigée par Millot, Anthony et Robineau (1958, 1965, 1978), aucune révision profonde de l'anatomie de ses nageoires, n'a été proposée depuis. Cette révision est toutefois nécessaire afin de pouvoir mieux comprendre les modalités de la terrestrialisation des vertébrés.

Nous nous sommes tout d'abord intéressés au développement squelettique des nageoires pectorales et pelviennes du cœlacanthe, à partir d'une série ontogénétique comprenant 3 stades pré-nataux, un stade juvénile et un stade adulte. Du fait de la rareté des embryons et des juvéniles de cœlacanthes, il n'a pas été envisagé de faire des dissections afin d'étudier leur anatomie interne. C'est donc à partir de l'utilisation de la tomographie par rayons X et par IRM que nous avons pu modéliser en trois dimensions le squelette des nageoires pour chacun des

stades. Le squelette des nageoires pectorale et pelvienne sont semblables dans leur organisation, à l'exception de l'élément radial pré-axial 0 de la nageoire pelvienne qui s'articule avec la ceinture pelvienne. Cet élément, déjà décrit dans les premières descriptions du cœlacanthe, pourrait remettre en cause une des synapomorphies des sarcoptérygiens, qui est la condition mono-basale des nageoires paires.

Comme chez la plupart des vertébrés, les nageoires pelviennes du cœlacanthe commencent leur développement plus tardivement que celui des nageoires pectorales. La mise en place des éléments radiaux pré-axiaux et post-axiaux se fait précocement à partir de la fragmentation des mésomères associés. Cette mise en place d'éléments radiaux par fragmentation est similaire chez les dipneustes, et a permis de clarifier l'origine de l'élément radial pré-axial 0 de la nageoire pelvienne. En effet, il semble que cet élément soit l'homologue sériel de l'élément radial pré-axial 1 de la nageoire pectorale. Sa position proximale et adjacente à la ceinture pelvienne viendrait de la forme particulière des mésomères de la nageoire pelvienne en forme d'arc de voûte, ce qui induit une fragmentation proximo-latérale du mésomère lors de la formation des éléments radiaux pré-axiaux. Après la fragmentation, nous avons pu mettre en évidence que les éléments radiaux les plus distaux, présents sous forme de plaques cartilagineuses, vont se segmenter en éléments radiaux pré-axiaux 3-4 et éléments pré-axiaux accessoires sur le bord pré-axial, et en élément radial distal et éléments radiaux post-axiaux sur le bord post-axial. Durant son développement, la ceinture pectorale montre une réorientation qui vient mettre en contact les clavicules droite et gauche.

Enfin, les données tomographiques ont permis de mettre en évidence la présence d'une ossification superficielle progressive de la partie antérieure de la ceinture pelvienne. Cette ossification est également associée à un système trabéculaire, qui n'a jamais été décrit chez le cœlacanthe. Nous avons supposé que ce système trabéculaire et cette ossification permettent de résister à d'importantes contraintes musculaires sur cette partie de la ceinture. L'étude des forces musculaires qui s'appliquent sur les différentes parties de la ceinture a permis de confirmer notre hypothèse, puisque les contraintes musculaires les plus importantes s'exercent sur ces parties partiellement ossifiées de la région antérieure de la ceinture pelvienne. Au niveau fossile, lorsque la ceinture pelvienne est préservée, elle montre souvent une ouverture concave sur son côté postérieur, au niveau de l'articulation avec les mésomères. Nous suggérons donc que seule la partie la plus ossifiée de la ceinture est préservée lors de la fossilisation, et que la tête articulaire cartilagineuse du cœlacanthe est manquante.

L'étude de l'anatomie musculaire des nageoires pectorales et pelviennes du cœlacanthe a per-

mis de mettre en évidence sa grande complexité musculaire. Les muscles de ces nageoires s'organisent selon trois couches : superficielle, moyenne et profonde. Nous avons pu mettre en évidence un nombre de muscles bien plus important par rapport à ce qui avait été décrit dans les précédentes descriptions, jusqu'à 86 faisceaux musculaires pour la nageoire pectorale. De plus, de nombreux faisceaux musculaires sont eux-même, divisés en sous-faisceaux avec des insertions différentes. Les nageoires pectorales et pelviennes montrent une organisation musculaire différente. En effet, un nombre important de muscles de la nageoire pectorale sont mono-articulaires et s'insèrent sur les éléments endosquelettiques de la nageoire. Pour la nageoire pelvienne, la plupart des muscles sont poly-articulaires, et relient la ceinture pelvienne aux rayons dermiques des nageoires. Cette organisation musculaire de la nageoire pelvienne est considérée comme plésiomorphe par rapport à celle de la nageoire pectorale. En effet, des muscles qui directement de la ceinture aux rayons de la nageoire se retrouvent chez les actinoptérygiens, tandis que chez les dipneustes et les tétrapodes, les muscles s'insèrent sur les éléments endosquelettiques des nageoires. L'étude de l'architecture musculaire des nageoires a permis de montrer que les nageoires pectorales sont deux fois plus puissantes que les nageoires pelviennes. En effet il a été possible de calculer, à partir des données de masse et de longueur des muscles, l'aire de section transversale anatomique (ACSA), qui est un proxy pour estimer la force produite par un muscle. L'ACSA de la nageoire pectorale est de 37 cm^2 tandis que celle de la nageoire pelvienne est de 20 cm^2. Les premières études de Fricke et ses collaborateurs (1992) sur la locomotion du coelacanthe ont montré que la propulsion se fait principalement par l'ondulation du corps et de la nageoire caudale, ainsi que par les nageoires médianes lobées anale et 2^{nde} dorsale. Les nageoires pectorales et pelviennes ont principalement un rôle dans la stabilisation et la manoeuvrabilité du coelacanthe, avec des nageoires pectorales plus actives que les nageoires pelviennes. Nos résultats supportent les résultats *in vivo* puisque les nageoires pectorales sont plus mobiles et apparaissent plus puissantes que les nageoires pelviennes.

Les résultats de dissection des nageoires du coelacanthe ont ensuite été intégrés dans une étude plus large portant sur l'évolution de l'architecture musculaire lors de la terrestrialisation des vertébrés. La transition nageoire-patte s'est accompagnée de nombreuses modifications anatomiques, dont l'augmentation relative de la taille de la ceinture pelvienne et de sa fusion avec le squelette axial au niveau du sacrum, qui permet finalement aux membres postérieurs de supporter le poids du corps. La propulsion des « poissons » est principalement produite par l'ondulation du corps et l'utilisation de la nageoire caudale et des nageoires pectorales, alors

que chez les tétrapodes la propulsion est principalement produite par les membres postérieurs. Si ce changement locomoteur semble confirmé au niveau fossile, il n'a jamais été étudié chez les espèces actuelles et aucune étude sur l'architecture musculaire n'a pour le moment été proposée. Pourtant il est nécessaire de prendre en compte aussi bien le squelette que les muscles lors des études sur la locomotion, puisque ce sont les muscles qui produisent les forces nécessaires à la locomotion. En nous basant sur les homologies musculaires proposées par Diogo et collaborateurs (2016), qui permettent de comparer la musculature des nageoires à celle bien plus complexe des pattes des tétrapodes, nous nous sommes alors intéressés à l'évolution de l'architecture musculaire dans le contexte de la terrestrialisation des vertébrés. Pour cette étude exploratoire, nous avons sélectionné trois actinoptérygiens (le polyptère *Polypterus senegalus*, l'esturgeon *Acipenser stellatus* et le bar sauvage *Dicentrarchus labrax*) et cinq tétrapodes (la salamandre *Necturus maculosus*, l'alligator *Alligator mississippiensis*, le tégu *Salvator merianae*, le grison *Galictis vittata* et la loutre *Lontra longicauda*). Ces espèces ont été choisies pour leur intérêt phylogénétique et écologique pour l'étude de la terrestrialisation des vertébrés. Nous avons pu montrer que la masse musculaire et la puissance musculaire totale des membres chiridiens, relativement à la masse corporelle, est plus importante chez les tétrapodes que chez les poissons. Cette augmentation de la masse musculaire confirme les observations faites sur le squelette au niveau fossile. Il est supposé que cette augmentation de la puissance des membres chiridiens est liée à la différence fonctionnelle entre les nageoires et les pattes, puisque les forces nécessaires au maintien du poids du corps et à la propulsion et la locomotion sont générées principalement par les membres chiridiens chez les tétrapodes.

Nos résultats soutiennent également l'hypothèse du transfert d'un système de propulsion antérieure vers un système de propulsion postérieure au cours de la terrestrialisation des vertébrés. En effet, nous pouvons avons pu quantifier chez les tétrapodes des augmentations relatives de la masse musculaire et de la force plus importantes au niveau du membre postérieur qu'au niveau du membre antérieur. Ainsi, le membre postérieur plus puissant des tétrapodes est le principal générateur de la force de propulsion lors de la locomotion. Nous avons également pu mettre en évidence une distribution musculaire différente entre les nageoires et les membres chiridiens. Alors que les groupes musculaires profonds sont les plus puissant pour les nageoires, ce sont les groupes musculaires superficiels qui sont plus puissants pour les membres chiridiens. Cette distribution différente des groupes musculaires semble être liée à un héritage phylogénétique, plutôt qu'à un rôle fonctionnel.

Les dissections nous ont également permis de mesurer la mobilité articulaire des nageoires du cœlacanthe et des membres chez les tétrapodes. Nous avons pu mettre en évidence dans un premier temps que la nageoire pectorale du cœlacanthe a une mobilité bien plus importante que celle de la nageoire pelvienne, notamment pour l'articulation proximale avec la ceinture. La faible mobilité de la nageoire pelvienne semble être liée à la présence du radial pré-axial 0 en contact avec la ceinture. La comparaison de la mobilité articulaire des nageoires du cœlacanthe avec celle des pattes des tétrapodes a montré que l'articulation au niveau de la ceinture pectorale est bien plus importante chez le cœlacanthe que chez les tétrapodes. Cette différence de mobilité est attribuée à la morphologie de l'articulation, puisque la surface articulaire glénoïde au niveau de la ceinture pectorale est convexe chez le cœlacanthe, et concave chez les tétrapodes. Cependant, alors que l'articulation de la ceinture pelvienne du cœlacanthe est également convexe, sa mobilité est moins importante que pour l'articulation de la hanche chez les tétrapodes, sans doute lié à la présence du radial pré-axial 0.

Comme pour la ceinture pelvienne, nous avons pu observer une ossification superficielle de la tête articulaire du scapulocoracoïde de la ceinture pectorale, non décrite donc la thèse. Au niveau fossile, lorsque préservé, le scapulocoracoïde est souvent un élément de petite taille, correspondant à sa partie ossifiée, mais la présence de rainure sur la face ventrale du cleithrum et de l'extracleithrum suggèrent que le scapulocoracoïde était plus massif, et que la partie cartilagineuse n'a pas été préservée lors du processus de fossilisation.
Les données musculaires ont permis de quantifier la puissance musculaire des nageoires paires du cœlacanthe, et de déterminer leur rôle durant sa locomotion. De nouvelles analyses sur la locomotion du cœlacanthe *in situ* pourront permettre de tester nos hypothèses et de compléter les résultats obtenus par Fricke et collaborateurs (1992). Les premiers résultats montrent que les nageoires pectorales semblent plus actives que les nageoires pelviennes lors de la locomotion, mais la propulsion du cœlacanthe semble être liée aux mouvements de la nageoire caudale pour les accélérations, et par les nageoires médianes lobées anale et 2^{nde} dorsale lors de la nage lente. De nouvelles dissections sur ces nageoires permettrons de quantifier de façon plus précise leur rôle dans la locomotion du cœlacanthe, ainsi que leur morphologie fonctionnelle. De plus, du point de vue évolutif, ces nageoires lobées sont spécifiques du clade Actinistia, et leur origine demeure inconnue. Per Erik Ahlberg (1992) a suggéré une origine de ces nageoires par la duplication du gène responsable du développement des nageoires pelviennes, mais cela reste toujours à tester. La découverte de nouveaux embryons pourrait permettre de travailler sur la question, en utilisant des données anatomiques, mais

également génétiques grâce à l'apport de l'ARN prélevé sur des spécimens non fixés.
Enfin, l'étude du cœlacanthe *Laugia groenlandica* du Trias inférieur et du squelette de ses nageoires paires, permettra de mieux comprendre l'évolution des nageoires paires au cours de l'histoire évolutive des cœlacanthes. Une étude préliminaire sur des données tomographiques centrées sur les nageoires pectorales de *Laugia* ont mis en évidence la présence d'un système trabéculaire dans les mésomères. Un tel système trabéculaire n'est pas présent chez *Latimeria* et son étude pourrait permettre d'apporter de nouvelles données sur l'évolution de l'ossification des nageoires chez les cœlacanthes, ainsi que l'évolution de la micro-structure osseuse chez les premiers sarcoptérygiens.

INTRODUCTION

General context and objectives of the thesis

---

1 - General context

History of the scientist discovery of the coelacanth

The first description of a coelacanth was made by Louis Agassiz (1839) on the basis of fossilized tail with hollow fin rays. He then erected the genus *Coelacanthus* (Gr. κοίλος hollow and ἄκανθα spine). For a century, a large number of species was described all over the world in the Paleozoic and Mesozoic record, with a vast range of sizes and shapes. Soon, scientists thought this clade went extinct at the end of the Mesozoic era (Smith, 1939; Forey, 1998). Indeed, no fossil from the Cenozoic has been assigned with certainty to coelacanths and the most recent fossil known is *Macropoma mantelli* (Agassiz, 1839) from the Turonian (Upper Cretaceous).

It is only in December 1938 that a living coelacanth was captured off the coast of South Africa by the Captain Hendrick Goosen. Marjorie Courtenay-Latimer, curator of the Natural History Museum of East London (Cape Town), recognized that this peculiar fish could be a major discovery, a so far unknown fish. J.L.B Smith from Grahamstown identified this fish as a living coelacanth (Smith, 1939). Smith named this new animal *Latimeria chalumnae* in honour of his friend Marjorie Courtnay-Latimer and from the location of its capture, close to the mouth of the Chalumna River in South Africa (Smith, 1939). This discovery had a huge impact on the scientific community, and J.L.B Smith made the discovery of a new coelacanth the purpose of an important part of his life (Fig. 0.1). This first coelacanth from South Africa was thought to be a lost individual from the Mozambique Channel and it is in this area that the search of coelacanths focused during many years. It is only at the end of December 1952, 14 years later, that a second coelacanth was captured in the water of the Comoros Archipelago, which were at this time administered by France.

Thenceforth, many coelacanths were collected and preserved in the collections of several institutions. More than 285 specimens were known in 2011, with 15 (whole animals) of them in the collections of the Muséum national d'Histoire naturelle, Paris (MNHN) (Nulens et al., 2011). *Latimeria chalumnae* is present throughout the Mozambique Channel, from Kenya to South Africa (Fig. 0.2). In 1997, a new population was discovered off the coast of Sulawesi in Indonesia, more than 10 000 km away from the population in the Mozambique Channel (Erdmann et al., 1998), and genetic studies showed that the Indonesian coelacanth was a new species, subsequently named *Latimeria menadoensis* (Pouyaud et al., 1999). More recently, another population of coelacanths was discovered in West Papua (Indonesia), 750 km away from the

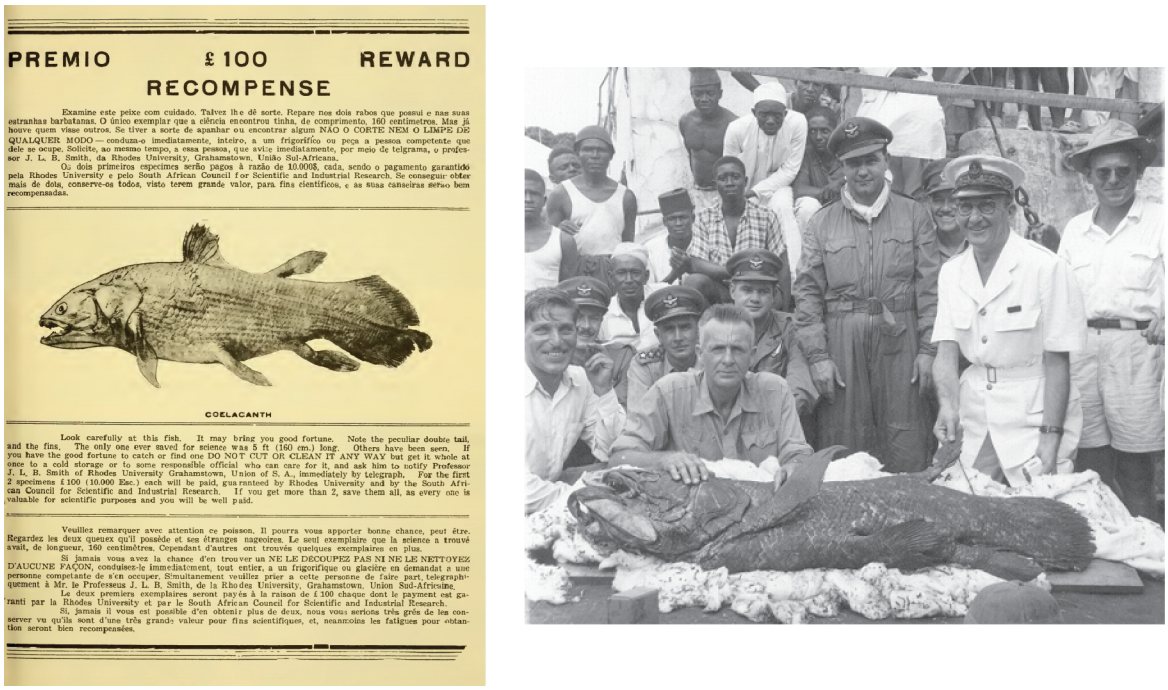

Figure 0.1: Wanted poster for the coelacanth distributed by J.L.B. Smith along the Mozambique Channel, and J.L.B. Smith posing in 1952 beside the second found coelacanth off the Comoro Islands. ©Thomson (1991)

population of Sulawesi, with a divergence time between the two populations estimated to 13 million years (Kadarusman et al., 2020).

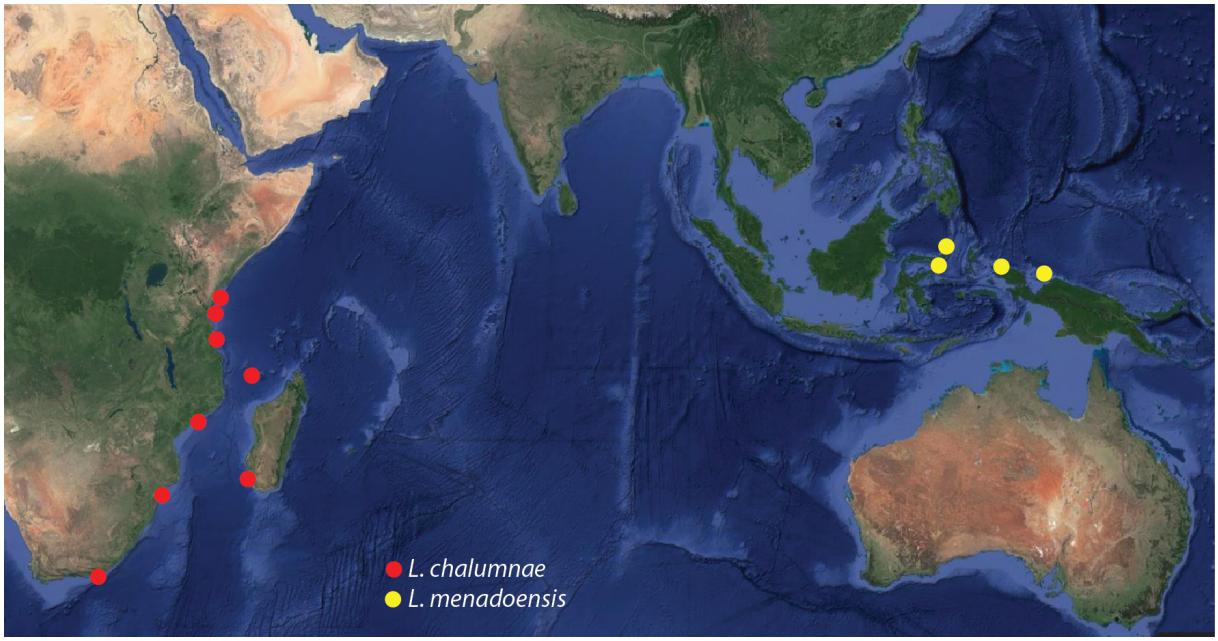

Figure 0.2: Known distribution of the two known coelacanth species *Latimeria chalumnae* and *L. menadoensis*.

Specific developmental and anatomical features of *Latimeria chalumnae*

Following its discovery, the African coelacanth *L. chalumnae* was the subject of an extensive monograph of three volumes named "Anatomie de *Latimeria chalumnae*" (Millot and Anthony, 1958, 1965; Millot et al., 1978). This monograph described in much detail the anatomy of the coelacanth and its specific features, previously only known in sarcopterygian fish fossils. Here I present a non-exhaustive list of specific developmental and anatomical features of *Latimeria* (Fig. 0.3).

- The coelacanth is an ovoviviparous animal (Lavett Smith et al., 1975; Atz, 1976). A female can carry 26 embryos in its oviduct (Bruton 1992), but it has been suggested that it could up to 30, since a specimen was captured with as many large eggs inside the oviduct (Suyehiro et al., 1982). For now on, only three pre-natal stages are known; an embryo of 5 cm total length, a pup with yolk-sac of about 32 cm long and a pup without yolk-sac near to the birth of 35 cm long. Together with a unique juvenile individual of about 42 cm long and adult specimens, this ontogenetic series allowed the description of the development of different organs of the coelacanth: the lung (Cupello et al., 2015), the head (Dutel et al., 2019), and the paired fins in this thesis (**Chapter I**).

- The anterior part of the oesophagus presents a ventral diverticulum, itself surrounded by a large fatty organ used for the buoyancy control (Cupello et al., 2015, 2019). Indeed the buoyancy control is ensured by the fatty organ and not by a swim bladder, an anatomical structure absent in *Latimeria*. This oesophageal diverticulum is a vestigial lung covered by small mineralized plates, homologous to the large ossified plates of the calcified organ of fossil coelacanths (Cupello et al., 2015, 2017). This lung is non-functional in the extant coelacanth which inhabits deep-water environments, but supposed to be in the process of functionality in the earliest developmental stages. In *Latimeria*, gas exchange take place exclusively at the level of the gills. In fossil coelacanths that lived in shallow brackish, fresh or marine waters, the lung is thought to have been functional, the large bony plates that covered the lung possibly allowing lung ventilation and protection against hydrostatic pressure (Brito et al., 2010; Cupello et al., 2017).

- The skull is separated into an anterior (ethmosphenoid) and a posterior (otoccipital) part by an intracranial joint. A divided skull is a character only found in the fossil record of sarcopterygian fishes, and lost independently in lungfishes and tetrapods. The intracranial joint is associated with the basicranial muscle. It was initially thought that this intra-cranial joint permits

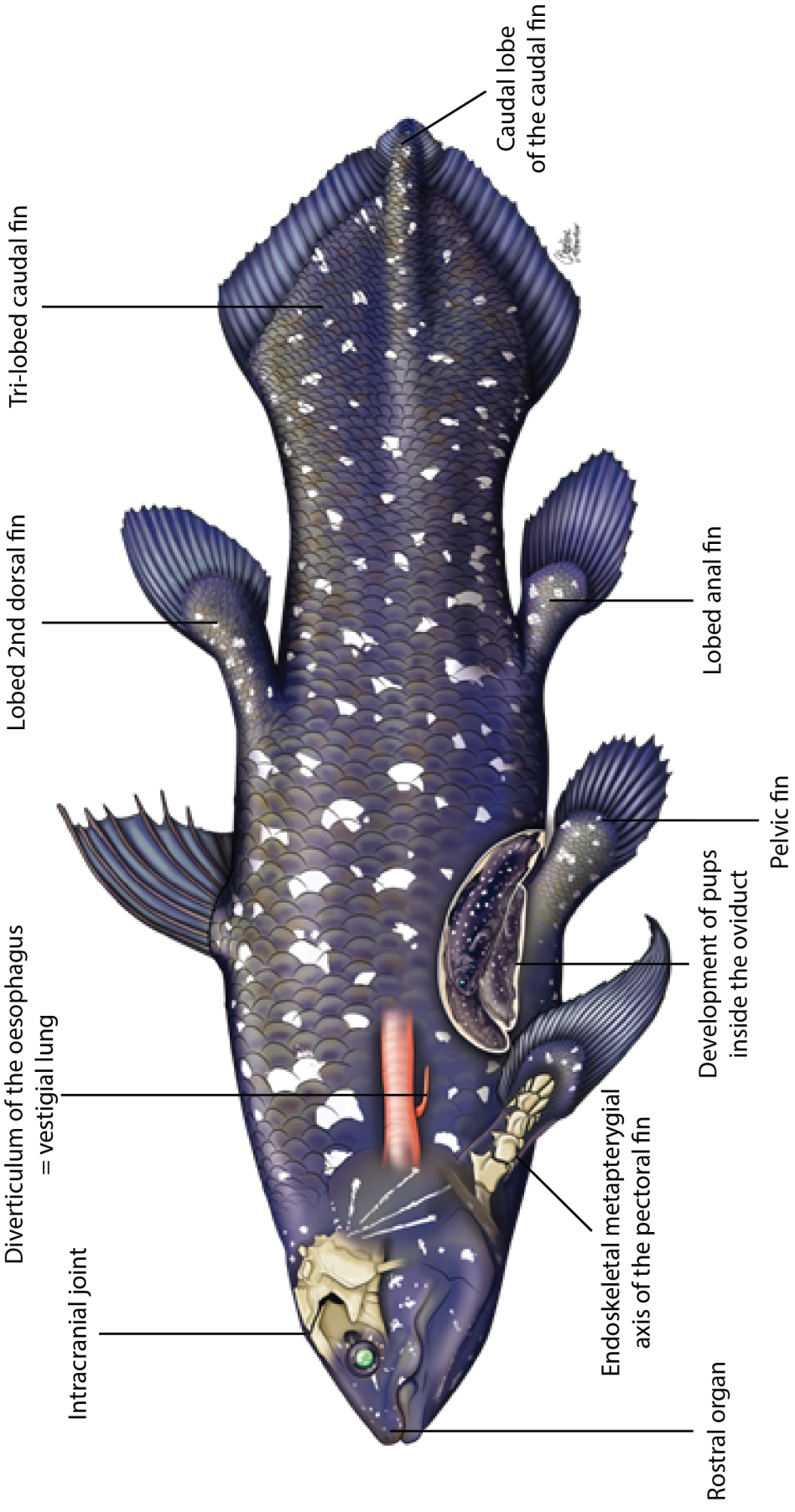

Figure 0.3: Anatomy of *Latimeria chalumnae* with overview of some specific features. ©Charlène Letenneur (MNHN).

an elevation of the snout by 15° to 21°, allowing a powerful suction by increasing mouth opening (Thomson, 1966; Robineau and Anthony, 1973). However, a recent study suggests that the intracranial joint mobility is less important than previously described, and that it is involved with the basicranial joint in the generation of bite force (Dutel et al., 2015).

- *L. chalumnae* possesses an electrosensitive organ in its snout (Millot and Anthony, 1956), the rostral organ, unique for vertebrates in its anatomy (Berquist et al., 2015). Indeed, it is formed by three pairs of large sensory canals, whereas in chondrichthyans and other osteichthyans (except neopterygian fishes and amniotes), the electro-sensitive organ is formed by hundreds or thousands of small sensory canals or ampullae. This organ is considered as an electro-detector of the low frequency electric fields produced by living tissues of preys (Berquist et al., 2015).

- The paired fins of the coelacanth are structurally different from the fins of actinopterygians. As in all sarcopterygian fishes the fin rays insert on an endoskeletal metapterygial axis that is articulated with the girdle by one element, the first mesomere. This mono-basal articulation permits a high mobility of the fin. The endoskeleton of the paired fins is covered by muscles.

- The anal and 2^{nd} dorsal fins are peculiar among extant osteichthyan fishes. In most sarcopterygian fishes, the fin rays are supported by radials elements supported by a basal plate, in a configuration similar to that of the median and paired fins of actinopterygians. In coelacanths, the anal and 2^{nd} dorsal fins have an organization similar to that of its paired fins, more like the pelvic fin, with the fin rays supported by a metapterygial axis that is articulated with a basal plate (Millot and Anthony, 1958; Ahlberg, 1992).

- The caudal fin is tri-lobed. It presents large dorsal and a ventral lobes, well developed and structurally similar, with around 25 lepidotrichia associated to each lobe. The third lobe, the caudal lobe, is much smaller and surrounds the extremity of the chord. It is associated with 30 to 35 lepidotrichia, arranged as a fan (Millot and Anthony, 1958). This caudal lobe is highly mobile (Fricke and Hissmann, 1992).

Ecology and swimming behaviour of the coelacanth

Whereas the anatomy of *Latimeria* is quite well known, mainly due to the monograph in three volumes (Millot and Anthony, 1958, 1965; Millot et al., 1978) and numbers of descriptive pa-

pers, many questions remain, especially concerning its behaviour, reproduction and ecology. Indeed, coelacanths are moderate deep-marine organisms and captured fishes cannot be kept alive in captivity. Since 2000, the coelacanth is classified as "critical endangered" (CR) species on the Red list of the IUCN, and since 1990 as "Vulnerable" (VU), and it is consequently not allowed to collect new specimens.

Following the description of some fin movements on a dying captured specimen (Locket and Griffith, 1972), Fricke and colleagues were able to observe for the first time a coelacanth in its natural environment with a submersible (Fricke et al., 1987). This observation was followed by many dives at different locations off the Comoros Islands resulting in hundreds of photographs and films. These dives showed that the coelacanth is a nocturnal species and brought some first information about its behaviour and ecology. Whereas the first descriptions of the coelacanth suggested that this animal was a bottom-crawler, direct observations showed that the coelacanth is instead a slow swimmer. It appears that coelacanths present a complex coordination of their fins, used both for locomotion and station holding when resting inside submarine caves (Fig. 0.4). In the Mozambique Channel, coelacanths live in moderate to deep water, between 115 and 200 m in Grande Comore (Fricke and Plante, 1988) and seems to prefer water below 18 °C and never above 20 °C. In 2000, a population of coelacanths was discovered in the Sodwana Bay, South Africa. This population lives in shallower water than the previous populations discovered in the Mozambique Channel, between 95 and 150 m, but sharing the same habitat condition as those in Comoros Islands, i.e. steep rocky environments with caves (Hissmann et al., 2006). No feeding or hunting has been recorded, but stomach contents showed that coelacanths are piscivorous predators that prefer benthic or epibenthic prey such as deep-sea fishes, eels, sharks and cuttlefishes (Uyeno, 1991).

Coelacanths live in small populations, the largest known being that of Grande Comore with few hundred individuals (Hissmann et al., 1998), whereas other populations are likely very small in size (estimated at 33 individuals in Sodwana Bay in 2013). Despite many dives and captures, only adults were observed, with the exception of two juvenile Indonesian coelacanths (Holden, 2009; Iwata et al., 2019, unpublished data). Many questions about the reproduction of the coelacanths remain to be answered, such as the mating behaviour, the gestation period, the places where the pregnant females give birth, or the life environment of the juveniles.

Figure 0.4: The extant coelacanth *Latimeria chalumnae* resting inside a submarine cave during the day. Picture taken during the "Gombessa" expedition in 2013, in Sodwana Bay, South Africa. ©Laurent Ballesta, Gombessa expeditions, Andromede Oceanology.

A brief overview of the evolutionary history of coelacanths

Fossil coelacanths have a worldwide distribution with occurrences in South America (e.g. Maisey, 1986; Soto et al., 2012; Yabumoto and Brito, 2013; Arratia and Schultze, 2015), North America (e.g. Schaeffer and Gregory, 1961; Lund and Lund, 1985; Schwimmer et al., 1994; Dutel et al., 2012; Wendruff and Wilson, 2012), Africa (e.g. Clément, 1999; Gottfried et al., 2004; Gess and Coates, 2015; Yabumoto et al., 2019), Asia (e.g. Liu, 1964; Gaudant, 1975; Tong et al., 2006; Wen et al., 2013; Yabumoto and Brito, 2016), Australia (e.g. Long, 1999; Clement, 2019), and Europe (e.g. Forey, 1981; Cavin et al., 2005, 2017, 2020; Friedman and Coates, 2006; Zaton et al., 2017; Renesto and Stockar, 2018). They also present an important ecological diversity, with for instance moderate to deep marine water habitats for *Latimeria, Macropoma, Holophagus* or *Coelacanthus* (Forey, 1998; Cupello et al., 2019), freshwater habitats for *Axelrodichthys, Indocoelacanthus* or *Mawsonia* (Jain, 1974; Patterson, 1975; Poyato-Ariza et al., 1998; Soto et al., 2012; Cavin et al., 2020) or brackish waters for *Mawsonia* or *Axelrodichthys* (Dutel et al., 2014; Cupello et al., 2019).

The evolutionary history of coelacanths is remarkably long, since the oldest supposed coelacanth known to date is *Styloichthys*, present in the fossil record of the Lochkovian (Early Devonian, 419.2 - 410.8 My) of the Witun Formation of East Yunnan (China) (Friedman, 2007). The second oldest supposed coelacanth, *Eoactinistia*, is present in the Fairy Formation (Australia) of the Pragian (Early Devonian, 410.8-407.6 My) but only as an isolated dentary (Johanson

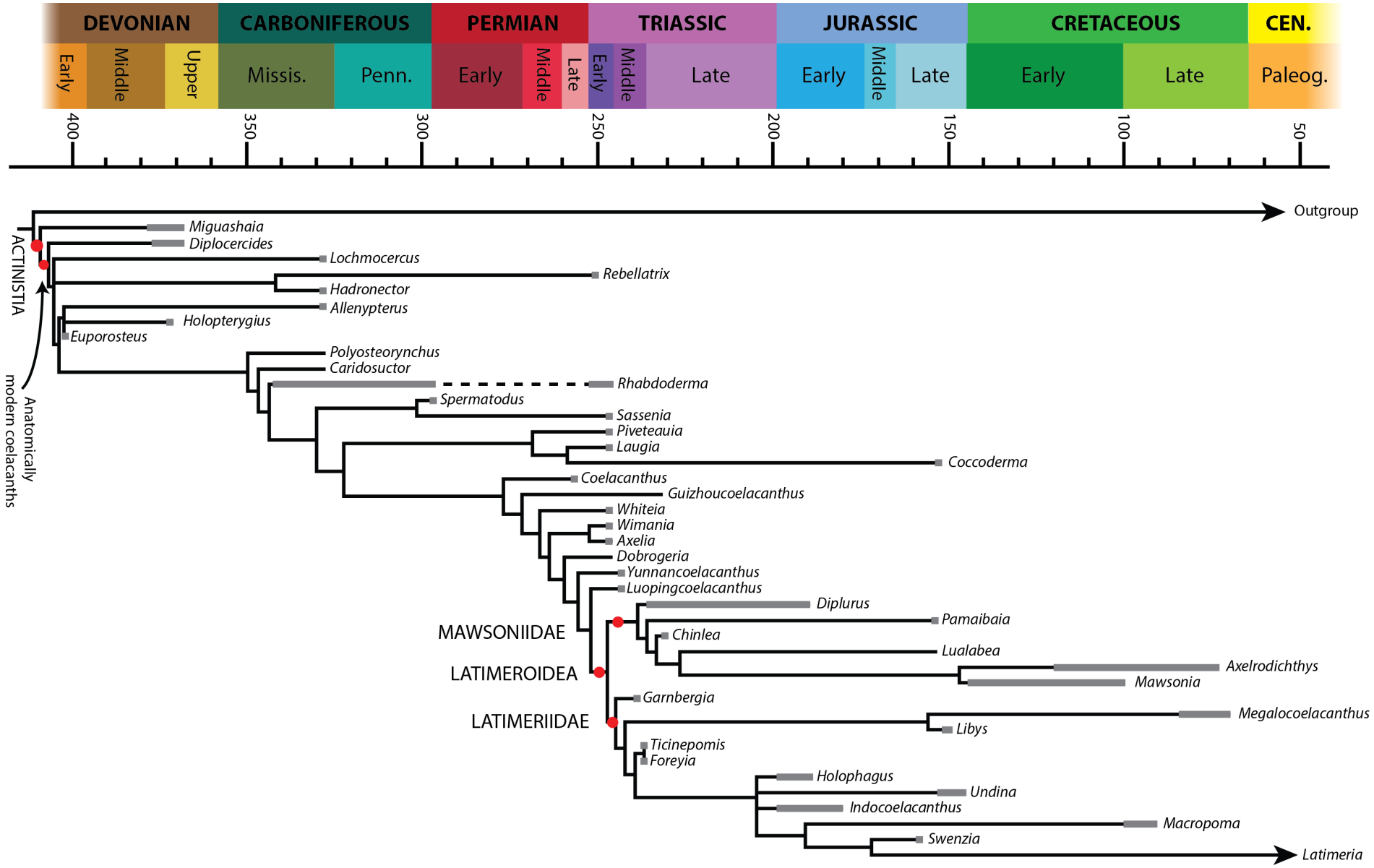
DEVONIAN
CARBONIFEROUS
PERMIAN
TRIASSIC
JURASSIC
CRETACEOUS
CEN.
Early
Middle
Upper
Missis.
Penn.
Early
Middle
Late
Early
Middle
Late
Early
Middle
Late
Early
Late
Paleog.
400
350
300
250
200
150
100
50
Outgroup
ACTINISTIA
Anatomically modern coelacanths
Miguashaia
Diplocercides
Lochmocercus
Rebellatrix
Hadronector
Allenypterus
Holopterygius
Euporosteus
Polyosteorynchus
Caridosuctor
Rhabdoderma
Spermatodus
Sassenia
Piveteauia
Laugia
Coccoderma
Coelacanthus
Guizhoucoelacanthus
Whiteia
Wimania
Axelia
Dobrogeria
Yunnancoelacanthus
Luopingcoelacanthus
Diplurus
MAWSONIIDAE
Pamaibaia
Chinlea
Lualabea
LATIMEROIDEA
Axelrodichthys
Mawsonia
Garnbergia
LATIMERIIDAE
Megalocoelacanthus
Libys
Ticinepomis
Foreyia
Holophagus
Undina
Indocoelacanthus
Macropoma
Swenzia
Latimeria

et al., 2006). This species, as *Euporosteus* from the Pragian of Germany and China, is considered as a modern coelacanth by its cranial morphology (Jaekel, 1927; Zhu et al., 2012). The most recent fossil coelacanth is *Megalocoelacanthus dobiei*, from the late Santonian to mid-Campanian age (Upper Cretaceous; 86.3-72.1 My) (Schwimmer et al., 1994; Dutel et al., 2012) (Fig. 0.5).

The main synapomorphy of Actinistia is the presence of an extracleithrum, a supernumerary dermal bone on the pectoral girdle (Forey, 1998; Arratia and Schultze, 2015). In their early history, coelacanths had a rapid diversification (Friedman and Coates, 2006). Devonian coelacanths as *Miguashaia*, *Gavinia* and *Styloichthys* possess plesiomorphic characters for sarcopterygians such as a heterocercal tail or an elongate post-orbital portion of the skull (Friedman, 2007; Zhu et al., 2012). Moreover, the exceptional fossilization of the pectoral endoskeleton of the Middle-Late Devonian coelacanth *Shoshonia* indicates an asymmetrical arrangement of the elements, as known in early sarcopterygians (Friedman et al., 2007). The presence of a symmetrical diphycercal tail or tri-lobed tail, an elongate preorbital and orbital portions of the skull and a more symmetrical endoskeleton of the pectoral fin are attributed to the modern coelacanths (Zhu et al., 2012). Moreover, the presence of lobe-shaped anal and 2^{nd} dorsal fins can also be considered as a synapomorphy of modern coelacanths, since early coelacanths such as *Miguashaia* do not show pedunculate median fins (Janvier, 1996; Forey, 1998).

Coelacanths are generally considered as a clade with a low rate of evolution and with a general morphology that did not change dramatically since the Early Devonian. This assumption was proposed first by Smith (1939) based on the gross resemblance of *Latimeria* with *Macropoma*. The living coelacanth was wrongly popularized as a 'living fossil' since the 50s'. In fact, coelacanths present vast specific, morphological and ecological diversity in the clade. Indeed, more than 37 genera and more than one hundred species have been described in the fossil record (Forey, 1998; Arratia and Schultze, 2015), with the maximum taxonomical diversity during the Lower Triassic and the Upper Jurassic (Forey, 1998) (Fig. 0.5). However, even if the term 'living-fossil' should not be used it is considered that the evolution rate of coelacanths is slow compared to other vertebrates, both with respect to morphological and molecular aspects

Figure 0.5: Time-scaled phylogeny of the Actinistia. Phylogeny modified from Cavin et al. (2017). Ages of the different genera are from Forey (1998); Cavin et al. (2013); Gess and Coates (2015); Cavin et al. (2020).The time-distribution is represented in grey.

(Amemiya et al., 2013; Casane and Laurenti, 2013; Cavin and Guinot, 2014).

There is a marked absence of well-preserved fin endoskeletons in the fossil record of the coelacanths, with the notable exceptions of *Shoshonia arctopteryx* from the Devonian of Wyoming, USA (Friedman et al., 2007) and *Laugia groenlandica* from the Early Triassic of Greenland (Stensiö, 1932). Whereas for *Latimeria* the pectoral fin endoskeleton is formed by four axial mesomeres (Millot and Anthony, 1958), it is different in these two fossil taxa. Indeed, *Laugia groenlandica* presents 3 axial mesomeres (Stensiö, 1932) (personal observations) and *Shoshonia* could have had up to 8 axial mesomeres (Friedman et al., 2007). With this absence of preserved fins in the fossil record of coelacanths, it is difficult to study and understand the evolution of the paired fins during the long history of the coelacanths. The paired fin morphology of the living coelacanths shows differences with those of the fossil coelacanths, but the exhaustive study of the paired fins in *Latimeria* is the only way to understand their functional role, and thus to predict modes of locomotion for fossil coelacanth taxa.

A model for the water-to-land transition?

Among vertebrates, coelacanths form a clade of sarcopterygian lobe-finned fishes inside the osteichthyans clade. Sarcopterygians are characterized by a monobasal articulation of their paired fins/limbs, with appendage musculature that extends onto the endoskeletal metapterygial axis of the fin/limb. Extant sarcopterygians comprise three clades: Actinistia (coelacanths), Dipnoi (lungfishes) and Tetrapoda (four-legged vertebrates) (Ahlberg, 1991; Janvier, 1996) (Fig. 0.6). The acquisition of appendages with digits was one of the key evolutionary steps in vertebrate history associated with the water-to-land transition that occurred during the Devonian.

The water-to-land transition is marked by many morphological and physiological transformations linked with ecological adaptations that ultimately permitted the terrestrialisation of vertebrates. Among the different transformations related to the appendages can be mentioned the reorientation of the glenoid and acetabulum in a more lateral position, the detachment of the pectoral girdle from the skull, the shift from pectoral to pelvic based locomotion, and the increase of the pelvic girdle size and its connection with the axial skeleton through the ilium (Carroll et al., 2005; Clack, 2012; Boisvert et al., 2013). Many Late Devonian fossils belonging to the tetrapodomorph clade are testimony to these transformations, such as *Eusthenopteron, Panderichthys, Tiktaalik, Acanthostega* or *Ichthyostega* (Fig. 0.6). Whereas for a long time, it was admitted that the presence of limbs was a proof of a terrestrial life-style, it has been shown

that Devonian tetrapods were mostly aquatic animals, and that the limbs had an aquatic function (Coates and Clack, 1995).

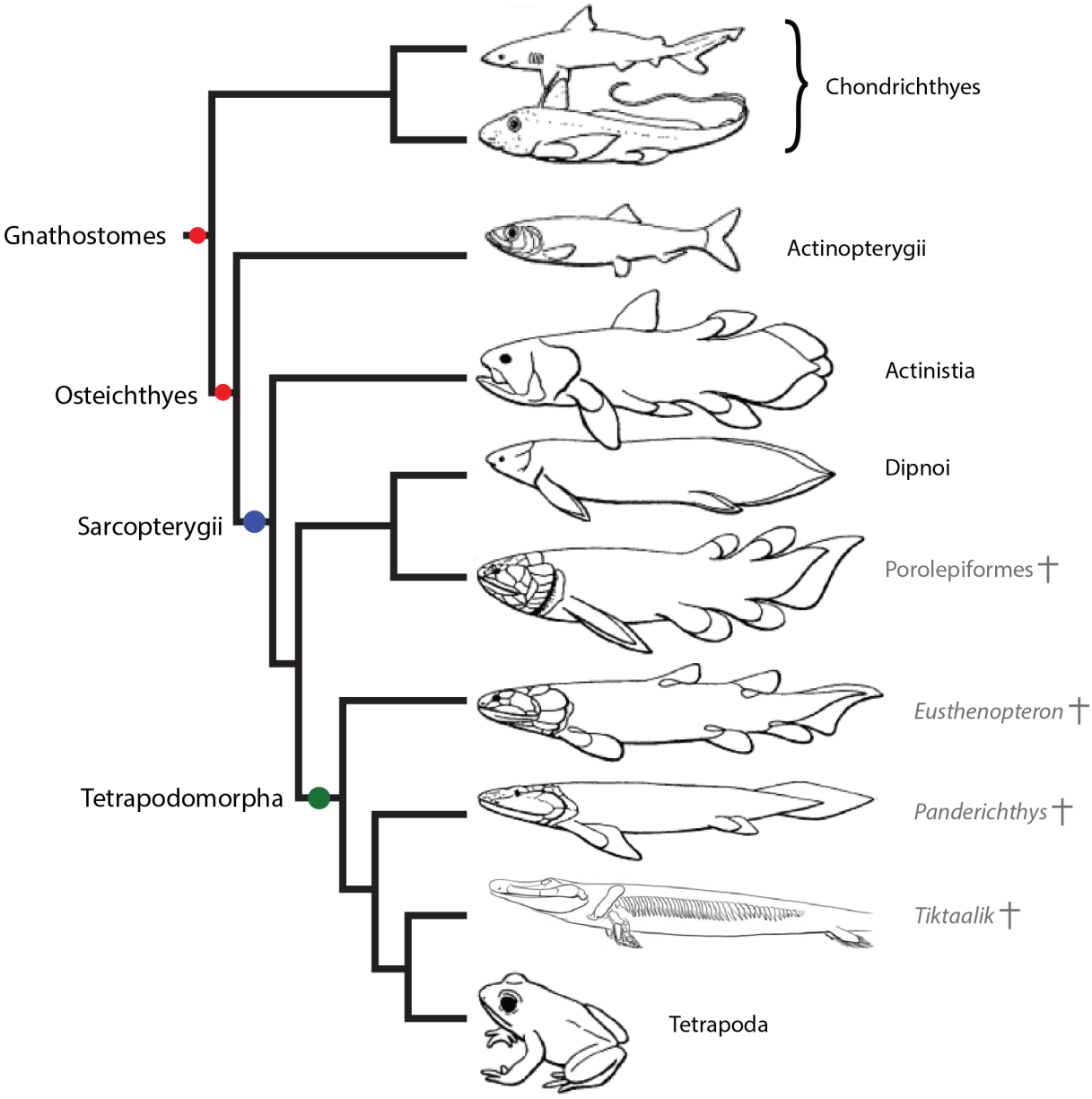

Figure 0.6: Simplified phylogeny of extant and extinct gnathostomes. Grey text indicates an extinct group. Modified from Janvier (1996), *Tiktaalik* position is from Daeschler et al. (2006).

The exact phylogenetic position of the actinistians was first controversial and different positions where proposed by different authors. They were considered as sister-taxa of chondrichthyans (Lovtrup, 1977), of all osteichthyans (Wiley, 1979) or of lungfishes (Northcutt, 1986). Only recently did morphological and molecular phylogenetic analyses comfort the hypothesis of a sister-taxa relationship to the clade lungfishes + tetrapods (Forey, 1998; Amemiya et al., 2013). Although the African and South American lungfishes have strongly reduced paired fins (e.g.

Criswell, 2015), the paired fins of the Australian lungfish *Neoceratodus* are used as a model for the study of the evolution of the fins development during the fin-to-limb transition (Shubin and Alberch, 1986; Johanson et al., 2007; Cole et al., 2011; Woltering et al., 2020). However, since early in their evolutionary history, the paired fins of lungfishes, including *Neoceratodus*, present a derived architecture with a large number of mesomeres on the metapterygial axis and a symmetrization of the fin (Friedman et al., 2007; Jude et al., 2014). Their anatomical study in the context of the fin-to-limb transition might consequently not be ideal. Indeed, the paired fins of early sarcopterygians are, among others, shorter and asymmetrical in their skeletal organization (Friedman et al., 2007). Even if the paired fins of the coelacanth *Latimeria* are derived, compared to the supposed highly asymmetrical plesiomorphic condition present in the Devonian coelacanth *Shoshonia* (Friedman et al., 2007), its skeletal anatomy is closer to that of the early tetrapodomorphs than that of lungfishes. *Latimeria* presents a smaller metapterygial axis, independent pre-axial radials and an asymmetrical organization of the radial elements along the metapterygial axis. Moreover, extant lungfishes are exclusively fresh-water animals (Clement, 2019) that have a locomotion based on the undulation of the body or the motion of the pectoral fins, but do not use the pelvic fins (Dean, 1906), whereas the extant coelacanth is a marine animal, similar to early tetrapodomorphs (Long et al., 2006; Clack, 2012), that likely actively used their pectoral and pelvic fins (Fricke and Hissmann, 1992). With its crucial position as sister-taxon of all extant sarcopterygians, the study of the paired fins of *Latimeria* seems appropriate to understand the evolution of the appendages in early sarcopterygians and during the fin-to-limb transition. However, this premise needs to be regarded cautiously, taking into consideration the unique evolutionary history of coelacanths.

2 - The paired fins of *Latimeria chalumnae* and objectives of the thesis

Since its discovery in 1938, the coelacanth has been extensively studied. Its lobed paired fins present a peculiar interest for biologists and palaeontologists in the understanding of the water-to-land transition in vertebrates. The first description of the paired fins anatomy was done by Millot & Anthony (1958). This description of the paired fins includes the description of the skeleton and the muscular anatomy. The dissections of *Latimeria* were made in a descriptive context, however, without taking account of the functional aspect of these fins.

No further detailed description of the skeletal anatomy of the paired fins of *Latimeria* has been done since this first description, except for a paper by Miyake and collaborators (2016) who argued the importance of the correct orientation of the mesomeres of the fins for comparison

with early tetrapodomorphs and a better understanding of the insertion of the muscles. Before any consideration of the impact of including the extant coelacanth in the evolutionary question of the fin-to-limb transition, it is necessary to have an exhaustive knowledge on the anatomy and development of the skeleton and associated muscles of its paired fins. The rare captures of some pregnant females permit an access to some ontogenetic stages of coelacanth allowing to obtain insights into the development of the paired fins.

In the **Chapter I**, I study the skeletal development of the pectoral and pelvic fins of *L. chalumnae*. This study allows the description of the morphological changes during the ontogeny of the coelacanth and the revision of the first descriptions of Millot and Anthony (1958). The development of the fins is compared with the development of the appendages in other osteichthyans.

More recently, new descriptions of the pectoral and pelvic fins musculature have been done to answer different questions. Miyake et al. (2016) compared the muscular anatomy of the pectoral fin of *Latimeria* with that of the lungfish *Neoceratodus* in order to investigate the evolutionary history and the muscular morphology of vertebrate limbs. Along the same vein, Diogo et al. (2016) investigated the evolutionary changes of the musculature of appendages during the water-to-land transition, with also a comparison with the muscular anatomy of the salamander *Ambystoma*. In their work, they proposed homologous relations between muscles of fishes and tetrapods. This latter work was then used to attempt a reconstruction of the muscular anatomy of fossils during the fin-to-limb transition (Molnar et al., 2018, 2020). Another publication proposed different homologies between muscles of *Latimeria, Neoceratodus* and the salamander *Necturus* (Boisvert et al., 2013). However, no dissections of the pelvic fins of *Latimeria* were used in this study, and the authors used the previous Millot and Anthony descriptions (1958) to propose homologies.

The muscular anatomy of the paired fins of *L. chalumnae* was used in different studies as a comparison for the muscular anatomy of other sarcopterygians. However, no study has described the muscle architecture of the fin muscles, crucial to characterize the role of the fins in locomotion. In **Chapter II**, I compare the muscle architecture of the pectoral and pelvic fins of the African coelacanth, and make inferences on the use of the fins for locomotion.

The fin-to-limb transition is marked by the increase in size of the pelvic appendages and a shift in the locomotory dominance from pectoral to pelvic appendages (Coates et al., 2002; Boisvert et al., 2013). These hypotheses are support by the fossil record from both sides of

the fin-to-limb transition. In previous studies on the muscular changes of appendages from fish to tetrapods, only the sarcopterygians are considered (Boisvert et al., 2013; Diogo et al., 2016; Molnar et al., 2018, 2020). Some rare studies on locomotion considered the actinopterygians such as the mudskipper *Periophtalmus* (Kawano and Blob, 2013) or the bichir *Polypterus* (Standen et al., 2014; Du and Standen, 2017, 2020), but without taking into account muscle anatomy. However, to test the shift of the locomotory dominance from pectoral to pelvic it is necessary to study the muscular anatomy and muscle architecture.

In the **Chapter III**, I focus on the changes in mucle architecture across the fin-to-limb transition. To address the hypothesis of a muscular shift from pectoral and pelvic appendages, I completed the results of the **Chapter II** with new dissections on the pectoral and pelvic appendages of species from both part of the fin-to-limb-transition, including some actinopterygians and tetrapods.

Bibliography

Agassiz, L. (1839). *Recherches sur les poissons fossiles - Tome II, Contenant l'Histoire de l'Ordre des Ganoïdes*. Petitpierre, Neuchâtel.

Ahlberg, P. E. (1991). A re-examination of sarcopterygian interrelationships, with special reference to the Porolepiformes. *Zoological Journal of the Linnean Society*, 103(3):241–287.

Ahlberg, P. E. (1992). Coelacanth fins and evolution. *Nature*, 358:459.

Amemiya, C. T., Alfoldi, J., Lee, A. P., Fan, S., Philippe, H., MacCallum, I., Braasch, I., Manousaki, T., Schneider, I., Rohner, N., Organ, C., Chalopin, D., Smith, J. J., Robinson, M., Dorrington, R. A., Gerdol, M., Aken, B., Biscotti, M. A., Barucca, M., Baurain, D., Berlin, A. M., Blatch, G. L., Buonocore, F., Burmester, T., Campbell, M. S., Canapa, A., Cannon, J. P., Christoffels, A., De Moro, G., Edkins, A. L., Fan, L., Fausto, A. M., Feiner, N., Forconi, M., Gamieldien, J., Gnerre, S., Gnirke, A., Goldstone, J. V., Haerty, W., Hahn, M. E., Hesse, U., Hoffmann, S., Johnson, J., Karchner, S. I., Kuraku, S., Lara, M., Levin, J. Z., Litman, G. W., Mauceli, E., Miyake, T., Mueller, M. G., Nelson, D. R., Nitsche, A., Olmo, E., Ota, T., Pallavicini, A., Panji, S., Picone, B., Ponting, C. P., Prohaska, S. J., Przybylski, D., Saha, N. R., Ravi, V., Ribeiro, F. J., Sauka-Spengler, T., Scapigliati, G., Searle, S. M., Sharpe, T., Simakov, O., Stadler, P. F., Stegeman, J. J., Sumiyama, K., Tabbaa, D., Tafer, H., Turner-Maier, J., Van Heusden, P., White, S., Williams, L., Yandell, M., Brinkmann, H., Volff, J. N., Tabin, C. J., Shubin, N. H., Schartl, M., Jaffe, D. B., Postlethwait, J. H., Venkatesh, B., Di

Palma, F., Lander, E. S., Meyer, A., and Lindblad-Toh, K. (2013). The African coelacanth genome provides insights into tetrapod evolution. *Nature*, 496(7445):311–316.

Arratia, G. and Schultze, H.-P. (2015). A new fossil actinistian from the Early Jurassic of Chile and its bearing on the phylogeny of Actinistia. *Journal of Vertebrate Paleontology*, 35(5):e983524.

Atz, J. W. (1976). *Latimeria* babies are born, not hatched. *Underwater Naturalist*, 9(4):4–7.

Berquist, R. M., Galinsky, V. L., Kajiura, S. M., and Frank, L. R. (2015). The coelacanth rostral organ is a unique low-resolution electro-detector that facilitates the feeding strike. *Scientific Reports*, 5(1):1–5.

Boisvert, C. A., Joss, J. M., and Ahlberg, P. E. (2013). Comparative pelvic development of the axolotl (*Ambystoma mexicanum*) and the Australian lungfish (*Neoceratodus forsteri*): conservation and innovation across the fish-tetrapod transition. *EvoDevo*, 4(3):1–19.

Brito, P. M., Meunier, F. J., Clément, G., and Geffard-Kuriyama, D. (2010). The histological structure of the calcified lung of the fossil coelacanth *Axelrodichthys araripensis* (Actinistia: Mawsoniidae). *Palaeontology*, 53(6):1281–1290.

Carroll, R. L., Irwin, J., and Green, D. M. (2005). Thermal physiology and the origin of terrestriality in vertebrates. *Zoological Journal of the Linnean Society*, 143(3):345–358.

Casane, D. and Laurenti, P. (2013). Why coelacanths are not 'living fossils'. *BioEssays*, 35:332–338.

Cavin, L., Buffetaut, E., Dutour, Y., Garcia, G., Le Loeuff, J., Méchin, A., Méchin, P., Tong, H., Tortosa, T., Turini, E., and Valentin, X. (2020). The last known freshwater coelacanths: New Late Cretaceous mawsoniid remains (Osteichthyes: Actinistia) from Southern France. *PLoS ONE*, 15(6):e0234183.

Cavin, L., Forey, P. L., Buffetaut, E., and Tong, H. (2005). Latest European coelacanth shows Gondwanan affinities. *Biology Letters*, 1(2):176–177.

Cavin, L., Furrer, H., and Obrist, C. (2013). New coelacanth material from the Middle Triassic of eastern Switzerland, and comments on the taxic diversity of actinistans. *Swiss Journal of Geosciences*, 106:161–177.

Cavin, L. and Guinot, G. (2014). Coelacanths as 'almost living fossils'. *Frontiers in Ecology and Evolution*, 2(49):1–5.

Cavin, L., Mennecart, B., Obrist, C., Costeur, L., and Furrer, H. (2017). Heterochronic evolution explains novel body shape in a Triassic coelacanth from Switzerland. *Scientific Reports*, 7:13695.

Clack, J. A. (2012). *Gaining Ground, Second Edition: The Origin and Evolution of Tetrapods*. Indiana University Press, Bloomington.

Clement, A. M. (2019). Sarcopterygian Fishes, the "Lobe-Fins". In Ziermann, J. M., Diaz Jr, R. E., and Diogo, R., editors, *Heads, Jaws, and Muscles*, pages 119–142. Springer.

Clément, G. (1999). The actinistian (Sarcopterygii) *Piveteauia madagascariensis* Lehman from the Lower Triassic of northwestern Madagascar: a redescription on the basis of new material. *Journal of Vertebrate Paleontology*, 19(2):234–242.

Coates, M. I. and Clack, J. A. (1995). ROMER's gap: tetrapod origins and terrestriality. *Bulletin du Museum national d'Histoire naturelle. Section C, Sciences de la Terre, paléontologie, géologie, minéralogie*, 17(1-4):373–388.

Coates, M. I., Jeffery, J. E., and Ruta, M. (2002). Fins to limbs: What the fossils say. *Evolution & Development*, 4(5):390–401.

Cole, N. J., Hall, T. E., Don, E. K., Berger, S., Boisvert, C. A., Neyt, C., Ericsson, R., Joss, J., Gurevich, D. B., and Currie, P. D. (2011). Development and evolution of the muscles of the pelvic fin. *PLoS Biology*, 9(10):16–18.

Criswell, K. E. (2015). The comparative osteology and phylogenetic relationships of African and South American lungfishes (Sarcopterygii: Dipnoi). *Zoological Journal of the Linnean Society*, 174(4):801–858.

Cupello, C., Brito, P. M., Herbin, M., Janvier, P., Dutel, H., and Clément, G. (2015). Allometric growth in the extant coelacanth lung during ontogenetic development. *Nature Communications*, 6:8222.

Cupello, C., Clément, G., Meunier, F. J., Herbin, M., Yabumoto, Y., and Brito, P. M. (2019). The long-time adaptation of coelacanths to moderate deep water : reviewing the evidences. *Bulletin of Kitakyushu Museum of Natural History and Human History*, 17:29–35.

Cupello, C., Meunier, F. J., Herbin, M., Janvier, P., Clément, G., and Brito, P. M. (2017). The homology and function of the lung plates in extant and fossil coelacanths. *Scientific Reports*, 7(1):1–8.

Daeschler, E. B., Shubin, N. H., and Jenkins Jr., F. A. (2006). A Devonian tetrapod-like fish and the evolution of the tetrapod body plan. *Nature*, 440:757–763.

Dean, B. (1906). Notes on the Living Specimens of the Australian Lungfish, *Cerutodus forsteri*, in the Zoological Society's Collection. *Proceedings of the Zoological Society of London*, 76:168–178.

Diogo, R., Johnston, P., Molnar, J. L., and Esteve-Altava, B. (2016). Characteristic tetrapod musculoskeletal limb phenotype emerged more than 400 MYA in basal lobe-finned fishes. *Scientific Reports*, 6:1–9.

Du, T. Y. and Standen, E. M. (2017). Phenotypic plasticity of muscle fiber type in the pectoral fins of *Polypterus senegalus* reared in a terrestrial environment. *The Journal of Experimental Biology*, 220(19):3406–3410.

Du, T. Y. and Standen, E. M. (2020). Terrestrial acclimation and exercise lead to bone functional response in *Polypterus* pectoral fins. *Journal of Experimental Biology*.

Dutel, H., Galland, M., Tafforeau, P., Long, J. A., Fagan, M. J., Janvier, P., Herrel, A., Santin, M. D., Clément, G., and Herbin, M. (2019). Neurocranial development of the coelacanth and the evolution of the sarcopterygian head. *Nature*, 569(7757):556–559.

Dutel, H., Herbin, M., Clément, G., and Herrel, A. (2015). Bite Force in the Extant Coelacanth *Latimeria*: The Role of the Intracranial Joint and the Basicranial Muscle. *Current Biology*, 25:1228–1233.

Dutel, H., Maisey, J. G., Schwimmer, D. R., Janvier, P., Herbin, M., and Clément, G. (2012). The Giant Cretaceous Coelacanth (Actinistia, Sarcopterygii) *Megalocoelacanthus dobiei* Schwimmer, Stewart & Williams, 1994, and Its Bearing on Latimerioidei Interrelationships. *PLoS ONE*, 7(11):e49911.

Dutel, H., Pennetier, E., and Pennetier, G. (2014). A giant marine coelacanth from the Jurassic of Normandy, France. *Journal of Vertebrate Paleontology*, 34(5):1239–1242.

Erdmann, M. V., Caldwell, R. L., and Moosa, M. K. (1998). Indonesian 'king of the sea' discovered. *Nature*, 395(6700):335.

Forey, P. L. (1981). The coelacanth *Rhabdoderma* in the Carboniferous of the British Isles. *Paleontology*, 24(1):203–229.

Forey, P. L. (1998). *History of the Coelacanth Fishes*. Thomson Science, London, chapman & edition.

Fricke, H. and Hissmann, K. (1992). Locomotion, fin coordination and body form of the living coelacanth *Latimeria chalumnae*. *Environmental Biology of Fishes*, 34(4):329–356.

Fricke, H. and Plante, R. (1988). Habitat Requirements of the Living Coelacanth. *Naturwissenschaflen*, 75:149–151.

Fricke, H., Reinicke, O., Hofer, H., and Nachtigall, W. (1987). Locomotion of the coelacanth *Latimeria chalumnae* in its natural environment. *Nature*, 329:331–333.

Friedman, M. (2007). *Styloichthys* as the oldest coelacanth: Implications for early osteichthyan interrelationships. *Journal of Systematic Palaeontology*, 5(3):289–343.

Friedman, M. and Coates, M. I. (2006). A newly recognized fossil coelacanth highlights the early morphological diversification of the clade. *Proceedings of the Royal Society B: Biological Sciences*, 273(1583):245–250.

Friedman, M., Coates, M. I., and Anderson, P. (2007). First discovery of a primitive coelacanth fin fills a major gap in the evolution of lobed fins and limbs. *Evolution & Development*, 9(4):329–337.

Gaudant, M. (1975). Sur la découverte de deux nouveaux Coelacanthes fossiles au Liban et la disparition apparente des Actinistiens au Crétacé. *Comptes Rendus de l'Académie des Sciences, Paris, Série D*, 280:959–962.

Gess, R. W. and Coates, M. I. (2015). Fossil juvenile coelacanths from the Devonian of South Africa shed light on the order of character acquisition in actinistians. *Zoological Journal of the Linnean Society*, 175(2):360–383.

Gottfried, M. D., Rogers, R. R., and Rogers, K. C. (2004). First record of Late Cretaceous coelacanths from Madagascar. In Arratia, G., Wilson, M. V. H., and Cloutier, R., editors, *Recent Advances in the Origin and Early Radiation of Vertebrates*, pages 687–691. Verlag Dr. Freidrich Pfeil, München, Germany.

Hissmann, K., Fricke, H., and Schauer, J. (1998). Population monitoring of the coelacanth (*Latimeria chalumnae*). *Conservation Biology*, 12(4):759–765.

Hissmann, K., Fricke, H., Schauer, J., Ribbink, A. J., Roberts, M., Sink, K., and Heemstra, P. C. (2006). The South African coelacanths - An account of what is known after three submersible expeditions. *South African Journal of Science*, 102(9-10):491–500.

Holden, C. (2009). Infant Fossil. *Science*, 326(5958):1327–1327.

Iwata, M., Yabumoto, Y., Saruwatari, T., Yamauchi, S., Fujii, K., Ishii, R., Mori, T., Hukom, F. D., Dirhamsyah, Peristiwady, T., Syahailatua, A., Masengi, K. W. A., Mandagi, I. F., Pangalila, F., and Abe, Y. (2019). Observation of the first juvenile Indonesian coelacanth, *Latimeria menadoensis* from Indonesian waters with a comparison to embryos of *Latimeria chalumnae*. *Bulletin of the Kitakyushu Museum of Natural History and Human History, Series A*, 17:57–65.

Jaekel, O. (1927). Der Kopf der Wirbeltiere. *Ergebnisse der Anatomie und Entwicklungsgeschichte*, 27:815–897.

Jain, S. L. (1974). *Indocoelacanthus robustus* n.gen., n.sp. (Coelacanthidae, Lower Jurassic), the First Fossil Coelacanth from India. *Journal of Paleontology*, 48(1):49–62.

Janvier, P. (1996). *Early vertebrates*. Oxford University Press, Oxford.

Johanson, Z., Joss, J., Boisvert, C. A., Ericsson, R., Sutija, M., and Ahlberg, P. E. (2007). Fish Fingers : Digit Homologues in Sarcopterygian Fish Fins. *Journal of Experimental Zoology Part B: Molecular and Developmental Evolution*, 308:757–768.

Johanson, Z., Long, J. A., Talent, J. A., Janvier, P., and Warren, J. W. (2006). Oldest coelacanth, from the Early Devonian of Australia. *Biology letters*, 2(3):443–6.

Jude, E., Johanson, Z., Kearsley, A., and Friedman, M. (2014). Early evolution of the lungfish pectoral-fin endoskeleton: evidence from the Middle Devonian (Givetian) *Pentlandia macroptera*. *Frontiers in Earth Science*, 2(August):1–15.

Kadarusman, Sugeha, H. Y., Pouyaud, L., Hocdé, R., Hismayasari, I. B., Gunaisah, E., Widiarto, S. B., Arafat, G., Widyasari, F., Mouillot, D., and Paradis, E. (2020). A thirteen-million-year divergence between two lineages of Indonesian coelacanths. *Scientific Reports*, 10(192):1–9.

Kawano, S. M. and Blob, R. W. (2013). Propulsive Forces of Mudskipper Fins and Salamander Limbs during Terrestrial Locomotion : Implications for the Invasion of Land. *Integrative and Comparative Biology*, 53(2):283–294.

Lavett Smith, C., Rand, C. S., Schaeffer, B., and Atz, J. W. (1975). *Latimeria*, the Living Coelacanth, Is Ovoviviparous. *Science*, 190:1105–1106.

Liu, H.-T. (1964). A new coelacanth from the marine Lower Triassic of N. W. Kwangsi, China. *Vertebrata PalAsiatica*, 8(2).

Locket, N. A. and Griffith, R. W. (1972). Observations on a living coelacanth. *Nature*, 237(5351):175.

Long, J. A. (1999). A new genus of fossil coelacanth (Osteichthyes: Coelacanthiformes) from the Middle Devonian of southeastern Australia. *Records of the Western Australian Museum*, 57:37–53.

Long, J. A., Young, G. C., Holland, T., Senden, T. J., and Fitzgerald, E. M. G. (2006). An exceptional Devonian fish from Australia sheds light on tetrapod origins. *Nature*, 444:199–202.

Lovtrup, S. (1977). *The Phylogeny of Vertebrata*. Wiley, London.

Lund, R. and Lund, W. L. (1985). Coelacanths from the Bear Gulch Limestone (Namurian) of Montana and the evolution of the Coelacanthiformes. *Bulletin of Carnegie Museum of Natural History*, 25:1–77.

Maisey, J. G. (1986). Coelacanths from the Lower Cretaceous of Brazil. *American Museum Novitates*, 2866:1–30.

Millot, J. and Anthony, J. (1956). L'organe rostral de *Latimeria* (crossoptérygien coelacanthidé). *Annales des sciences Naturelles Zoologie*, 18:381–389.

Millot, J. and Anthony, J. (1958). *Anatomie de Latimeria chalumnae - Tome I: Squelette, Muscles et Formations de soutien*. CNRS, Paris, cnrs edition.

Millot, J. and Anthony, J. (1965). *Anatomie de Latimeria chalumnae - Tome II: Système nerveux & Organes des sens*. CNRS, Paris.

Millot, J., Anthony, J., and Robineau, D. (1978). *Anatomie de Latimeria chalumnae - Tome III: Appareil digestif, Appareil respiratoire, Appareil urogénital, Glandes endocrines, Appareil circulatoire, Téguments-écailles, Conclusions générales*. CNRS, Paris.

Miyake, T., Kumamoto, M., Iwata, M., Sato, R., Okabe, M., Koie, H., Kumai, N., Fujii, K., Matsuzaki, K., Nakamura, C., Yamauchi, S., Yoshida, K., Yoshimura, K., Komoda, A., Uyeno, T., and Abe, Y. (2016). The pectoral fin muscles of the coelacanth *Latimeria chalumnae*: Functional and evolutionary implications for the fin-to-limb transition and subsequent evolution of tetrapods. *The Anatomical Record*, 299(9):1203–1223.

Molnar, J. L., Diogo, R., Hutchinson, J. R., and Pierce, S. E. (2018). Reconstructing pectoral appendicular muscle anatomy in fossil fish and tetrapods over the fins-to-limbs transition. *Biological Reviews*, 93:1077–1107.

Molnar, J. L., Diogo, R., Hutchinson, J. R., and Pierce, S. E. (2020). Evolution of Hindlimb Muscle Anatomy Across the Tetrapod Water-to-Land Transition, Including Comparisons With Forelimb Anatomy. *Anatomical Record*, 303(2):218–234.

Northcutt, R. G. (1986). Lungfish Neural Characters and Their Bearing on Sarcopterygian Phylogeny. *Journal of Morphology*, 190(S1):277–297.

Nulens, R., Scott, L., and Herbin, M. (2011). An updated inventory of all known specimens of the coelacanth, *Latimeria* spp. *Smithiana Publications in Aquatic Biodiversity*, 3:1–52.

Patterson, C. (1975). The distribution of Mesozoic freshwater fishes. *Mémoires du Muséum National d'Histoire Naturelle (Paris)*, 88:155–174.

Pouyaud, L., Wirjoatmodjo, S., Rachmatika, I., Tjakrawidjaja, A., Hadiaty, R., and Hadie, W. (1999). Une nouvelle espèce de coelacanthe. Preuves génétiques et morphologiques. *Comptes Rendus de l'Academie des Sciences - Serie III*, 322(4):261–267.

Poyato-Ariza, F. J., Talbot, M. R., Fregenal-Martínez, M. A., Meléndez, N., and Wenz, S. (1998). First isotopic and multidisciplinary evidence for nonmarine coelacanths and pycnodontiform fishes: Palaeoenvironmental implications. *Palaeogeography, Palaeoclimatology, Palaeoecology*, 144(1-2):65–84.

Renesto, S. and Stockar, R. (2018). First record of a coelacanth fish from the Middle Triassic Meride Limestone of Monte San Giorgio (Canton Ticino, Switzerland). *Rivista Italiana di Paleontologia e Stratigrafia*, 124(3):639–653.

Robineau, D. and Anthony, J. (1973). Biomécanique du crâne de *Latimeria chalumnae* (Poisson crossoptérygien coelacanthidé). *Comptes Rendus de l'Académie des Sciences, Paris, Série D*, 276:1305–1308.

Schaeffer, B. and Gregory, J. T. (1961). Coelacanth Fishes from the Continental Triassic of the Western United States. *American Museum Novitates*, 2036:1–18.

Schwimmer, D. R., Stewart, J. D., and Williams, G. D. (1994). Giant fossil coelacanths of the Late Cretaceous in the eastern United States. *Geology*, 22(6):503–506.

Shubin, N. H. and Alberch, P. (1986). A Morphogenetic Approach to the Origin and Basic Organization of the Tetrapod Limb. *Evolutionary Biology*, 20:319–387.

Smith, J. L. B. (1939). A Living Fish of Mesozoic Type. *Nature*, 143(3620):455–456.

Soto, M., De Carvalho, M. S., Maisey, J. G., Perea, D., and Silva, J. D. (2012). Coelacanth remains from the Late Jurassic-?Earliest Cretaceous of Uruguay: The southernmost occurrence of the Mawsoniidae. *Journal of Vertebrate Paleontology*, 32(3):530–537.

Standen, E. M., Du, T. Y., and Larsson, H. C. E. (2014). Developmental plasticity and the origin of tetrapods. *Nature*, 513(7516):54–58.

Stensiö, V. E. A. (1932). *Triassic Fishes from East Greenland, collected by the Danish Expeditions in 1929-1931*. Meddelelser om Grønland.

Suyehiro, Y., Uyeno, T., and Suzuki, N. (1982). Coelacanth, dissecting a living fossil. *Newton (Graphic Science Magazine)*, 2(8):82–93.

Thomson, K. S. (1966). Intracranial Mobility in the Coelacanth. *Science*, 153:999–1000.

Thomson, K. S. (1991). *Living Fossil: the Story of the Coelacanth*. Norton & Co, New York.

Tong, J., Zhou, X., Erwin, D. H., Zuo, J., and Zhao, L. (2006). Fossil Fishes from the Lower Triassic of Majiashan, Chaohu, Anhui Province, China. *Journal of Paleontology*, 80(1):146–161.

Uyeno, T. (1991). Observations on locomotion and feeding of released coelacanths, *Latimeria chalumnae*. *Environmental Biology of Fishes*, 32:267–273.

Wen, W., Zhang, Q. Y., Hu, S. X., Benton, M. J., Zhou, C.-Y., Tao, X., Huang, J.-Y., and Chen, Z.-Q. (2013). Coelacanths from the Middle Triassic Luoping Biota, Yunnan, South China, with the earliest evidence of ovoviviparity. *Acta Palaeontologica Polonica*, 58(1):175–193.

Wendruff, A. J. and Wilson, M. V. (2012). A fork-tailed coelacanth, *Rebellatrix divaricerca*, gen. et sp. nov. (Actinistia, Rebellatricidae, fam. nov.), from the Lower Triassic of Western Canada. *Journal of Vertebrate Paleontology*, 32(3):499–511.

Wiley, E. O. (1979). Ventral gill arch muscles and the interrelationships of gnathostomes, with a new classification of the Vertebrata. *Zoological Journal of the Linnean Society*, 67(2):149–179.

Woltering, J. M., Irisarri, I., Ericsson, R., Joss, J. M. P., Sordino, P., and Meyer, A. (2020). Sarcopterygian fin ontogeny elucidates the origin of hands with digits. *Science Advances*, 6:eabc3510.

Yabumoto, Y. and Brito, P. M. (2013). The second record of a mawsoniid coelacanth from the Lower Cretaceous Crato Formation, Araripe Basin, northeastern Brazil, with comments on the development of coelacanths. In Arratia, G., Schultze, H., and Wilson, M. V., editors, *Mesozoic Fishes vol.5. Global Diversity and Evolution*, pages 489–497. Verlag Dr. Freidrich Pfeil, Munich.

Yabumoto, Y. and Brito, P. M. (2016). A New Triassic Coelacanth, *Whiteia oishii* (Sarcopterygii, Actinistia) from West Timor, Indonesia. *Paleontological Research*, 20(3):233–246.

Yabumoto, Y., Brito, P. M., Iwata, M., and Abe, Y. (2019). A new Triassic coelacanth, *Whiteia uyenoteruyai* (Sarcopterygii, Actinistia) from Madagascar and paleobiogeography of the family Whiteiidae. *Bulletin of Kitakyushu Museum of Natural History and Human History*, 17:15–27.

Zaton, M., Broda, K., Qvarnström, M., Niedźwiedzki, G., and Ahlberg, P. E. (2017). The first direct evidence of a late devonian coelacanth fish feeding on conodont animals. *Science of Nature*, 104(3-4):1–5.

Zhu, M., Yu, X., Lu, J., Qiao, T., Zhao, W., and Jia, L. (2012). Earliest known coelacanth skull extends the range of anatomically modern coelacanths to the Early Devonian. *Nature Communications*, 3:772–778.

MATERIAL AND METHODS

1 - Material

Specimens of the African coelacanth, *Latimeria chalumnae*

The study materiel included in this thesis consists of several specimens of adult coelacanth, a juvenile specimen, and three prenatal specimens. Most of the specimens are stored in the collections of the Museum national d'Histoire naturelle, Paris, France (MNHN). Among the adults (developmental stage 5), we used the following specimens: CCC6, CCC7, CCC14, CCC19, CCC22 and CCC27 (CCC for Coelacanth Conservation Council) (Nulens et al., 2011).

- CCC6 (collection number: MNHN-ZA-AC-2012-4) corresponds to an isolated pectoral fin endoskeleton of an adult male of 126cm in total length (TL) that weighed 33kg, stored in the collections of the MNHN. It was used as comparison material for the endoskeleton anatomy (**Chapter I**).

- CCC7 (MNHN-ZA-AC-2012-5) corresponds to an isolated paired fin endoskeleton from a male of 130 cm TL that weighed 30kg. The fins were used as comparison material for the endoskeleton anatomy (**Chapter I**).

- CCC14 (MNHN-ZA-AC-2012-11) is an adult male of 134 cm TL that weighed 39kg. It was captured in the region of Dzahadjou, Hambou, off the coast of Grande Comore Island in 1956. It is preserved in a 6-7% formaldehyde solution. This specimen was used for dissections and measurements of the joint mobility along the metapterygial axis (**Chapter II**), and as a material comparison for the endoskeleton anatomy (**Chapter I**).

- CCC19 (MNHN-ZA-AC-2012-15) corresponds to an isolated pectoral fin of an adult male of 132 cm TL that weighed 35kg. The pectoral fin was used as comparison material for the endoskeleton anatomy (**Chapter I**) and to measure the joint mobility of the fin along the metapterygial axis (**Chapter II**).

- CCC22 (MNHN-ZA-AC-2012-18) is an adult male of 130 cm TL and weighed 31kg. It was captured off the coast of Grande Comore in 1960, in the region of Itsoundzu, Canton de Badjini. It is preserved in a 6-7% formaldehyde solution. This specimen was used for imaging and reconstructions of the endoskeleton of the pectoral fin (**Chapter I**).

- CCC27 (MNHN-ZA-AC-2012-21) is an adult male of 132 cm TL and weighed 38kg. It was captured off the coast of Grande Comore in 1961. It is preserved in a 6-7% formaldehyde solution. This specimen was used for imaging and reconstructions of the endoskeleton of the pelvic fin (**Chapter I**) and dissection of the pelvic fin (**Chapter II**).

The juvenile specimen CCC94 (MNHN-ZA-AC-2012-27) (developmental stage 4) is a young female of 42.5 cm TL and weighs 800g. It was captured off the coast of Grande Comore, in the region of Iconi in 1974. It is preserved in a 6-7% formaldehyde solution. It was used for imaging and reconstruction of its fin anatomy (**Chapter I**).

The three prenatal specimens correspond to three different developmental stages: a fetus, a pup with yolk sac and a more mature pup without yolk sac (respectively developmental stages 1, 2 and 3).

- CCC202.1 (SAIAB 76199) is a fetus of 5 cm TL found in the female specimen CCC202, captured off the coast of Tanzania, in the Muheaza District in 2005. It is preserved in an aqueous ethanol solution (70°) in the collections of the South African Institute for Aquatic Biodiversity (SAIAB) in Grahamstown. The specimen was used for imaging and reconstructions of its fins anatomy (**Chapter I**).

- CCC29.5 (MNHN-ZA-AC-2012-22) is a pup with yolk sac of 32.3 cm TL and weighs 530 g. It was found with four other pups in female specimen CCC29, captured off the coast of Mutsamudu, Anjouan, in the Comoros Archipelagos in 1969. It is preserved in a 6-7% formaldehyde solution. It was used for imaging and reconstructions of its fins anatomy (**Chapter I**).

- CCC162.21 (ZSM 28409) is a pup without yolk sac of 35.6 cm TL and weighs around 500g. It was found in the female specimen CCC162 in 1991 that contained 26 pups, captured off the port of Pebane, Mozambique. It is preserved in an aqueous ethanol solution (70°) in the collections of the Zoologische Staatssammlung of Munich. The specimen was used for imaging and reconstructions of its fins anatomy (**Chapter I**).

The specimens CCC22, CCC29.5, CCC94, CCC162.21 and CCC202.1 were selected before the beginning of the PhD project, since they were already scanned for previous studies (Cupello et al., 2015; Dutel et al., 2019). During the thesis, the specimens CCC14 and CCC27 were selected for dissections of the paired fins, and the pelvic fins of CCC27 were added for imaging acquisitions since the data on the specimen CCC22 were inadequate for an accurate segmentation. Other specimens (CCC6, CCC7, CCC19) were used since they were already prepared and available as comparison material in the collections of the MNHN. We used CCC19 for the measures of joint mobility since this isolated pectoral fin still had its ligaments.

Other vertebrate specimens used in the Chapter III

- Actinopterygians

Three actinopterygians were used during this thesis.

- The bichir *Polypterus senegalus* is a specimen of 80g. It was fixed in a 6-7% formaldehyde solution and preserved to a 70% ethanol solution.

- The sturgeon *Acipenser stellatus* is a sprecimen of 1131g. It was frozen, fixed in a 6-7% formaldehyde solution, then transferred to a 70% ethanol solution for preservation.

- The European bass *Dicentrarchus labrax* is a specimen of 770g. It was frozen, fixed in a 6-7% formaldehyde solution, then transferred to a 70% ethanol solution.

- Tetrapods

Specimens of tetrapods were chosen to represent the diversity of clades and lifestyles.

- Among lissamphibians, we used a mudpuppy *Necturus maculosus* of 36g, fixed in a 6-7% formaldehyde solution, then transferred to a 70% ethanol solution. This specimen was incomplete, with the distal part of the tail being absent.

- A crocodylian *Alligator mississipiensis* female from the Aquarium de la Porte Dorée, partly dissected and frozen, gave only access to the isolated right fore- and hind limbs. Before the dissections, the limbs were placed in a 6-7% formaldehyde solution, in order to fix the muscles, then transferred to a 70% ethanol solution. The body mass was unknown, and we estimated it based on the femur length, with a linear regression using the data of adult *Alligator* from Allen et al. (2010).

- A tegu lizard (*Salvator merianae* male of 2kg was used for dissections. It was preserved in a 6-7% formaldehyde solution. It appeared during the dissections that the ligaments of this specimen were damaged by the fixation and preservation in formaldehyde solution. We used a second male specimen (not weighted), that was also fixed in a 6-7% formaldehyde solution, then transferred to a 70% ethanol solution and that had intact ligaments to measure the joint mobility.

- Two mammals were included in the study: the grison *Galictis vittata* and the otter *Lontra longicauda*. The data from the mammals were available from a previous unpublished study (two otters and four grisons; courtesy of Anne-Claire Fabre and Benoit de Thoisy), and the results of the body mass, muscle masses, muscle length and fibre length were obtained by taking the mean. Two grison specimens are a male (M3017, M3018), one is a female (M178) and one is undetermined sex (M2209). The two otters are of undetermined sex (M3022, M3024). Both *Galictis* and *Lontra* were dissected fresh with no fixation of the muscles. The specimens are

from the collections of the Institut Pasteur, Cayenne.

All these specimens were chosen since they represent taxa that are phylogenetically (tetrapods) or ecologically (actinopterygians) of interest to understand the fin-to-limb transition and because they were available. Specimens were obtained from the Aquarium tropical de la Porte Dorée (Paris, France), the collection Jaguars of the Institut Pasteur (Cayenne, French Guyana) and the research collection of Anthony Herrel. The European bass was obtained a local fish monger. The number of actinopterygians and tetrapods specimens was limited by the long required time for dissections, especially for the fins of *Latimeria*.

2 - Methods

MRI and X-ray tomography and 3D reconstruction

Imaging

We used different non-destructive tomographic techniques to be able to quantify the anatomy of the paired fins of the coelacanths. Long propagation phase-contrast X-ray synchrotron micro-tomography was used for the fetus, the two pups and the juvenile. Conventional µCT-scanning was used for the adult specimen. MRI was used for the juvenile and data allow the observation of the soft tissues and the endoskeleton of the paired fins, in complementarity with theX-ray synchrotron tomography data. The different types of organs (endoskeleton, muscle, bone, cartilaginous, etc.) show a different contrast in the virtual slices obtained. The long propagation phase-contrast X-ray synchrotron micro-tomography, CT-scan, and the MRI permits to show preferentially different organs, and are complementary. The first two methods are more efficient for hard tissues (i.e. the different types of bones), whereas the MRI permit to visualize soft tissues.

All the specimens were already imaged before the beginning of the project. However it has been necessary to get new acquisitions for the pelvic fin of the adult CCC27 at the CT-scan AST-RX platform of the MNHN, and for the two pup specimens CCC29.5 and CCC162.21 at the European Synchrotron Radiation Facility (ESRF). The pup without yolk sac had been only partially scanned in previous study, and data concerning the posterior part of the specimen, including the pelvic fin, were missing. The original imaging data of the pup with yolk sac did not have enough contrast to permit accurate visualisation and segmentation of the endoskeleton (Fig. 0.7A). For these reasons, I wrote a proposal for beam time at the ESRF, and its accep-

tance allowed me to scan these two specimens on the ESRF beam line ID19 in May 2018 (Fig. 0.7B).

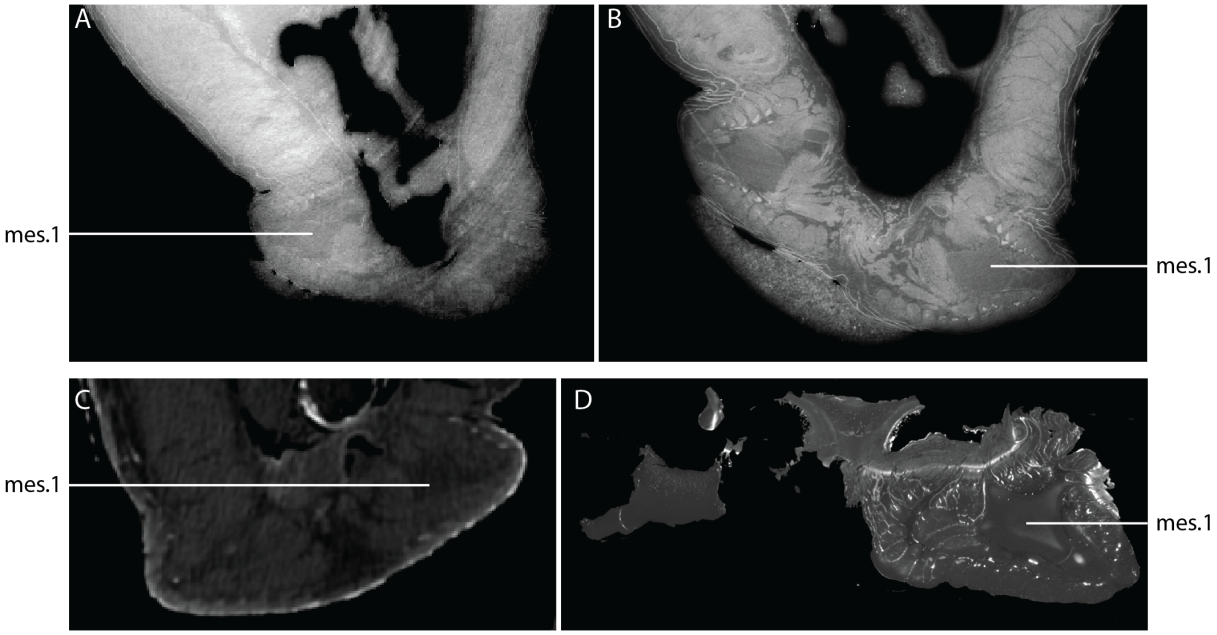

Figure 0.7: Comparison between the first (A, C) and second (B, D) µ-tomographic data acquisitions for the pelvic fins of the pup with yolk sac CCC29.5 (A, B) (synchroton) and the adult specimens CCC22 (C) and CCC27 (D) (CT-scan), at the level of the first mesomere (mes.1). Not to scale.

Given the scarcity of the material, it was not possible to used contrast agent before the data acquisitions. Indeed, for some specimens (e.g., the juvenile specimen CCC94, see Fig. 0.8A-B) the grayscale value (representing the X-ray beam attenuation to the tissue) was very close between soft tissues and the endoskeleton, and the 3D-segmentation of the fins took time. We did not have the possibility to scan the juvenile specimen a second time at the ESRF a second time, despite the difficulty of segmenting the most distal endoskeleton elements of the paired fins with the original synchrotron data. The MRI data permitted to segment these distal elements, but in a much lower resolution than that of the synchrotron data (Fig. 0.8C), and some of the smaller elements were not easily distinguishable.

The adult specimen CCC22 was originally scanned in a quite low resolution, that did not permit to visualize properly the pelvic fin anatomy (Fig. 0.7C). Moreover, the first data showed a strange high density structure inside the pelvic girdle. The scanning of the isolated pelvic fin of the adult specimen CCC27 permitted to have access to the inner structure of the pelvic girdle. It was necessary for the latter to have finished the dissections of the muscles of the fins to scan it, and it was the reason to separate the **Chapter I** into two different articles. After the

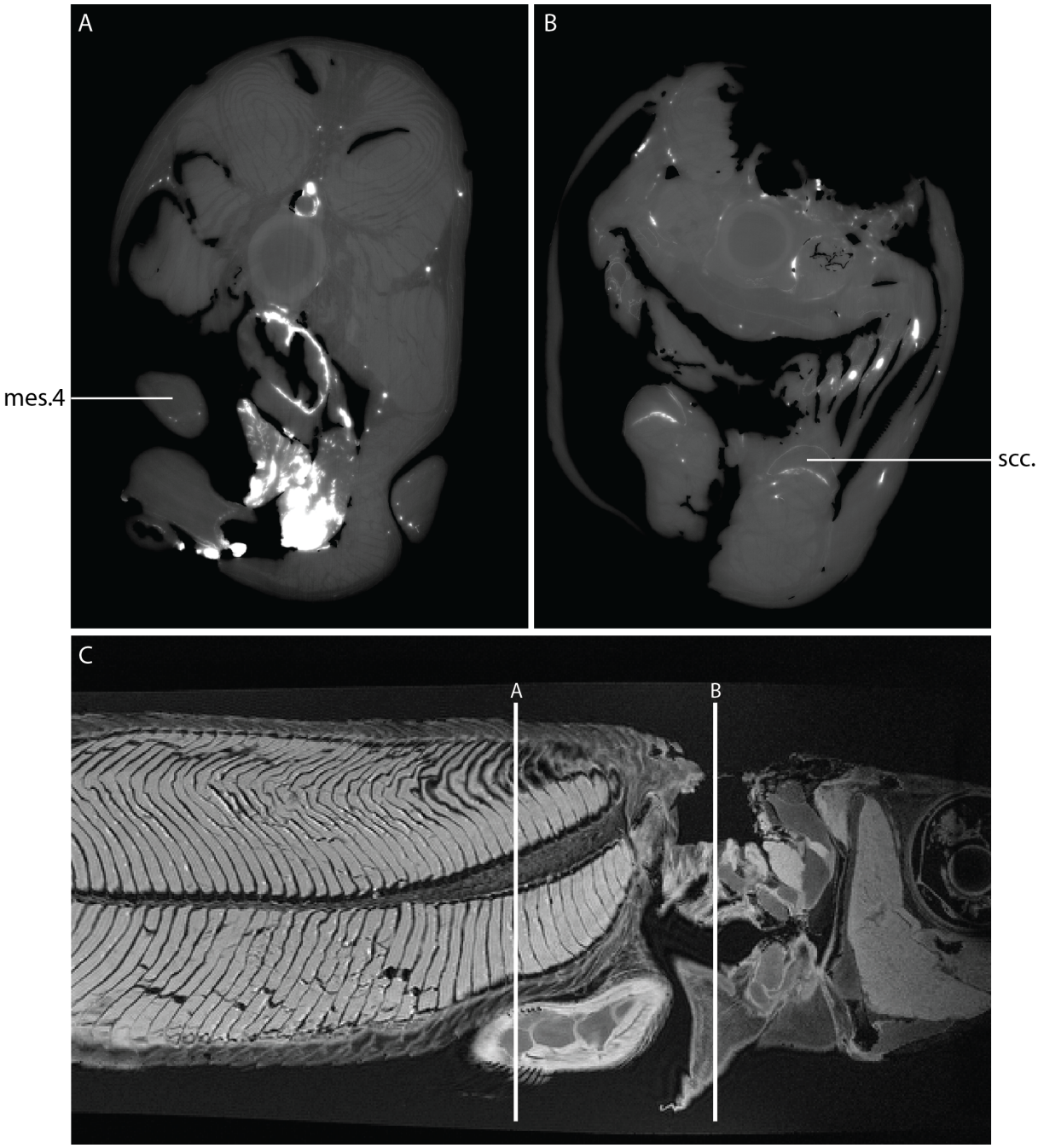

Figure 0.8: Comparison of the X-ray synchrotron tomography (A-B) and MRI (C) data of the juvenile specimen (CCC94) at the level of the scapulocoracoid (scc.) and fourth mesomere (mes.4) of the pectoral fins. The contrast between the muscles and endoskeletal elements is too low to reconstruct the distal part of the fin. The MRI data shows a better contrast, but with a lower resolution. Not to scale.

dissections, I wrote a proposal for scanning the fins in on the µCT-scan at the AST-RX platform of the MNHN, and the fins were scanned in September 2019 (Fig. 0.7D).

The problem of contrast between the muscles and the endoskeletal elements observed in X-ray tomography data in some specimens can be attributed to the preservation liquid of the specimens. Indeed, the formaldehyde fixation can cause a demineralization of the tissues, when the

pH of the solution is too acidic (Simmons, 2014).

Segmentation and 3D-reconstruction

For all specimens, segmentation and three-dimensional rendering were done using the software MIMICS Innovation Suite 20.0 (Materialise) (developmental stages 1-4) and MIMICS Innovation Suite 21.0 (Materialise) (pelvic fin of the developmental stage 5). The different objects were exported in STL format and transformed into a 3D PDF with the software 3-matic 11.0 (Materialise) and 3-matic 13.0 (Materialise).

Muscular data

Dissections

Before dissections, all the specimens were immersed in water, in order to remove the formaldehyde. For each appendage, the origin and insertion sites of each muscle bundle were noted and muscle bundles were photographed, removed with care and classified into functional groups (Fig. 0.9). Pictures were taken *in situ* at each stage of the dissection before removing the muscle bundles that were directly placed in a 70% aqueous solution of ethanol. After the complete dissection of each fin, the length of all muscle bundles was measured using a ruler (± 1mm), blotted dry and weighed to 0.00001g or 0.001g using an electronic balance (Mettler AE100; Ohaus Scout pro). The total length of each muscle bundle was defined as the maximal distance between the origin and insertion of the muscle bundle (from the most proximal origin of the muscular part to the most distal insertion, excluding tendons or aponeuroses). Dissections of the pectoral fin of *Latimeria* were done by Alessia Huby, and I dissected the pelvic fin of *Latimeria* and the appendages of the other vertebrates taxa (except for the two mammals since data were already available, as explained above).

Muscular properties

To quantify the muscle architecture we recorded muscle mass and muscle length that was measured during the dissection, and the fibre length.

For some of the large specimens (*Alligator*, *Acipenser*, *Salvator*, *Galictis* and *Lontra*), with muscle fibres clearly visible with the naked eyes, the fibre length was directly measured on the muscle with a ruler. In order to measure the fibre length, muscles were cut parallel to the fibre orientation, which allow a clear identification of each fibre. After dissections of *Dicentrarchus,*

Figure 0.9: Dissections of the dorsal side of the pelvic fin of *Latimeria* CCC27 (A) and isolated muscular fibres of the corresponding muscle (B). (C) Identification of the intrinsic muscles of the right forelimb of *Alligator* during the dissections.

Polypterus, Necturus and *Latimeria*, muscles were gently dried, and placed for a minimum of 24 hours in a 30% solution of nitric acid to dissolve all connective tissue, in order to dissociate the muscle fibres (Loeb and Gans, 1986). For some muscles, especially the superficial muscles of *Latimeria*, this dissociation period in the nitric acid lasted up to a week, due to the long-time muscle fixation in the formaldehyde solution. Once the connective tissues surrounding the fibres have been digested, nitric acid was removed and replaced by a 50% aqueous solution of glycerol (Antón, 1999; Herrel et al., 2008) (Fig. 0.9B). For each muscle, 10 fibres were selected randomly. A photo was taken of the smaller fibres. Large fibres were drawn using a binocular scope with *camera lucida* and then scanned to measure them. Measurements of the fibres, both on the photos and drawings, were done using the software Fiji (version ImageJ 1.52p, Java 1.8.0_172) and mean fibre length was then calculated.

The different parameters allowed us to determine the anatomical and physiological cross-section area (ACSA and PCSA) for each muscle. The detail for the calculation of ACSA and PCSA is presented in the **Chapter II** and **Chapter III**.

Classification of muscles

To compare the muscles of the fins and limbs, it has been necessary to define the homology between the muscles of the fins and limbs. The appendage muscles were classified into four general groups: the *abductor superficialis*, *abductor profundus*, *adductor superficialis* and *adductor profundus*, using the homologies between fin and limbs muscles proposed by Diogo et al. (2016). Some of extrinsic pectoral muscles were excluded from the analysis, since they insert only on the pectoral girdle, and have no homologous relations with the muscles of the pectoral fin of fishes. On the analysis of the pelvic appendages, however, we chose to include the caudofemoralis muscle of tetrapods, despite its uncertain origin, since this muscle inserts on the femur, and thus has a function in the motion of the hind limb.

Joints mobility

To compare the mobility of the different articulations of the pectoral and pelvic appendages, We measured the mobility of each joint after complete dissection with ligaments and capsule joints intact. To do so, we introduced two needles parallel to one another in the two elements that composed the joint (Moon, 1999). Then, the elements were moved maximally without damaging ligaments or joint capsules to estimate the degree of freedom of the joint for adduction/abduction, the protraction/retraction and pronation/supination movements. For each movement, five measures were taken, after returning the joint to the resting position of the fin, and a picture was taken for each measure (Fig. 0.10). The resting position of each fin is defined in the results. The angle formed by the needles was then determined using the software Fiji (version ImageJ 1.52p, Java 1.8.0_172), and the mean maximal angle was calculated for each movement.

We measured the joint mobility along the metapterygial axis for the paired fins of *Latimeria chalumnae* (**Chapter II**), but we only focused on the two proximal joints for the pectoral and pelvic limbs of tetrapods (**Chapter III**). In order to measure the abduction/adduction of the elbow and knee of tetrapods, it was necessary to extend the joint to the maximum, otherwise supination/pronation mobility would be included in the abduction/adduction mobility measurement. The different movements for a joint are defined as following:

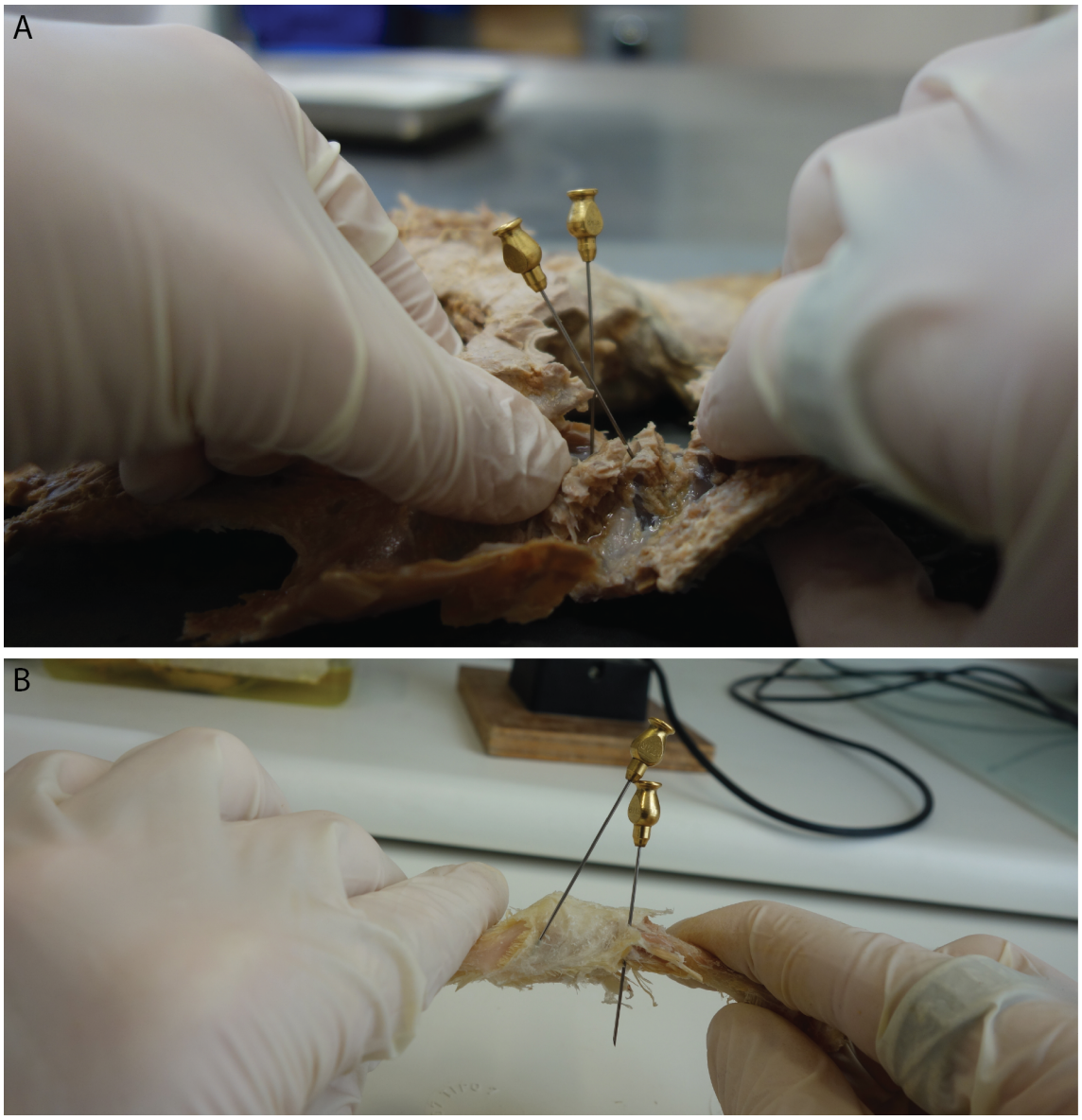

Figure 0.10: Measurement of flexion/extension mobility for joint between the first and second mesomeres of the pelvic fin of *Latimeria* CCC27 (A) and the knee of the tegu lizard *Salvator* (B).

- Pronation/supination corresponds to the long-axis rotation for both fins and limbs

- Protraction/retraction corresponds to the mobility along the antero-posterior axis of the body for the proximal joint for both fins and limbs. For the second joint (elbow and knee), it corresponds to flexion/extension.

- Abduction/adduction shows the range of mobility along the dorso-ventral axis for the proximal joint (shoulder and hip), and shows the lateral/medial mobility of the joint for the second joint (elbow and knee) (i.e. pre-axial/post-axial mobility of the joint for *Latimeria*).

It was necessary to define a reference position for the paired fins of *Latimeria* before assigning

the movements to the joints, since these fins have a large mobility (especially the pectoral fin that can have a fully 180° rotation). We defined the movement of the joint for the pectoral fin in its resting position, i.e. along the body with the leading edge of the fin in dorsal position. The resting position of the pelvic fin is defined as being along the ventral side of the body with its leading edge directed laterally. It was not easy to defined the movements of the fins of *Latimeria*, since the two fins are oriented in two different planes of the body (the sagittal plane and the frontal plane), whereas in tetrapods the fore- and hind limbs are in the same plane.

Mobility measures were realized for *Latimeria*, *Alligator* and *Salvator*. For *Alligator*, its was not possible to measure the mobility of the hip since we dissected an isolated hind limb, without associated pelvic girdle. It was not possible to measure the mobility of joints in *Necturus* since the epiphyses of long bones were not ossified and thus flexible. Joint mobility data for the fore- and hind limbs was not available for *Lontra* and *Galictis* since the data of their musculature were obtained from a previous study. Since there are few taxa included in this study of the fin and limb mobility, the results presented here are a preliminary work that will be completed later in view of publication. We thus plan to dissect additional taxa including amphibians, turtles and mammals for which we will be able to measure all variables and which will replace the taxa included for the current preliminary analysis (*Lontra*, *Galictis*).

Statistical analysis

We used statistical analyses in the **Chapter III** in order to study the difference in muscle architecture between different taxa. Analyses were performed using the software R v.4.0.2 (R Core Team, 2020). Since the different taxa used in this study present a large variation of size and body mass, the measures of interest (muscle mass, ACSA, PCSA) were $\log_{10}$-transformed to fulfil the assumption of normality and homoscedasticity. The $\log_{10}$-transformed data were then regressed against the $\log_{10}$-transformed body mass for each taxon, to remove the effect of size in our analyses. Univariate analyses of covariance (ANCOVA) were performed to test our hypotheses. The detail of each hypothesis is present in the **Chapter III**.

Bibliography

Allen, V. R., Elsey, R. M., Jones, N., Wright, J., and Hutchinson, J. R. (2010). Functional specialization and ontogenetic scaling of limb anatomy in *Alligator mississippiensis*. *Journal of Anatomy*, 216:423–445.

Antón, S. C. (1999). Macaque Masseter Muscle: Internal Architecture, Fiber Length and Cross-Sectional Area. *International Journal of Primatology*, 20(3):441–462.

Cupello, C., Brito, P. M., Herbin, M., Janvier, P., Dutel, H., and Clément, G. (2015). Allometric growth in the extant coelacanth lung during ontogenetic development. *Nature Communications*, 6:8222.

Diogo, R., Johnston, P., Molnar, J. L., and Esteve-Altava, B. (2016). Characteristic tetrapod musculoskeletal limb phenotype emerged more than 400 MYA in basal lobe-finned fishes. *Scientific Reports*, 6:1–9.

Dutel, H., Galland, M., Tafforeau, P., Long, J. A., Fagan, M. J., Janvier, P., Herrel, A., Santin, M. D., Clément, G., and Herbin, M. (2019). Neurocranial development of the coelacanth and the evolution of the sarcopterygian head. *Nature*, 569(7757):556–559.

Herrel, A., Vanhooydonck, B., Porck, J., and Irschick, D. J. (2008). Anatomical Basis of Differences in Locomotor Behavior in *Anolis* Lizards : A Comparison Between Two Ecomorphs. *Bulletin of the Museum of Comparative Zoology*, 159(4):213–238.

Loeb, G. and Gans, C. (1986). *Electromyography for experimentalists*. Chicago, the univer edition.

Moon, B. R. (1999). Testing an inference of function from structure: Snake vertebrae do the twist. *Journal of Morphology*, 241(3):217–225.

Nulens, R., Scott, L., and Herbin, M. (2011). An updated inventory of all known specimens of the coelacanth, *Latimeria* spp. *Smithiana Publications in Aquatic Biodiversity*, 3:1–52.

R Core Team (2020). A Language and Environment for Statistical Computing (Version 4.0.2). *Vienna: R Foundation for Statistical Computing*.

Simmons, J. E. (2014). *Fluid preservation: a Comprehensive Reference*. Rowman & Littlefield, Lanham, Maryland.

CHAPTER I

Development of the paired fins of the African coelacanth *Latimeria chalumnae*

Context of the Chapter I

The ontogeny is studied from long time in vertebrates, and the development of the paired fins is nowadays well known in both chondrichthyans (e.g. Cole and Currie, 2007; Riley et al., 2017), actinopterygians (e.g. Davis et al., 2004; Mabee and Noordsy, 2004; Sfakianakis et al., 2005; Thorsen and Hale, 2005) and sarcopterygians (e.g. Shubin and Alberch, 1986; Rieppel, 1992; Johanson et al., 2004; Boisvert et al., 2013). Among sarcopterygians, the development of the coelacanth remains poorly known, since it is not possible to maintain it in captivity, neither to breed it. However, the development is an important source of information in the evolutionary process and the morphological transitions, and the coelacanth is crucial in our understanding of the fin-to-limb transition. The ovoviviparity of the coelacanth (Lavett Smith et al., 1975) permits to have access to different ontogenetic stages (Nulens et al., 2011), and the development of non-invasive techniques allows the study of the inner anatomy of the coelacanth and its development (Cupello et al., 2015; Dutel et al., 2019). In sarcopterygians, three different processes of development of the appendages have been proposed by Shubin and Alberch (1986): the branching process, the segmentation process and the *de novo* process. Here we investigate the development of the pectoral and pelvic fins of *Latimeria* to understand the processes used for their formation, and the evolution of the appendage development in the fin-to-limb transition.

Even if the ontogenetic series of *Latimeria* was scanned before the beginning of the thesis, it was necessary to perform new acquisitions at the European Synchrotron Radiation Facility (Grenoble, France). Indeed, it would have been interesting to scan again the early embryonic stage housed in the SAIAB colections (collection number: SAIAB 76199), since the image contrast was not sufficient on the distal part of the fins for an accurate vizualisation and segmentation. But it was decided that it would be too dangerous for this precious and unique specimen to borrow it again for another X-ray acquisition. In the same way, the pup with yolk sac did not have enough image contrast, the pup without yolk sac was only partially scanned and the pelvic fins were missing in the original data. Moreover the pelvic fins of the adult specimen needed to be rescanned since it was originally scanned with a too resolution. In order to obtain a higher resolution of the pelvic fins, it was necessary to scan isolated fins, after their dissection. This chapter is divided in two different articles, because there was a delay to the complete dissections of the fins and to obtain access of the AST-RX platform of the MNHN. I started with the pectoral fins and continued with the pelvic ones. I segmented all the data and wrote the two associated papers.

Bibliography

Boisvert, C. A., Joss, J. M., and Ahlberg, P. E. (2013). Comparative pelvic development of the axolotl (*Ambystoma mexicanum*) and the Australian lungfish (*Neoceratodus forsteri*): conservation and innovation across the fish-tetrapod transition. *EvoDevo*, 4(3):1–19.

Cole, N. J. and Currie, P. D. (2007). Insights From Sharks : Evolutionary and Developmental Models of Fin Development. *Developmental Dynamics*, 236:2421–2431.

Cupello, C., Brito, P. M., Herbin, M., Janvier, P., Dutel, H., and Clément, G. (2015). Allometric growth in the extant coelacanth lung during ontogenetic development. *Nature Communications*, 6:8222.

Davis, M. C., Shubin, N. H., and Force, A. (2004). Pectoral fin and girdle development in the basal actinopterygians *Polyodon spathula* and *Acipenser transmontanus*. *Journal of Morphology*, 262(2):608–628.

Dutel, H., Galland, M., Tafforeau, P., Long, J. A., Fagan, M. J., Janvier, P., Herrel, A., Santin, M. D., Clément, G., and Herbin, M. (2019). Neurocranial development of the coelacanth and the evolution of the sarcopterygian head. *Nature*, 569(7757):556–559.

Johanson, Z., Joss, J. M., and Wood, D. (2004). The scapulocoracoid of the Queensland lungfish *Neoceratodus forsteri* (Dipnoi: Sarcopterygii): morphology, development and evolutionary implications for bony fishes (Osteichthyes). *Zoology*, 107(2):93–109.

Lavett Smith, C., Rand, C. S., Schaeffer, B., and Atz, J. W. (1975). *Latimeria*, the Living Coelacanth, Is Ovoviviparous. *Science*, 190:1105–1106.

Mabee, P. M. and Noordsy, M. (2004). Development of the paired fins in the paddlefish, *Polyodon spathula*. *Journal of Morphology*, 261(3):334–344.

Nulens, R., Scott, L., and Herbin, M. (2011). An updated inventory of all known specimens of the coelacanth, *Latimeria* spp. *Smithiana Publications in Aquatic Biodiversity*, 3:1–52.

Rieppel, O. (1992). Studies on skeleton formation in reptiles. I. The postembryonic development of the skeleton in *Cyrtodactylus pubisulcus* (Reptilia: Gekkonidae). *Journal of Zoology*, 227(1):87–100.

Riley, C., Cloutier, R., and Grogan, E. D. (2017). Similarity of morphological composition and developmental patterning in paired fins of the elephant shark. *Scientific Reports*, 7(1):1–10.

Sfakianakis, D. G., Doxa, C. K., Kouttouki, S., Koumoundouros, G., Maingot, E., Divanach, P., and Kentouri, M. (2005). Osteological development of the vertebral column and of the fins in *Diplodus puntazzo* (Cetti, 1777). *Aquaculture*, 250(1-2):36–46.

Shubin, N. H. and Alberch, P. (1986). A Morphogenetic Approach to the Origin and Basic Organization of the Tetrapod Limb. *Evolutionary Biology*, 20:319–387.

Thorsen, D. H. and Hale, M. E. (2005). Development of zebrafish (*Danio rerio*) pectoral fin musculature. *Journal of Morphology*, 266(2):241–255.

CHAPTER I a

Development and growth of the pectoral girdle and fin skeleton in the extant coelacanth *Latimeria chalumnae*

Manuscript published

Journal of Anatomy 236(3), pp 493-509. DOI: 10.1111/joa.13115

Development and growth of the pectoral girdle and fin skeleton in the extant coelacanth *Latimeria chalumnae*

Mansuit Rohan[1,2], Clément Gaël[1], Herrel Anthony[2], Hugo Dutel[3], Paul Tafforeau[4], Mathieu D. Santin[5] and Herbin Marc[2]

[1] UMR 7207 Centre de Recherche en Paléontologie, Paris, MNHN – Sorbonne Université – CNRS, Département Origines & Evolution, Muséum national d'Histoire naturelle, 57 rue Cuvier, 75005 Paris, France

[2] UMR 7179 MECADEV, MNHN – CNRS, Département Adaptations du Vivant, Muséum national d'Histoire naturelle, 57 rue Cuvier, 75005 Paris, France

[3] School of Earth Sciences, University of Bristol, 24 Tyndall avenue, BS8 1TQ, United-Kingdom.

[4] European Synchrotron Radiation Facility, BP 220, 6 Rue Jules Horowitz, 38043 Grenoble Cedex, France.

[5] Inserm U 1127, CNRS UMR 7225, Centre for NeuroImaging Research, ICM (Brain & Spine Institute), Sorbonne University, Paris, France

Address for correspondence

Rohan Mansuit
UMR 7179 MECADEV, MNHN – CNRS,
Département Adaptations du Vivant
55 rue Buffon
75005 Paris, France
e-mail : rohan.mansuit@mnhn.fr

Abstract

The monobasal pectoral fins of living coelacanths and lungfishes are homologous to the forelimbs of tetrapods and are thus critical to investigate the origin thereof. However, it remains unclear whether the similarity in the asymmetrical endoskeletal arrangement the pectoral fins of coelacanths reflects the evolution of the pectoral appendages in sarcopterygians. Here, we describe for the first time the development of the pectoral fin and shoulder girdle in the extant coelacanth *Latimeria chalumnae*, based on the tomographic acquisition of a growth series. The pectoral girdle and pectoral fin endoskeleton are formed early in the development with a radially outward growth of the endoskeletal elements. The visualization of the pectoral girdle during development shows a reorientation of the girdle between the fetus and pup 1 stages, creating a contact between the scapulocoracoids and the clavicles in the ventro-medial region. Moreover, we observed a splitting of the pre- and post-axial cartilaginous plates in respectively pre-axial radials and accessory elements on one hand, and in post-axial accessory elements on the other hand. The mechanisms involved in the splitting of the cartilaginous plates appear, however, different from those involved in the formation of radials in actinopterygians. Our results show a proportional reduction of the proximal pre-axial radial of the fin rendering the external morphology of the fin more lobe-shaped and a spatial reorganization of elements resulting from the fragmentation of the two cartilaginous plates. *Latimeria* development hence supports previous interpretations of the asymmetrical pectoral fin skeleton as being plesiomorphic for coelacanths and sarcopterygians.

Keywords

Actinistia, sarcopterygian, ontogeny, fin, endoskeleton, pectoral girdle, tomography

Introduction

Among the sarcopterygians, the clade Actinistia is today only represented by the coelacanth genus *Latimeria*, and is considered as the sister group to the Rhipidistia, represented by living lungfishes and tetrapods (Ahlberg, 1991; Forey, 1998; Friedman et al., 2007; Clack, 2012; Amemiya et al., 2013). This clade presents a long evolutionary history with its origin dating back to the Early Devonian (Johanson et al., 2006; Friedman, 2007; Zhu et al., 2012b). Coelacanths are well represented in the fossil record, with about 40 described genera and more than 130 species (Forey, 1998). The clade also presents an important diversity of form, size and ecology (Forey, 1998; Friedman and Coates, 2006; Casane and Laurenti, 2013; Cavin et al., 2017), and was considered to have gone extinct at the end of the Mesozoic Era (Smith, 1939). Today, there are two known species: *Latimeria chalumnae* (Smith, 1939) in Western Indian Ocean and *L. menadoensis* (Erdmann et al., 1998; Pouyaud et al., 1999) discovered offshore of Sulawesi, Indonesia.

Because of their close relationships with tetrapods, many aspects of the biology and development of the coelacanths are of interest to better understand the origin, the anatomical characteristics and the evolution of osteichthyans (Dutel et al., 2019) and early land vertebrates (Fricke and Hissmann, 1992). Pectoral fins of coelacanths are moreover of particular interest, partly due to the fact that the paired fin skeleton of the coelacanth is organized along a metapterygial axis (Millot and Anthony, 1958). This organisation is similar to that of the endochondral skeletal elements of lungfishes, and tetrapod limbs (Shubin and Alberch, 1986; Mabee, 2000). Consequently, the paired lobed-fin of sarcopterygian fishes is considered homologous to the tetrapod limb (i.e. Gregory and Raven, 1941; Westoll, 1943; Fricke and Hissmann, 1992; Clack, 2009). Moreover, the first elements of the pectoral fin of the coelacanth (the first mesomere, the first pre-axial radial, and the second mesomere) are considered to be homologous to the stylopodal and zeugopodal elements of the tetrapod limb (Fricke and Hissmann, 1992; Johanson et al., 2007; Miyake et al., 2016). The majority of studies concerning the water-to-land transition of vertebrates have focused on the pectoral appendages given their importance during locomotion in transitional and early terrestrial vertebrates (Shubin et al., 2006; Pierce et al., 2012; Standen et al., 2014). Coelacanths have also been considered as being relevant in the context of terrestrialization because they move their fins in an alternating manner, reminiscent of the movements of tetrapod limbs (Fricke et al., 1987; Forey, 1998; Clack, 2012). However, the fins of the extant coelacanth clearly do not have a function of “legs”, i.e. crawling on sea bottom, as had been supposed by (Smith, 1956). Whereas lungfishes are more closely related to

tetrapods than coelacanths, as early as the beginning of their evolutionary history, they present modified paired fins with a high degree of symmetry that do not reflect the pectoral fin of early sarcopterygians (Ahlberg, 1989; Coates et al., 2002; Coates, 2003; Friedman et al., 2007). One the other hand, early tetrapodomorphs and coelacanths show asymetrical fins (Ahlberg, 1989; Friedman et al., 2007), where the pre-axial and post-axial side of the fin do not have the same arrangement around the metapterygial axis. It remains unknown, however, whether the evolution of the pectoral fin of coelacanths is informative about the evolution of the pectoral appendages in sarcopterygians more generally.

The pectoral fin and girdle development of the living coelacanth remains unknown. Consequently, a detailed anatomical description of the morphology and anatomy of the pectoral fin and girdle at different ontogenetic stages of the extant coelacanth is crucial for an understanding of the development of the pectoral fin of *Latimeria* in comparison to fossil coelacanths and tetrapodomorphs. The development of the endoskeleton of the pectoral fin and girdle in *Latimeria* is likely to be informative for reconstructing the plesiomorphic configuration of the pectoral appendages in sarcopterygians (Coates et al., 2002; Amaral and Schneider, 2018). Here, we study the development of the pectoral fin and girdle in the extant coelacanth by describing this anatomical complex in a unique ontogenetic series of five stages constitued of three prenatal stages and two post-natal stages (Dutel et al., 2019).

Materials and methods

Specimens

The developmental series includes five stages from several museum collections (Fig. 1a.1). The first stage is a fetus of 5 cm total length (TL) (CCC 202.1) (Nulens et al., 2011) found inside the female specimen CCC 202 captured off the Tanzanian coast in 2005 and conserved in the collection of the South African Institute for Aquatic Biodiversity, Grahamstown, South Africa (SAIAB 76199). Stage 2 is a pup of 32.3 cm TL with a yolk sac (CCC 29.5), found inside the female specimen CCC 29 captured off the Comores Island in 1969 and conserved in the collection of the MNHN, Paris, France (MNHN AC 2012-22). Stage 3 is a late pup which yolk sac is resorbed of 34.8 cm TL (CCC 162.21) found inside the female CCC 162 captured off the coast of Mozambique in 1991, and conserved in the collection of the Zoologische Staatssammlung, Munich, Germany (ZSM 28409). Stage 4 is a juvenile of 42.5 cm TL (CCC 94) captured off Grande Comore in 1974 and conserved in the collection of the MNHN, Paris, France (MNHN

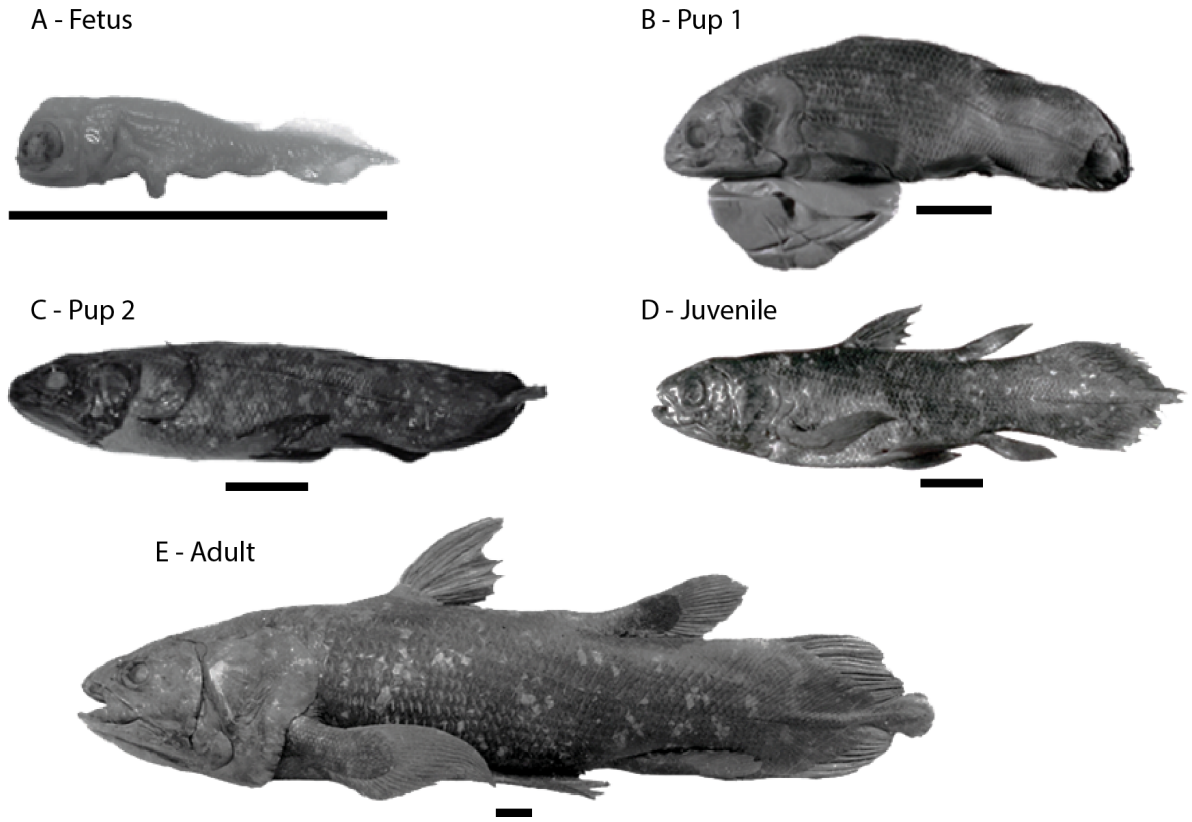

Figure 1a.1: *Latimeria chalumnae* – Ontogenetic series in left lateral view. (A) Fetus (CCC 202.1). (B) First pup (CCC 29.5). (C) Second pup (CCC 162.21). (D) Juvenile (CCC 94). (E) Adult (CCC 22). Scale bar: 5 cm.

AC 2012-27). The adult specimen (stage 5) principally used in this study is a male of 130 cm TL (CCC 22) captured in Grande Comore in 1960 and conserved in the collection of the MNHN, Paris, France (MNHN AC 2012-18). Direct anatomical observations were also made on isolated pectoral fin skeleton of several adult specimens: CCC 6 (MNHN AC 2012-4), CCC 7 (MNHN AC 2012-5), CCC 14 (MNHN AC 2012-11) and CCC 19 (MNHN AC 2012-15). Specimens from the MNHN, Paris are preserved in a 6-7% formaldehyde solution, while the others are preserved in a 70% aquaeous ethanol solution.

Imaging

Stage 1 – Fetus (CCC 202.1)

The specimen was scanned using long propagation phase-contrast synchrotron X-ray microtomography at the ID19 beamline of the European Synchrotron Radiation Facility (ESRF), Grenoble (France). It was imaged at a voxel size 6.5 µm using a pink beam achieved with a W150 wiggler at a gap of 50 mm and filtered with 2 mm of aluminium, 0.25 mm of copper and 0.2 mm of gold. The scintillator was a 250-µm-thick LuAG:Ce (lutetium–aluminium–garnet) crystal.

The resulting detected spectrum was centred on 73 keV with a bandwidth of 17 keV FWHM (full width at half maximum). The detector was a FreLoN 2K14 charge coupled device (CCD) camera mounted on a lens system. To obtain a sufficient propagation phase-contrast effect, a distance of 3m between the sample and the detector was used. The final reconstruction (13µm) was obtained after binning with the software ImageJ.

Stage 2 – Pup 1 (with yolk sac) (CCC 29.5)

The specimen was scanned using long propagation phase-contrast synchrotron X-ray microtomography at the ID19 beamline of the European Synchrotron Radiation Facility (ESRF), Grenoble (France). It was scanned at a voxel size of 23.34 µm and using a propagation distance of 13m to maximize the phase-contrast effect. The beam produced by the ID19 W150 wiggler at a gap of 59mm was filtred by 2.8mm of aluminium and 1.4mm of copper, resulting in an average detected energy of 77.4 keV. The scintillator was a 2000-µm-thick LuAG:Ce (lutetium–aluminium–garnet) crystal. The detector was a PCO edge 4.2 sCMOS. The final reconstruction (46.68µm) was obtained after binning with the software ImageJ.

Stage 3 – Pup 2 (with yolk sac resorbed) (CCC 162.21)

The specimen was scanned using long propagation phase-contrast synchrotron X-ray microtomography at the ID19 beamline of the European Synchrotron Radiation Facility (ESRF), Grenoble (France). It was scanned at a voxel size of 30.45 µm using the ID19 W150 wiggler at a gap of 50mm filtered by 2mm of aluminium, 0.25mm of copper and 0.25mm of tungsten. The scintillator, detector and distance between the sample and the detector were the same as for fetus. The final reconstruction (60.90µm) was obtained after binning in ImageJ.

Stage 4 – Juvenile (CCC 94)

The specimen was scanned twice, once at the ESRF (Grenoble, France) and once using an MRI scan at the ICM (Paris, France). At the ESRF, the specimen was scanned at a voxel size of 28.43µm and using a propagation distance of 13m to maximize the phase-contrast effect. The beam produced by the ID19 W150 wiggler at a gap of 30mm was filtered by 2mm of aluminium and 15mm of copper, resulting in an average detected energy of 170 keV with a bandwidth of 85 keV FWHM. The detector camera was a FreLoN 2K charge coupled device mounted on a lens system composed of a 750-mm-thick LuAG:Ce scintillator. The final reconstruction (56.86µm) was obtained after binning in ImageJ, and used for the 3D-rendering of the pectoral girdle. As the contrast was not excellent, possibly due to a historical treatment by injection of a colloidale

baryte solution (Anthony, 1980), the specimen was re-scanned in MRI at the Centre for NeuroImaging Research, ICM (Brain & Spine Institute). MRI was performed at 3T with a Siemens Tim TRIO (Siemens, Germany) system. Images were acquired with a 3D Flash sequence with an isotropic resolution of 300 µm. Parameters were: Matrix size = 640*300*256; TR/TE (ms) = 18/4.73; Flip Angle = 10°; Spectral Width = 100 kHz; Number of averages = 20; Total acquisition time was 7 hours and 41 minutes. The RMI data were used for the 3D-rendering of the pectoral fin endoskeleton.

Synchrotron data were reconstructed using a filtered back-projection algorithm coupled with a single distance phase-retrieval process (Paganin et al., 2002; Sanchez et al., 2012). For each sample, all the sub-scans were reconstructed separately, converted into 16-bit TIFF stacks and then concatenated to generate a single complete scan of each specimen. The ring artefacts were corrected on the reconstructed slices using a specific tool developed at the European Synchrotron Radiation Facility (Lyckegaard et al., 2011).

Stage 5 – Adult (CCC 22)

The specimen CCC 22 was scanned with a high-resolution computerized axial tomography scanning (CAT scan) in a Parisian Hospital (France) using the following scanning parameters: effective energy 120 kV, current 158 mA, voxel size 742 µm and 1,807 views.

The slices were reconstructed and exported into 16-bit TIFF stacks using the phoenix datos|x 2.0 reconstruction software, and exported into 16-bit TIFF stacks.

Segmentation and 3D-reconstruction method

For all the specimens, segmentation and three-dimensional rendering were done using the software MIMICS Innovation Suite 20.0 (Materialise).

Results

The pectoral girdle

In the adult, the pectoral girdle is composed of four flattened and elongated dermal bones – the clavicle, the cleithrum, the anocleithrum and the extracleithrum – and one endochondral bone, the scapulocoracoid as described by Millot and Anthony (1958) (Fig. 1a.2). The girdle forms an arc posterior to the branchial arches. Since the general morphlogy of the pectoral girdle does not change between the different stages, our illustrations depict pup 2 only (Fig. 1a.2).

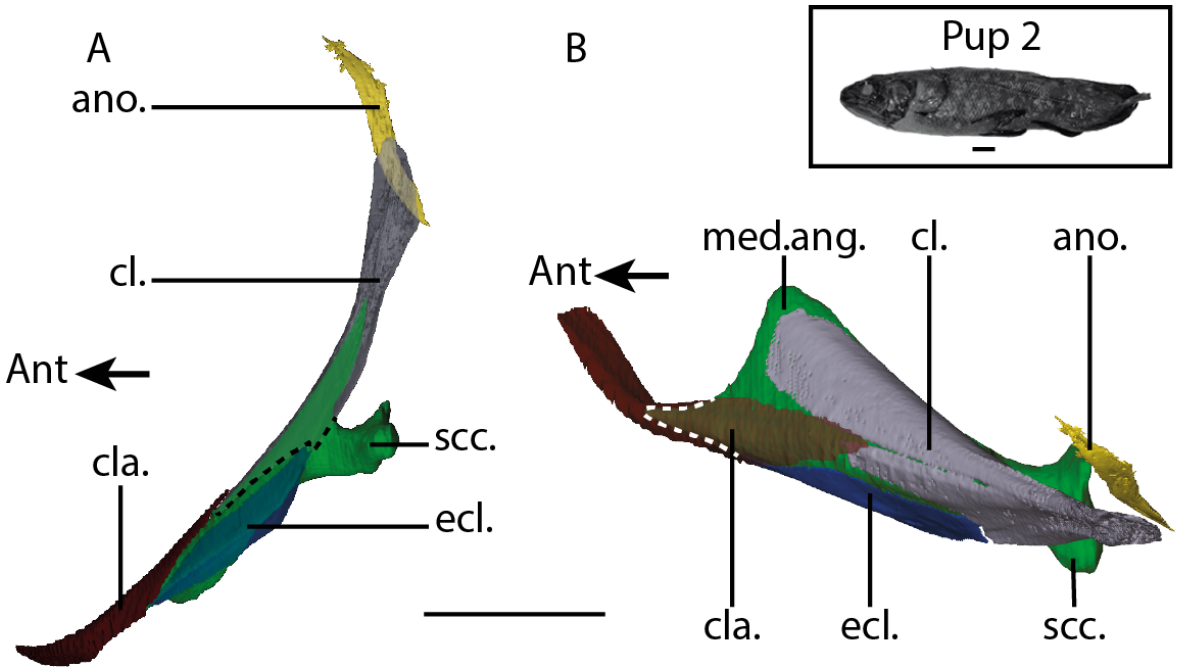

Figure 1a.2: *Latimeria chalumnae* – Second pup. Left pectoral girdle in lateral (A) and dorsal (B) view. The cleithrum and extracleithrum are transparent in (A), revealing the general shape of the scapulocoracoid. The clavicle is transparent in (B), revealing the lateral angle of the scapulocoracoid. The dotted line shows the edge of the cleithrum in (A) and the edge of the scapulocoracoid in (B). ano., anocleithrum; cl., cleithrum; cla., clavicle; ecl., extracleithrum; lat.ang., lateral angle of the scapulocoracoid; med.ang., medial angle of the scapulocoracoid; scc., scapulocoracoid. Scale bar: 20 mm.

The pectoral girdle is already well developed in the fetus, and does not change dramatically in the four successive stages (Fig. 1a.3). Indeed, the bones continue to grow, but conserve their general shape. However, there is a shift in orientation of the complete pectoral complex (Fig. 1a.4) between the fetus and pup 1. In the fetus, the medial margins of the girdles are oriented toward the ventral side of the embryo, there is no contact between the anterior part of the girdles, and the extracleithrum has a dorsal position on the scapulocoracoid. In pup 1, the medial margins of the girdles rotate in a dorsal direction, leading to the contact between their two anterior extremities, also observed in the following stages, and the extracleithrum has a more lateral position on the scapulocoracoid (Fig. 1a.4). In the juvenile the cleithrum, extracleithrum and clavicle of the pectoral girdle move progressively in closer contact to one another. In the adult stage, these three bones are in close contact with one another with the edges of the bones overlapping. On the µCT scan the three bones appear fused, yet this may be due to the limited resolution of the scan. Indeed, the observation of isolated pectoral girdles shows that the three bones are not fused and that each bone is independent.

- The anocleithrum (ano.)

It is the most dorsal bone of the pectoral girdle, closely located, but without contact, to the

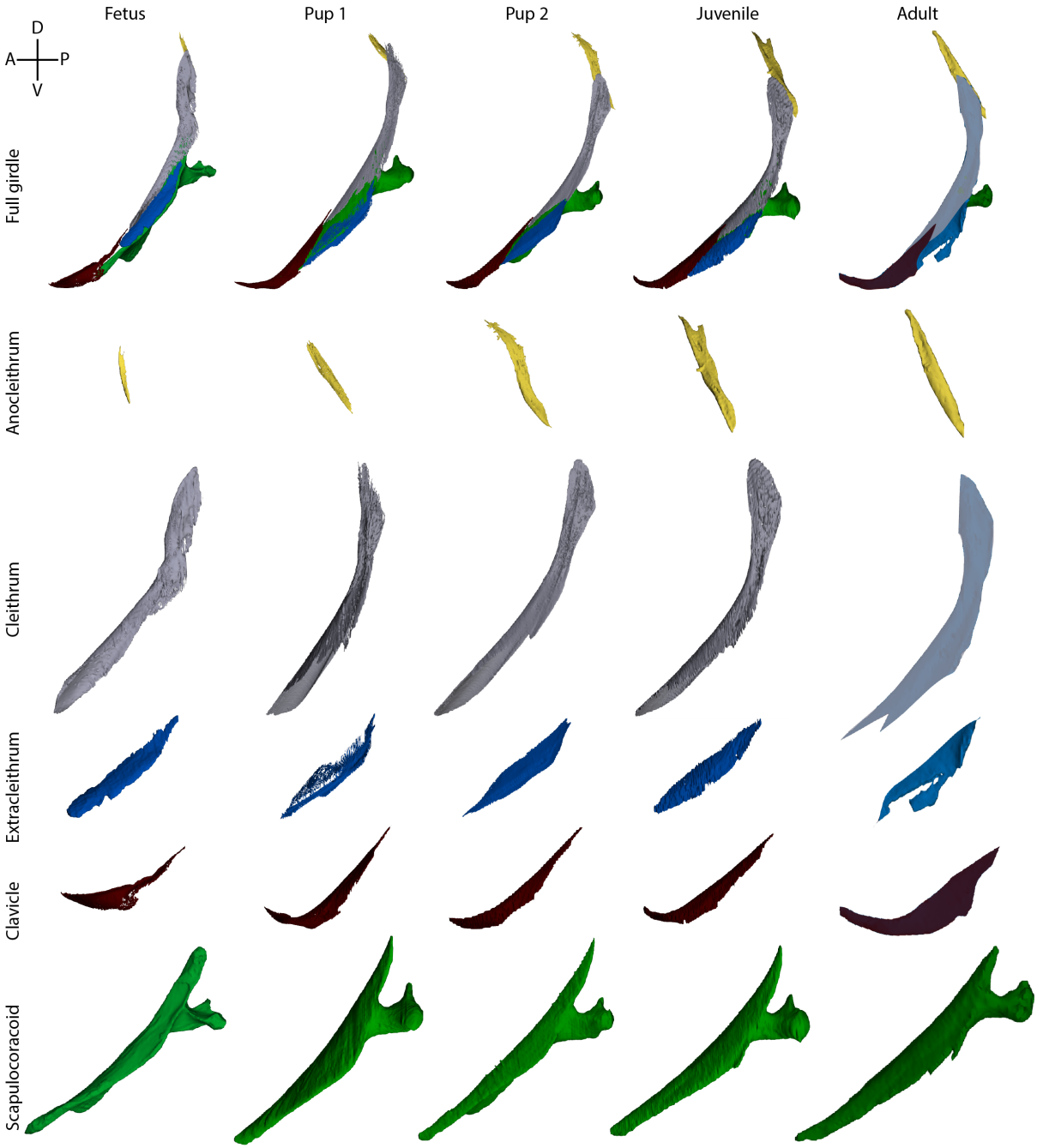

Figure 1a.3: *Latimeria chalumnae*. Elements of the left pectoral girdle in lateral view at five different developmental stages (1–5). The different stages are not to scale, but the different bones within a given stage are to scale.

medial side of the dorsal end of the cleithrum. It is a small flat and straight bone, oriented dorso-ventrally. The anocleithrum is attached to the cleithrum by a ligament, as described previously by Millot and Anthony (1958). The general morphology of this dermal bone changes dramatically during development.

In the fetus, the anocleithrum is straight and proportionally smaller compared to other stages

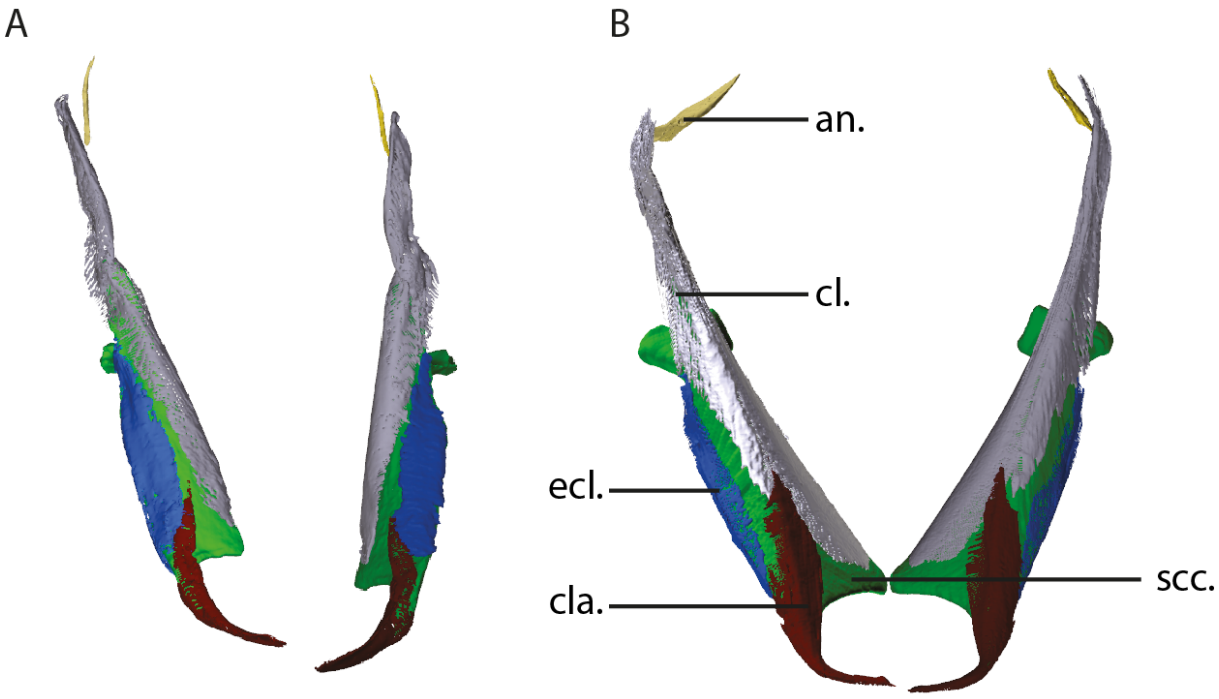

Figure 1a.4: *Latimeria chalumnae* – The fetus and the first pup. Anterior views of the pectoral girdles of the fetus (A) and first pup (B), illustrating the reorientation of the pectoral girdles during the development of the coelacanth. cl., cleithrum; cla., clavicle; ecl., extracleithrum; scc., scapulocoracoid. Not to scale.

(Fig. 1a.3). In lateral view, it extends beyond the antero-dorsal margin of the dorsal end of the cleithrum. In pup 1, the anocleithrum is proportionally longer, and gently curved to follow the lateral body surface. It also extends beyond the antero-dorsal margin of the dorsal end of the cleithrum. From pup 2 onwards, it extends beyond both the antero-dorsal and postero-ventral margins of the dorsal end of the cleithrum (Fig. 1a.5).

The anocleithrum shows some individual variability and asymmetry. Pup 1 has a right anocleithrum with a convex shape in anterior direction, whereas the left one is straight (Fig. 1a.5A). In pup 2, the left anocleithrum is S-shaped whereas the right one is straighter (Fig. 1a.5B). The right anocleithrum of the adult is bifid with a backward pointing process whereas the left one is straight (Fig. 1a.5D). This condition was previously noticed by Millot and Anthony (1958) in another adult specimen (MNHN AC-2012-1 = CCC 3).

- The cleithrum (cl.)

In the adult, the cleithrum is an elongated bone fused with the extracleithrum and the clavicle, and overlapping the dorsal surface of the scapulocoracoid (Fig. 1a.2). The medial margin of the cleithrum forms a gutter to accommodate the medial margin of the scapulocoracoid. The cleithrum contacts the extracleithrum at its lateral edge, and in its posterior part forms a

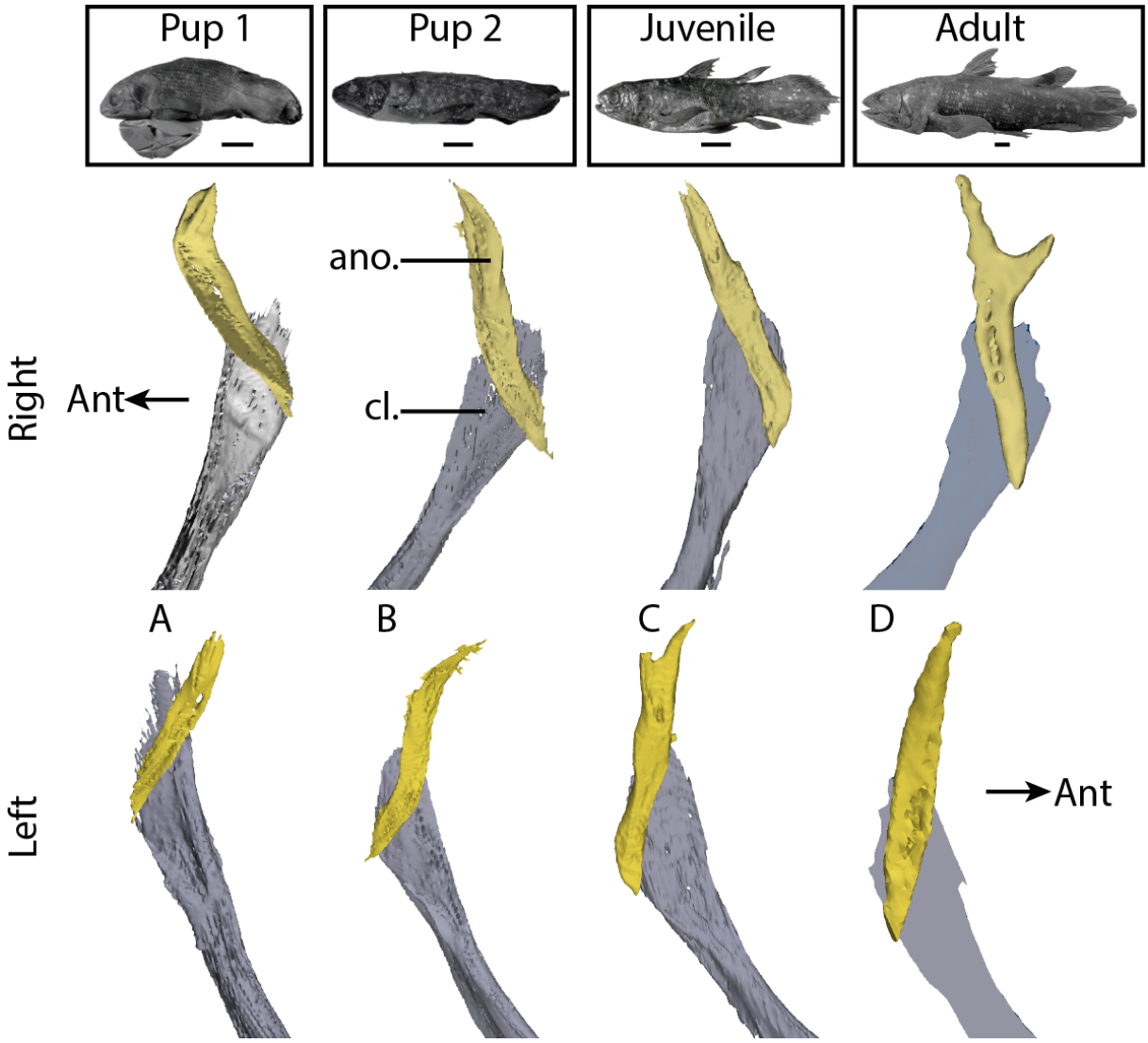

Figure 1a.5: *Latimeria chalumnae* – Stages 2–5. Right anocleithrum (top) and left anocleithrum (bottom) in medial view. Note the intraspecific asymmetry and the individual asymmetry of the anocleithrum. ano., anocleithrum; cl., cleithrum. Scale bar: 5 cm. 3D models are not to scale.

gutter surrounding the lateral margin of the scapulocoracoid until the level of the articular process of the scapulocoracoid. The dorsal part of the cleithrum surrounds the dorsal tip of the scapulocoracoid. The uppermost part of the cleithrum is flattened latero-medially and flared dorso-ventrally, with a more or less pronounced longitudinal ridge on the lateral side of the bone. In the fetus, the dorsal lamina of the cleithrum is dorso-medially oriented. Its dorsal tip is pointed and its anterior margin slightly convex (Fig. 1a.3). In later stages, the dorsal tip is spatula-shaped and the anterior margin tends to be progressively more concave (Fig. 1a.3).

- The extracleithrum (ecl.)

The extracleithrum has an elongated diamond shape and its lateral margin extends lower than the lateral margin of the scapulocoracoid (Fig. 1a.2). Its postero-medial edge contacts the

cleithrum and its antero-medial margin is overlapped by the clavicle. The scapulocoracoid fits in the gutter-shaped internal side of the lateral margin of the extracleithrum (Fig. 1a.2). In the fetus, the lateral margin of the extracleithrum simply follows the lateral margin of the scapulocoracoid. The gutter-type contact present in later stages is not formed yet.

The extracleithrum is separated from the clavicle by a gap that decreases during the development and disappears from the juvenile onwards. In pup 1, the lateral margin of the extracleithrum extends beyond the lateral margin of the scapulocoracoid and a long gutter appears on its internal side from pup 2 onwards.

- The clavicle (cla.)

In the adult, the enlarged posterior part of the clavicle is positioned at the antero-lateral part of the scapulocoracoid (Fig. 1a.2). In cross-section, it appears that the posterior tip of the clavicle overlaps the margins of the cleithrum and extracleithrum (Fig. 1a.6). The medial and lateral margins of the clavicle form two gutters where the lateral angle of the scapulocoracoid fits into, then extends antero-ventrally as a twisted shank (Fig. 1a.2). This shank is horizontal, medially concave and reaches the median plane of the ventral side of the body. According to Millot and Anthony (1958), both twisted shanks articulate with a narrow basal lamina, located at the mid-line, but this basal lamina cannot be observed in the imaging data.

In the fetus, the medial and lateral margins of the clavicle do not form a gutter and the clavicle does not totally surround the lateral angle of the scapulocoracoid (Fig. 1a.6A). The posterior part of the clavicle is only in contact with the extracleithrum. There is no contact between the anterior twisted shanks of the right and the left clavicles. From pup 1 onwards, the clavicles are ventrally in contact and form with the scapulocoracoid a hemi-circle and the posterior part of the clavicle partially overlaps the cleithrum (Fig. 1a.6B-C). In this stage, the lateral margin of the clavicle extends ventrally and begins to form a gutter. In pup 2 and the following stages, the lateral and medial margins of the clavicle form two small gutters that surround the lateral angle of the scapulocoracoid. From pup 2 onwards, the posterior tip of the clavicle overlaps both the margins of the cleithrum and extracleithrum.

- The scapulocoracoid (scc.)

This massive element is overlapped by the cleithrum, extracleithrum and clavicle (Fig. 1a.2, Fig. 1a.3). It is the only endochondral bone of the pectoral girdle. It is composed of two parts:

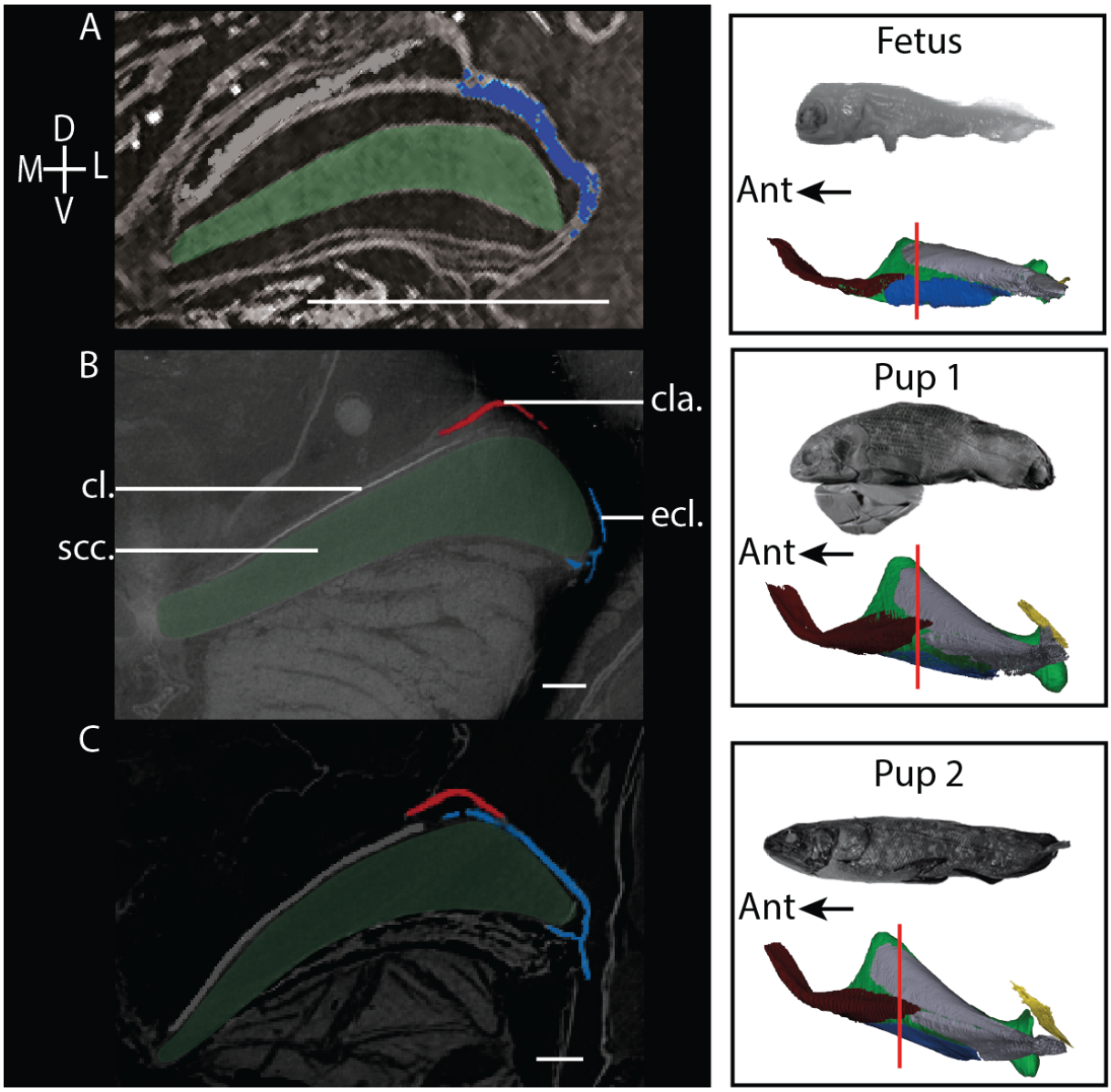

Figure 1a.6: *Latimeria chalumnae* – The fetus (A), the first (B) and second (C) pup. Left pectoral girdle in transverse section. The location of the transverse sections are shown by a red line on the dorsal view of the 3D models of the pectoral girdles. In the fetus, the anterior part of the clavicle is not well developed and partially overlaps the posterior part of the cleithrum (not visible in the transverse section). In the first pup, the anterior part of the clavicle partially overlaps the cleithrum, but not the extracleithrum, whereas from the second pup onwards the anterior part of the clavicle partially covers both the cleithrum and the extracleithrum. cl., cleithrum; cla., clavicle; ecl., extracleithrum; scc., scapulocoracoid. D, dorsal; L, lateral; V, ventral; M, medial. Specimens and 3D models are not to scale. Scale bar: 1 mm.

a long triangular-shaped blade, with a dorsal tip and a ventral base, positioned on the internal side of the cleithrum, and a short and massive articular process for the pectoral fin, posteriorly oriented. The anterior margin of the triangular-shaped blade is concave. The lateral and dorsal angles of the scapulocoracoid are very sharp and respectively surrounded by the the clavicle and the cleithrum (Fig. 1a.2A). The massive articular process of the scapulocoracoid is posteriorly oriented along the body axis, and round in transverse section. The end of this process is

a flat quadrangular surface with a small articular head at the supero-lateral angle. This articular head corresponds to the glenoid process and forms a ball-and-socket joint (Miyake et al., 2016), and articulates with the first endoskeletal element of the fin.

In the fetus, the dorsal angle of the scapulocoracoid is rounded and slightly curved towards its outer side (Fig. 1a.3). The dermal elements of the girdle do not lie directly on the triangular part of the scapulocoracoid, but are separated by a large space (Fig. 1a.6A). The articular process presents four concave faces in transverse section. From pup 1 onwards the dorsal angle is straight and sharp. The dermal bones closely overlap the scapulocoracoid (Fig. 1a.6). The articular process is more robust and large, rounded in transverse section (Fig. 1a.3).

The pectoral fin (Fig. 1a.7)

The pectoral fin of *Latimeria* is composed of different elements: mesomeres on the metapterygial axis, pre-axial elements (corresponding to the pre-axial radials and pre-axial accessory elements), and post-axial elements (corresponding to the post-axial accessory elements and the distal radial) (Fig. 1a.7). According to Millot and Anthony (1958), the metapterygial axis of the fin consists of five axial elements, named “articles” and numbered from proximal to distal. However, Ahlberg (1989) identified four mesomeres and one distal radial element. There are four pre-axial radial elements (Millot and Anthony, 1958; Forey, 1998), a variable number of pre-axial and post-axial accessory elements (Millot and Anthony, 1958) (Fig. 1a.7). The fin rays insert on the pre- and post-axial accessory elements, on the fourth pre-axial radial and on the distal radial (Fig. 1a.7). According to Millot and Anthony (1958), the fifth axial element is different in shape from the first to fourth ones, and the fin rays articulate at its distal edge, whereas the previous axial elements do not articulate with the fin rays. In this regard, and following Forey (1998), we here refer to four mesomeres on the metapterygial axis and one distal radial that belongs to the post-axial elements. The term of “mesomeres” is used after (Jarvik, 1980) as the subcylindrical radial segments of the principal axis in sarcopterygian fins.

According to Johanson et al. (2007), the three first axial elements are homologous to the humerus, ulna and ulnare of tetrapodomorphs and tetrapods. Similarly, the two first pre-axial radial elements are considered homologous to the radius and intermedium of tetrapods (Johanson et al., 2007). The reference position of the pectoral fin is with the fin positioned along the body, its leading edge oriented dorsally. This position corresponds to the position of the pectoral fin of embryos within the oviduct (Forey, 1998).

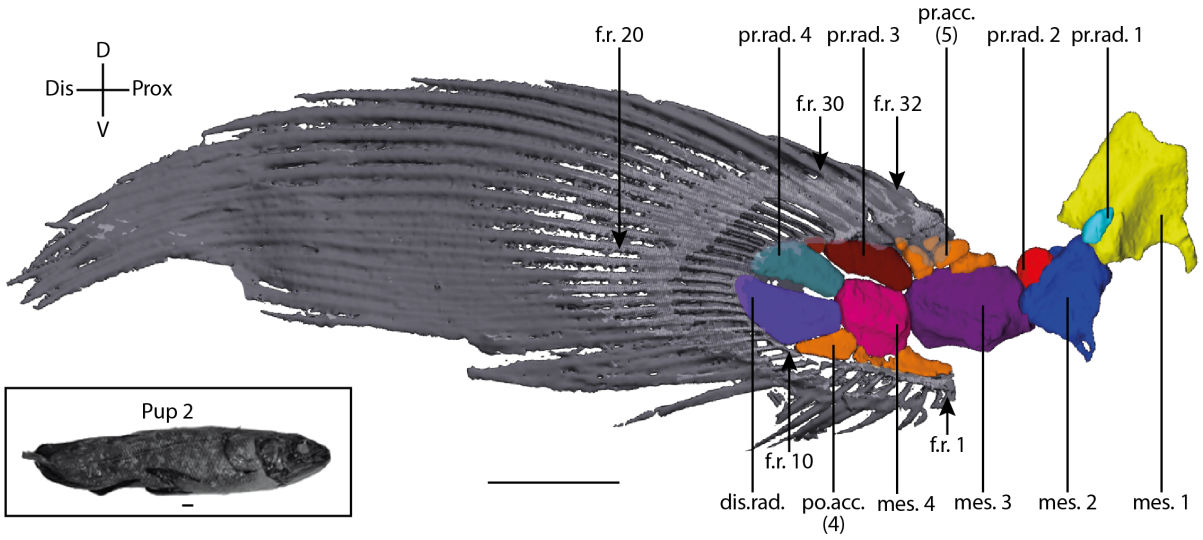

Figure 1a.7: *Latimeria chalumnae* – Second pup. Right pectoral fin in lateral view. f.r., fin ray; dis.rad., distal radial; mes., mesomere; po. acc., post-axial accessory elements; pr. acc., pre-axial accessory elements; pr. rad., pre- axial radial. Scale bar: 10 mm.

1) The metapterygial axis

The first and second mesomeres (Forey, 1998) have a similar quadrangular prismatic shape with slightly concave faces, as described by Millot and Anthony (1958). The dorsal and ventral edges ("*bord supérieur*" and "*bord inférieur*" cfr. Millot and Anthony, 1958) of the first mesomere form both a ridge directed from the proximal to the distal side. The dorsal ridge is well developed and extends further than the distal end of the bone. The distal part of the ridge is directed to the medial plane ("*interne*" for Millot and Anthony), when the fin is in resting position. The ventral ridge is also well developed and has a hook ("*crochet*" for Millot and Anthony) directed towards the medial plane (Fig. 1a.7, Supplementary Fig. 1a.1). The lateral and medial edge ("*externe*" and "*interne*" edge for Millot and Anthony, 1958) of the mesomeres are angular but smooth and they do not form a ridge (Supplementary Fig. 1a.1).

Each mesomere is longer than wide and presents a proximal joint ("*extrémité antérieure*" for Millot and Anthony, 1958) that is concave and a distal joint convex ("*extrémité postérieure*" for Millot and Anthony, 1958).

- The first mesomere (mes. 1)

This mesomere has the same orientation in our virtual dissection as described by Millot and Anthony (1958) and we can define the four facets: the dorso-medial, the dorso-lateral, the ventro-lateral and ventro-medial ("*supéro-interne*", "*supéro-externe*", "*inféro-externe*" and "*inféro-interne*" for Millot and Anthony, 1958) (Supplementary Fig. 1a.1). It is the largest mesomere of the fin.

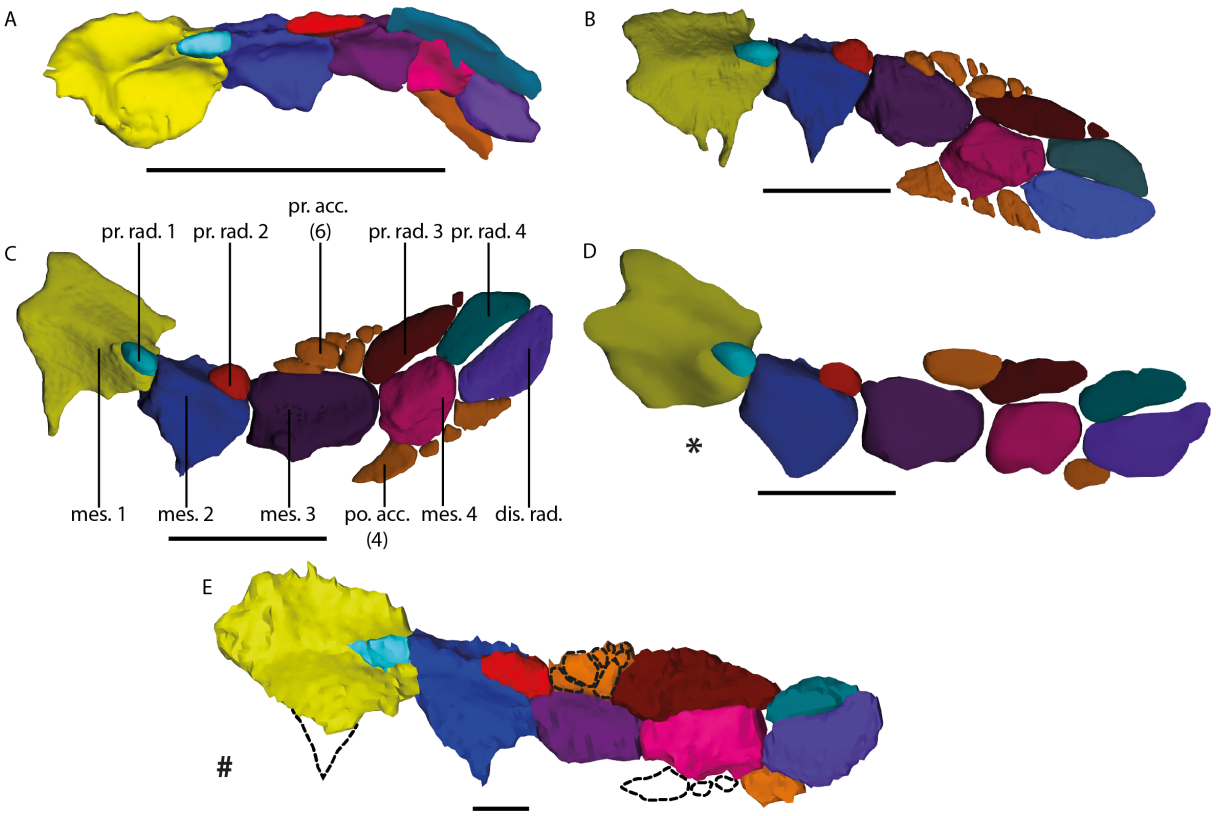

Figure 1a.8: *Latimeria chalumnae*. Pectoral fin of five different developmental stages in left lateral view (B–D) and right lateral view (mirrored, A,E). (A) The fetus. (B) The first pup. (C) The second pup. (D) The juvenile. (E) The adult. * The juvenile was scanned with MRI at low resolution, preventing the segmentation of the smallest elements. # The adult was scanned using a regular CT-scan and the resolution of the data did not allow the segmentation of some elements. Corresponding elements of the fin have been indicated in the same colour. The dotted line represents the pre-axial accessory elements, post-axial accessory elements and the hook on the mes. 1 of the stage 5 not segmented but known to exist based on pre- pared pectoral fins. dis.rad., distal radial; mes., mesomere; po. acc., post-axial accessory elements; pr. acc., pre-axial accessory elements; pr. rad., pre-axial radial. Scale bar: 2 mm (A), 10 mm (B–E).

In the fetus, the transverse section of this mesomere shows four highly concave facets (Fig. 1a.9 A). The joint with the scapulocoracoid (called glenoid surface by Millot and Anthony, 1958) is also concave, and located on the lateral side of the mesomere, extending proximally (Fig. 1a.8, Fig. 1a.9 C, D). The dorsal and ventral ridges of the first mesomere are slightly oblique to the medial plane at the distal end of the mesomere. These ridges begin at the level of the joint with the scapulocoracoid and end at the distal part of the first mesomere. From pup 1 onwards, the first mesomere is fully formed and presents a quadrangular prismatic shape. Its cross section shows that its facets are less concave than in fetus (Fig. 1a.9 B). The articular surface with the head of the scapulocoracoid is highly concave. As in the following stages, it is mainly located on the lateral side of the mesomere with only a lateral swollen margin (Supple-

mentary Fig. 1a.1). From pup 1 to the adult, the morphology of the first mesomere does not change (except in size). In these stages, we can observe an asymmetry between the right and left side. The left mesomere has a double hook that forms the beginning of a loop (Fig. 1a.9 E), whereas the right mesomere has only a single hook (Fig. 1a.9 F).

• The second mesomere (mes. 2)

This mesomere is smaller than the first one. As described by Millot and Anthony (1958), its proximal joint is less concave than that of the first mesomere. Despite a similar morphology as the first mesomere, its orientation is different and the bone shows a rotation around the fin axis (Supplementary Fig. 1a.1). The dorsolateral face of the mesomere 1 corresponds to the dorsal face of the mesomere 2, the ventrolateral face corresponds to the lateral face, the ventromedial face to the ventral face and the dorsomedial face to the medial face (Supplementary Fig. 1a.1). The proximal joint of this mesomere is not in lateral position as in the first mesomere, but it covers the proximal surface (Supplementary Fig. 1a.1). This joint surface is less deep compared to the first mesomere and a peripheral swollen edge surrounds it, whereas the first mesomere has only a lateral swollen edge around the proximal joint (Supplementary Fig. 1a.1). In fetus, its morphology is similar to that of the first mesomere: longer than wide, thin, and with highly concaves faces (Fig. 1a.9 C, D). In this stage, it is not clear that there is a rotation of the elements along the metapterygial axis. From pup 1 onwards, it is fully formed with a quadrangular prismatic shape and concave faces. As for the first mesomere, the second mesomere shows some asymmetry. In pup 2, the ventrolateral ridge of the right fin wears a double hook that forms a loop (Fig. 1a.9 G), whereas on the left fin, the second mesomere only has a single hook (Fig. 1a.8, Fig. 1a.9 H).

• The third mesomere (mes. 3)

As for the second mesomere, this element shows a rotation around the axis of the fin. Here, the dorsal face of the second mesomere corresponds to the dorsomedial face, the lateral face corresponds to the dorsolateral face, the ventral face to the ventrolateral face and the medial face to the ventromedial face. Therefore, the dorsal edge of the first mesomere corresponds to the medial edge of this mesomere and the dorsolateral face of the first mesomere corresponds to the dorsomedial face. This mesomere is more transversely flattened than the previous one. The dorsal and ventral ridges of the first mesomere corresponds to the medial and lateral ridges. As for the previous mesomere, the ridges are on the medial and lateral edge of the third mesomere (corresponding to the dorsal and ventral edge of the first mesomere) separating the dorsome-

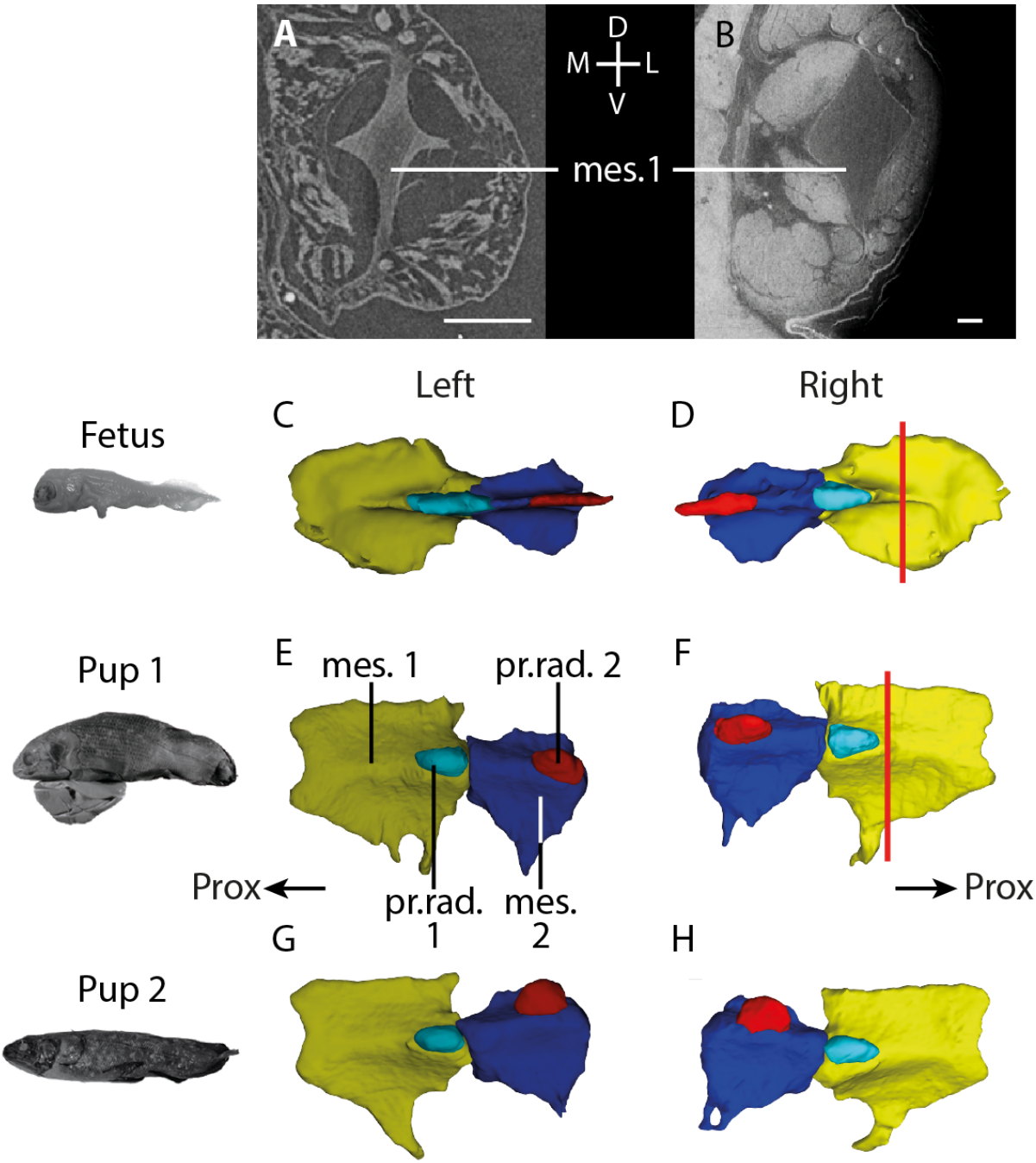

Figure 1a.9: *Latimeria chalumnae* – Stages 1–3. Transverse sections of the first mesomere in the fetus (A) and the first pup (B), and lateral views of the left (C,E,G) and right (D,F,H) proximal elements of the pectoral fin of the fetus (C,D), the first pup (E,F) and the second pup (G,H). The location of the transverse sections are shown in the 3D models of the corresponding mesomeres (red line). In the fetus, the mesomeres have strongly concave faces (A,C,D) compared with the following stages (B,E–H). Pre-axial radial elements 1 and 2 are proportionally longer than in the next stages, and extend more distally than the end of the corresponding mesomere (C,D). In the first (E,F) and second pup (G,H), the pre-axial radial elements are proportionally shorter and have an ovoid shape. The left first mesomere of the first pup (E) shows a double hook on the ventral ridge, whereas the right first mesomere of first pup (F) and the first mesomeres of the second pup show only a single hook (G,H). The right second mesomere of the second pup (H) has a loop-like hook on the ventro-lateral edge, whereas the left second mesomere (G) and the second mesomere of the first pup (E,F) show a single hook. mes., mesomere; pr. rad., pre-axial radial; D, dorsal; L, lateral; M, medial; V, ventral. Scale bar: 1 mm. 3D models are not to scale.

dial and ventromedial faces (and dorsolateral and ventrolateral faces) of the mesomere. These two ridges, directed from the proximal to distal, present the same shape. The proximal first third is oblique and slopes down to the ventral side. The distal two-thirds slope slightly up until the distal extremity of the mesomere (Fig. 1a.10 C-F). The lateral ridge does not present a hook, unlike the ventral ridge of the first mesomere and the ventro-lateral ridge of the second mesomere. The concave proximal joint is less deep than that of the previous mesomere. The distal end of this mesomere is highly convex and articulates with the fourth mesomere and the third pre-axial radial. In the fetus, its morphology is similar to previous mesomeres. From pup 1 onwards, it is fully formed, and its morphology does not change until adult stage (Fig. 1a.8, Fig. 1a.10).

- The fourth mesomere (mes. 4)

It is the smallest mesomere of the fin. It has the same orientation as the third mesomere and it has the same transverse flattening. Its ventral edge forms a large ridge whereas its dorsal edge is flat (Fig. 1a.7, Fig. 1a.10). The lateral and medial edge of the fourth mesomere form a large bulge and there is a small oblique ridge on the proximal part of the medial edge. This mesomere is surrounded by the third pre-axial radial element at its dorsal edge and by the post-axial accessory elements at its ventral edge (Fig. 1a.7, Fig. 1a.10). In the fetus, as for the previous elements, the fourth mesomere is thin, with its faces highly concave in transverse cross section. The ventral edge shows a small ridge, smaller than in the next stages (Fig. 1a.10 A-B). The dorsal edge of the fourth mesomere forms a massive ridge. The lateral and medial edge of the mesomere form each a thin ridge directed from proximal to distal. The medial thin ridge follows the proximo-distal midline along the medial face of mesomere and the lateral ridge is located more ventrally on the fourth mesomere. From pup 1 onwards, it is fully formed and its morphology does not change until the adult stage (Fig. 1a.8, Fig. 1a.10 C-F). The dorsal edge no longer has its triangular shape and becomes flat. The lateral and medial ridges of the fetus now form a bulge directed from proximal to distal and it is more difficult to distinguish the dorsolateral and ventrolateral faces on the lateral side of the mesomere (and the dorsomedial and ventromedial faces from the medial side of the mesomere) (Fig. 1a.10 C-F).

2) The pre-axial elements

The pre-axial radial elements are located on the dorsal side of the fin (corresponding to the pre-axial side of the fin/limb of most sarcopterygians; Forey, 1998), near to the joint between the mesomeres of the fin. The first and second pre-axial radials have a different morphology

from the third and fourth pre-axial radials (Millot and Anthony, 1958). The two first pre-axial radials have an egg-like shape whereas the others are thin and elongated.

• The first pre-axial radial (pr. rad. 1)

It is positioned at the distal part of the lateral edge of the first mesomere (pre-axial edge), near the joint with the second mesomere. It is slightly shifted towards the dorsolateral face of the first mesomere (Fig. 1a.7, Fig. 1a.8, Fig. 1a.9). It is egg-shaped and slightly thinner on the proximal side. In the fetus, this radial extends to the proximal part of the second mesomere and the distal part of the first mesomere (Fig. 1a.9 C-D), but from pup 1 onwards, it only covers the first mesomere (Fig. 1a.9 E-H). The right and left first pre-axial radials present a different shape. Whereas the right element already shows its ovoid shape, the left element is thinner in transverse section and elongated and extends to the second mesomere more broadly.

• The second pre-axial radial (pr. rad. 2)

It covers the distal part of the dorsolateral edge of the second mesomere, near the joint with the third mesomere. As for the first pre-axial radial, it is slightly shifted towards the dorsal face of the second mesomere and it is egg-shaped (Fig. 1a.7, Fig. 1a.8, Fig. 1a.9). According to Millot and Anthony (1958), this element is thinner and more elongated than the first pre-axial radial. However, our segmentation and the different isolated pectoral fins of adult specimens (CCC 6; CCC 7; CCC 14; CCC 19) show a similar size and shape of the two elements. In the fetus, this second pre-axial radial is elongated and thin in transverse section and covers the proximal part of the third mesomere (Fig. 1a.8, Fig. 1a.9 C-D). From pup 1 onwards, the second pre-axial radial is less elongated and egg-shaped, and covers only the distal part of the second mesomere (Fig. 1a.8, Fig. 1a.9 E-H).

• The third pre-axial radial (pr. rad. 3)

This radial differs from the previous radials in shape. It is thin and elongated, oval-shaped, and taller than the fourth mesomere that it covers (Fig. 1a.7). At its distal end, there is a small pointed element, which is the tip of the third pre-axial radial. This element carries fin rays 25 to 28 (Fig. 1a.7). The proximal part of this element is straight and it articulates with the third mesomere. In the fetus, it could only be segmented for the right fin. This element is closely associated with the fourth pre-axial radial and the pre-axial accessory elements and is part of a large cartilaginous plate (Fig. 1a.10 A-B). In pup 1, the cartilaginous plate is segmented and the third pre-axial radial is differentiated from the fourth pre-axial radial and the pre-axial

accessory elements (Fig. 1a.10). From pup 1 onwards, the third pre-axial radial presents its elongated oval shape and has a small separated tip.

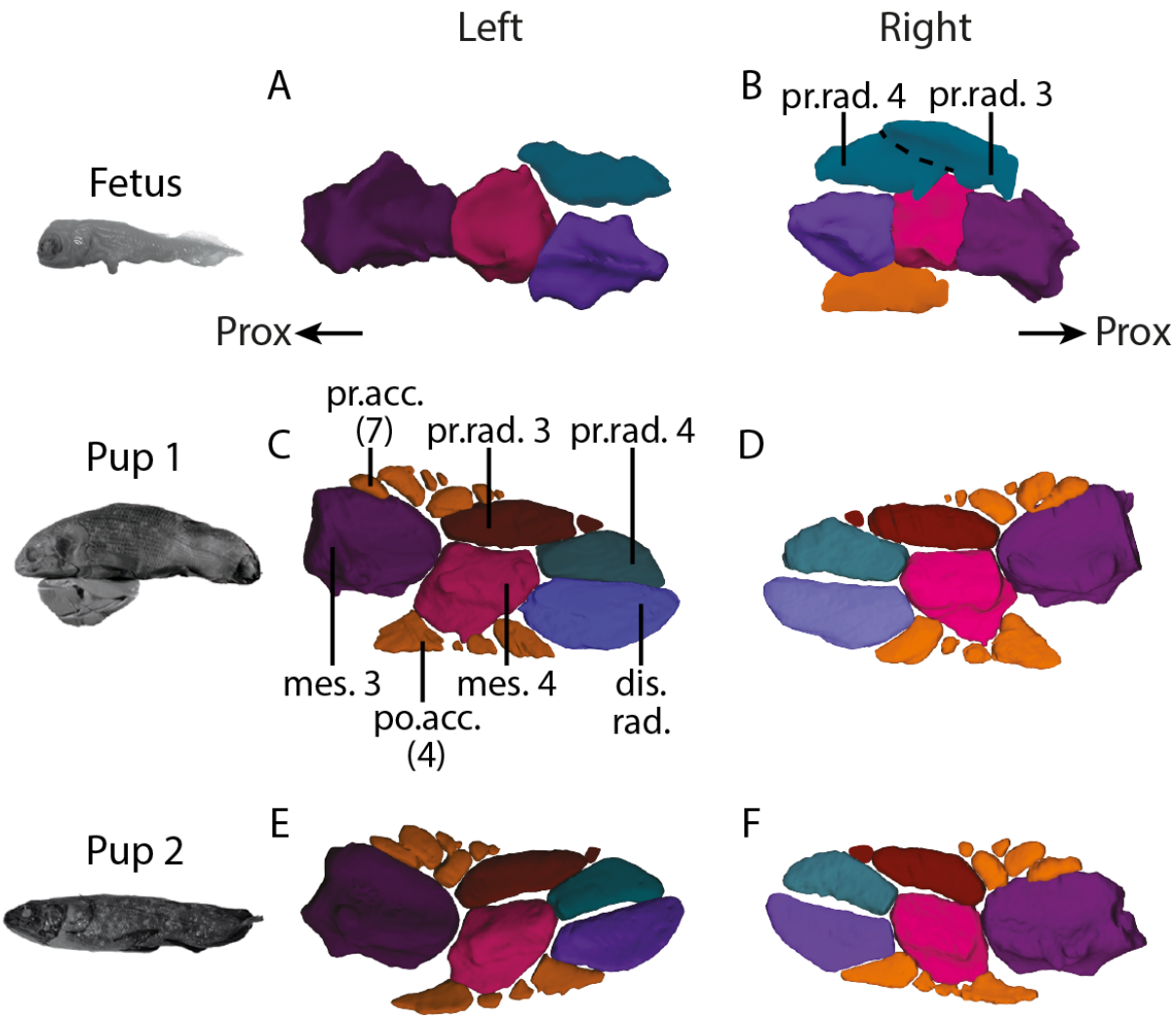

Figure 1a.10: *Latimeria chalumnae* – Stages 1–3. Distal part of the left (A,C,E) and right (B,D,F) pectoral fins of the fetus (A,B), the pup 1 (C, D) and the pup 2 (E,F) in lateral views. In the fetus, the right pectoral fin shows a large cartilaginous plate (blue) that corresponds to pre-axial radials 3 and 4 and the pre-axial accessory elements in the following stages. The first and second pups show variation and asymmetry in the number of pre-axial accessory elements. dis.rad, distal radial; mes., mesomere; po. acc., post-axial accessory elements; pr. acc., pre-axial accessory elements; pr. rad., pre-axial radial. Not to scale.

- The fourth pre-axial radial (pr. rad. 4)

This element is positioned at the distal end of the fin endoskeleton in association with the distal radial. As for the third pre-axial radial, this element is elongated and thin, but it has a trapezoidal shape with three straight edges and one curved edge (Fig. 1a.7, Fig. 1a.10). The ventral straight edge is in contact with the distal radial and its dorsal edge is in contact with the third pre-axial radial and its tip. It articulates with distal part of the fourth mesomere by its proximal

straight edge (Fig. 1a.10). Its distal edge is curved and carries fin rays 20 to 24 (Fig. 1a.7). In the fetus it appears that the third pre-axial radial and the fourth pre-axial radial form a unique cartilaginous plate that covers at least the fourth mesomere and the distal radial in the left fin (Fig. 1a.10 A) and also the third mesomere in the right fin (Fig. 1a.10 B). Between the fetus stage and the pup 1 stage, this element becomes segmented into several elements: the third pre-axial radial with its pre-axial accessory elements and its tip, and the fourth pre-axial radial described just above (Fig. 1a.8, Fig. 1a.10). From pup 1 onwards, the fourth pre-axial radial presents its trapezoidal shape (Fig. 1a.10 C-F).

- Pre-axial accessory elements (pr. acc.)

These elements (called "*éléments accessoires de la troisième pièce radiale préaxiale*" by Millot and Anthony, 1958) are positioned at the dorsal edge of the third mesomere and associated to the third pre-axial radial. There is one large element in contact with the third mesomere, one large element in contact with both the third mesomere and the previous element that carries the fin rays 31 and 32, and one large element in contact with the third mesomere and the third pre-axial radial that carries the fin rays 29 and 30 (Fig. 1a.7). There are also several smaller elements, between two and four, in contact with the larger elements or with the third pre-axial radial, but their number varies depending on the development stage (Fig. 1a.7, Fig. 1a.8, Fig. 1a.10). In the fetus, there are no differentiated pre-axial accessory elements. These elements belong to the same large cartilaginous plate as the third pre-axial radial and the fourth pre-axial radial (Fig. 1a.10 A-B). From pup 1 onwards, the cartilaginous plate becomes segmented in several elements and the pre-axial accessory elements are differentiated from the third pre-axial radial and the fourth pre-axial radial (Fig. 1a.10). It seems that the number of pre-axial accessory elements is not fixed and can differ between the right and left fins within an individual (Fig. 1a.7). In pup 1, there are six elements on the right fin with three small elements, whereas there are seven elements on the left fin with four small elements. In pup 2, there is the same organization with three small pre-axial accessory elements of the right fin, but only two small elements on the left fin (associated with the three large elements). In the adult, Millot and Anthony (1958) described seven elements on the pre-axial accessory elements, three large elements and four small elements. Our 3D segmentation shows only one large cartilaginous element identified by µCT, but the different isolated pectoral fin skeletons show seven elements, as described by Millot and Anthony (1958).

3) The post-axial elements

• The distal radial (dis. rad.) (Fig. 1a.7)

As described by Millot and Anthony (1958), this element is transversely flattened and it has an elongated trapezoid shape. Its shape is similar to the fourth pre-axial radial and it is its symmetric, but slightly taller (Fig. 1a.7, Fig. 1a.10). It has three straight edges and one curved convex edge. In transverse section the distal radial present two slightly convex faces (Supplementary Fig. 1a.2). Its dorsal straight edge is aligned with the proximo-distal axis of the fourth mesomere and it is close to the fourth pre-axial radial element. The proximal joint is straight. Its ventral edge is straight and in contact with the distal post-axial accessory element. The curved edge is positioned at the distal part of the ventral edge of this element. It is on this edge that the fin rays 11 to 19 are inserted (Fig. 1a.7). In the fetus, the distal radial already presents a shape similar to that observed in the adult. It is transversely flattened, but presents a lateral ridge directed from proximal to distal (Fig. 1a.10 A-B). In pup 1, there is no lateral ridge on this element (Fig. 1a.10 C-D). From pup 2 onwards, there is a small swelling on its dorsal edge. This swelling is triangular shaped, as wide as its edge on the proximal part, then decreasing in size (Fig. 1a.10 E-F).

• The post-axial accessory elements (po. acc.)

According to Millot and Anthony (1958), there are five post-axial accessory elements in the adult stage. However, in the different isolated pectoral fins of adult specimens observed (CCC 6; CCC 7; CCC 14; CCC 19), we can see only four elements, aligned along the ventral ridge of the fourth mesomere. The proximal and the distal post-axial accessory elements are the largest ones and have a similar shape. The proximal element articulates with the proximal part of the ventral edge of the fourth mesomere. It is triangular-shaped with the tip directed to the proximal side of the fin and leaves a large gap between this element and the third mesomere (Fig. 1a.7, Fig. 1a.8, Fig. 1a.10). The second and third post-axial accessory elements are small and globular. The distal element is similar to the first element. This element is in contact with the distal part of the ventral edge of the fourth mesomere and the ventral edge of the distal radial. The first ten fin rays insert on the ventral edge of these post-axial accessory elements: 1 to 5 on the first element, ray 6 on the second element, ray 7 on the third, and rays 8 to 10 on the fourth element (Fig. 1a.7). In the fetus, there is only one large post-axial accessory element identified in the µCT (Fig. 1a.10 B). This element is in contact with the fourth mesomere and the proximal part of the ventral edge of the distal radial. It appears segmented at pup 1 and pup 2, as for the pre-axial cartilaginous plate. In pup 1, we can observe an asymmetry between the

right and left fin for these elements. In the right fin, the elements are as described above, but in the left fin, the third element is slightly different, being flat and trapezoidal-shaped (Fig. 1a.10 C). In pup 2, there is no asymmetry between the right and left pectoral fins for these elements. In the juvenile and adult, the µCT data do not allow us to identify more than one small element (Fig. 1a.8).

4) The fin rays

There are 32 fin rays on the pectoral fin. There are numbered 1 to 32 from the ventral side to the dorsal side (Fig. 1a.7). As described by Millot and Anthony (1958) the proximal part of the fin ray is bifurcated, and one branch inserts on the lateral side of the fin and the other on the medial side. The first ray is very small and the next becomes longer until ray 20 after which the length of the fin rays decreases. The fins rays of the pre-axial side of the fin insert largely on the pre-axial radials elements: rays 29 to 32 insert on the pre-axial accessory elements, rays 25 to 28 insert on the third pre-axial radial, and rays 20 to 24 insert on the curved edge of the fourth pre-axial radial. On the post-axial side of the fin, the fin rays insert only on the edge of the elements: the fin rays 11 to 19 on the curved edge of the distal radial and rays 1 to 10 on the edge of the post-axial accessory elements. In the fetus, the fin web is rounded and there seems to be no clear leading edge. From pup 1 onwards, the fin web has the same morphology as in the adult, forming a fin web that is elongated and pointed, with a convex leading edge and a concave trailing edge.

Discussion

As the period of gestation remain unknown in the extant coelacanths, it was consequently not possible to establish precise relationships between the known ontogenetic stages in vertebrates and those described here for *Latimeria*. We have gathered five clearly different ontogenetic stages: three prenatal stages, one juvenile and one adult.

The pectoral girdle

The pectoral girdle shows different arrangements within the different vertebrate groups, with various types of relations between the dermal and endoskeletal elements in relation to the mode of locomotion (McGonnell, 2001). The dermal anocleithrum (in sarcopterygians) or post-cleithrum (in actinopterygians), cleithrum and clavicle are primitively present in all osteichthyans (Gosline, 1977; Friedman and Brazeau, 2010; Zhu et al., 2012a). The majority of osteichthyans

also has a supracleithrum and/or a post-temporal, both small elements located in the most dorsal part of the girdle as in early tetrapodomorphs (Coates and Ruta, 2007; Friedman and Brazeau, 2010). Coelacanths have the anocleithrum, cleithrum and clavicle in common with the other osteichthyans, but also a supernumerary dermal bone, the extracleithrum, which is considered as a synapomorphy of the group (Forey, 1998). The endoskeletal element of the pectoral girdle, the scapulocoracoid, is present in all vertebrates and is covered by the cleithrum and clavicle in osteichthyans (McGonnell, 2001). In osteichthyan fishes, the scapulocoracoid is usually small compared to other elements of the pectoral girdle and the cleithrum forms a large part of the girdle (Janvier, 1996; McGonnell, 2001; Zhu and Schultze, 2001). However, in *Latimeria chalumnae* the scapulocoracoid is proportionally massive (Fig. 1a.3, Fig. 1a.6) and is, together with the cleithrum, the largest element of the girdle. A large scapulocoracoid is also present in the lungfish *Neoceratodus forsteri* (Rosen et al., 1981; Johanson et al., 2004) and considered convergent with coelacanths by (Coates and Ruta, 2007). Within tetrapodomorphs, there is an evolutionary trend towards a reduction of the dermal part of the girdle (clavicle, cleithrum) while the endochondral scapulocoracoid becomes the main component of the girdle in tetrapods (McGonnell, 2001; Vickaryous and Hall, 2006). The presence of a large scapulocoracoid or scapula + coracoid in tetrapods and in the coelacanth *Latimeria* is also considered convergent. Indeed, early tetrapodomorphs as *Eusthenopteron* (Andrews and Westoll, 1970) have proportionally small scapulocoracoids, as for extinct coelacanths as observed in the Triassic coelacanth *Laugia groenlandica* (Stensiö, 1932; Millot and Anthony, 1958) and the Devonian coelacanth *Diplocercides* (Stensiö, 1922). However, it is necessary to be careful with this assumption. Indeed, unlike the dermal elements of the girdle, the coelacanth scapulocoracoid is largely cartilaginous and it is consequently possible that only the most ossified part of this element is preserved in fossils (Forey, 1998). According to Forey (1981), the scapulocoracoid of the Carboniferous coelacanth *Rhabdoderma* was probably more substantial than the preserved mineralized portion, and fit into the groove present in the internal face of the cleithrum as observed in *Latimeria*. If this assumption is correct, the presence of groove on the internal side of dermal bones of the girdle in fossil coelacanths, as in *Diplurus* (Schaeffer, 1952), *Rhabdoderma* (Forey, 1981) or *Trachymetopon* (Dutel et al., 2015), delimit the lateral expansion of the scapulocoracoid.

In most osteichthyans the pectoral girdle is formed early in development before the fins or limbs. The cleithrum and clavicle are dermal bones and are known to be the first to appear, the scapulocoracoid appearing later in the development of actinopterygians (Jollie, 1980; Faustino

and Power, 1999; Koumoundouros et al., 2001) and of the lungfish *Neoceratodus* (Johanson et al., 2004; Joss and Johanson, 2007). In *Latimeria chalumnae*, our observations suggest a similar development since all the elements of the pectoral girdle are present in the fetus. Yet the scapulocoracoid seems deflated and is not in tight contact with the dermal bones (Fig. 1a.3, Fig. 1a.6). Later in development an expected radially outward growth of the scapulocoracoid leads to the close overlapping of the scapulocoracoid by the cleithrum, the extracleithrum and the clavicle, as observed from pup 1 onwards (Fig. 1a.6). These observations let us assume that the scapulocoracoid is formed later in the development than the dermal bones in *Latimeria* as in most vertebrates. The scapulocoracoid consists of a single massive element (Millot and Anthony, 1958) in the early development of the pectoral girdle. This development of the scapulocoracoid of *Latimeria* agrees with Schaeffer's (1941) observation of a complete co-ossification of the scapular and coracoid elements of the girdle for *Undina* and *Macropoma*. However, the development of the endoskeletal bone of the pectoral girdle is different from the actinopterygians. Indeed, in actinopterygians (except for acipenseriforms (Jollie, 1980; Davis et al., 2004), there are two ossifications regions inside the cartilaginous scapulocoracoid plate that correspond to the scapular and coracoid regions of the girdle (Patterson, 1982; Cubbage and Mabee, 1996; Grandel and Schulte-Merker, 1998). In *Neoceratodus*, as for *Latimeria*, there are no distinct ossification centers for the scapular and coracoid regions inside the scapulocoracoid. However, unlike the coelacanth, these two regions are distinct in the adult lungfish and are not co-ossified (Johanson et al., 2004).

The anocleithrum is the element of the girdle that proportionally grows the most during development despite remaining the smallest bone of the girdle at the adult stage (Fig. 1a.3). The small and rod-like anocleithrum in Latimeria is different in size and proportion from anocleithra known in other sarcopterygian fishes such as Neoceratodus or tetrapodomorph fishes (Coates and Ruta, 2007). The anocleithrum of *Latimeria* provides an insertion for the large *levator externus 5* muscle of the branchial arches musculature (Millot and Anthony, 1958; Forey, 1998; Carvalho et al., 2013), likely similar to *Neoceratodus* (Carvalho et al., 2013). However, the homology between the anocleithrum bones of different sarcopterygians has been previously challenged (Campbell et al., 2006) and remains to be validated.

In the early stages of development there is a reorientation of the pectoral girdle inside the body. The reorientation of bones during development has been shown in several groups of vertebrates. It is well documented for the pelvic girdle in lissamphibians (Ročková and Roček,

2005; Pomikal et al., 2011; Manzano et al., 2013), the chicken (Nowlan and Sharpe, 2014) and in mice (Pomikal and Streicher, 2010), and for the pectoral girdle in chelonians (Nagashima et al., 2007). However, the mechanisms of rotation and reorientation of the girdles remain largely unknown. As for the reorientation of the digits during the development in some birds (Botelho et al., 2014), the reorientation of the pectoral girdle in *Latimeria* is probably tightly linked to its interactions with the development of the adjacent muscles.

The pectoral fin

The endoskeletal elements of the pectoral fin known in adult stage are already present in the fetus, except the pre-axial accessory elements and the pre-axial radial elements 3 and 4. The axial elements of the pectoral fin, like the scapulocoracoid, seem deflated in the fetus, and their development between the fetus and pup 1 suggests a significant process of radially outward growth (Fig. 1a.8). The large distal cartilaginous plate in the fetus corresponds to the most distal radial elements (pre-axial radial 3 and 4, pre-axial accessory elements) in pup 1. The post-axial accessory elements show a similar development with the post-axial cartilaginous plate in the fetus corresponding to four post-axial accessory elements in pup 1 (Fig. 1a.8). Millot and Anthony (1958) already proposed the fragmentation of a unique cartilaginous plate to form the radial elements. Observations made on the earliest stage confirm the presence of non-differentiated large plates and support this hypothesis. Moreover, in the fetus, the cartilaginous plate articulates with the third and fourth mesomeres and the distal radial, suggesting a positional homology to the pre-axial accessory elements and the pre-axial radial 3 and 4, since these elements are respectively articulated with the third and fourth mesomeres and the distal radial in the later stages of development (Fig. 1a.8; Fig. 1a.10).

This splitting of a single endochondral plate to form the elements of the fin is also known in some other groups of vertebrates. This mechanism has been observed in actinopterygians such as *Polyodon* (Davis et al., 2004; Mabee and Noordsy, 2004), the zebrafish *Danio rerio*, the bichir *Polypterus senegalus* (Grandel and Schulte-Merker, 1998), the sturgeon *Acipenser* (Davis et al., 2004). The splitting of the endoskeleton of the fin is made by a decomposition of the extracellular matrix of the endoskeletal plate leading to the formation of the proximal radials (pro- and mesopterygium) (Davis et al., 2004; Nakamura et al., 2016). The primitive condition of the pectoral fin of sarcopterygians is thought to be polybasal with pro-, meso- and metapterygium, as in actinopterygians (Zhu and Yu, 2009). However, crown sarcopterygians, including coelacanths, have lost their pro- and mesopterygium and only retain the metapterygium leading

to the mono-basal condition of the fin (Rosen et al., 1981; Janvier, 1996; Zhu and Yu, 2009). In the acipenseriforms *Acipenser* and *Polyodon*, the metapterygial elements are formed outside the endoskeletal plate as an extension of the scapulocoracoid (Davis et al., 2004; Mabee and Noordsy, 2004). These elements are formed in a similar way as are the distal radials of the fins of non-tetrapod sarcopterygians and the limbs in tetrapods (Davis et al., 2004), with a condensation of the mesenchyme from proximal to distal (Shubin and Alberch, 1986; Joss and Longhurst, 2001).

The development of the metapterygial axis in *Latimeria* might result from a process of segmentation as known in other sarcopterygians and in *Polyodon*. However, this process occurs in the earliest stages of the development of the fin or limb, and only for the formation of the different cartilaginous elements of the endoskeletal axis before the ossification of these elements (Shubin and Alberch, 1986; Joss and Longhurst, 2001; Cohn et al., 2002). Due to the reduced ontogenetic series used in this study we cannot confirm a segmentation process since the elements are already formed and only a growth of the separated endoskeletal elements can be observed. For coelacanths, it is then not possible to identify the mechanism involved in the formation of the metapterygial axis or in the splitting of the cartilaginous plate into pre-axial radial elements or post-axial accessory elements. The splitting of the two pre-axial and post-axial cartilaginous plates to form, respectively, the third and fourth pre-axial radials and the pre-axial accessory elements, and the post-axial accessory elements, seems, however, to be different from the decomposition process of the extracellular matrix of the endoskeletal disc to form the radial elements as known in actinopterygians. Indeed, in actinopterygians, it is the precartilaginous plate that splits during development and that forms the different radial elements. However, this splitting occurs before the condensation of the precartilaginous plate (Grandel and Schulte-Merker, 1998; Davis et al., 2004). In *Latimeria*, it appears that the cartilaginous plate is already condensed in the fetus. This is clearly visible on the µCT data and the different elements of the fins have the same contrast than that of other endochondral bones of the body.

Evolution of the pectoral fin morphology in coelacanths and tetrapodomorph fishes

The radials elements of the pectoral fin are asymmetrically organized around the metapterygial axis. Indeed, each mesomere of the fin is associated with a pre-axial element (radial and/or accessory), whereas only the fourth mesomere is associated with radial elements on its post-axial region (distal radial and accessory elements; Fig. 1a.7). However, the general shape of

the first and second pre-axial radials, small and rounded, is clearly different from that of the more distal radials which are longer and flattened (Fig. 1a.7), as previously reported (Millot and Anthony, 1958). This difference in shape between the pre-axial radial elements gives lobe-shaped morphology to the pectoral fin of *Latimeria* compared to the fan-shaped fin morphology known in tetrapodomorph fishes. By contrast, the dermal fin rays are arranged almost symmetrically around the main axis of the pectoral fin and they do not insert on the pre-axial radial 1 and 2 (Fig. 1a.7). The asymmetrical condition of the pectoral fin is more pronounced in the early stage of the development. In the fetus, the first and second pre-axial radials, extending on the next mesomere, are proportionally longer than in the following stages (Fig. 1a.8, Fig. 1a.9 C-D), where these elements are small and only associated with one mesomere (Fig. 1a.7, Fig. 1a.8, Fig. 1a.10 E-H). The proportional reduction of the size of the proximal pre-axial radials with respect to the rest of endochondral elements gives a more lobe-shaped aspect to the fin. Developmental data seem corroborate the scenario of an evolution of the pectoral fin towards a lobe-shaped morphology based on rare fossil coelacanth specimens. Indeed, the species *Shoshonia arcopteryx* (Friedman et al., 2007) from the Devonian of the United States, has elongated and flattened radials on the pre-axial side of the fin. The most proximal pre-axial radials are elongated in *Shoshonia* and are different from the short and rounded first and second pre-axial radials in adult *Latimeria*, providing a more fan-shaped morphology to the fin. Interestingly, the earliest stage of *Latimeria* also presents elongated proximal pre-axial radials. As seen in *Latimeria* since the fetus stage, only the distal mesomere is associated with a post-axial radial. The fin rays of *Shoshonia* are associated with all the pre-axial radials, which gives the fin a more asymmetrical profile of the fin web (Friedman et al., 2007). This asymmetrical disposition of the fin rays is also observed in other fossil coelacanths (Forey, 1998; Friedman et al., 2007) including *Laugia groenlandica* (Stensiö, 1932) from the Triassic of Greenland. The condition observed in these fossils is thus different from the near-symmetrical arrangement of the fin rays in *Latimeria*. An asymmetrical arrangement of the radial elements and fin rays along the metapterygial axis is also observed in tetrapodomorph fishes (Andrews and Westoll, 1970; Shubin et al., 2006; Friedman et al., 2007), whereas in dipnomorph fishes the pectoral fin is very symmetrical (Ahlberg, 1989; Friedman et al., 2007). The fin rays usually insert on the pre- and post-axial radial elements, except in osteolepiforms where they also insert on the post-axial process of the mesomeres (Friedman et al., 2007). According to several authors it is possible that the post-axial process and the post-axial radials have a same ontogenetic origin which could explain the insertion of the fin rays on the mesomere (Jarvik, 1980; Friedman et al., 2007).

In contrast, the endochondral elements in the pectoral fin of dipnomorphs are nearly symmetrical with an arrangement of pre-axial and post-axial radials all along the metapterygial axis (Ahlberg, 1989; Friedman et al., 2007; Jude et al., 2014). Yet, the condition observed in lungfish appears to be highly derived with respect to the ancestral condition of sarcopterygian. The presence of an internally and externally asymmetrical pectoral fin in coelacanths and other lobe-finned fishes suggests that this condition is ancestral for sarcopterygians, as firstly proposed by Ahlberg (1989). This interpretation is supported by our observations made on the development of *Latimeria*. The particular morphology of the pectoral fin in *Latimeria* might be linked to changes in the mobility of the fin and in the locomotion, but this hypothesis remains to be tested.

Conclusion

The bony elements of the girdle and pectoral fin of the extant coelacanth *Latimeria* are nearly fully developed in the earliest stage of the ontogenetic series described here. During the first steps of pectoral fin development there is a re-orientation of the girdle putting the scapulocoracoids and the clavicles in the ventro-medial region of the two girdles in contact. The anocleithrum is the dermal bone of the girdle that proportionally grows the most during the development, further showing considerable morphological plasticity. The scapulocoracoid is robust which is unusual in most osteichthyans with the exception of tetrapods. The earliest developmental stage specimen shows a deflated scapulocoracoid and a lack of contact between the mesomeres and the scapulocoracoid with the dermal bones of the girdle. This early stage specimen also presents two large cartilaginous plates, on pre-axial and post-axial sides of the fin that later split into the pre-axial accessory elements and the third and fourth pre-axial radial, and in the post-axial accessory elements. The internal shape of the pectoral fin further becomes progressively more lobe-shaped due to a proportional reduction of the proximal pre-axial radials during development. Our developmental data corroborate previous fossil evidence, and reinforce the hypothesis that the lobe-shaped pectoral fin in the living coelacanth derives from the primitive fan-shaped condition of sarcopterygians.

Abbreviations

ano., anocleithrum; cl., cleithrum; cla., clavicle; dis. rad., distal radial; ecl., extracleithrum; f. r., fin ray; mes., mesomere; po. acc., post-axial accessory elements; pr. acc., pre-axial accessory

elements; pr. rad., pre-axial radial; scc., scapulocoracoid

Acknowledgements

We thank R. Bills and A. Paterson (South African Institute for Aquatic Biodiversity, SAIAB) and D. Neumann (Zoologische Staatssammlung München, ZSM) for the loan of the fetus and pup 2 specimens respectively. We are grateful to the European Synchrotron Radiation Facility (ESRF, Grenoble, France) for granting beam time and providing assistance in using beamline ID19 (Proposal EC-1023), M. Garcia at "AST-RX, plate-forme d'accès scientifique à la tomographie à rayons X" (UMS 2700, MNHN, Paris, France) for the X-ray tomography scans. We thank F. Goussard (UMR 7207 CR2P MNHN-CNRS-Sorbonne Université, Paris, France) for his assistance in the 3D imaging work. This work was supported by a grant from Agence Nationale de la Recherche under the LabEx ANR-10-LABX-0003-BCDiv, in the program "Investissements d'avenir" n° ANR-11-IDEX-0004-02.

Data Availability Statement

All the data are available by request from the authors.

Author contributions

R.M, G.C and M.H designed the project. H.D and P.T performed the synchrotron scans. M.D.S made the magnetic resonance imaging acquisitions. H.D, G.C and M.H made the conventional microtomographical acquisitions with the assistance of local staff. R.M segmented the scans and made the three-dimensional rendering of all of the developmental stages. R.M, G.C, A.H and M.H interpreted the results. R.M wrote the manuscript. G.C, A.H, H.D, P.T and M.H revised the manuscript.

Bibliography

Ahlberg, P. E. (1989). Paired fin skeletons and relationships of the fossil group Porolepiformes (Osteichthyes: Sarcopterygii). *Zoological Journal of the Linnean Society*, 96(2):119–166.

Ahlberg, P. E. (1991). A re-examination of sarcopterygian interrelationships, with special reference to the Porolepiformes. *Zoological Journal of the Linnean Society*, 103(3):241–287.

Amaral, D. B. and Schneider, I. (2018). Fins into limbs : Recent insights from sarcopterygian fish. *Genesis*, 56:e23052.

Amemiya, C. T., Alfoldi, J., Lee, A. P., Fan, S., Philippe, H., MacCallum, I., Braasch, I., Manousaki, T., Schneider, I., Rohner, N., Organ, C., Chalopin, D., Smith, J. J., Robinson, M., Dorrington, R. A., Gerdol, M., Aken, B., Biscotti, M. A., Barucca, M., Baurain, D., Berlin, A. M., Blatch, G. L., Buonocore, F., Burmester, T., Campbell, M. S., Canapa, A., Cannon, J. P., Christoffels, A., De Moro, G., Edkins, A. L., Fan, L., Fausto, A. M., Feiner, N., Forconi, M., Gamieldien, J., Gnerre, S., Gnirke, A., Goldstone, J. V., Haerty, W., Hahn, M. E., Hesse, U., Hoffmann, S., Johnson, J., Karchner, S. I., Kuraku, S., Lara, M., Levin, J. Z., Litman, G. W., Mauceli, E., Miyake, T., Mueller, M. G., Nelson, D. R., Nitsche, A., Olmo, E., Ota, T., Pallavicini, A., Panji, S., Picone, B., Ponting, C. P., Prohaska, S. J., Przybylski, D., Saha, N. R., Ravi, V., Ribeiro, F. J., Sauka-Spengler, T., Scapigliati, G., Searle, S. M., Sharpe, T., Simakov, O., Stadler, P. F., Stegeman, J. J., Sumiyama, K., Tabbaa, D., Tafer, H., Turner-Maier, J., Van Heusden, P., White, S., Williams, L., Yandell, M., Brinkmann, H., Volff, J. N., Tabin, C. J., Shubin, N. H., Schartl, M., Jaffe, D. B., Postlethwait, J. H., Venkatesh, B., Di Palma, F., Lander, E. S., Meyer, A., and Lindblad-Toh, K. (2013). The African coelacanth genome provides insights into tetrapod evolution. *Nature*, 496(7445):311–316.

Andrews, S. M. and Westoll (1970). The Postcranial Skeleton of *Eusthenopteron foordi* Whiteaves. *Earth and Environmental Science Transactions of the Royal Society of Edinburgh*, 68(9):207–329.

Anthony, J. (1980). Evocation des travaux français sur *Latimeria* notamment depuis 1972. *Proceedings of the Royal Society of London. Series B. Biological sciences*, 208:349–367.

Botelho, J. F., Smith-Paredes, D., Nuñez-Leon, D., Soto-Acuña, S., and Vargas, A. O. (2014). The developmental origin of zygodactyl feet and its possible loss in the evolution of Passeriformes. *Proceedings of the Royal Society B: Biological Sciences*, 281:20140765.

Campbell, K. S. W., Barwick, R. E., and den Blaauwen, J. L. (2006). Structure and Function of the Shoulder Girdle in Dipnoans : New Material from *Dipterus valenciennesi*. *Senckenbergiana lethaea*, 86(1):77–91.

Carvalho, M., Bockmann, F. A., and de Carvalho, M. R. (2013). Homology of the Fifth Epibranchial and Accessory Elements of the Ceratobranchials among Gnathostomes: Insights from the Development of Ostariophysans. *PLoS ONE*, 8(4).

Casane, D. and Laurenti, P. (2013). Why coelacanths are not 'living fossils'. *BioEssays*, 35:332–338.

Cavin, L., Mennecart, B., Obrist, C., Costeur, L., and Furrer, H. (2017). Heterochronic evolution explains novel body shape in a Triassic coelacanth from Switzerland. *Scientific Reports*, 7:13695.

Clack, J. A. (2009). The Fin to Limb Transition: New Data, Interpretations, and Hypotheses from Paleontology and Developmental Biology. *Annual Review of Earth and Planetary Sciences*, 37(1):163–179.

Clack, J. A. (2012). *Gaining Ground, Second Edition: The Origin and Evolution of Tetrapods*. Indiana University Press, Bloomington.

Coates, M. I. (2003). The Evolution of Paired Fins. *Theory in Biosciences*, 122:266–287.

Coates, M. I., Jeffery, J. E., and Ruta, M. (2002). Fins to limbs: What the fossils say. *Evolution & Development*, 4(5):390–401.

Coates, M. I. and Ruta, M. (2007). Skeletal Changes in the Transition from Fins to Limbs. In Hall, B. K., editor, *Fins Into Limbs: Evolution, Development, and Transformation*, chapter Chapter 2, pages 15–38. Chicago, the univer edition.

Cohn, M. J., Lovejoy, C. O., Wolpert, L., and Coates, M. I. (2002). Branching, segmentation and the metapterygial axis: Pattern versus process in the vertebrate limb. *BioEssays*, 24(5):460–465.

Cubbage, C. C. and Mabee, P. M. (1996). Development of the Cranium and Paired Fins in the Zebrafish *Danio rerio* (Ostariophysi, Cyprinidae). *Journal of Morphology*, 229:121–160.

Davis, M. C., Shubin, N. H., and Force, A. (2004). Pectoral fin and girdle development in the basal actinopterygians *Polyodon spathula* and *Acipenser transmontanus*. *Journal of Morphology*, 262(2):608–628.

Dutel, H., Galland, M., Tafforeau, P., Long, J. A., Fagan, M. J., Janvier, P., Herrel, A., Santin, M. D., Clément, G., and Herbin, M. (2019). Neurocranial development of the coelacanth and the evolution of the sarcopterygian head. *Nature*, 569(7757):556–559.

Dutel, H., Herbin, M., Clément, G., and Herrel, A. (2015). Bite Force in the Extant Coelacanth *Latimeria*: The Role of the Intracranial Joint and the Basicranial Muscle. *Current Biology*, 25:1228–1233.

Erdmann, M. V., Caldwell, R. L., and Moosa, M. K. (1998). Indonesian 'king of the sea' discovered. *Nature*, 395(6700):335.

Faustino, M. and Power, D. M. (1999). Development of the pectoral, pelvic, dorsal and anal fins in cultured sea bream. *Journal of Fish Biology*, 54(5):1094–1110.

Forey, P. L. (1981). The coelacanth *Rhabdoderma* in the Carboniferous of the British Isles. *Paleontology*, 24(1):203–229.

Forey, P. L. (1998). *History of the Coelacanth Fishes*. Thomson Science, London, chapman & edition.

Fricke, H. and Hissmann, K. (1992). Locomotion, fin coordination and body form of the living coelacanth *Latimeria chalumnae*. *Environmental Biology of Fishes*, 34(4):329–356.

Fricke, H., Reinicke, O., Hofer, H., and Nachtigall, W. (1987). Locomotion of the coelacanth *Latimeria chalumnae* in its natural environment. *Nature*, 329:331–333.

Friedman, M. (2007). *Styloichthys* as the oldest coelacanth: Implications for early osteichthyan interrelationships. *Journal of Systematic Palaeontology*, 5(3):289–343.

Friedman, M. and Brazeau, M. D. (2010). A reappraisal of the origin and basal radiation of the Osteichthyes. *Journal of Vertebrate Paleontology*, 30(1):36–56.

Friedman, M. and Coates, M. I. (2006). A newly recognized fossil coelacanth highlights the early morphological diversification of the clade. *Proceedings of the Royal Society B: Biological Sciences*, 273(1583):245–250.

Friedman, M., Coates, M. I., and Anderson, P. (2007). First discovery of a primitive coelacanth fin fills a major gap in the evolution of lobed fins and limbs. *Evolution & Development*, 9(4):329–337.

Gosline, W. A. (1977). The structure and function of the dermal pectoral girdle in bony fishes with particular reference to ostariophysines. *Journal of Zoology*, 183(3):329–338.

Grandel, H. and Schulte-Merker, S. (1998). The development of the paired fins in the zebrafish (*Danio rerio*). *Mechanisms of Development*, 79(1-2):99–120.

Gregory, W. K. and Raven, H. C. (1941). Part I: Paired Fins and Girdles in Ostracoderms, Placoderms, and Other Primitive Fishes. *Annals of the New York Academy of Sciences*, 42:275–291.

Janvier, P. (1996). *Early vertebrates*. Oxford University Press, Oxford.

Jarvik, E. (1980). *Basic structure and evolution of vertebrates*. London.

Johanson, Z., Joss, J., Boisvert, C. A., Ericsson, R., Sutija, M., and Ahlberg, P. E. (2007). Fish Fingers : Digit Homologues in Sarcopterygian Fish Fins. *Journal of Experimental Zoology Part B: Molecular and Developmental Evolution*, 308:757–768.

Johanson, Z., Joss, J. M., and Wood, D. (2004). The scapulocoracoid of the Queensland lungfish *Neoceratodus forsteri* (Dipnoi: Sarcopterygii): morphology, development and evolutionary implications for bony fishes (Osteichthyes). *Zoology*, 107(2):93–109.

Johanson, Z., Long, J. A., Talent, J. A., Janvier, P., and Warren, J. W. (2006). Oldest coelacanth, from the Early Devonian of Australia. *Biology letters*, 2(3):443–6.

Jollie, M. (1980). Development of Head and Pectoral Girdle Skeleton and Scales in *Acipenser*. *Copeia*, 1980(2):226–249.

Joss, J. and Johanson, Z. (2007). Is *Palaeospondylus gunni* a Fossil Larval Lungfish ? Insights From *Neoceratodus forsteri* Development. *Journal of Experimental Zoology Part B: Molecular and Developmental Evolution*, 308(B):163–171.

Joss, J. and Longhurst, T. (2001). Lungfish paired fins. In Ahlberg, P. E., editor, *Major Events in Early Vertebrate Evolution*, chapter 21, pages 370–376. London, taylor & f edition.

Jude, E., Johanson, Z., Kearsley, A., and Friedman, M. (2014). Early evolution of the lungfish pectoral-fin endoskeleton: evidence from the Middle Devonian (Givetian) *Pentlandia macroptera*. *Frontiers in Earth Science*, 2(August):1–15.

Koumoundouros, G., Divanach, P., and Kentouri, M. (2001). Osteological development of *Dentex dentex* (Osteichthyes: Sparidae): Dorsal, anal, paired fins and squamation. *Marine Biology*, 138(2):399–406.

Lyckegaard, A., Johnson, G., and Tafforeau, P. (2011). Correction of ring artifacts in X-ray tomographic images. *International Journal of Tomography and Statistics*, 18:1–9.

Mabee, P. M. (2000). Developmental Data and Phylogenetic Systematics: Evolution of the Vertebrate Limb. *American Zoologist*, 40:789–800.

Mabee, P. M. and Noordsy, M. (2004). Development of the paired fins in the paddlefish, *Polyodon spathula*. *Journal of Morphology*, 261(3):334–344.

Manzano, A., Abdala, V., Ponssa, M. L., and Soliz, M. (2013). Ontogeny and tissue differentiation of the pelvic girdle and hind limbs of anurans. *Acta Zoologica*, 94(4):420–436.

McGonnell, I. M. (2001). The evolution of the pectoral girdle. *Journal of Anatomy*, 199:189–194.

Millot, J. and Anthony, J. (1958). *Anatomie de Latimeria chalumnae - Tome I: Squelette, Muscles et Formations de soutien*. CNRS, Paris, cnrs edition.

Miyake, T., Kumamoto, M., Iwata, M., Sato, R., Okabe, M., Koie, H., Kumai, N., Fujii, K., Matsuzaki, K., Nakamura, C., Yamauchi, S., Yoshida, K., Yoshimura, K., Komoda, A., Uyeno, T., and Abe, Y. (2016). The pectoral fin muscles of the coelacanth *Latimeria chalumnae*: Functional and evolutionary implications for the fin-to-limb transition and subsequent evolution of tetrapods. *The Anatomical Record*, 299(9):1203–1223.

Nagashima, H., Kuraku, S., Uchida, K., Ohya, Y. K., Narita, Y., and Kuratani, S. (2007). On the carapacial ridge in turtle embryos : its developmental origin , function and the chelonian body plan. *Development*, 134:2219–2226.

Nakamura, T., Gehrke, A. R., Lemberg, J., Szymaszek, J., and Shubin, N. H. (2016). Digits and fin rays share common developmental histories. *Nature*, 537(7619):225–228.

Nowlan, N. C. and Sharpe, J. (2014). Joint shape morphogenesis precedes cavitation of the developing hip joint. *Journal of Anatomy*, 224(4):482–489.

Paganin, D., Mayo, S. C., Gureyev, T. E., Miller, P. R., and Wilkins, S. W. (2002). Simultaneous phase and amplitude extraction from a single defocused image of a homogeneous object. *Journal of Microscopy*, 206(1):33–40.

Patterson, C. (1982). Morphology and Interrelationships of Primitive Actinopterygian Fishes. *American Zoologist*, 22:241–259.

Pierce, S. E., Clack, J. A., and Hutchinson, J. R. (2012). Three-dimensional limb joint mobility in the early tetrapod *Ichthyostega*. *Nature*, 486(7404):523–526.

Pomikal, C., Blumer, R., and Streicher, J. (2011). Four-dimensional analysis of early pelvic girdle development in *Rana temporaria*. *Journal of Morphology*, 272:287–301.

Pomikal, C. and Streicher, J. (2010). 4D-Analysis of early pelvic girdle development in the mouse (*Mus musculus*). *Journal of Morphology*, 271(1):116–126.

Pouyaud, L., Wirjoatmodjo, S., Rachmatika, I., Tjakrawidjaja, A., Hadiaty, R., and Hadie, W. (1999). Une nouvelle espèce de coelacanthe. Preuves génétiques et morphologiques. *Comptes Rendus de l'Academie des Sciences - Serie III*, 322(4):261–267.

Ročková, H. and Roček, Z. (2005). Development of the pelvis and posterior part of the vertebral column in the Anura. *Journal of Anatomy*, 206:17–35.

Rosen, D. E., Forey, P. L., Gardiner, B. G., and Patterson, C. (1981). Lungfishes, tetrapods, paleontology, and plesiomorphy. *Bulletin of the American Museum of Natural History*, 167(4):159–276.

Sanchez, S., Ahlberg, P. E., Trinajstic, K. M., Mirone, A., and Tafforeau, P. (2012). Three-dimensional synchrotron virtual paleohistology: A new insight into the world of fossil bone microstructures. *Microscopy and Microanalysis*, 18:1095–1105.

Schaeffer, B. (1952). The Triassic coelacanth fish *Diplurus*, with observations on the evolution of the Coelacanthini. *Bulletin of the American Museum of Natural History*, 99(2):25–78.

Shubin, N. H. and Alberch, P. (1986). A Morphogenetic Approach to the Origin and Basic Organization of the Tetrapod Limb. *Evolutionary Biology*, 20:319–387.

Shubin, N. H., Daeschler, E. B., and Jenkins, F. A. J. (2006). The pectoral fin of *Tiktaalik roseae* and the origin of the tetrapod limb. *Nature*, 440.

Smith, J. L. B. (1939). A Living Fish of Mesozoic Type. *Nature*, 143(3620):455–456.

Smith, J. L. B. (1956). *Old Fourlegs: the Story of the Coelacanth*. London.

Standen, E. M., Du, T. Y., and Larsson, H. C. E. (2014). Developmental plasticity and the origin of tetrapods. *Nature*, 513(7516):54–58.

Stensiö, V. E. A. (1922). Über zwei Coelacanthiden aus dem Oberdevon von Wildungen. *Paläontologische Zeitschrift*, 4(2-3):167–210.

Stensiö, V. E. A. (1932). *Triassic Fishes from East Greenland, collected by the Danish Expeditions in 1929-1931*. Meddelelser om Grønland.

Vickaryous, M. K. and Hall, B. K. (2006). Homology of the reptilian coracoid and a reappraisal of the evolution and development of the amniote pectoral apparatus. *Journal of Anatomy*, 208:263–285.

Westoll, T. S. (1943). The origin of the tetrapods. *Biological Reviews*, 18(2):78–98.

Zhu, M. and Schultze, H.-p. (2001). Interrelationships of basal osteichthyans. In *Major Events in Early Vertebrate Evolution*, number 1996, pages 289–314.

Zhu, M. and Yu, X. (2009). Stem sarcopterygians have primitive polybasal fin articulation. *Biology Letters*, 5(3):372–375.

Zhu, M., Yu, X., Choo, B., Qu, Q., Jia, L., Zhao, W., Qiao, T., and Lu, J. (2012a). Fossil fishes from China provide first evidence of dermal pelvic girdles in osteichthyans. *PLoS ONE*, 7(4).

Zhu, M., Yu, X., Lu, J., Qiao, T., Zhao, W., and Jia, L. (2012b). Earliest known coelacanth skull extends the range of anatomically modern coelacanths to the Early Devonian. *Nature Communications*, 3:772–778.

Supplementary informations

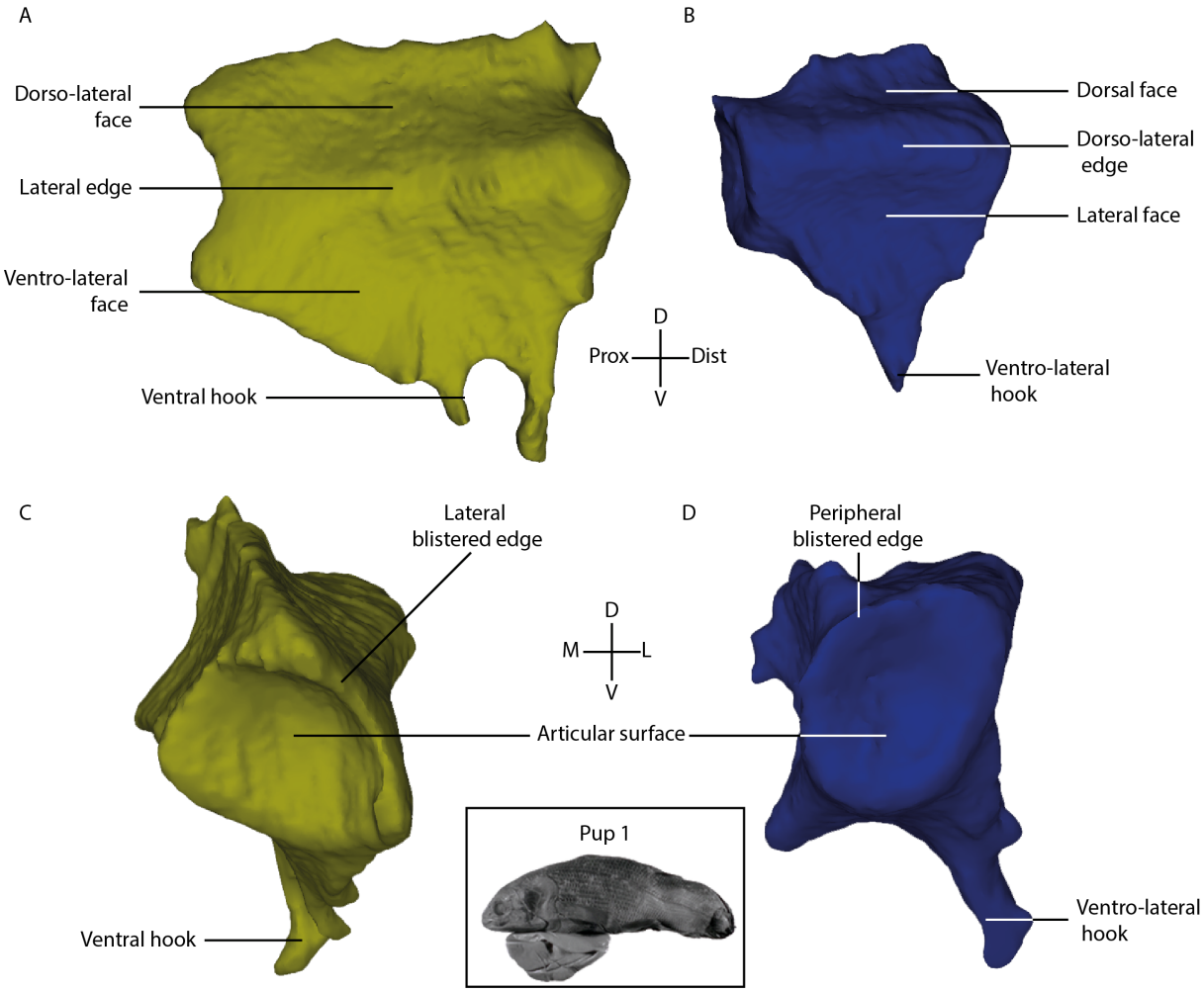

Supplementary Figure 1a.1: *Latimeria chalumnae* – First pup. First (A, C) and second (B, D) mesomeres of the left pectoral fin in lateral view (A, B) and proximal view (C, D). The lateral view of the two mesomeres shows the different faces and the reorientation of the mesomeres along the axis. The proximal view shows the differ- ent articular surfaces of the first and second mesomeres. D = dorsal; L = lateral; M = medial; V= ventral. Not to scale.

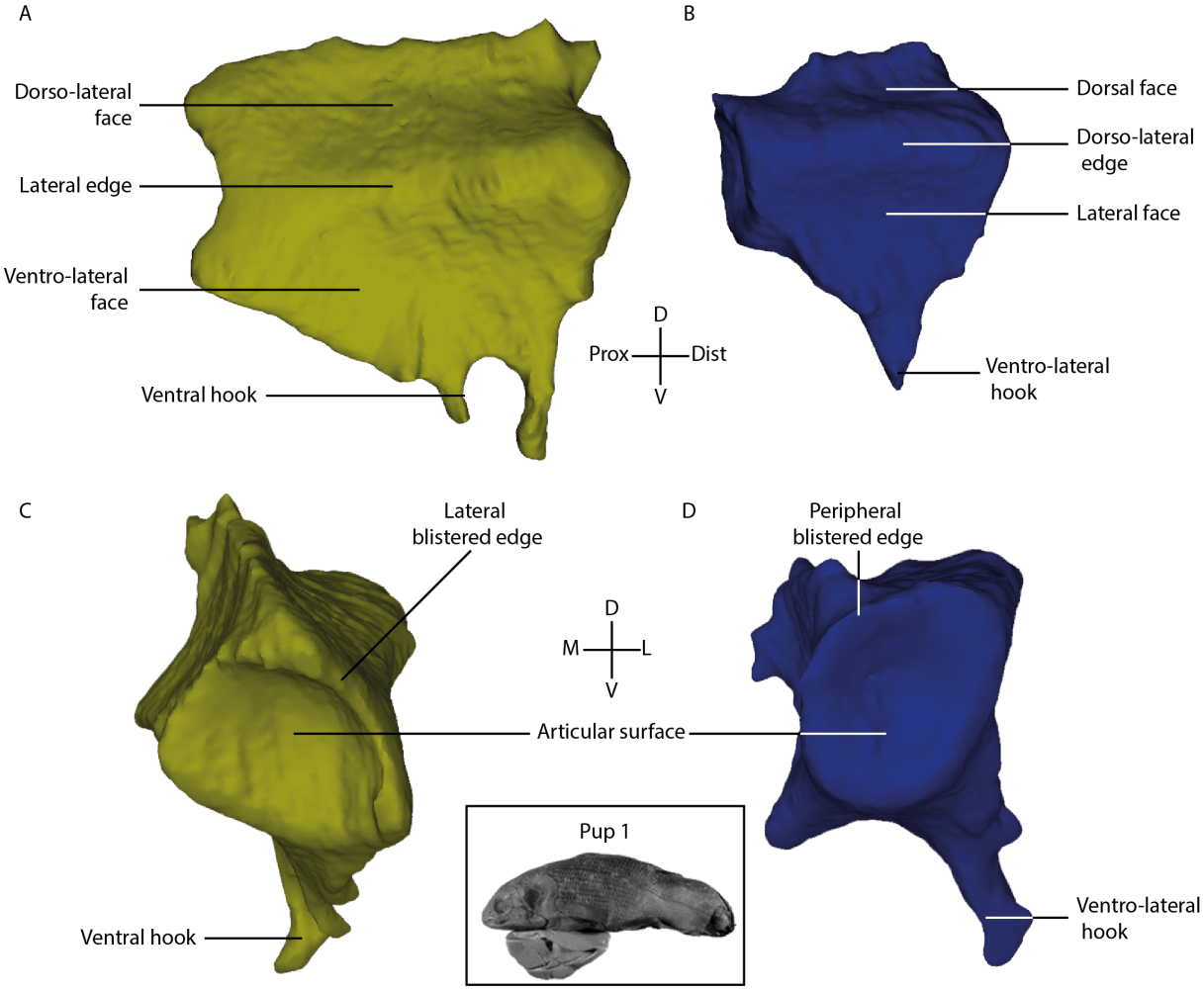

Supplementary Figure 1a.2: *Latimeria chalumnae* – Second pup. Transverse section of the distal end of the right fin (A) and its location on the lateral view of the 3D model (B). The distal radial presents only two convex faces, different from the previous axial elements of the fin that have four concave faces. dis.rad = distal radial; mes. = mesomere; po. acc. = post-axial accessory elements; pr. rad. = pre-axial radial. D = dorsal; L = lateral; M = medial; V= ventral. Not to scale.

CHAPTER I b

Development and growth of the pelvic fin in the extant coelacanth *Latimeria chalumnae*

Manuscript published

The Anatomical Record. DOI: 10.1002/ar.24452

Development and growth of the pelvic fin in the extant coelacanth *Latimeria chalumnae*

Mansuit Rohan[1,2], Clément Gaël[1], Herrel Anthony[2], Hugo Dutel[3,4], Paul Tafforeau[5], Mathieu D. Santin[6] and Herbin Marc[2]

[1] UMR 7207 Centre de Recherche en Paléontologie, Paris, MNHN – Sorbonne Université – CNRS, Département Origines & Evolution, Muséum national d'Histoire naturelle, 57 rue Cuvier, 75005 Paris, France

[2] UMR 7179 MECADEV, MNHN – CNRS, Département Adaptations du Vivant, Muséum national d'Histoire naturelle, 57 rue Cuvier, 75005 Paris, France

[3] School of Earth Sciences, University of Bristol, 24 Tyndall avenue, BS8 1TQ, United-Kingdom.

[4] School of Engineering and Computer Science, University of Hull, Hull, UK

[5] European Synchrotron Radiation Facility, BP 220, 6 Rue Jules Horowitz, 38043 Grenoble Cedex, France.

[6] Inserm U 1127, CNRS UMR 7225, Centre for NeuroImaging Research, ICM (Brain & Spine Institute), Sorbonne University, Paris, France

Address for correspondence

Rohan Mansuit
UMR 7179 MECADEV, MNHN – CNRS,
Département Adaptations du Vivant
55 rue Buffon
75005 Paris, France
e-mail : rohan.mansuit@mnhn.fr

Running title

Ontogeny of the pelvic appendage of Latimeria

Grant information

Grant sponsor: Agence Nationale de la Recherche in the LabEx ANR-10-LABX-0003-BCDiv
Grant number: program 'Investissements d'avenir' n° ANR-11-IDEX-0004-02

Abstract

The ontogeny of the paired appendages has been extensively studied in lungfishes and tetrapods, but remains poorly known in coelacanths. Recent work has shed light on the anatomy and development of the pectoral fin in *Latimeria chalumnae*. Yet, information on the development of the pelvic fin and girdle is still lacking. Here, we described the development of the pelvic fin and girdle in *Latimeria chalumnae* based on 3D reconstructions generated from conventional and X-ray synchrotron microtomography, as well as MRI acquisitions. As in other jawed vertebrates, the development of the pelvic fin occurs later than that of the pectoral fin in *Latimeria*. Many elements of the endoskeleton are not yet formed at the earliest stage sampled. The four mesomeres are already formed in the fetus, but only the most proximal radial elements (pre-axial radial 0-1) are formed and individualized at this stage. We suggest that all the pre-axial radial elements in the pelvic and pectoral fin of *Latimeria* are formed through the fragmentation of the mesomeres. We document the progressive ossification of the pelvic girdle, and the presence of a trabecular system in the adult. This trabecular system likely reinforces the cartilaginous girdle to resist the muscle forces exerted during locomotion. Finally, the presence of a pre-axial element in contact with the pelvic girdle from the earliest stage of development onwards questions the mono-basal condition of the pelvic fin in *Latimeria*. However, the particular shape of the mesomeres may explain the presence of this element in contact with the girdle.

Keywords

Actinistia, sarcopterygians, ontogeny, appendages, endoskeleton

Introduction

Among sarcopterygians, the living coelacanths *Latimeria chalumnae* (Smith, 1939) and *L. menadoensis* (Pouyaud et al., 1999) are the only living representatives of the Actinistia, a clade closely related to lungfishes and tetrapods (Forey, 1998; Friedman et al., 2007; Clack, 2012; Amemiya et al., 2013). Although the anatomy of *Latimeria chalumnae* is well known (Millot and Anthony, 1958, 1965; Millot et al., 1978), its development remains largely unknown. Indeed, only a few embryos and one juvenile are present in collections worldwide (Nulens et al., 2011). Due to the improvement of non-invasive imaging techniques such as conventional and synchrotron micro-tomography, as well as magnetic resonance imaging, it is now possible to study the development of small and complex internal structures of the coelacanth like the lung (Cupello et al., 2015), the neurocranium (Dutel et al., 2019) and the pectoral fin (Mansuit et al., 2020).

The endoskeleton elements of the paired fins or limbs are organized along a single metapterygial axis in sarcopterygians (Millot and Anthony, 1958; Shubin and Alberch, 1986). However, whereas the development of paired appendages in lungfishes and tetrapods is relatively well known (Shubin and Alberch, 1986; Boisvert et al., 2013; Jude et al., 2014), it remains poorly studied in coelacanths (but see Mansuit et al., 2020). Yet, the development of the pelvic appendages of vertebrates occurs later than the pectoral appendages (Cubbage and Mabee, 1996; Mabee and Trendler, 1996; Mabee and Noordsy, 2004). Therefore, documenting of the development of the pelvic fin of *Latimeria* is important to fully understand the development of the paired fins in this species. Following our recent work on pectoral fin development (Mansuit et al., 2020), we here describe the anatomy and development of the pelvic appendage of *Latimeria* based on an ontogenetic series of five different stages.

Materials and methods

Specimens

The developmental series includes five stages including specimens from several Museum collections (Fig. 1b.1). The first stage is a fetus of 5 cm total length (TL) (international number: CCC 202.1) found inside the female specimen CCC 202 captured off the coast of Tanzania in 2005 and conserved in the collection of the South African Institute for Aquatic Biodiversity (SAIAB) in Grahamstown (collection number: SAIAB 76199). The stage two is a pup with yolk sac

of 32.3 cm TL (CCC 29.5) found inside the female specimen CCC 29 captured in the Comores in 1969 and conserved in the collection of the Muséum national d'Histoire naturelle (MNHN), Paris (collection number: MNHN AC 2012-22). The stage three is a late pup without yolk sac of 34.8 cm TL (CCC 162.21) found inside the female CCC 162 captured off the coast of Mozambique in 1991 and conserved in the collections of the Zoologische Staatssammlung of Munich (collection number: ZSM 28409). The stage four is a juvenile of 42.5 cm TL (CCC 94) captured off the coast of Grande Comore Island in 1974 and conserved in the collections of the MNHN, Paris (collection number: MNHN AC 2012-27). Imaging reconstructions and observations on adult stage (stage 5) were mainly based on a male specimen of 132 cm TL (CCC 27) captured off the coast of Grande Comore Island in 1961 and conserved in the collections of the MNHN, Paris (collection number: MNHN AC 2012-21) (Nulens et al., 2011). Direct anatomical observations were also made from on a dissected and prepared pelvic fin skeleton of adult specimen CCC 7 (collection number: MNHN AC 2012-5). All specimens of the MNHN, Paris are conserved in a 6-7% formaldehyde solution, while the others are preserved in an aquaeous ethanol solution (70°).

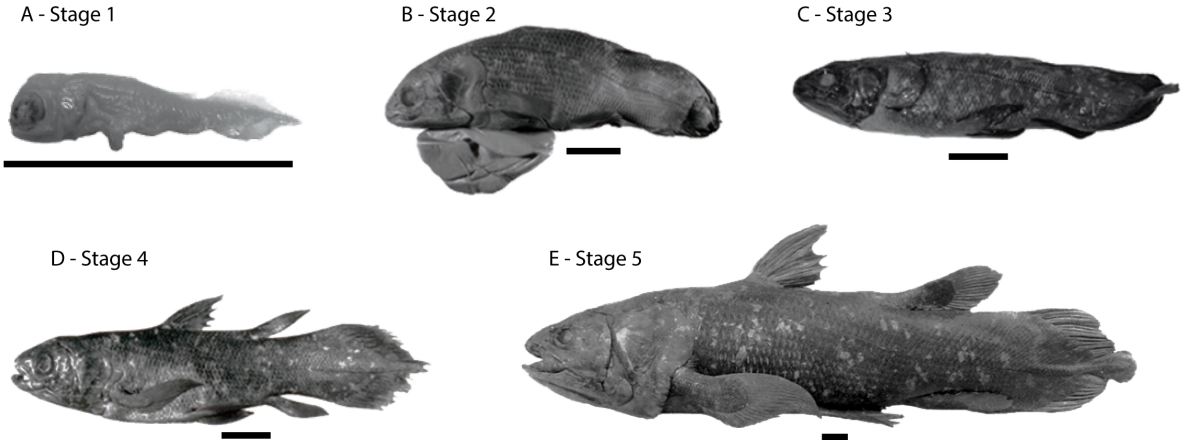

Figure 1B.1: *Latimeria chalumnae* — Ontogenetic series in left lateral view. (a) Early embryo (CCC 202.1), (b) Embryo with yolk sac (CCC 29.5), (c) Late embryo without yolk sac (CCC 162.21), (d) Juvenile (CCC 94), (e) Adult (CCC 27). Scale bar = 5 cm

Imaging

Figure Fig. 1b.2 illustrates sections through the girdle and fins of the different specimens illustrating the quality of the raw data used in this paper.

Stage 1 – Fetus (CCC 202.1)

The specimen was scanned using long propagation phase-contrast synchrotron X-ray microto-

mography at the ID19 beamline of the European Synchrotron Radiation Facility (ESRF), Grenoble (France). It was imaged in a glass cylinder filled with ethanol, at a voxel size of 6.5µm, with a high-quality pink beam using the ID19 W150 wiggler and a gap of 50 mm filtered by 2 mm of aluminium, 0.25 mm of copper and 0.2 mm of gold. The scintillator was a 250-µm-thick LuAG:Ce (lutetium–aluminium–garnet) crystal. The resulting detected spectrum was then centred on 77 keV, with a bandwidth of 17 keV FWHM (full width at half maximum). The detector was a FreLoN 2K charge coupled device (CCD) camera mounted on a lens system. To obtain a sufficient propagation phase-contrast effect, a distance of 3m between the sample and the detector was used. Synchrotron data were reconstructed using a filtered back-projection algorithm coupled with a single distance phase-retrieval process (Paganin et al., 2002; Sanchez et al., 2012). All the sub-scans were reconstructed separately, converted into 16-bit TIFF stacks and then concatenated to generate a single complete volume. The ring artefacts were corrected on the reconstructed slices using a specific tool developed at the ESRF (Lyckegaard et al., 2011). The final volume used for the present study (13µm voxel size) was obtained after isotropic 2-times binning with the software ImageJ.

Stage 2 – Pup 1 (with yolk sac) (CCC 29.5)

The specimen was scanned on the ID19 beamline on the ESRF in a empty plastic tube, at a voxel size of 23.34µm, using a propagation distance of 13m to maximize the phase-contrast effect. The beam produced by the W150 wiggler at a gap of 59mm was filtered by 2.8mm of aluminium and 1.4mm of copper, resulting in an average detected energy of 77,4 keV. The scintillator was a 2000-µm-thick LuAG:Ce (lutetium–aluminium–garnet doped with cerium) crystal. The detector was a PCO edge 4.2 sCMOS. Tomographic slices were reconstructed using the same protocol than the one described above. The final volume (46.68µm voxel size) was obtained after isotropic 2-times binning with the softward ImageJ.

Stage 3 – Pup 2 (with yolk sac resorbed) (CCC 162.21)

The specimen was scanned in a similar manner to stage 2, at a voxel size of 23.34µm. The scintillator, detector and distance between the sample and the detector were the same as for the stage 2 embryo. The final volume (46.68µm voxel size) was obtained after isotropic 2-times binning in ImageJ.

Stage 4 – Juvenile (CCC 94)

The specimen was scanned twice, once at the ESRF on the beamline ID19, and once using

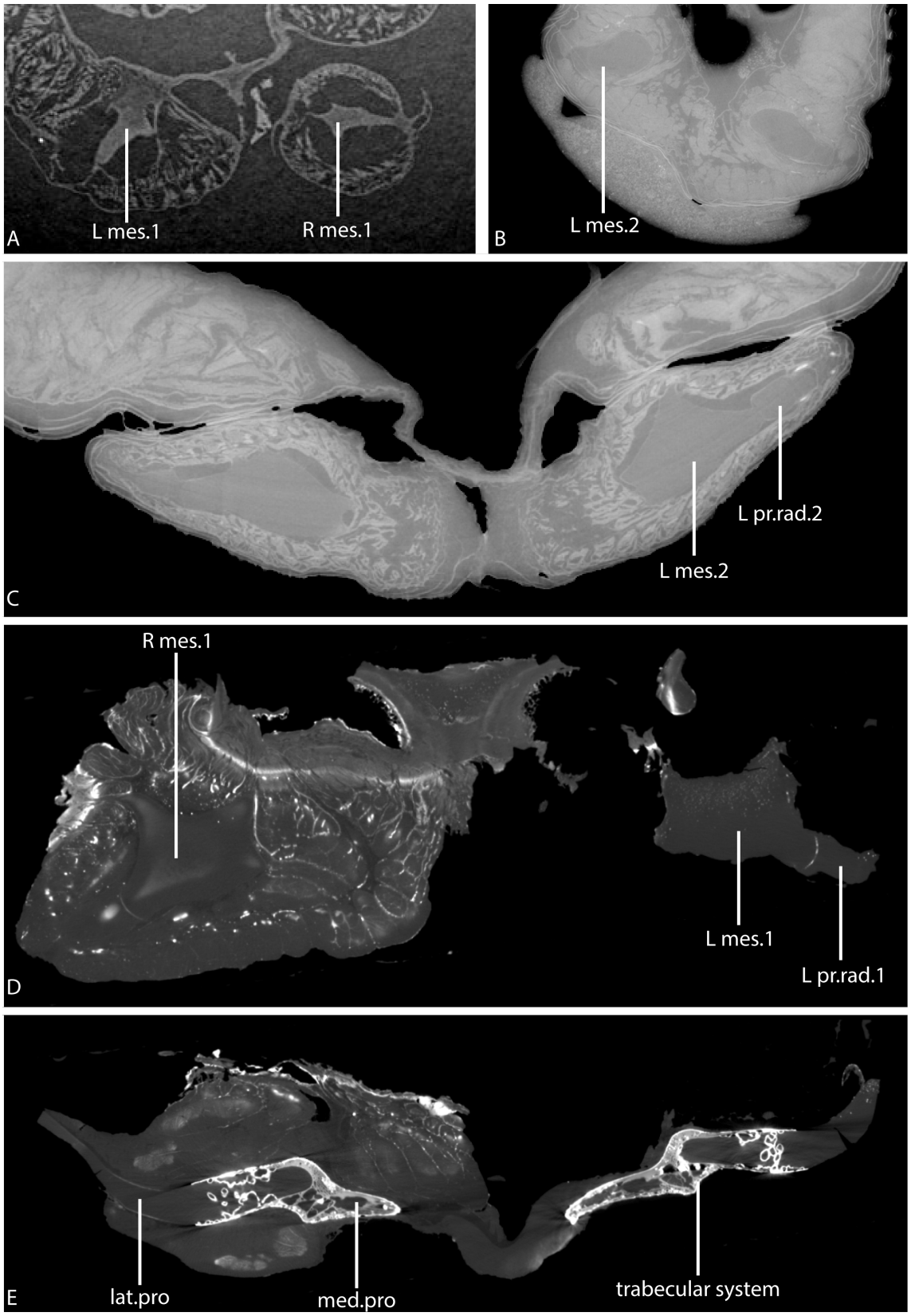

Figure 1b.2: Transverse section of the pelvic fin and girdle in the fetus (a), pup 1 (b), pup 2 (c), and adult (d, e) showing the quality of the scans and the contrast for the different stages, at different section along the fin. Transverse section for the fetus, pup 1, and 2 are zoomed on the pelvic fin (a, b, c). Concerning the adult stage, the pelvic fins were isolated and the left fin was dissected (d, e). lat.pro., lateral process; med.pro., medial process; mes., mesomere; pr.rad., preaxial radial

magnetic resonance imaging (MRI). At the ESRF, the specimen was scanned in a plastic tube filled with water, at a voxel size of 28.43 µm, using a propagation distance of 13m to maximize the phase-contrast effect. The beam produced by the W150 wiggler at a gap of 30mm was filtered by 2mm of aluminium and 15mm of copper, resulting in an average detected energy of 170 keV with a bandwidth of 85 keV FWHM. The detector camera was a FreLoN 2K charge coupled device mounted on a lens system coupled to a 750-mm-thick LuAG:Ce scintillator. Tomographic slices were reconstructed using the same protocol than the ones described above. The final volume (56.86 µm voxel size) was obtained after isotropic 2-times binning with the software ImageJ.

As the contrast was not sufficient due to the partial demineralisation of the bones linked to the long preservation in formalin solution, the specimen was re-scanned using MRI at lower resolution. The MRI was performed at 3T with a Siemens Tim TRIO (Siemens, Germany) system. Images were acquired with a 3D Flash sequence using an isotropic resolution of 300 µm. Parameters were: Matrix size = 640*300*256; TR/TE (ms) = 18/4.73; Flip Angle = 10°; Spectral Width = 100 kHz; Number of averages = 20; Total acquisition time was 7 hours and 41 minutes.

Stage 5 – Adult (CCC 27)

The specimen CCC 27 was scanned at the AST-RX facility of the MNHN (Paris, France) using stacking of multiple scans with the following scanning parameters: voltage 110 kV, current 950 µA, filter 0.2 mm Cu, voxel size 105 µm and 3,258 views.

Segmentation and 3D-reconstruction method

For all the specimens, segmentation and three-dimensional rendering were done using the softwares MIMICS Innovation Suite 20.0 (Materialise) (Stage 1-4) and MIMICS Innovation Suite 21.0 (Materialise) (Stage 5). The different objects were exported in STL format and transformed into a 3D PDF with the software 3-matic 11.0 (Materialise) (Stages 1-4) and 3-matic 13.0 (Materialise) (Stage 5).

Results

The pelvic appendages are located on the ventral side of the animal, in the middle of the body on both sides of the cloaca (Millot et al., 1978).

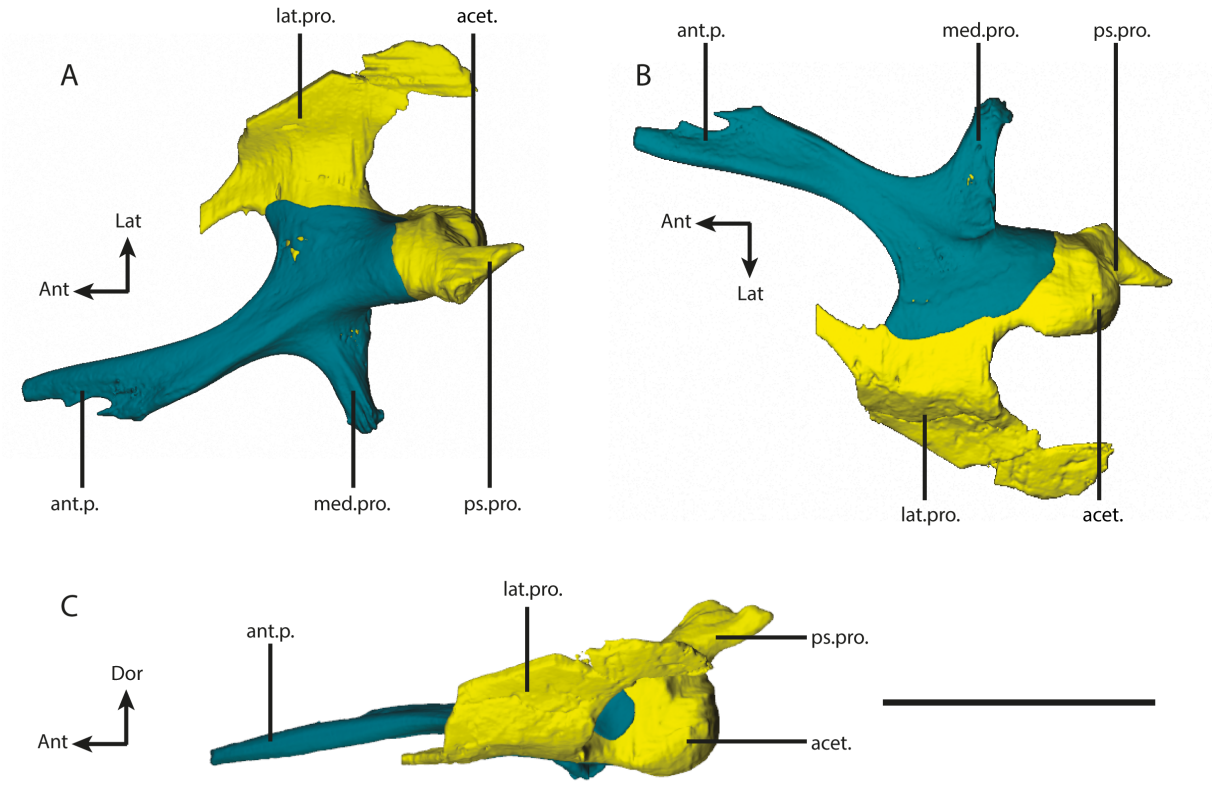

Figure 1b.3: *Latimeria chalumnae* — Adult stage. Right pelvic girdle in dorsal view (a), ventral view (b), and lateral view (c). act., acetabulum; ant.p., anterior process; lat.p., lateral process; med.pro., medial process; pos.p., posterior part; ps.pro., posterosuperior process. Blue = dense part of the girdle; yellow = endoskeletal pelvic girdle. Scale bar = 50 mm

The pelvic girdle

In the adult stage, the pelvic girdle is a massive element and supports several processes: the anterior process (ant.p) ("*segment antérieur*" according to Millot and Anthony), the lateral process (lat.pro.) ("*apophyse latérale externe*" according to Millot and Anthony), the medial process (med.pro) ("*apophyse latérale interne*" according to Millot and Anthony) and the postero-superior process (ps.pro) ("*apophyse postéro-supérieure*" according to Millot and Anthony) (Fig. 1b.2 E, Fig. 1b.3). The anterior process is a long cartilaginous and rod-like structure that gently flares anteriorly to form a flattened blade. The lateral process is large and flat, concave on its dorsal side, with an anterior peak, whereas the medial process is a short and triangular expansion. The postero-superior process is robust and short, with a flattened apex. The posterior part of the girdle presents a convex articular head, called the acetabulum, which articulates with the first axial element of the fin. The two girdles are not fused in *Latimeria* (Fig. 1b.4 C), but joined by ligaments between the two medial processes and between the distal edge of the two anterior processes. The microtomographic data allow, for the first time, the visualization of a partially denser region at the surface of the pelvic girdle that could correspond to an en-

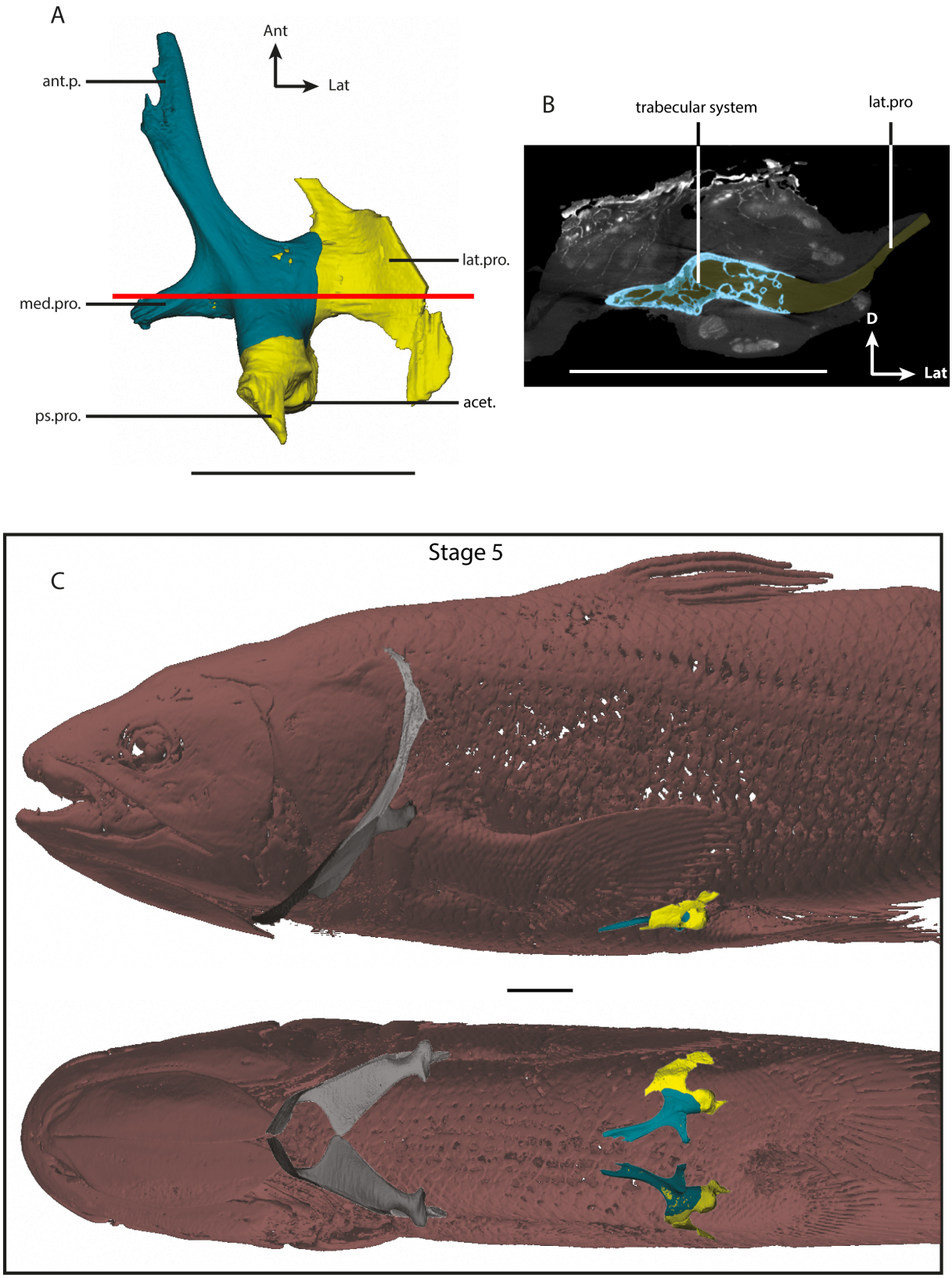

Figure 1b.4: *Latimeria chalumnae* — Adult stage. Right pelvic girdle in dorsal view (a) and transverse section (b). Location of the pectoral and pelvic girdle inside the body in the left and ventral view (c). The red line in A shows the location of the transverse section. The trabecular system and the dense radio-opaque part of the girdle are clearly visible. The color code of the transverse section and the 3D model is identical. act., acetabulum; ant.p., anterior process; lat.p., lateral process; med.pro., medial process; pos.p., posterior part; ps.pro., posterosuperior process. Blue = dense part of the pelvic girdle; yellow = endoskeletal pelvic girdle; grey = pectoral girdle. Scale bar = 50 mm

dochondral ossification of the girdle (Fig. 1b.2, Fig. 1b.3, Fig. 1b.4). In the adult, this region covers the anterior process, the medial process, and extends posteriorly until the base of the postero-superior process and of the lateral process with a convex expansion. This denser area is internally associated with a trabecular system (Fig. 1b.2 E, Fig. 1b.4 B) that is well developed in the posterior part and the medial process of the girdle. The anterior process and the base of the lateral process present a trabecular system appears to be less developed. This ossification is also visible on the isolated pelvic girdle of the specimen CCC 7.

In the fetus, the pelvic girdle is relatively smaller and shows a very different shape from what is observed in the next stages (Fig. 1b.5 A). The different processes have morphologies different from those observed in the adult stage. The anterior process of the girdle is only represented by a small pointed extension. The medial process is large with a square shape and the lateral process forms only a short crest. The postero-superior process is a reduced convex process. From pup 1 onwards, the girdle becomes more complete and all its processes are fully formed (Fig. 1b.5 B-E). In pup 1, the anterior process of the right girdle does not form a blade, but a bifid process. The dense superficial surface only partially covers the anterior process of the girdle (Fig. 1b.5 B). From pup 2 onwards, the anterior process of the girdle forms a blade. The dense superficial surface covers almost the entire anterior process of the girdle, and the most anterior part of the girdle (Fig. 1b.5 C). In the juvenile, the ossification expands to the posterior part of the girdle and partially covers the medial process (Fig. 1b.5 D). No trabecular system can be observed, in contrast to the adult stage.

The pelvic fin (Fig. 1b.6)

The pelvic fin is composed of several elements: mesomeres on the metapterygial axis, pre-axial elements (pre-axial radials + pre-axial accessory elements) and post-axial elements (post-axial radials + distal radial). According to Millot and Anthony (1958), the metapterygial axis of the fin consists of five axial elements (named "*articles*"), numbered from proximal to distal, while Forey (1998) identified 4 mesomeres and one distal radial element. There are five pre-axial radial elements (Millot and Anthony, 1958; Forey, 1998), a variable number of pre-axial accessory elements and post-axial radials (Millot and Anthony, 1958). The fin rays insert on the pre-axial and post-axial elements of the fin (see descriptions below). As described by Millot and Anthony (1958), the so-called "fifth article" of the metapterygial axis has a different shape compared to the previous elements of the metapterygial axis, and the fin rays insert on it. Following Forey (1998), we therefore consider this element as a distal radial belonging to the post-axial

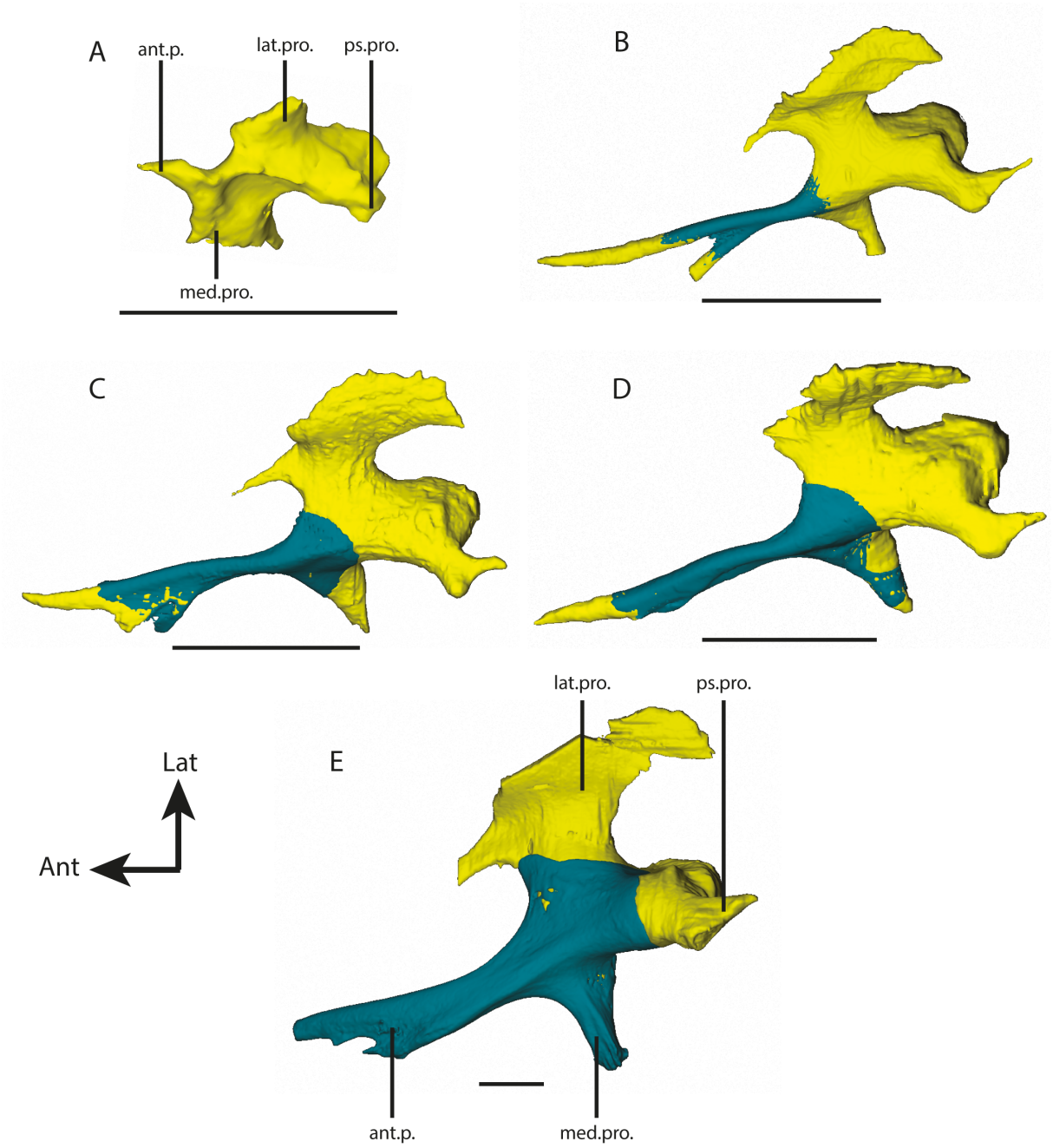

Figure 1b.5: *Latimeria chalumnae*. Right pelvic girdle in dorsal view at five different developmental stages. a: Stage 1, b: Stage 2, c: Stage 3, d: Stage 4, and e: Stage 5. ant.p., anterior process; lat.p., lateral process; med.pro., medial process; pos.p., posterior part; ps.pro., posterosuperior process. Blue = dense part of the girdle; yellow = endoskeletal pelvic girdle. a: Scale 2 mm; b – e: Scale bar = 10 mm

elements (Fig. 1b.6). In the adult stage, the organization of the endoskeleton of the pelvic fin is similar to that observed for the pectoral fin (Millot and Anthony, 1958; Mansuit et al., 2020) (Fig. 1b.7). However, unlike in the pelvic girdle, there is no trabecular system in any element of the pelvic fin (as for the pectoral fin) (Fig. 1b.2).

1) The metapterygial axis

As for the pectoral fin of *L. chalumnae* (Mansuit et al., 2020), we use the term mesomere for subcylindrical radial segments of the principal axis in sarcopterygian fins (Jarvik, 1980). As described by Millot and Anthony (1958) for the adult stage, the four mesomeres have a similar length, and the three first mesomeres have a similar shape (Fig. 1b.6 A). There is a progressive dorso-ventral flattening of the mesomeres from proximal to distal (Fig. 1b.6 B). From proximal to distal, the ridges on the dorsal side of the mesomeres are also progressively less developed and have an increasingly medial position from the first to the third mesomere.

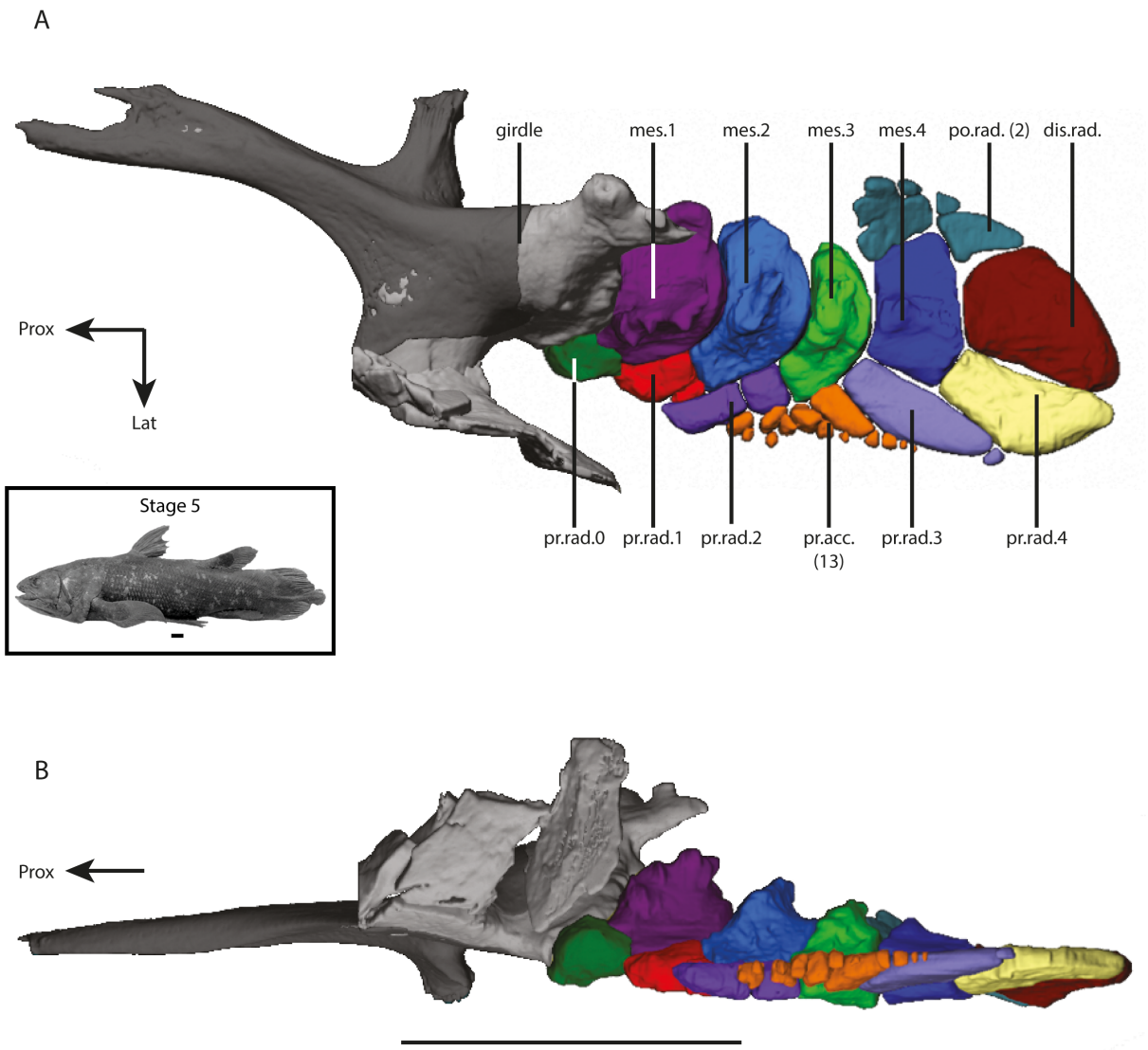

Figure 1b.6: *Latimeria chalumnae* — Adult stage. Left pelvic fin in dorsal (a) and lateral (b) view. The lateral process of the girdle is broken. mes., mesomere; po.rad., postaxial radial; pr.acc., preaxial accessory elements; pr.rad., preaxial radial. Scale bar = 50 mm

- The first mesomere (mes.1)

As described by Millot and Anthony (1958) in the adult stage the first mesomere is wider than long and slightly arc-shaped. It articulates with the acetabulum of the pelvic girdle by its concave proximal edge and with the next mesomere by its convex distal edge (Fig. 1b.6). The angle between the distal edge and the medial edge forms a large process. The dorsal side presents a strong but irregular oblique crest, directed from proximo-lateral to disto-medial. The ventral facet of the mesomere is flatter with only a small swelling on the medial part of its surface.

In the fetus, the shape of the first mesomere is similar to that seen in the adult specimen: concave on the proximal edge and convex on the distal edge, with a ridge on its dorsal face (Fig. 1b.8 A). There is a bilateral asymmetry to the morphology of the mesomere, since the ridge is oblique on the right fin whereas it is longitudinal on the left fin (Fig. 1b.10 A). This first mesomere is squarer in the fetus than in the adult stage. There is no process on the medial side of the mesomere. The ventral side of the mesomere does not have a swelling on the medial part of the surface, but a longitudinal ridge close to the medial edge. From pup 1 onwards, the first mesomere has already its adult shape, arc-shaped and slightly wider than long (Fig. 1b.8 B-E). The dorsal ridge is well developed, with an irregular surface. In pup 1, the ventral face of the first mesomere has an important swelling on the medial part of its surface. From pup 2 onwards, the swelling is less important and the ventral side of the mesomere is flatter. The oblique crest on the ventral face of this mesomere described by Millot and Anthony (1958) is not present from pup 1 onwards, neither is it on the isolated pelvic fin.

- The second mesomere (mes.2)

In the adult stage, the second mesomere has a morphology similar to that of the first mesomere, but more flattened and slightly shorter (Fig. 1b.6). The medial process is smaller and the dorsal ridge less developed. The latter is less oblique and more latero-medially oriented than on the mesomere 1.

In the fetus, the second mesomere is trapezoid in shape. There is no process on its medial edge, and the ridge is poorly developed (Fig. 1b.8 A). Moreover, this ridge is longitudinal on the left fin whereas it is more oblique on the right fin (Fig. 1b.10 A). From pup 1 onwards, the second mesomere has its adult shape (Fig. 1b.8 B-E). As for the first mesomere, the swelling surface on the ventral face of the second mesomere is well marked in pup 1, yet becomes flatter from pup 2 onwards.

• The third mesomere (mes.3)

In the adult stage, the length of this element is smaller than those of previous mesomeres, but the width is more or less the same (Fig. 1b.6). The general morphology is boomerang-liked. Like for the previous mesomeres the dorsal ridge is well developed, but less pronounced. However, the medial process is barely visible.

In the fetus, the third mesomere is square in shape, with a proximo-lateral extension (Fig. 1b.8 A). This extension could correspond to the second pre-axial radial in a fragmentation process of this early mesomere. The dorsal ridge is longitudinal and in medial position. From pup 1 onwards, the third mesomere has its boomerang shape and its well-developed ridge, as in the adult (Fig. 1b.8 B-E). As for the previous mesomeres, the ventral side of the third mesomere has an important swelling that becomes flatter from pup 2 onwards.

• The fourth mesomere (mes.4)

In the adult stage, this mesomere is trapezoid in shape, less wide than the previous mesomeres and without the presence of a medial process (Fig. 1b.6). The proximal edge of the mesomere is slightly concave and the distal edge slightly convex, whereas the lateral and medial edges are straight. This mesomere is the only one in contact with the post-axial elements. The medial edge of this mesomere is thinner than the lateral edge. As for the previous mesomeres, there is a small ridge on the dorsal side of this mesomere. This ridge has a proximo-distal orientation and decreases in height from proximal to distal. This element is not aligned with the previous axial elements, but is medially shifted. It is surrounded by the pre-axial radial 3, the pre-axial radial 4, the distal radial, and the post-axial radials from its pre-axial side (corresponding to its lateral edge) to its post-axial side (corresponding to the medial edge).

In the fetus, the fourth mesomere of the right fin presents an arrowhead-shape, wider than long with a strongly concave proximal edge (Fig. 1b.8 A). The shape of the left mesomere is elongated, with a slightly concave proximal edge (Fig. 1b.10 A). From pup 1 onwards, the mesomere has its trapezoidal shape, as in the adult (Fig. 1b.8 B-E).

2) The pre-axial elements

The pre-axial elements are situated on the lateral edge of the pelvic fin. The organization of the radial elements along the metapterygial axis is similar on the pelvic fin and on the pectoral

fin, except for the presence of a pre-axial radial (called pre-axial radial 0) on the pelvic fin only (Fig. 1b.7). As in the pectoral fin (Millot and Anthony, 1958; Mansuit et al., 2020) there is an important difference in morphology of the pre-axial radial elements between the most proximal elements (pr.rad. 0-2) and the distal elements (pr.rad. 3-4).

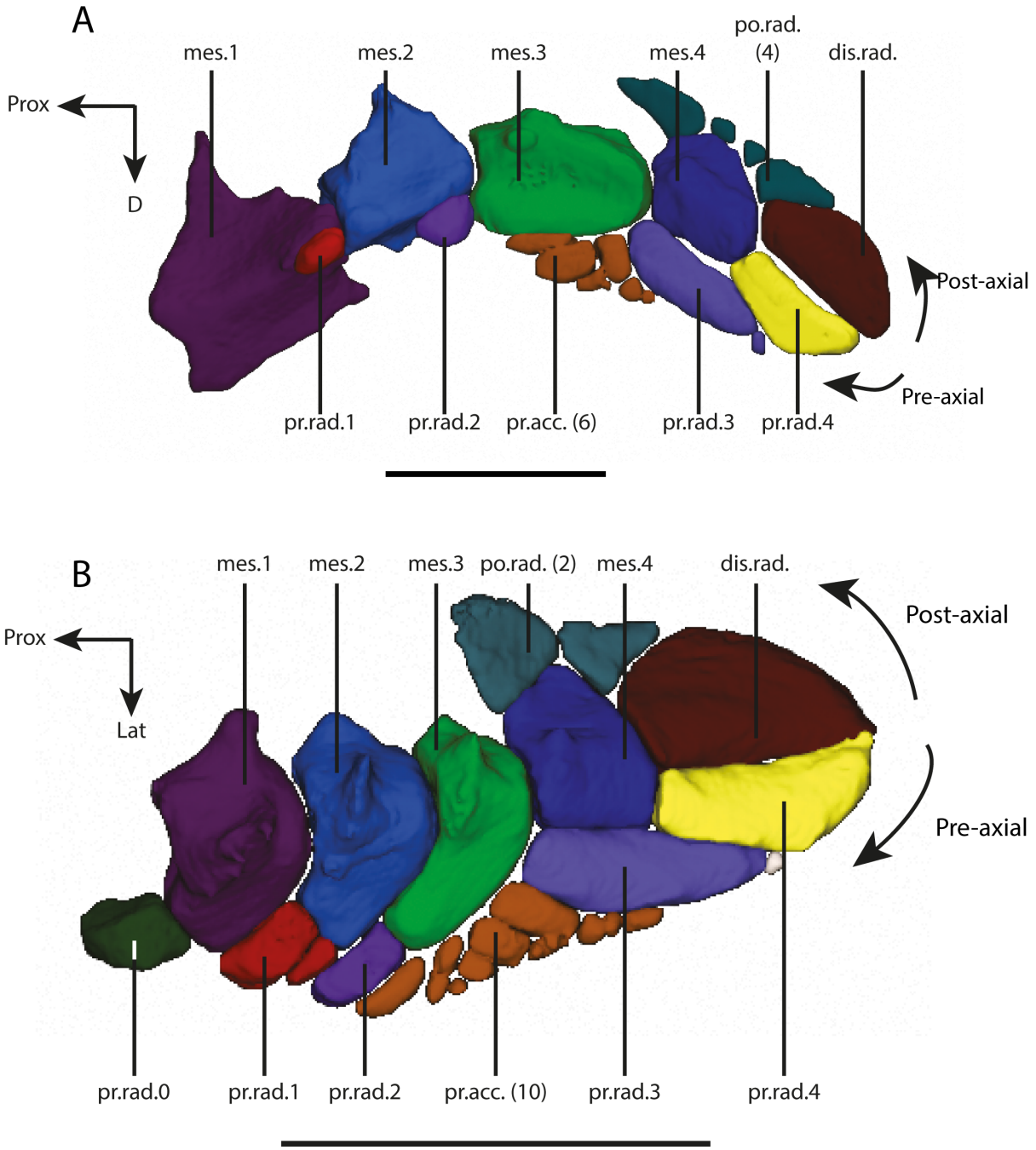

Figure 1b.7: *Latimeria chalumnae* — pup 2. Comparison between the left pectoral (a) and pelvic fin (b). The pectoral fin is reversed to have a better comparison with the pelvic fin. The organization of the endoskeletal elements of the pectoral and pelvic fins is the same, except for the presence of the preaxial radial 0 on the pelvic fin. mes., mesomere; po.rad., postaxial radial; pr.acc., preaxial accessory elements; pr.rad., preaxial radial. Scale bar = 10 mm

• The pre-axial radial 0 (pr.rad.0)

In the adult stage, this element has a square shape and lies in the prolongation of the lateral edge of the first mesomere. It is in contact with the ventral side of the latero-distal part of the pelvic girdle (Fig. 1b.6). The medial articular surface of the pre-axial radial 0, in contact with the pelvic girdle, is slightly concave.

In the fetus, this element is rectangular in dorsal view with a triangular section (Fig. 1b.8 A). From pup 1 onwards, this element is square in shape (Fig. 1b.8 B-E).

• The pre-axial radial 1 (pr.rad.1)

In the adult stage, this element forms the prolongation of the lateral edge of the second mesomere and is in contact with the lateral part of the distal edge of the first mesomere (Fig. 1b.6). The pre-axial radial 1 is formed by two parts, a large and rectangular proximal element and a small distal element with a triangular shape.

In the fetus, this element is single and elongated (Fig. 1b.8 A). In pup 1, this element is also single and rectangular in shape (Fig. 1b.8 B). In pup 2, the pre-axial radial 1 is fully formed and composed of two elements (Fig. 1b.8 C-E). In the juvenile, only one element can be reconstructed from the MRI scans but this may be due to the lack of precision in the MRI data (Fig. 1b.8 D).

• The pre-axial radial 2 (pr.rad.2)

In the adult stage, the pre-axial radial 2 forms the prolongation of the lateral side of the third mesomere and lies in contact with the lateral part of the distal edge of the second mesomere (Fig. 1b.6). The pre-axial radial 2 is formed by two elements, a basal square element, adjacent to the mesomere 3, and a rectangular element aligned with the basal element (Fig. 1b.7 B). This element carries fin rays 1-6 on its dorsal side, whereas it only carries the fin rays 1-4 inserting more distally on its ventral side (Fig. 1b.9).

In the fetus, this element does not appear individualized from the mesomere 3. From pup 1 onwards, the pre-axial radial 2 has its adult shape, with its elongated rectangular shape and the two aligned pieces (Fig. 1b.8 B). There is some variation in the morphology of this element as in pup 2 and the juvenile specimens the pre-axial radial 2 only consists of a single elongated element (Fig. 1b.8 C-D), instead of two aligned elements (Fig. 1b.8 B, E). However, these

observations could be due to the low resolution of the MRI data of the juvenile specimen.

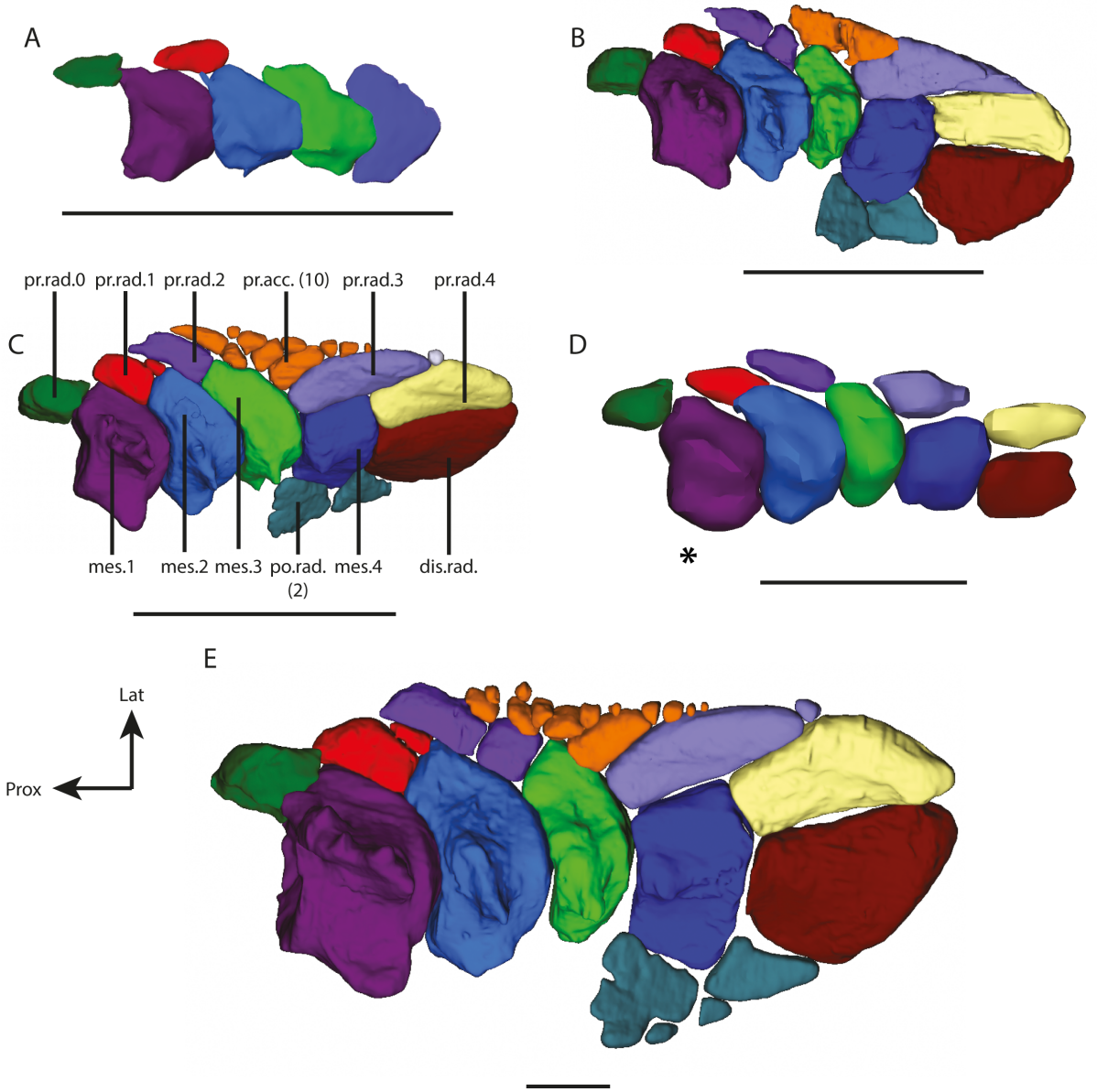

Figure 1b.8: *Latimeria chalumnae*. Right (a – d) and left (e - mirror) pelvic fin of five different stages in dorsal view. a: fetus, b: pup 1, c: pup 2, d: juvenile, e: adult. * : The juvenile was scanned using magnetic resonance imaging (MRI) at a low resolution, which did not allow the segmentation of the smallest elements (po.rad., pr.acc.). Corresponding elements of the fin are indicated in the same color. mes., mesomere; po.rad., postaxial radial; pr.acc., preaxial accessory elements; pr.rad., preaxial radial. (a) Scale 2 mm; (b – e) Scale bar = 10 mm

- The pre-axial radial 3 (pr.rad.3)

In the adult stage, the pre-axial radial 3 is a thin and elongated element, longer than the fourth mesomere, with three straight edges and one distal convex edge (Fig. 1b.6). The proximal edge of this element is straight and articulates with the third mesomere. A very small globular element is present at its distal tip. This pre-axial radial carries the fin rays 10-13 (Fig. 1b.9).

In the fetus, this element is not separated from the fourth mesomere (Fig. 1b.8 A, Fig. 1b.10 A). In pup 1, the pre-axial radial 3 is thin and elongated, without a separated tip (Fig. 1b.8 B). Its medial edge is straight and its latero-distal corner forms a concave angle to fit a pre-axial accessory element. This angle could correspond to some elements of pre-axial accessory elements that are segmented later in the pup 2 to form the three most distal elements (Fig. 1b.8 B-C). On the left fin, the distal part of the radial is surrounded by the pre-axial radial 4. From pup 2 onwards, this element has its adult shape, with an elongated trapezoidal shape and a separated distal small element (Fig. 1b.8 C-E).

- The pre-axial radial 4 (pr.rad.4)

The pre-axial radial 4, situated at the distal end of the fin endoskeleton, closely resembles the mirror image of the distal radial. As the pre-axial radial 3 this element is elongated with three straight edges and a convex distal edge (Fig. 1b.6). This element carries the fin rays 14-18 (Fig. 1b.9).

In the fetus, the data do not allow the separation of the pre-axial radial 4 from the fin rays and muscles on the right fin (Fig. 1b.8 A), so this element was not segmented. However, it is assumed that the pre-axial radial 4 is already present on the right fin. On the left fin, this radial is not separated from the distal radial (Fig. 1b.10 A). In pup 1, there is a bilateral asymmetry, since the medial edge of the pre-axial radial 4 is straight on the right fin (Fig. 1b.8 B), but concave on the left fin, forming a space between this element and the distal radial (Fig. 1b.10 B). The lateral edge of the pre-axial radial 4 forms an angle that surrounds the distal part of the pre-axial radial 3. From pup 2 onwards, the pre-axial radial 4 has the same trapezoidal shape as described for the adult (Fig. 1b.8 C-E).

- The pre-axial accessory elements (pr.acc.)

In adult stage, these small elements (called “éléments accessoires de la troisième pièce radiale préaxiale” by Millot and Anthony, 1958) are positioned in a patch between the distal edges of the third mesomere, the pre-axial radial 2, and the lateral edge of the pre-axial radial 3 (Fig. 1b.6). According to Millot and Anthony (1958), the pelvic fin presents four of these elements at the adult stage. However, both our segmentation of the scan of the pelvic fin and the observation of the isolated fin show a variation in the number of pre-axial accessory elements. Indeed, there are 13 elements in adult stage CCC 27 (Fig. 1b.6, Fig. 1b.8 E), whereas there are at least

five accessory elements in the isolated fin of CCC 7. The difference in numbers of elements observed in the different fins can be explained by the size of the smallest elements, not visible to the naked eyes and hidden by dermal fin rays covering them. The pre-axial accessory elements carry the fin rays 7-9 on the dorsal side of the fin and the fin rays 5-9 on the ventral side of the fin (Fig. 1b.9).

These elements are not present in the fetus, and appear at the pup 1 stage (Fig. 1b.8). In the pup 1 stage there are only two elements, as large as the pre-axial radials 2 (Fig. 1b.8 B). These two elements become fragmented during development since there are at least ten small elements in pup 2 (Fig. 1b.8 C), and 13 elements in the adult. In the juvenile, we assume that the pre-axial accessory elements are present, but the MRI data did not allow the visualization of the pre-axial accessory elements.

3) The post-axial elements

• The distal radial (dis.rad.)

In adult stage, the distal radial is similar in shape to the pre-axial radial 4 as a mirror image, although almost twice as wide (Fig. 1b.6). It has three more or less straight edges and a convex distal edge. It carries the fin rays 19-27 (Fig. 1b.9).

In the fetus, only the left distal radial could be segmented (Fig. 1b.10 A). We assumed that the right distal radial is also present at this stage, but as for the pre-axial radial 4, the data did not allow the separation of this element from the muscles and the fin web. This element is small and square except for its proximal edge that is slightly concave. In pup 1, the left fin presents an ovoid space between the distal radial and the pre-axial radial 4 (Fig. 1b.10 B). Such a space is not present on the right fin (Fig. 1b.8 B). Its medial edge forms an angle that surrounds the post-axial radials in the left fin. From pup 2 onwards, the distal radial is fully formed with the trapezoidal shape observed in adult stage (Fig. 1b.8 C-E). According to Millot and Anthony (1958) there is a longitudinal ridge on the dorsal side of this element, but such a ridge does not appear on the 3D modellings nor on the observed isolated pelvic fin.

• The post-axial radials (po.rad.)

The post-axial radials are located at the medial edge of the pelvic fin in articulation with the fourth mesomere and the distal radial. In adult stage, Millot and Anthony (1958) described three elements among the post-axial radials. The proximal element presents a large triangular

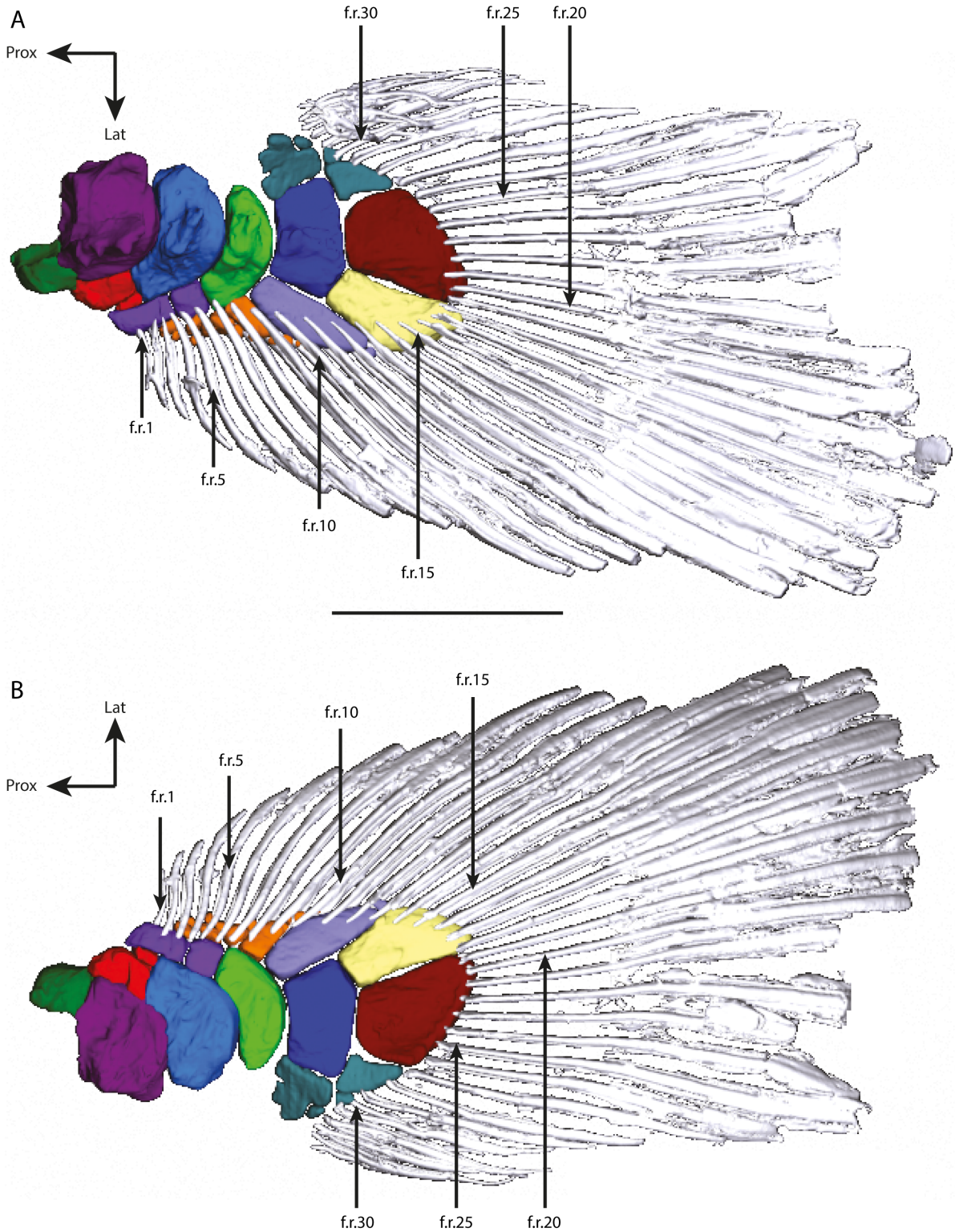

Figure 1b.9: *Latimeria chalumnae* — Adult stage. Insertion of the fin rays on the endoskeletal elements of the left fin in dorsal (a) and ventral view (b). The insertion of the fin rays on the preaxial edge of the fin is more proximal on the dorsal edge compared to the ventral edge. f.r., fin ray. Scale bar = 50 mm

shape, and is located on the medial edge of the fourth mesomere. On the left fin of CCC 27, this element is split into a large piece and a small one (Fig. 1b.6), whereas there is only one proximal element on the right fin, as is observed for the isolated prepared fin of CCC 7 and as

described by Millot and Anthony (1958). The distal element is slightly smaller, with a quadrangular shape and located on the medial part of the distal edge of the fourth mesomere and on the medial edge of the distal radial (Fig. 1b.6). The third element is very small compared to the other post-axial radials, triangular-shaped, and located between the proximal and the distal one. The post-axial radials carry the fin rays 28-34 (Fig. 1b.9).

In the fetus these elements cannot be individually identified or separated from the mesomere 4 in the right fin (Fig. 1b.8 A; Fig. 1b.10). In the pup 1 and pup 2 the post axial radials are well developed, but with only two elements (Fig. 1b.8 B- C).

4) The fin rays (Fig. 1b.9)

The pelvic fin in adult stage present 37 fin rays, which are numbered 1 from the pre-axial (lateral) to 37 at post-axial (medial) side of the fin. As for the pectoral fin, the proximal part of each fin ray is bifurcated, one branch inserting on the dorsal face of the fin and one branch inserts on the ventral face of the fin. The first ray is very small, and the next rays become longer along the pre-axial side of the fin, up to the axis of the fin, to progressively decrease in size along the post-axial side of the fin. As for the pectoral fin, the rays of the pre-axial side of the fin insert largely on the pre-axial elements, whereas the rays on the post-axial side of the fin insert only on the medial edges of the distal radial and the post-axial radials. The three last fin rays 35-37 are free and do not insert on fin elements. The fins rays are inserted more proximally on the dorsal than on the ventral side on the pre-axial side of the fin.

Discussion

As discussed in our previous study (Mansuit et al., 2020), even if the gestation time for coelacanths is estimated at more to 13 months (Hureau and Ozouf, 1977), it is not possible to precisely determine the time between the different stages.

Morphology of the pelvic girdle

Unlike the pectoral girdle, the pelvic girdle is only formed by a unique endoskeletal bone as described by Millot and Anthony (1958). Unlike in lungfishes as *Neoceratodus* (Boisvert et al., 2013) the two hemi-girdles are not fused (Fig. 1b.4 C) but only linked by ligaments (Millot and Anthony, 1958). The general shape of the pelvic girdle of *Latimeria chalumnae* is similar to what

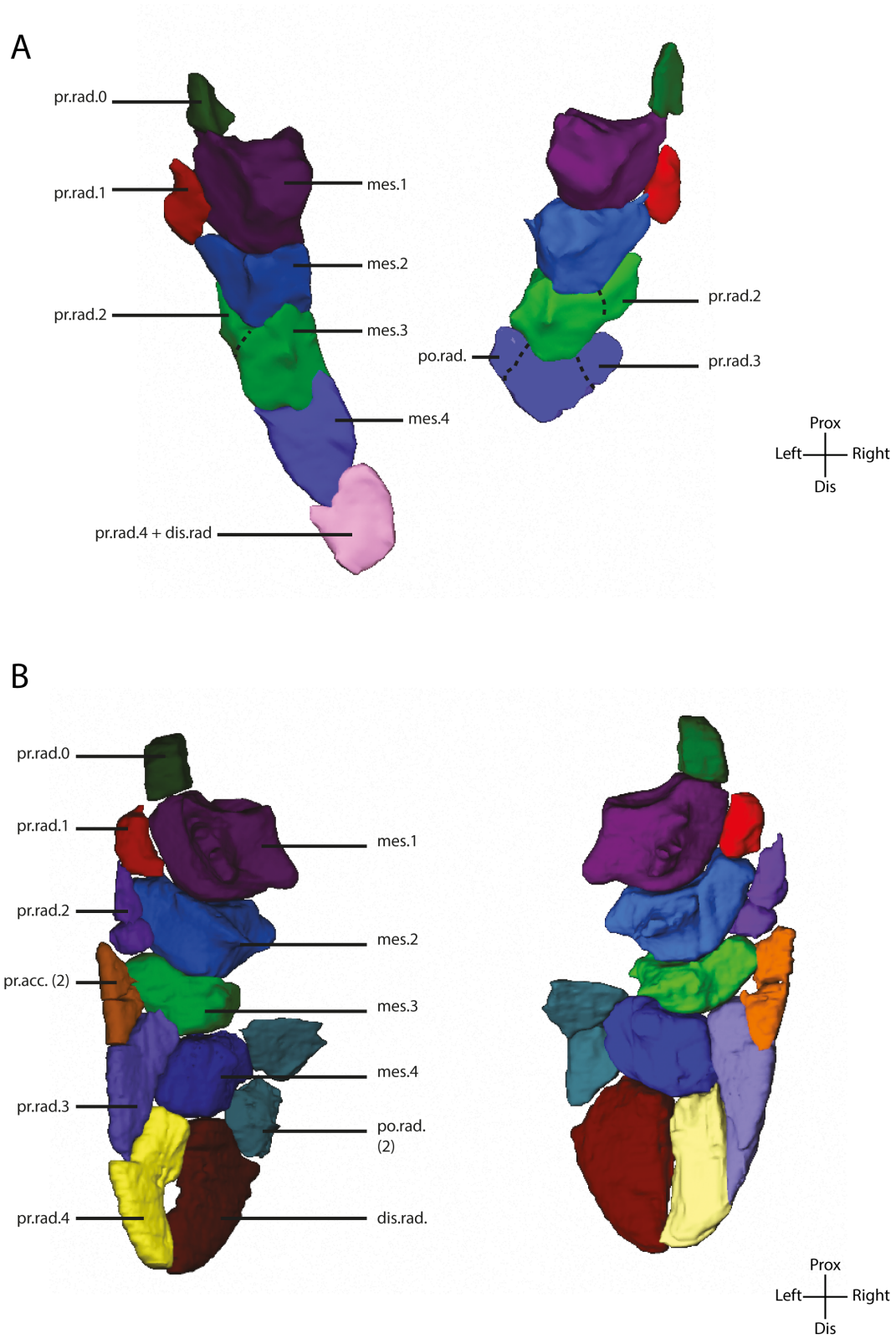

Figure 1b.10: *Latimeria chalumnae* — Fetus (a) and pup 1 (b) stages. Right and left pelvic fins in dorsal. Dotted lines show the supposed splitting zone between the mesomere and the preaxial and postaxial elements. (b) There is an asymmetry between the right and left fin in the pup 1 stage, on the distal part of the fin. mes., mesomere; po.rad., postaxial radial; pr.acc., preaxial accessory elements; pr.rad., preaxial radial. Not to scale

is observed in fossil coelacanths with an anterior rod-like process, a lateral and a medial processes (Forey, 1998). According to Forey (1998), the lateral process corresponds to the ilium (iliac process of Coates and Ruta, 2007), the medial process to the ischium (ischial process of Coates and Ruta, 2007) and the anterior process to the pubis of the pelvic girdle of tetrapods. However, the homology between the lateral and medial processes with the illium and ischium remains uncertain (Ahlberg, 1989). Therefore we preferred to use the neutral terminology proposed by Millot and Anthony (1958) (i.e., medial and lateral processes, and anterior process) to avoid any ambiguities regarding the homology of these structures. In extant tetrapods, the ilium, ischium and pubis are formed through different ossification centers (Malashichev, 2001; Ročková and Roček, 2005; Maxwell and Larsson, 2009). In the extant coelacanth *Latimeria*, as in lungfish (Schultze, 1986) the girdle is cartilaginous (Millot and Anthony, 1958) and there is only an ossification of the anterior part of the girdle and medial process, but not for the lateral process (Fig. 1b.2 E, Fig. 1b.3, Fig. 1b.4). Moreover, the ossification of the pelvic girdle begins at the anterior process of the girdle, subsequently extending to the medial process of the girdle (Fig. 1b.5). Consequently, only a single ossification center appears to be present in the pelvic girdle of *Latimeria*. Only based on anatomical observations, it is thus not possible to assign a homology to the different parts of the girdle in *Latimeria* relative to the different bones of the girdle of tetrapods.

The anterior process/blade of the pelvic girdle seems to be common in actinopterygian fishes (e.g. Andrews and Westoll, 1970; Grandel and Schulte-Merker, 1998; Faustino and Power, 1999; Yamanoue et al., 2010) and sarcopterygian fishes (Andrews and Westoll, 1970; Forey, 1998; Boisvert et al., 2013). According to Andrews and Westoll (1970), this anterior process forms an insertion area for abdominal muscles and ligaments. In *Latimeria*, however, only the extremity of this process supports the abdominal muscles. The main part of the blade forms the attachment site for the pelvic fin muscles (Millot and Anthony, 1958) (personal observations).

As for the articular head of the pectoral girdle (Millot and Anthony, 1958), the acetabulum of the pelvic girdle of *Latimeria* is convex. This convex articular surface is a feature shared by coelacanths and dipnomorphs (Shubin, 1995; Boisvert et al., 2013). In tetrapodomorphs, the pelvic girdle shows a concave acetabulum, where the first mesomere fits (Ahlberg, 1989; Shubin, 1995; Boisvert et al., 2013). A concave acetabulum was considered as the primitive condition for sarcopterygians (Ahlberg, 1989), and the convex acetabulum of coelacanths and dipnomorphs as a derived character. Even if the precise interrelationships of sarcopterygians

remain debated, the current consensus presents coelacanths as sister-taxa of tetrapods and lungfishes (e.g. Ahlberg, 1991; Cloutier and Ahlberg, 1996; Friedman et al., 2007; Amemiya et al., 2013). It thus appears that a convex acetabulum is the primitive condition for sarcopterygians.

The micro-tomographic imaging highlights, for the first time, the presence of a dense surface around part of the pelvic girdle, and the presence of a dense trabecular system within the girdle (Fig. 1b.4 B). The pelvic girdle of *Latimeria* is cartilaginous (Millot and Anthony, 1958; Forey, 1998), and this dense surface and trabecular system might be an endochondral ossification of the girdle. The presence of a trabecular system in the pelvic girdle of *Latimeria* might reinforce its structural resistance when loaded by pelvic muscle forces. Indeed, many *levator* and *depressor* muscles of the pelvic fin insert on the anterior part of the girdle and on the medial process (Millot and Anthony, 1958) (personal observations). In tetrapods, it has been shown that the ossification of the bones is influenced by muscular activity during the embryonic development (Hall, 1986; Newman and Müller, 2005; Boisvert et al., 2013). It is therefore likely that the same process occurs in *Latimeria* where the young develop in the mother and likely show muscular contractions before birth. The ossification of the bone occurs only from the pup 1 stage. Forey (1998) noted that the pelvic girdle of extinct coelacanths often presents an open concave posterior end, and that the acetabulum is missing. It could be assumed that only the ossified part of the pelvic girdle is preserved in the fossil record, and that the cartilaginous posterior part of the girdle does not fossilize. The trabecular system highlighted in *Latimeria* has never been described in the fossil records for coelacanths and other osteichthyan fishes, and remains to be determined whether this feature is specific to *Latimeria* or if other bony fishes possess a trabecular system in the pelvic girdle.

Morphology of the pelvic fin

In *Latimeria*, the general organization of the pelvic fin endoskeleton is similar to that of the pectoral fin (Millot and Anthony, 1958; Panchen and Smithson, 1990), particularly the distal part of the fin (pr.rad. 3-4, pr.acc., dis.rad., po.rad.) (Fig. 1b.7). This endoskeletal morphology of the pectoral and pelvic fins/limbs is shared by all sarcopterygians (Rosen et al., 1981). In all crown-sarcopterygians these paired appendages are connected to their respective girdle via a mono-basal articulation (Rosen et al., 1981; Janvier, 1996; Clack, 2012), whereas stem-sarcopterygians are assumed to have a poly-basal fin articulation (Zhu and Yu, 2009). In *Latimeria* and in other sarcopterygian fishes, the pelvic fin is smaller than the pectoral one (e.g.

Andrews and Westoll, 1970; Ahlberg, 1989; Forey, 1998; Boisvert, 2005; Jeffery et al., 2018). The major difference between the pelvic and pectoral fins, in Latimeria, lies in the presence of a pre-axial radial 0, which articulates with the pelvic girdle and the first mesomere (Fig. 1b.7 B). This element is absent in the pectoral fin (Fig. 1b.7 A). The pre-axial radial 0 was previously described (Millot and Anthony, 1958) and is also present in the pelvic fin of the Triassic coelacanth *Laugia groenlandica* (Stensiö, 1932) (specimen NHMD 152716, personal observation), but never received developmental or phylogenetic consideration. Indeed, the presence of this small element questions the mono-basal condition of the pelvic fin of *Latimeria* and coelacanths in general, and may question the synapomorphy of crown-sarcopterygians (a mono-basal articulation of paired fins (Rosen et al., 1981; Janvier, 1996; Zhu and Yu, 2009)). The development of the pelvic fin suggests that the presence of this element in contact with the girdle is due to the particular morphology of the mesomeres. This element may correspond to the pre-axial radial 1 of the pectoral girdle (see below). Thus, the pluri-basal condition of the pelvic fin of Latimeria would be a specificity of coelacanths.

Although the general organization of the endoskeleton of the pelvic and pectoral fins are similar, some differences can be observed (Fig. 1b.7). The mesomeres of the pectoral fin are longer than wide, with a quadrangular shape (Millot and Anthony, 1958; Mansuit et al., 2020). By contrast, the mesomeres of the pelvic fin are shorter than wide with an arc shape, dorso-ventrally flattened, with a ridge on their dorsal side. These differences between the shape of the mesomeres of the pelvic and pectoral fin appears to be also present in the Triassic coelacanth *Laugia groenlandica* (Stensiö, 1932) (personal observations).

There are marked differences in the size and shape of the most proximal radial elements between the pectoral and pelvic fins. The pre-axial radials 1-2 of the pectoral fin are small compared to the mesomeres, ovoid in shape, and in contact with the distal part of the associated mesomere (Fig. 1b.7 A). By contrast, the pre-axial radials 1-2 of the pelvic fin are proportionally larger and in contact with both the associated and the following mesomeres (Fig. 1b.6, Fig. 1b.7 B). In the fossil tetrapodomorph fishes *Eusthenopteron* and *Panderichthys*, the pre-axial radials 1-2 of the pelvic fin have a similar shape, although slightly smaller, than those of the pectoral fin (Andrews and Westoll, 1970; Boisvert, 2005). Their morphology is different from that of *Latimeria*: they are elongated elements that articulate with the distal edge of the associated mesomere, and more or less parallel to the long edge of the following mesomere.

According to Forey (1998), the pelvic fin of *Latimeria* presents an important degree of asymmetry to the central axis compared to the pectoral fin, i.e. the organization and arrangement of the elements is different between the pre-axial and the post-axial edge of the fin. As for the pectoral fin (Millot and Anthony, 1958; Mansuit et al., 2020), the arrangement of the pre- and post-axial elements along the metapterygial axis of the pelvic fin of *Latimeria* is asymmetrical. The mesomeres of the pelvic fin are all associated with pre-axial radials, whereas only the fourth mesomere is associated with post-axial elements (post-axial radials and distal radial). Moreover, the presence of the pre-axial radial 0 on the pelvic fin, not present on the pectoral fin, increases the asymmetry to the central axis of the pelvic fin. However, as for the pectoral fin, the most proximal pre-axial radials (0-2) of the pelvic fin are small and globular or rectangular shape, whereas the distal pre-axial radials (3-4) are thin and elongate (Millot and Anthony, 1958) (Fig. 1b.7). This difference of shape is related to muscle insertions. Indeed, some muscles insert on the pre-axial radials 0-2, whereas for the pre-axial radial 3-4, the muscles inserted at the base of the fin rays that are associated with the radials (Mansuit et al., in prep.). Considering the general endoskeletal arrangement, the pelvic fin of *Latimeria* shows a short lobe-shaped silhouette compared to that of the more elongate lobed pectoral fin. The insertion of the fin rays on the fin is also more asymmetrical on the pelvic fin compared to the pectoral fin (Millot and Anthony, 1958; Friedman et al., 2007). Fin rays of the pelvic fin insert more proximally on the pre-axial side than on the post-axial side (Fig. 1b.9) compared to the pectoral fin where the fin web shows a more symmetrical arrangement around the metapterygial axis. However, as for the pectoral fin, the most proximal pre-axial radials (pre-axial radial 0-1) are not associated with the pelvic fin rays. An asymmetrical arrangement of the pelvic fin rays along the metapterygial axis has also been suggested in the Triassic coelacanth *Laugia groenlandica* (Stensiö, 1932; Forey, 1998). An asymmetry is also present on the fin ray arrangements between the dorsal and ventral sides of the pelvic fin. Indeed, the fin rays insert more proximally on the dorsal side of the fin than on the ventral side (Fig. 1b.9). This asymmetrical coverage of the paired fin rays is also shared by the fossil coelacanths *Laugia groenlandica* (Stensiö, 1932; Forey, 1998), the extant lungfish *Neoceratodus* and fossil tetrapodomorph fishes, such as *Eusthenopteron* and *Tiktaalik* (Stewart et al., 2019).

Development of the pelvic appendage

The most pronounced changes in the pelvic girdle morphology occurs between the fetus and pup 1, and notably entail the elongation of the anterior part of the girdle (Fig. 1b.5 A-B). The elongation of the girdle during the development seems to be common in osteichthyan fishes,

since it is observed both in actinopterygians, for example in *Pagrus major* (Matsuoka, 1985), *Chanos chanos* (Taki et al., 1986), *Danio rerio* (Grandel and Schulte-Merker, 1998) and *Sparus aurata* (Faustino and Power, 1999), and in the lungfish *Neoceratodus forsteri* (Boisvert et al., 2013). However, the pelvic girdle mainly grows in a posterior direction in the axolotl *Ambystoma mexicanum* (Boisvert et al., 2013), whereas the pubis has a small anterior growth.

Although very similar, the development of the pelvic fin appears to lag behind that of the pectoral fin in *Latimeria*. The assumption of a delay in the development of the pelvic appendage is based on the morphology of the endoskeletal elements observed in the fetus. At this stage, all mesomeres of the pectoral fin are formed, and the radial elements are present, at least as cartilaginous plates. However, most of the radial elements are not differentiated from the mesomere 4 and the distal radial in the pelvic fin (Fig. 1b.8; Fig. 1b.10 A), which suggests that its development is delayed compared to the pectoral fin. A delay in the development of the pectoral and pelvic appendages is also observed in chondrichthyans (Ballard et al., 1993; Didier et al., 1998; Ziermann et al., 2017), actinopterygians (Grandel and Schulte-Merker, 1998; Faustino and Power, 1999) and sarcopterygians (Joss and Longhurst, 2001; Boisvert et al., 2013). Therefore, *Latimeria* likely follows the general gnathostome pattern of paired appendages development. In *Latimeria* fetus, only the most proximal pre-axial radials (pr.rad. 0-1) are present in the pelvic fin (Fig. 1b.8). However, from pup 1 stage onwards all the elements of the fin are present. Contrary to what is observed during the development of the pectoral fin (Mansuit et al., 2020), there is no cartilaginous plate around the metapterygial axis of the pelvic fin.

Based on the comparison of the morphology of the mesomeres during the development, we suggest a developmental mechanism for the endoskeletal elements of the pelvic fin. Along the pre-axial edge of the fin, the distribution of the radials matches that of the mesomeres (e.g. mes.1 and pr.rad.0) in the pups and adult. In the fetus, only the radial 0 and 1 are present. In addition, the mesomere 3 presents a general shape that is different from that observed in later stages, with the presence of a well-developed proximo-lateral extension (Fig. 1b.8; Fig. 1b.10 A). Similarly, the mesomere 4 (observed in the right pelvic fin), which is the most distal endoskeletal element in the fetus fin, has an arrow-head shape with lateral and medial extensions around the distal end of the mesomere 3. These lateral extensions of the mesomeres 3 and 4 are lost in later developmental stages (Fig. 1b.8), while there is a progressive increase in the number of elements on the pre-axial side of the fin. An additional pre-axial radial and

two pre-axial accessory elements are observed in pup 1, and the number of pre-axial accessory elements increases in pup 2 (10) and in the adult (13) (Fig. 1b.8). This pattern suggest that the pre-axial radials are formed through the fragmentation of the radial extension of the adjacent mesomere, following a proximo-distal sequence during the development (i.e. the first mesomere splits first). In this scenario, the extension of mesomere 3 observed in the fetus gives rise to the pre-axial radial 2 in the pup. From pup 1 onwards, a series of pre-axial and post-axial radials surrounds the mesomere 4. We suggest that these elements derive respectively from the lateral and medial extensions of the mesomere 4 observed in the fetus. The distal end of the left fin is formed by a distal plate in the fetus, which might correspond to the distal radial and the pre-axial radial 4 from pup 1 onwards (Fig. 1b.10). Yet, additional developmental stages are needed to better understand the origin of the distal elements of the pelvic fin, such as the pre-axial radial 3, and the potential contribution of the mesomere 4 and distal plate in the formation of these elements.

The formation of the pre-axial radials is not clearly understood in the extant lungfish *Neoceratodus*. Previous studies suggest two different patterns of development to explain their formation. In the first scenario, the radials arise *de novo* process (Joss and Longhurst, 2001): they are formed by a distinct mesenchymal condensation and are unconnected to other elements (Shubin and Alberch, 1986; Johanson et al., 2007). In the second scenario, the radials arise from the fragmentation of the associated mesomere (Joss and Longhurst, 2001), i.e. the element is formed by a continuous plate of precartilage that subsequently breaks up into two separate elements (Shubin and Alberch, 1986). This second scenario could corroborate our hypothesis of the splitting of the mesomere. However, we suggested previously that the pre-axial radials are formed by the fragmentation of the following mesomeres, and not the associated mesomeres as in *Neoceratodus*. Since the mesomeres of the pelvic fin of *Latimeria* have an arc-shape it is possible that the position of the pre-axial radials is different compared to that observed for the pectoral fin. If so, this would suggest that the pre-axial radial 0 of the pelvic fin corresponds to the pre-axial radial 1 of the pectoral fin (and the pr.rad.1 of pelvic fin to the pr.rad. 2 of the pectoral fin). The pre-axial radial 3 of the pelvic fin would then not correspond to any pre-axial radial in the pectoral fin, and this element could have been lost in the pectoral fin. If there is a correspondence between pectoral and pelvic pre-axial radials, the poly-basal condition of the pelvic fin in Latimeria may be a derived character in sarcopterygians due to the shape of the mesomeres. Concerning the formation of the post-axial elements, these elements are supposed to arise *de novo* in *Neoceratodus* (Joss and Longhurst, 2001; Johanson et al., 2007),

but a fragmentation process cannot be excluded in *Latimeria*, as explained above.

Conclusion

As in other vertebrates, the development of the pelvic fin occurs later than that of the pectoral fin in *Latimeria*: many elements of the endoskeleton are not formed yet in the earliest stage sampled here. In the fetus, only the four mesomeres and the most proximal radial elements (pre-axial radial 0-1) are formed. The mesomeres 3 and 4 show prominent extensions in the fetus, but not in later stages. We suggest that the radial elements (pre-axial radials 0-4, pre-axial accessory elements and post-axial radials) originate from the fragmentation of the mesomeres (e.g. pr.rad. 0 fragments from mes. 1). Since the pectoral and pelvic fins show a similar organization of their endoskeleton and development, it is most probable that the same mechanism underpins the formation of both paired fins. The progressive ossification of the pelvic girdle and the formation of a trabecular system in the adult stage is documented here. This trabecular system might reinforce the cartilaginous girdle to withstand the muscle forces exerted during locomotion. However, it remains unknown whether this trabecular system is unique to *Latimeria chalumnae* or shared by other extinct coelacanths or early sarcopterygians. Finally, the presence of a pre-axial element in contact with the pelvic girdle from the earliest stage of development onwards questions the mono-basal condition of the pelvic fin in *Latimeria*. The presence of this element raises questions a synapomorphy of crown-sarcopterygians: the mono-basal articulation of paired fins. But the particular shape of the mesomeres of the pelvic fin and the process of development of pre-axial radials may explain the presence of this element in contact with the girdle. This element could be homologous to the pre-axial radial 1 on the pectoral fin.

Abbreviations

act. = acetabulum; ant.p. = anterior process; lat.p. = lateral process; med.pro. = medial process; mes. = mesomere; po.rad. = post-axial radial; pos.p. = posterior part; pr.acc. = pre-axial accessory elements; pr.rad. = pre-axial radial ps.pro. = postero-superior process.

Data Availability Statement

The synchrotron data will be available on the ESRF data- base, at the following address: http://paleo.esrf.fr/ (fetus, pup1, pup2, juvenile). The CT-scan data are available at the following address: http://coldb.mnhn.fr/catalognumber/mnhn/za/ac-2012-21 (adult). The MRI data will

be available at the following address: https://www.morphosource.org/ (juvenile). All the data are also available by request from the authors.

Acknowledgements

We thank R. Bills and A. Paterson (South African Institute for Aquatic Biodiversity, SAIAB) and D. Neumann (Zoologische Staatssammlung München, ZSM)for the loan of the fetus and pup 2 specimens, respectively. We are grate ful to the European Synchrotron Radiation Facility (ESRF, Grenoble, France) for granting beam time and providing assistance in using beamline ID19 (Proposal EC-1023), and M. Garcia and M. Bellato at AST-RX, plateforme d'accès scientifique à la tomographie à rayons X (UMS 2700, MNHN, Paris, France) for the X-ray tomography scans. We thank F. Goussard (UMR 7207 CR2P MNHN-CNRS-Sorbonne Université, Paris, France) for his assistance in the 3D imaging work. We thank C. Bens and A. Verguin of the Collections de Pièces anatomiques en Fluides of the MNHN de Paris. We thank B. Lindow (Natural History Museum of Denmark) for the loan of fossils of *Laugia groenlandica*. This work was supported by a grant from Agence Nationale de la Recherche in the LabEx ANR-10-LABX-0003-BCDiv, program "Investissements d'avenir" No. ANR-11-IDEX-0004-02.

Author contributions

Rohan Mansuit: Conceptualization; data curation; formal analysis; methodology; software; writing-original draft. Gaël Clément: Conceptualization; data curation; formal analysis; funding acquisition; supervision; validation; writing-review and editing. Anthony Herrel: Conceptualization; data curation; formal analysis; funding acquisition; supervision; validation; writing-review and editing. Hugo Dutel: Formal analysis; methodology; software; validation; writing-review and editing. Paul Tafforeau: Formal analysis; methodology; software; validation; writing-review and editing. Mathieu Santin: Formal analysis; methodology; software; validation; writing-review and editing. Marc Herbin: Conceptualization; data curation; formal analysis; funding acquisition; supervision; validation; writing-review and editing.

Bibliography

Ahlberg, P. E. (1989). Paired fin skeletons and relationships of the fossil group Porolepiformes (Osteichthyes: Sarcopterygii). *Zoological Journal of the Linnean Society*, 96(2):119–166.

Ahlberg, P. E. (1991). A re-examination of sarcopterygian interrelationships, with special reference to the Porolepiformes. *Zoological Journal of the Linnean Society*, 103(3):241–287.

Amemiya, C. T., Alfoldi, J., Lee, A. P., Fan, S., Philippe, H., MacCallum, I., Braasch, I., Manousaki, T., Schneider, I., Rohner, N., Organ, C., Chalopin, D., Smith, J. J., Robinson, M., Dorrington, R. A., Gerdol, M., Aken, B., Biscotti, M. A., Barucca, M., Baurain, D., Berlin, A. M., Blatch, G. L., Buonocore, F., Burmester, T., Campbell, M. S., Canapa, A., Cannon, J. P., Christoffels, A., De Moro, G., Edkins, A. L., Fan, L., Fausto, A. M., Feiner, N., Forconi, M., Gamieldien, J., Gnerre, S., Gnirke, A., Goldstone, J. V., Haerty, W., Hahn, M. E., Hesse, U., Hoffmann, S., Johnson, J., Karchner, S. I., Kuraku, S., Lara, M., Levin, J. Z., Litman, G. W., Mauceli, E., Miyake, T., Mueller, M. G., Nelson, D. R., Nitsche, A., Olmo, E., Ota, T., Pallavicini, A., Panji, S., Picone, B., Ponting, C. P., Prohaska, S. J., Przybylski, D., Saha, N. R., Ravi, V., Ribeiro, F. J., Sauka-Spengler, T., Scapigliati, G., Searle, S. M., Sharpe, T., Simakov, O., Stadler, P. F., Stegeman, J. J., Sumiyama, K., Tabbaa, D., Tafer, H., Turner-Maier, J., Van Heusden, P., White, S., Williams, L., Yandell, M., Brinkmann, H., Volff, J. N., Tabin, C. J., Shubin, N. H., Schartl, M., Jaffe, D. B., Postlethwait, J. H., Venkatesh, B., Di Palma, F., Lander, E. S., Meyer, A., and Lindblad-Toh, K. (2013). The African coelacanth genome provides insights into tetrapod evolution. *Nature*, 496(7445):311–316.

Andrews, S. M. and Westoll (1970). The Postcranial Skeleton of *Eusthenopteron foordi* Whiteaves. *Earth and Environmental Science Transactions of the Royal Society of Edinburgh*, 68(9):207–329.

Ballard, W. W., Mellinger, J., and Lechenault, H. (1993). A Series of Normal Stages for Development of *Scyliorhinus canicula*, the Lesser Spotted Dogfish (Chondrichthyes: Scyliorhinidae). *The Journal of Experimental Zoology*, 267:318–336.

Boisvert, C. A. (2005). The pelvic fin and girdle of *Panderichthys* and the origin of tetrapod locomotion. *Nature*, 438(7071):1145–1147.

Boisvert, C. A., Joss, J. M., and Ahlberg, P. E. (2013). Comparative pelvic development of the axolotl (*Ambystoma mexicanum*) and the Australian lungfish (*Neoceratodus forsteri*): conservation and innovation across the fish-tetrapod transition. *EvoDevo*, 4(3):1–19.

Clack, J. A. (2012). *Gaining Ground, Second Edition: The Origin and Evolution of Tetrapods*. Indiana University Press, Bloomington.

Cloutier, R. and Ahlberg, P. E. (1996). Morphology, Characters, and the Interrelationships of Basal Sarcopterygians. *Interrelationships of Fishes*, pages 445–479.

Coates, M. I. and Ruta, M. (2007). Skeletal Changes in the Transition from Fins to Limbs. In Hall, B. K., editor, *Fins Into Limbs: Evolution, Development, and Transformation*, chapter Chapter 2, pages 15–38. Chicago, the univer edition.

Cubbage, C. C. and Mabee, P. M. (1996). Development of the Cranium and Paired Fins in the Zebrafish *Danio rerio* (Ostariophysi, Cyprinidae). *Journal of Morphology*, 229:121–160.

Cupello, C., Brito, P. M., Herbin, M., Janvier, P., Dutel, H., and Clément, G. (2015). Allometric growth in the extant coelacanth lung during ontogenetic development. *Nature Communications*, 6:8222.

Didier, D. A., Leclair, E. E., and Vanbuskirk, D. R. (1998). Embryonic staging and external features of development of the chimaeroid fish, *Callorhinchus milii* (Holocephali, Callorhinchidae). *Journal of Morphology*, 236(1):25–47.

Faustino, M. and Power, D. M. (1999). Development of the pectoral, pelvic, dorsal and anal fins in cultured sea bream. *Journal of Fish Biology*, 54(5):1094–1110.

Forey, P. L. (1998). *History of the Coelacanth Fishes*. Thomson Science, London, chapman & edition.

Friedman, M., Coates, M. I., and Anderson, P. (2007). First discovery of a primitive coelacanth fin fills a major gap in the evolution of lobed fins and limbs. *Evolution & Development*, 9(4):329–337.

Grandel, H. and Schulte-Merker, S. (1998). The development of the paired fins in the zebrafish (*Danio rerio*). *Mechanisms of Development*, 79(1-2):99–120.

Hall, B. K. (1986). The role of movement and tissue interactions in the development and growth of bone and secondary cartilage in the clavicle of the embryonic chick. *Journal of Embryology and Experimental Morphology*, 93:133–152.

Hureau, J.-C. and Ozouf, C. (1977). Détermination de l'âge et croissance du coelacanthe *Latimeria chalumnae* Smith, 1939 (Poisson, Crossoptérygien, Coelacanthidé). *Cybium*, 2:129–137.

Janvier, P. (1996). *Early vertebrates*. Oxford University Press, Oxford.

Jarvik, E. (1980). *Basic structure and evolution of vertebrates*. London.

Jeffery, J. E., Storrs, G. W., Holland, T., Tabin, C. J., and Ahlberg, P. E. (2018). Unique pelvic fin in a tetrapod-like fossil fish, and the evolution of limb patterning. *Proceedings of the National Academy of Sciences*, 115(47):201810845.

Johanson, Z., Joss, J., Boisvert, C. A., Ericsson, R., Sutija, M., and Ahlberg, P. E. (2007). Fish Fingers : Digit Homologues in Sarcopterygian Fish Fins. *Journal of Experimental Zoology Part B: Molecular and Developmental Evolution*, 308:757–768.

Joss, J. and Longhurst, T. (2001). Lungfish paired fins. In Ahlberg, P. E., editor, *Major Events in Early Vertebrate Evolution*, chapter 21, pages 370–376. London, taylor & f edition.

Jude, E., Johanson, Z., Kearsley, A., and Friedman, M. (2014). Early evolution of the lungfish pectoral-fin endoskeleton: evidence from the Middle Devonian (Givetian) *Pentlandia macroptera*. *Frontiers in Earth Science*, 2(August):1–15.

Lyckegaard, A., Johnson, G., and Tafforeau, P. (2011). Correction of ring artifacts in X-ray tomographic images. *International Journal of Tomography and Statistics*, 18:1–9.

Mabee, P. M. and Noordsy, M. (2004). Development of the paired fins in the paddlefish, *Polyodon spathula*. *Journal of Morphology*, 261(3):334–344.

Mabee, P. M. and Trendler, T. A. (1996). Development of the Cranium and Paired Fins in *Betta splendens* (Teleostei: Percomorpha): Intraspecific Variation and interspecific Comparisons. *Journal of Morphology*, 227:249–287.

Malashichev, Y. B. (2001). Sacrum and Pelvic Girdle Development in Lacertidae. *Russian Journal of Herpetology*, 8(1):1–16.

Mansuit, R., Clément, G., Herrel, A., Dutel, H., Tafforeau, P., Santin, M. D., and Herbin, M. (2020). Development and growth of the pectoral girdle and fin skeleton in the extant coelacanth *Latimeria chalumnae*. *Journal of Anatomy*, 236(3):493–509.

Matsuoka, M. (1985). Osteological development in the red sea bream, *Pagrus major*. *Japanese Journal of Ichthyology*, 32(1):35–51.

Maxwell, E. E. and Larsson, H. C. (2009). Comparative ossification sequence and skeletal development of the postcranium of palaeognathous birds (Aves: Palaeognathae). *Zoological Journal of the Linnean Society*, 157(1):169–196.

Millot, J. and Anthony, J. (1958). *Anatomie de Latimeria chalumnae - Tome I: Squelette, Muscles et Formations de soutien*. CNRS, Paris, cnrs edition.

Millot, J. and Anthony, J. (1965). *Anatomie de Latimeria chalumnae - Tome II: Système nerveux & Organes des sens*. CNRS, Paris.

Millot, J., Anthony, J., and Robineau, D. (1978). *Anatomie de Latimeria chalumnae - Tome III: Appareil digestif, Appareil respiratoire, Appareil urogénital, Glandes endocrines, Appareil circulatoire, Téguments-écailles, Conclusions générales*. CNRS, Paris.

Newman, S. A. and Müller, G. B. (2005). Origination and innovation in the vertebrate limb skeleton: An epigenetic perspective. *Journal of Experimental Zoology*, 304(6):593–609.

Nulens, R., Scott, L., and Herbin, M. (2011). An updated inventory of all known specimens of the coelacanth, *Latimeria* spp. *Smithiana Publications in Aquatic Biodiversity*, 3:1–52.

Paganin, D., Mayo, S. C., Gureyev, T. E., Miller, P. R., and Wilkins, S. W. (2002). Simultaneous phase and amplitude extraction from a single defocused image of a homogeneous object. *Journal of Microscopy*, 206(1):33–40.

Panchen, A. L. and Smithson, T. R. (1990). The pelvic girdle and hind limb of *Crassigyrinus scoticus* (Lydekker) from the Scottish Carboniferous and the origin of the tetrapod pelvic skeleton. *Transactions of the Royal Society of Edinburgh: Earth Sciences*, 81:31–44.

Pouyaud, L., Wirjoatmodjo, S., Rachmatika, I., Tjakrawidjaja, A., Hadiaty, R., and Hadie, W. (1999). Une nouvelle espèce de coelacanthe. Preuves génétiques et morphologiques. *Comptes Rendus de l'Academie des Sciences - Serie III*, 322(4):261–267.

Ročková, H. and Roček, Z. (2005). Development of the pelvis and posterior part of the vertebral column in the Anura. *Journal of Anatomy*, 206:17–35.

Rosen, D. E., Forey, P. L., Gardiner, B. G., and Patterson, C. (1981). Lungfishes, tetrapods, paleontology, and plesiomorphy. *Bulletin of the American Museum of Natural History*, 167(4):159–276.

Sanchez, S., Ahlberg, P. E., Trinajstic, K. M., Mirone, A., and Tafforeau, P. (2012). Three-dimensional synchrotron virtual paleohistology: A new insight into the world of fossil bone microstructures. *Microscopy and Microanalysis*, 18:1095–1105.

Schultze, H. (1986). Dipnoans as sarcopterygians. *Journal of Morphology*, 190(1 S):39–74.

Shubin, N. H. (1995). The Evolution of Paired Fins and the Origin of Tetrapods Limbs. In *Evolutionary Biology*, pages 39–86. Boston, springer edition.

Shubin, N. H. and Alberch, P. (1986). A Morphogenetic Approach to the Origin and Basic Organization of the Tetrapod Limb. *Evolutionary Biology*, 20:319–387.

Smith, J. L. B. (1939). A Living Fish of Mesozoic Type. *Nature*, 143(3620):455–456.

Stensiö, V. E. A. (1932). *Triassic Fishes from East Greenland, collected by the Danish Expeditions in 1929-1931*. Meddelelser om Grønland.

Stewart, T. A., Lemberg, J. B., Taft, N. K., Yoo, I., Daeschler, E. B., and Shubin, N. H. (2019). Fin ray patterns at the fin-to-limb transition. *Proceedings of the National Academy of Sciences*, pages 1–9.

Taki, Y., Kohno, H., and Hara, S. (1986). Early Development of Fin-supports and Fin-rays in the Milkfish *Chanos chanos*. *Japanese Journal of Ichthyology*, 32(4):413–420.

Yamanoue, Y., Setiamarga, D. H., and Matsuura, K. (2010). Pelvic fins in teleosts: Structure, function and evolution. *Journal of Fish Biology*, 77(6):1173–1208.

Zhu, M. and Yu, X. (2009). Stem sarcopterygians have primitive polybasal fin articulation. *Biology Letters*, 5(3):372–375.

Ziermann, J. M., Freitas, R., and Diogo, R. (2017). Muscle development in the shark *Scyliorhinus canicula*: Implications for the evolution of the gnathostome head and paired appendage musculature. *Frontiers in Zoology*, 14(1):1–17.

CHAPTER II

Revision of the muscular anatomy of the paired fins of the living coelacanth *Latimeria chalumnae*

Manuscript submitted

Biological Journal of the Linnean Society

Context of the Chapter II

The muscle anatomy of the paired fins of the African coelacanth was described by Millot and Anthony (1958), in their monograph of the anatomy of the coelacanth. With the scarcity of available specimens of coelacanths in the different worldwide collections, these descriptions are used in different studies that compare the muscle anatomy of the coelacanth with actinopterygian, sarcopterygian fishes or tetrapods (e.g. Boisvert et al., 2013). However, recent studies showed that the muscle anatomy of the skull of *Latimeria* is much more complex than previously described by Millot and Anthony (Dutel et al., 2013, 2015b). With the new functional descriptions of the muscle anatomy of the skull, it was possible to assess the role of the different muscles, to have a functional analysis of the jaw-closing system and to estimate the bite force of the coelacanth (Dutel et al., 2015a), that can be used in an evolutionary context.

The muscular anatomy of the paired fins of *Latimeria* is of high interest in the context of the fin-to-limb transition. In this context, Millot and Anthony's descriptions and new dissections were used to compare the coelacanth anatomy with those of other sarcopterygians (Boisvert et al., 2013; Diogo et al., 2016; Miyake et al., 2016). However, the new dissections focused only on the pectoral fin of the coelacanth and lacked the functional aspect given by the muscles properties. The new detailed descriptions of the muscle anatomy of the pectoral and pelvic fins of *Latimeria* presented in this chapter permit a functional understanding of these two paired fins. Moreover, these results permit to complete the *in vivo* observations of the locomotion of the coelacanth (Fricke and Hissmann, 1992) by characterizing the role of the different paired fins.

The dissections and interpretations of the muscle anatomy of the pectoral fin of *Latimeria* were done in collaboration with Alessia Huby (Laboratory of Functional and Evolutionary Morphology, Department of Biology, Ecology and Evolution, University of Liège, Belgium), that permitted a collaboration for a more global publication on the pectoral and pelvic fins musculatures. The muscles were firstly named according to their function, i.e. the *abductor* muscles on the dorsal edge of the fin and the *adductor* muscles on the ventral edge. However, since the description of the muscle anatomy will be used in a more global context for following studies, and to be compared with other species in the **Chapter III**, it has been decided to revise this nomenclature. Thus, *abductor* muscles are on the lateral face and *adductor* muscles on the medial face of the pectoral fin, similar to the muscles of actinopterygians (e.g. Adriaens et al., 1993; Wilhelm et al., 2015). This nomenclature is so the reverse of that of Millot and Anthony (1958). Indeed,

the authors named the muscles considering the fin in a different reference posture than that used in our study, the pectoral fin perpendicular to the body, with the leading edge of the fin directed forward. Thus, the *abductor* muscles are those inserting on the "dorsal" face of the fin, that corresponds to the medial face with the pectoral fin position along the body with the leading edge in dorsal position.

If the development of the muscle anatomy is of high interest, it is however not possible to dissected embryos and juvenile specimens of coelacanths, due to the scarcity of these specimens. Moreover, it was not possible to virtually dissected the muscular anatomy of these specimens with the imaging data, since most of them (fetus, juvenile, adult) do not have enough contrast to visualize the different muscles bundles, or the muscles were seemingly damaged, dessicated and retracted by the preservative fluid (pup without yolk sac). Only the pup with yolk sac (CCC29.5) permits the visualization of some muscles of the fins, but due to the time-consuming operation of segmentation and the incompleteness of the muscular data, it has been decided to not entertain this work.

It as also been decided to study the joint mobility of the pectoral and pelvic fins of *Latimeria*, in order to determine, among others, if the presence of the supernumerary pre-axial radial 0 on the pelvic fin described on the **Chapter Ib** could imply a limitation in the mobility of the fin relative to the girdle.

Bibliography

Adriaens, D., Decleyre, D., and Verraes, W. (1993). Morphology of the pectoral girdle in *Pomatoschistus lozanoi* De Buen, 1923 (Gobiidae), in relation to pectoral fin adduction. *Belgian journal of zoology*, 123(2):135–157.

Boisvert, C. A., Joss, J. M., and Ahlberg, P. E. (2013). Comparative pelvic development of the axolotl (*Ambystoma mexicanum*) and the Australian lungfish (*Neoceratodus forsteri*): conservation and innovation across the fish-tetrapod transition. *EvoDevo*, 4(3):1–19.

Diogo, R., Johnston, P., Molnar, J. L., and Esteve-Altava, B. (2016). Characteristic tetrapod musculoskeletal limb phenotype emerged more than 400 MYA in basal lobe-finned fishes. *Scientific Reports*, 6:1–9.

Dutel, H., Herbin, M., Clément, G., and Herrel, A. (2015a). Bite Force in the Extant Coelacanth

Latimeria: The Role of the Intracranial Joint and the Basicranial Muscle. *Current Biology*, 25:1228–1233.

Dutel, H., Herrel, A., Clément, G., and Herbin, M. (2013). A reevaluation of the anatomy of the jaw-closing system in the extant coelacanth *Latimeria chalumnae*. *Naturwissenschaften*, 100(11):1007–1022.

Dutel, H., Herrel, A., Clément, G., and Herbin, M. (2015b). Redescription of the hyoid apparatus and associated musculature in the extant coelacanth *Latimeria chalumnae*: Functional implications for feeding. *Anatomical Record*, 298(3):579–601.

Fricke, H. and Hissmann, K. (1992). Locomotion, fin coordination and body form of the living coelacanth *Latimeria chalumnae*. *Environmental Biology of Fishes*, 34(4):329–356.

Millot, J. and Anthony, J. (1958). *Anatomie de Latimeria chalumnae - Tome I: Squelette, Muscles et Formations de soutien*. CNRS, Paris, cnrs edition.

Miyake, T., Kumamoto, M., Iwata, M., Sato, R., Okabe, M., Koie, H., Kumai, N., Fujii, K., Matsuzaki, K., Nakamura, C., Yamauchi, S., Yoshida, K., Yoshimura, K., Komoda, A., Uyeno, T., and Abe, Y. (2016). The pectoral fin muscles of the coelacanth *Latimeria chalumnae*: Functional and evolutionary implications for the fin-to-limb transition and subsequent evolution of tetrapods. *The Anatomical Record*, 299(9):1203–1223.

Wilhelm, B. C., Du, T. Y., Standen, E. M., and Larsson, H. C. (2015). *Polypterus* and the evolution of fish pectoral musculature. *Journal of Anatomy*, 226(6):511–522.

Revision of the muscular anatomy of the paired fins of the living coelacanth *Latimeria chalumnae*

Alessia Huby*[1], Rohan Mansuit*[2,3], Marc Herbin[3], Anthony Herrel[3]

* Alessia Huby and Rohan Mansuit are co-first authors of the paper

[1] Laboratory of Functional and Evolutionary Morphology, FOCUS Research Unit, Department of Biology, Ecology and Evolution, University of Liège, Liège, Belgium

[2] UMR 7207 Centre de Recherche en Paléontologie, Paris, Muséum national d'Histoire naturelle – Sorbonne Université – CNRS, Département Origines & Evolution, Muséum national d'Histoire naturelle, 8 rue Buffon, CP38, 75005 Paris, France

[3] UMR 7179 Mécanismes Adaptatifs et Evolution, Muséum national d'Histoire naturelle – Sorbonne Université – CNRS, Département Adaptations du Vivant, Muséum national d'Histoire naturelle, CP55, 57 rue Cuvier, 75005 Paris, France

Abstract

As a sarcopterygian fish, the extant coelacanth *Latimeria* has muscular paired fins, different in their skeletal and muscular anatomy from the paired fins of actinopterygians. Despite the muscular anatomy of the pectoral and pelvic fins of *Latimeria* was described by several studies, a precise functional description of the muscular and its architecture was never done. With our detailed functional description of the muscles of the paired fins, and the study of their properties, we showed a more complex organization of the muscles than previously known. The pectoral and pelvic fins have a different organization of the muscular anatomy, with an important number of mono-articular muscles inserting on the endoskeletal elements in the pectoral fin. The pelvic fin showed a more plesiomorphic configuration of the muscles, since most of them are poly-articular and run from the pelvic girdle to the fin rays, a typical actinopterygian muscular anatomy. We found that the pectoral fins are stronger than the pelvic fins, supposed to the greater contribution of the pectoral fins to the locomotion and manoeuvring. The muscles properties of the pelvic fins highlighted that the superficial ossification of the pelvic girdle and the trabecular system are associated with stronger muscles than the rest of the pelvic girdle. This ossification and trabecular system are supposed to permit to the cartilaginous pelvic girdle to resist to the muscular constraints. Finally, the study of the joint mobility along the paired fins showed that the pectoral fin has a greater mobility than the pelvic fins. The reduced mobility of the pelvic fin is supposed to be linked with the morphology of the mesomeres and the large pre-axial radials.

Keywords

Anatomical cross-section area, mobility, muscles, pectoral fin, pelvic fin, sarcopterygians.

Introduction

Most living vertebrates are bony fishes (Osteichthyes) whose evolutionary success is in part due to the morphological diversification of the paired appendages allowing their expensive invasion of novel environments (Drucker and Lauder, 2002; Kardong, 2018). Based on the anatomical organization of pectoral and pelvic appendages, osteichthyan fishes are divided into two groups: the ray-finned fishes (Actinopterygii) grouping the vast majority of extant bony fishes and the sarcopterygians including lobe-finned fishes (extant coelacanths, lungfishes) and tetrapods (Diogo and Abdala, 2007; Amemiya et al., 2013; Nelson et al., 2016; Amaral and Schneider, 2018; Kardong, 2018). The pectoral and pelvic fins of actinopterygian fishes are internally supported by bony spines (fin rays or lepidotrichia) that are directly attached to the body at the level of the pectoral and pelvic girdles by several basal skeletal elements (radials) connected to three basal cartilages (polybasal articulation). By contrast, the lepidotrichia of the paired fins of sarcopterygian fishes are connected to an endoskeleton composed of several adjacent elements (mesomeres) forming an axis (metapterygial axis) that is joined to the body by a single endoskeletal element (monobasal articulation), the first mesomere (Johanson et al., 2007; Zhu and Yu, 2009; Kardong, 2018). In addition to endoskeletal differences, fin movements in actinopterygians are mainly controlled by relatively small abductor and adductor muscles located within the body, whereas these muscles are larger and located largely outside the body within the lobed fins in sarcopterygians (Millot and Anthony, 1958; Wilhelm et al., 2015; Diogo et al., 2016; Miyake et al., 2016; Kardong, 2018).

Among sarcopterygians, coelacanths (Actinistia) include two modern species, i.e. the African coelacanth *Latimeria chalumnae* and the Indonesian coelacanth *Latimeria menadoensis*. However, fossil forms were extremely diverse from the Early Devonian to the Late Cretaceous and varied in shape, size, and ecology (Agassiz, 1839; Erdmann et al., 1998; Forey, 1998; Nulens et al., 2011). Living coelacanths are large-bodied marine fishes, which measure up to two meters in length and weigh up to 105 kilograms (Nulens et al., 2011). They are predatory fishes that live around deep-water caves and rugged terrains at the depths between 110 and 400 meters (Fricke et al., 1987; Fricke and Hissmann, 1992; Hissmann et al., 2006). The anatomy of pectoral and pelvic fins of the African coelacanth *Latimeria chalumnae* was extensively studied by Millot and Anthony (1958) and subsequently revised by many authors (Ahlberg, 1992; Diogo et al., 2016; Miyake et al., 2016). Recently, Miyake and co-authors (2016) studied the arrangement and function of the pectoral fin muscles.

Even though coelacanths are bottom dwelling, the hypothesis that these animals walked on the bottom similar to tetrapods has been refuted by numerous observations in their natural environment (Fricke et al., 1987, 1991; Fricke and Hissmann, 1992; Hissmann et al., 2006). Coelacanths most often swim in a rather and extremely slow manner while maintaining a stiff and inflexible body. Propulsion is generated by the lobed, paired and unpaired fins (Fricke and Hissmann, 1992). The caudal fin is used mainly during the accelerations. During slow continuous locomotion the second dorsal fin and anal fin as well as both pectoral fins typically show large amplitude movements whereas the amplitude of pelvic fins is lower (Fricke and Hissmann, 1992). Moreover, the paired fins are highly mobile and display atypical movements including figure-eight motions of the pectoral fin during the forward swimming, or the elliptical motions of the pelvic fins (Décamps et al., 2017). Fricke and Hissmann (1992) hypothesized that the muscular part of the pelvic fin is shorter than that of the pectoral fin and that the mobility of the pelvic fin is limited compared to the pectoral fin, yet this remains to be test.

Although the paired fins of the coelacanths are a derived condition in sarcopterygian fish, they are structurally comparable to the limbs of tetrapods and appear to develop in a similar way (Shubin and Alberch, 1986; Ahlberg, 1992; Diogo et al., 2016). Compared to lungfish fins, the paired fins of coelacanths have been hypothesized to better reflect the ancestral sarcopterygian condition (Coates et al., 2002; Friedman et al., 2007). Consequently, coelacanths have been considered as one of the best living models to infer the basal tetrapod condition in terms of anatomy, development, and genetics (Ahlberg, 1992; Coates, 1994; Diogo and Abdala, 2007; Diogo et al., 2016; Miyake et al., 2016; Amaral and Schneider, 2018). Despite several studies describing the anatomy of the muscular system of the pectoral and pelvic fins in coelacanths, little is known about the precise architecture of the musculo-skeletal system of these paired appendages. Yet, an understanding of the muscle architecture is essential to understand the function and role of the different appendages during locomotion and the changes that occurred during the water-to-land transition.

The aim of the present study is to provide a detailed functional description of the muscular anatomy (i.e. muscle arrangement, muscle mass, anatomical cross-section area) of the paired fins of the living coelacanth *Latimeria chalumnae*. Moreover, we provide data on the mobility of the endoskeletal axis (e.g. joint mobility) and compare it between the pectoral and pelvic fins. This will allow a better understanding of the specific role of paired fins in the unique swimming mode of the extant coelacanth in addition to provide base-line data for future modelling studies.

Materials & Methods

Specimens studied

Two specimens of the extant African coelacanth *Latimeria chalumnae* were used for dissections: CCC 14 and CCC 27 (Nulens et al., 2011). The specimen CCC 14 is an adult male specimen of 134 cm in total length (TL) and weighs 39kg. It was captured in the region of Dzahadjou, Hambou, off the coast of Grande Comore Island in 1956. The specimen CCC 27 is an adult male specimen of 132 cm TL and weighs 38kg, captured off the coast of Grande Comore Island in 1961. Both specimens are preserved in a 6-7% formaldehyde solution and stored in the collections of the Museum national d'Histoire naturelle (MNHN) in Paris, France, under the collection number MNHN-ZA-AC-2012-11 and MNHN-ZA-AC-2012-21 respectively. The isolated pectoral fin of a third specimen was used for the study of the joint mobility of the fins, specimen CCC 19 (MNHN-ZA-AC-2012-15) (Nulens et al., 2011). This specimen is a male of 140 cm TL and weighs 35kg, captured in 1959 off the coast of Grande Comore. It was dissected and the pectoral fin is preserved in a 6-7% formaldehyde solution.

Dissections

The two specimens of *L. chalumnae* were immersed in water for one week before anatomical dissections in order to remove the formaldehyde. The left pectoral fin of the specimen CCC 14 and the left pelvic fin of the specimen CCC 27 were dissected. For each fin, the origin and insertion sites of muscle bundles were noted and muscle bundles were photographed, removed with care and classified into functional groups. Photographs were taken in situ at each stage of the dissection before removing the muscle bundles that were directly placed in a 70% aqueous solution of ethanol. After the complete dissection of each fin, the length of all muscle bundles was measured using a ruler (± 1mm), blotted dry and weighed using an analytical balance (Mettler AE100, ± 0.00001g) or an electronical balance (Ohaus Scout pro, ± 0.01g). The total length of each muscle bundle was defined as the maximal distance between the origin and insertion of the muscle bundle (from the most proximal origin of the muscular part to the most distal insertion, excluding tendons or aponeuroses).

Muscle architecture

The mass and length of the muscles was used to quantify the anatomical cross-section area (ACSA) of each muscle bundle as an estimator of its force-generating capacity (Loeb and Gans, 1986). The ACSA is based on the bundle mass (m), a standard muscular density (ρ) and the

muscle lenght (L) using the following equation:

$$ACSA[cm^2] = m[g]/(\rho[g.cm^{-3}] * L[cm])$$

Since the value of the muscular density of *L. chalumnae*, and more generally of lobe-finned fishes, remains unknown, we used here the values for fishes (1.06 g.cm^{-3}) (Dabrowski, 1978).

Joint mobility

To compare the mobility of the different articulations of the pectoral and pelvic fins, we measured the mobility of each joint along the metapterygial axis after complete dissection but with the ligaments intact. We also had the opportunity to measure the joint mobility of the already dissected pectoral fin of CCC 19. To do so, we introduced two needles parallel to one another in the two bony elements involved in the joint (Moon, 1999). Then, the elements were moved maximally without damaging ligaments or joint capsules to estimate the degree of freedom of the joint for adduction/abduction, the protraction/retraction and pronation/supination movements. For example, we introduced one needle on the mesomere 1 and the other on the mesomere 2 to determine the mobility of the joint between the mesomere 1 and the mesomere 2 and we photographed each maximum position. For each movement, five measures were taken, after returning the joint to the resting position of the fin. The resting position of each fin is defined in the results. The angle formed by the needles was then determined using the software Fiji (version ImageJ 1.52p, Java 1.8.0_172), and the mean maximal angle was calculated for each movement.

Results

The first anatomical description of the paired fins of *L. chalumnae* was done by Millot and Anthony (1958). The nomenclature used in the present study follows that of Diogo et al. (2016). The nomenclature used by Miyake et al. (2016) for the pectoral fin of the coelacanth is similar to that used by Diogo et al. (2016). The correspondence between the nomenclature used by Millot and Anthony (1958), Diogo et al. (2016) and the present work is shown in Tables 2.1 to 2.6. As previously described, both the pectoral and pelvic fin musculature are organized along three different layers: the superficial layer just beneath the scales, the middle layer, and the deep layer that overlaps the endoskeleton of the fin (Millot and Anthony, 1958; Diogo et al., 2016; Miyake et al., 2016).

Osteological anatomy of the paired fins

We provide here a short description of the osteology of the pectoral and pelvic fins of *L. chalumnae* (Fig. 2.1). A more extensive description is available in the literature (see Millot and Anthony, 1958; Mansuit et al., 2020a,b).

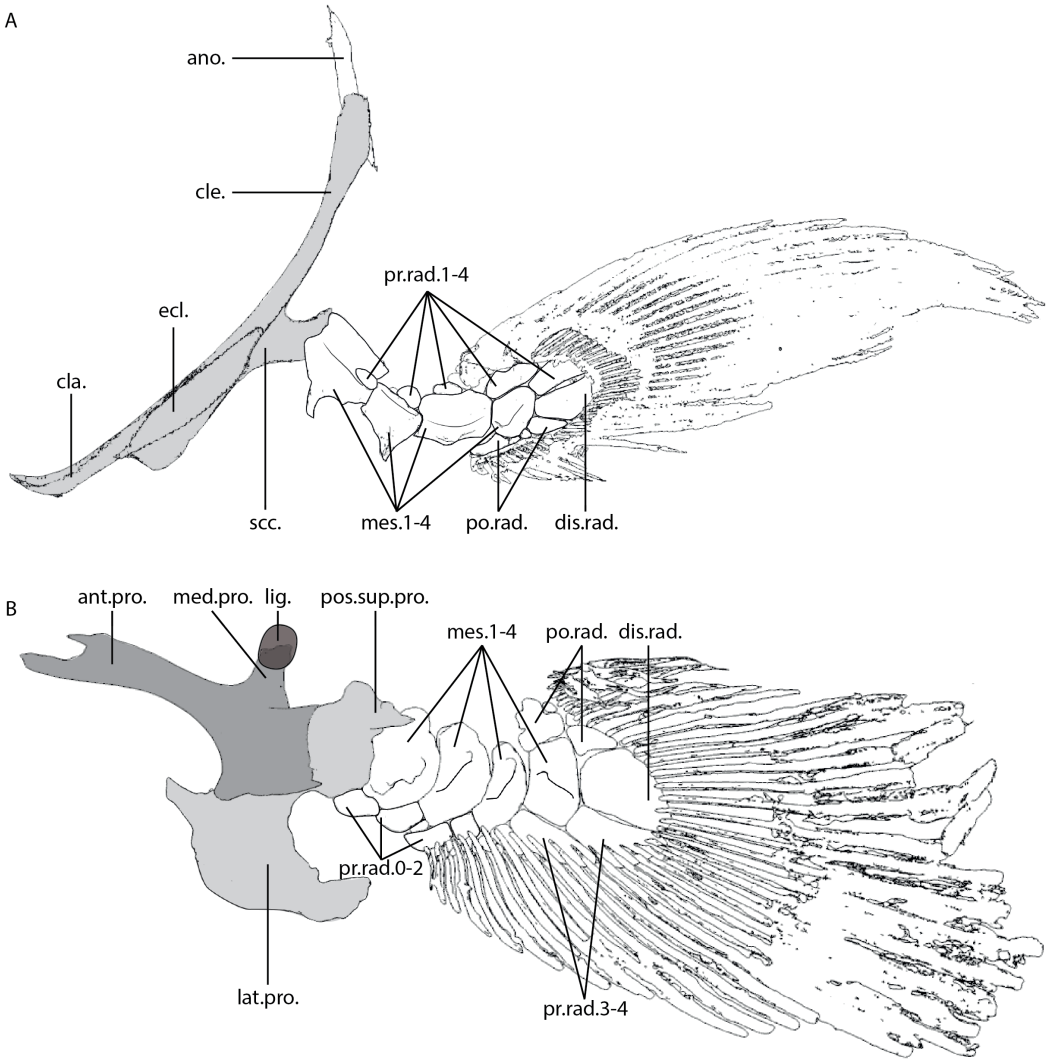

Figure 2.1: Comparison of the skeletal anatomy of the pectoral (A) and pelvic (B) fin of *Latimeria chalumnae*. The shaded parts correspond to the pectoral (A) and pelvic (B) girdle. The dark grey part (B) corresponds to the dense ossification of the pelvic girdle associated with a trabecular system. ano.: anocleithrum; ant.pro.: anterior process; cla.: clavicle; cle.: cleithrum; dis.rad.: distal radial; ecl.: extracleithrum; lat.pro.: lateral process; lig.: "ligament-ball"; med.pro.: medial process; mes.: mesomere; pos.sup.pro.: postero-superior process; pr.rad.: pre-axial radial; scc.: scapulocoracoid.

The pectoral girdle has an ark-shape and is formed by four flattened dermal bones (anocleithrum, cleithrum, extracleithrum and clavicle) and a massive endoskeletal scapulocoracoid element (Fig. 2.1 A). The pelvic girdle is formed by a single endoskeletal bone, surrounded by a

flat and curved lateral process, a short and triangular medial process, a rod-like cartilaginous anterior process and a small postero-superior process. The anterior part of the pelvic girdle presents also a highly ossified surface and internal trabecular system (Fig. 2.1 B). The left and right medial processes are linked to each other by a "ligament ball".

The pectoral and pelvic fins have a similar organization, with the metapterygial axis formed by four mesomeres associated with pre-axial radial elements, and post-axial radial elements. The most proximal pre-axial radial elements are small and globular in shape, whereas the most distal pre-axial radials (pr.rad.3-4) are elongated, trapezoidal in shape, and associated with dermal fin rays in both fins. The post-axial elements are formed by the post-axial radials and the distal radial (elongate and trapezoidal in shape), and they are associated with dermal fin rays. The pelvic fin presents a supernumerary pre-axial radial, called pre-axial radial 0, associated with the mesomere 1 and the pelvic girdle (Millot and Anthony, 1958; Mansuit et al., 2020b).

Pectoral musculature anatomy

Eighty-six muscle bundles, organized into 13 functional groups, were identified here in the pectoral fin of *L. chalumnae*. Similarly to Mansuit et al. (2020a), the resting position of the pectoral fin is considered as the fin positioned along the body with its leading edge oriented dorsally (Fig. 2.2). In this position, the muscles on the lateral side are *abductor* muscles protracting the fin and those on the medial side are the *adductor* muscles retracting the fin. Following this position, movements of the pectoral fin are defined as follow:

-Protraction: the lateral side of the fin has a forward movement

-Retraction: the medial side of the fin has a backward movement

-Abduction: the pre-axial edge of the fin has an upward movement

-Adduction: the pre-axial edge of the fin has a downward movement

-Pronation: the lateral side of the fin has a downward pivoting movement around the axis of the fin

-Supination: the lateral side of the fin has an upward pivoting movement around the axis of the fin.

Superficial layer (Table 2.1)

The superficial layer of the pectoral fin is formed by two muscle masses: the *abductor superficialis* muscles on the lateral side and the *adductor superficialis* muscles on the medial side of the pectoral fin (Fig. 2.3).

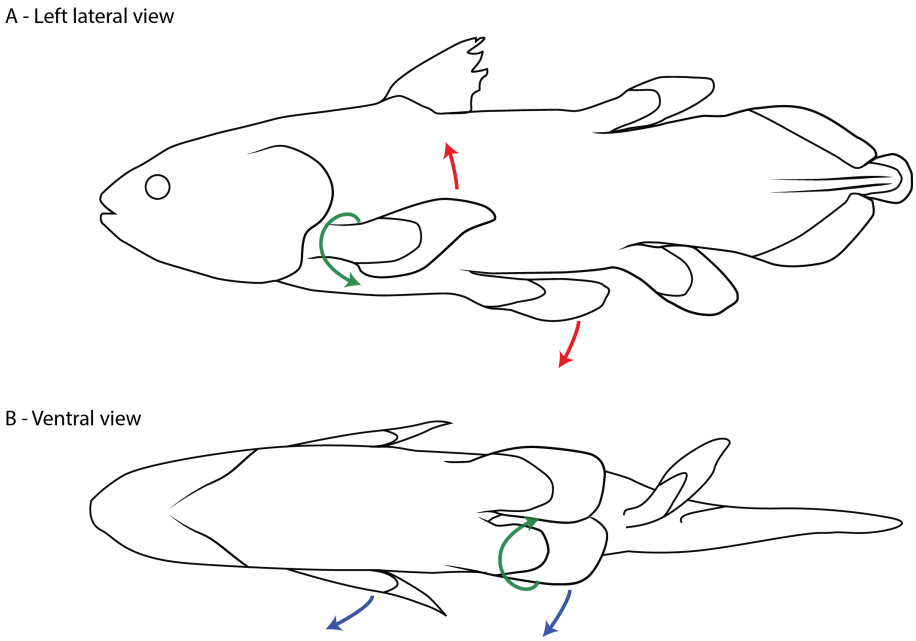

Figure 2.2: Pectoral and pelvic fins in their resting position in lateral (A) and ventral (B) views. The red arrows correspond to the abduction movement of the fins, the blue arrows for the protraction movement of the fins and the green arrows corresponds to the pronation movement of the fins. The antagonist movements are not represented here.

Abductor superficialis

The *abductor superficialis* muscle is formed by eight different muscle bundles having different origins and insertions (Table 2.1; Fig. 2.3 A). Six bundles (*abductor superficialis 1-6*) are mono-articular, meaning they cross only one joint, and two other bundles (*abductor superficialis 7-8*) are poly-articular, meaning they cross more than one joint.

Abductor superficialis 1: originates on the lateral side of the fin, on the latero-posterior edge of the cleithrum dorsally to the extracleithrum. It inserts on the proximal portion of the dorsal ridge and the dorso-lateral facet of the mesomere 1. This muscle bundle permits abduction and protraction of the mesomere 1.

Abductor superficialis 2: originates on the lateral edge of the extracleithrum. It inserts on the proximal portion of the ventro-lateral aspect of the mesomere 1. It permits the adduction and protraction of the mesomere 1.

Abductor superficialis 3: originates on the dorso-lateral aspect of the mesomere 1 and on its dorsal ridge, both on lateral and medial face of the fin. It inserts on the proximal portion of the dorsal part and dorso-medial ridge of the mesomere 2. It permits the abduction and protraction of the mesomere 2.

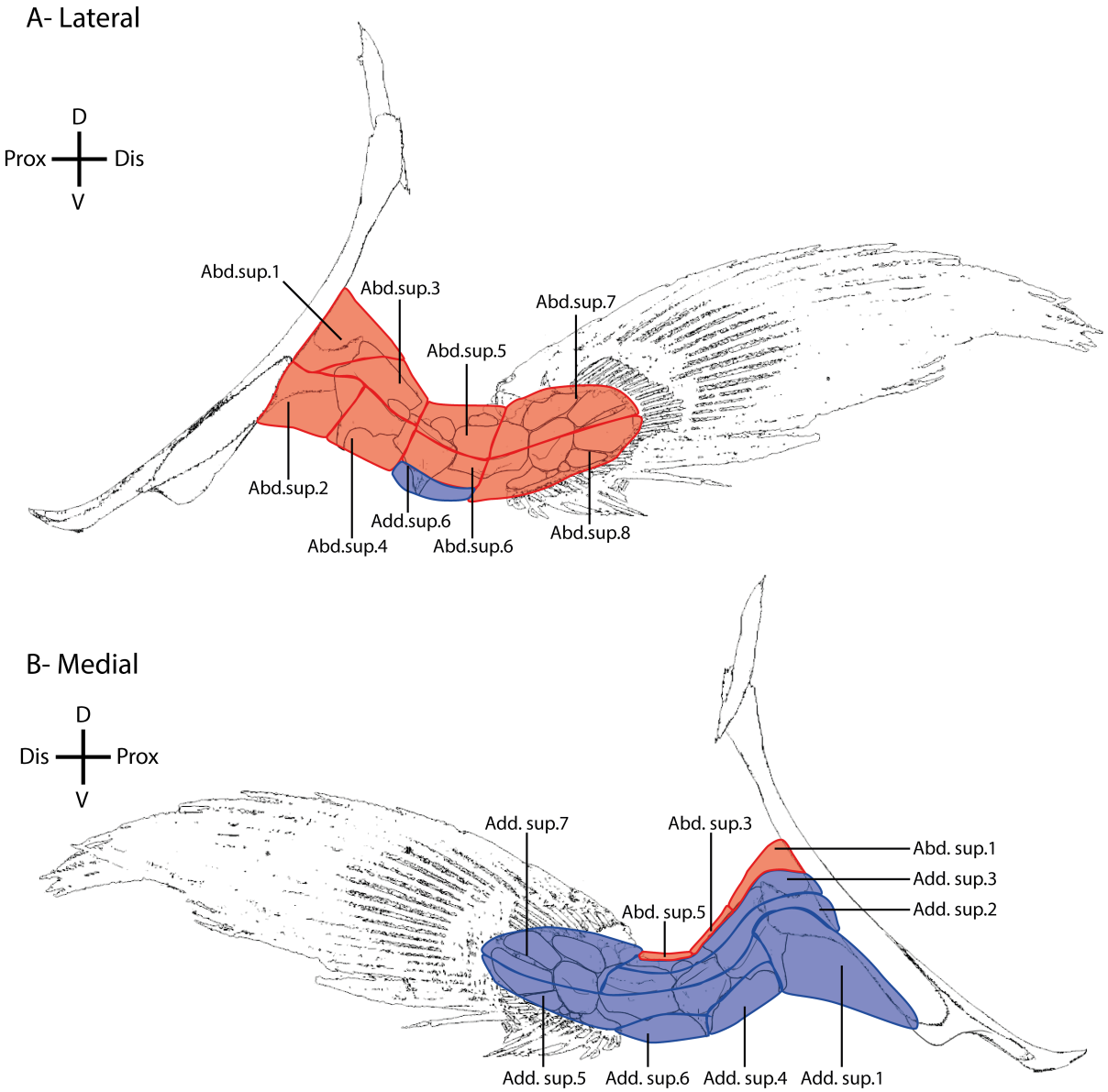

Figure 2.3: Superficial muscle layer of the pectoral fin of the coelacanth *Latimeria chalumnae* in lateral (A) and medial (B) views. Abd.sup: *abductor superficialis*; Add.sup: *adductor superficialis*; D: dorsal; Dis: distal; Prox: proximal; V: ventral.

Table 2.1: Muscles of the superficial layer of the pectoral fin of the coelacanth *Latimeria chalumnae*.

	Muscle	Diogo *et al* (2016)	Millot & Anthony (1958)	Origin(s)	Insertion(s)	Articulation mode	Function	Mass (g)	Bundle lenght (cm)	ACSA (cm²)
Lateral	*Abductor superficialis 1*	*Abductor superficialis*	Adducteur superficiel	Cleithrum: inner surface	Mesomere 1	Mono-articular	Abduction and protraction	9,000	4,25	1,998
	Abductor superficialis 2			Extracleithrum: posterior portion	Mesomere 1	Mono-articular	Adduction and protraction	3,653	5,00	0,689
	Abductor superficialis 3			*Mesomere 1: distal portion of the dorsal edge; *Scapulocoracoid: articulatory head of glenoid process	Mesomere 2 and pre-axial radial 1	Mono-articular	Abduction and protraction	4,042	2,25	1,695
	Abductor superficialis 4			Mesomere 1: lateral edge	Mesomere 2	Mono-articular	Adduction and protraction	3,980	3,50	1,073
	Abductor superficialis 5			Mesomere 2: distal portion of the dorso-medial edge	Mesomere 3	Mono-articular	Abduction and protraction	2,899	2,00	1,367
	Abductor superficialis 6			Mesomere 2: dorso-lateral edge	Mesomere 3	Mono-articular	Protraction	2,423	2,75	0,831
	Abductor superficialis 7			Mesomere 3: lateral ridge	Fin rays 1-12	Poly-articular	Protraction	1,786	3,00	0,562
	Abductor superficialis 8			Mesomere 3: lateral ridge	Fin rays 13-33	Poly-articular	Protraction	2,732	4,50	0,573
Medial	*Adductor superficialis 1*	*Adductor superficialis*	Adducteur superficiel	Scapulocoracoid	Mesomere 1	Mono-articular	Adduction and retraction	14,000	8,00	1,651
	Adductor superficialis 2			Cleithrum: anterior edge	Mesomeres 1-3	Poly-articular	Retraction	7,000	10,00	0,660
	Adductor superficialis 3			Cleithrum: anterior edge	Mesomeres 1-3	Poly-articular	Retraction	2,612	10,00	0,246
	Adductor superficialis 4			Mesomere 1: ventral ridge	Mesomere 2	Mono-articular	Adduction and retraction	2,838	4,50	0,595
	Adductor superficialis 5			Mesomere 1: ventral ridge	Mesomere 3 + fin rays 22-33	Poly-articular	Retraction	2,477	10,50	0,223
	Adductor superficialis 6			Mesomere 2: dorso-lateral edge	Mesomere 3	Mono-articular	Adduction and retraction	2,238	3,50	0,603
	Adductor superficialis 7			Mesomere 3: distal portion of the dorsal edge	Fin rays 1-21	Poly-articular	Retraction	2,265	2,50	0,855

Abductor superficialis 4: originates on the ventro-lateral aspect of the mesomere 1. It inserts on the proximal portion of the ventral part of the mesomere 2. It permits the adduction and protraction of the mesomere 2.

Abductor superficialis 5: originates on the dorsal part of the mesomere 2, on its dorso-lateral and dorso-medial edge. It inserts on the dorso-lateral aspect of the mesomere 3 and on its dorsal ridge, both on lateral and medial sides of the fin. It permits the abduction and protraction of the mesomere 3.

Abductor superficialis 6: originates on the proximal part of lateral aspect of the mesomere 2. It inserts on the proximal portion of the ventro-lateral aspect of the mesomere 3. It permits the protraction of the mesomere 3.

Abductor superficialis 7: originates on the distal portion of the dorso-lateral aspect of the mesomere and inserts at the base of the fin rays 1 to 12 via an aponeurosis at the lateral side of the fin. It permits the protraction of the distal part of the fin and fin rays 1 to 12.

Abductor superficialis 8: originates on the distal portion of the ventro-lateral aspect of the mesomere 3 and inserts at the base of the fin rays 13 to 33 via an insertion aponeurosis at the lateral side of the fin. It permits the protraction of the distal part of the fin and fin rays 13 to 33.

Adductor superficialis

The adductor superficialis muscle mass is formed by seven different muscle bundles having different origins and insertions (Table 2.1; Fig. 2.3 B). Three bundles (*adductor superficialis 1, 4* and *6*) are mono-articular, and four bundles (*adductor superficialis 2, 3, 5* and *7*) are poly-articular.

Adductor superficialis 1: originates on the ventro-medial edge of the cleithrum, the ventral side of the scapulocoracoid and the ventral edge of the extracleithrum. It inserts on the proximal portion of the ventro-medial aspect of the mesomere 1 and on the large ventral ridge of this mesomere. It permits the adduction and retraction of the mesomere 1.

Adductor superficialis 2-3: they originate from the anterior edge of the cleithrum, and insert on the distal portion of the medial aspect of the mesomere 3. They are also attached to me-

someres 1 and 2 with strong fibrous connective tissue. The *adductor superficialis 3* is dorsal to the *adductor superficialis 2*. They permit the retraction of mesomeres 1 to 3.

Adductor superficialis 4: originates on the distal portion of the ventral ridge of the mesomere 1, on its medial side. It inserts on the proximal portion of the ventro-medial ridge of the mesomere 2. It permits the adduction and retraction of the mesomere 2.

Adductor superficialis 5: originates on the proximal portion of the ventro-medial aspect of the mesomere 1, just dorsal to the origin of the *adductor superficialis 4*. It inserts on the medial side of the mesomere 3 and at the base of the fin rays 22 to 33 via an aponeurosis. It permits the retraction of the mesomere 3 and fin rays 22 to 33.

Adductor superficialis 6: originates on the medial and lateral sides of the fin, on the distal portion of the ventro-medial ridge of the mesomere 2. It inserts on the ventral side of the mesomere 3. It permits the adduction and retraction of the mesomere 3.

Adductor superficialis 7: originates on the distal portion of the mesomere 3. It inserts at the base of the fin rays 1 to 21 via an aponeurosis at the medial side of the fin. It permits the retraction of the distal part of the fin and fin rays 1 to 21.

Middle layer (Table 2.2)

The middle layer is also formed by two muscle masses: the *abductor profundus* on the lateral side and the *adductor profundus* on the medial side of the pectoral fin (Fig. 2.4).

Abductor profundus

The *abductor profundus* muscle is formed by 31 different muscle bundles (Fig. 2.4 A). Among them, 24 bundles are mono-articular (*abductor profundi 1-2, 10-31*) and seven are poly-articular (*abductor profundi 3-7* and *9-10*).

Abductor profundi 1-2: originate on the medio-caudal edge of the superior part of the cleithrum (Table 2.2). They insert on the distal part of the dorso-lateral aspect of the mesomere 1. They permit the abduction and protraction of the mesomere 1.

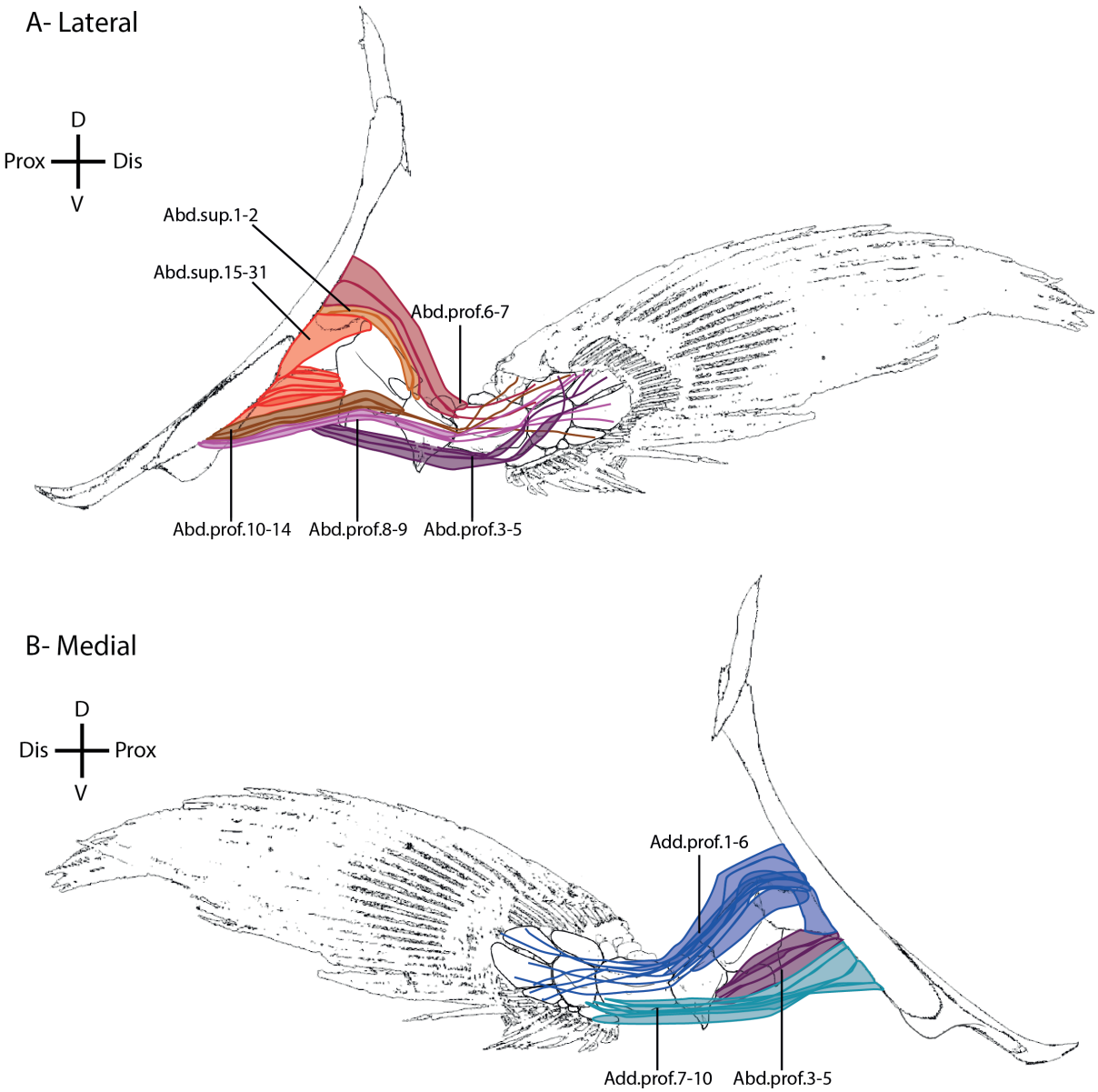

Figure 2.4: Middle muscle layer of the pectoral fin of the coelacanth *Latimeria chalumnae* in lateral (A) and medial (B) views. Abd.prof: *abductor profundus*; Add.prof: *adductor profundus*; D: dorsal; Dis: distal; Prox: proximal; V: ventral.

Table 2.2: Muscles of the middle layer of the pectoral fin of the coelacanth *Latimeria chalumnae*.

	Muscle	Diogo et al (2016)	Millot & Anthony (1958)	Origin(s)	Insertion(s)	Articulation mode	Function	Mass (g)	Bundle lenght (cm)	ACSA (cm²)
Lateral face	*Abductor profundus 1*	*Abductor profundus*	Adducteur profond	Cleithrum: inner surface	Mesomere 1: distal portion of the dorso-lateral facet	Mono-articular	Abduction and protraction	2,327	4,30	0,511
	Abductor profundus 2			Cleithrum: inner surface	Mesomere 1: distal portion of the dorso-lateral facet	Mono-articular	Abduction and protraction	1,545	4,00	0,364
	Abductor profundus 3			Scapulocoracoid: proximal portion of internal posterior surface	Mesomeres 2-3 along the ventral edge (lateral face)	Poly-articular	Adduction and protraction	1,568	14,00	0,106
	Abductor profundus 4			Scapulocoracoid: proximal portion of internal posterior surface	Mesomere 3 along the ventral edge (lateral face)	Poly-articular	Adduction and protraction	7,000	18,00	0,367
	Abductor profundus 5			Scapulocoracoid: proximal portion of internal posterior surface	Mesomeres 1-3 along the ventral edge (lateral face)	Poly-articular	Adduction and protraction	1,495	10,00	0,141
	Abductor profundus 6			Scapulocoracoid: proximal portion of internal posterior surface	Mesomeres 1-3 (lateral face)	Poly-articular	Abduction and protraction	0,327	11,00	0,028
	Abductor profundus 7			Scapulocoracoid: proximal portion of internal posterior surface	Mesomeres 1-3 (lateral face)	Poly-articular	Abduction and protraction	1,482	11,00	0,127
	Abductor profundus 8			Scapulocoracoid: proximal portion of internal posterior surface	Mesomeres 1-2 along the ventral edge (lateral face)	Mono-articular	Adduction and protraction	1,642	10,50	0,148
	Abductor profundus 9			Scapulocoracoid: proximal portion of internal posterior surface	Mesomeres 1-2 along the ventral edge (lateral face)	Poly-articular	Adduction and protraction	1,032	8,00	0,122

Table 2.2 (suite)

	Muscle	Diogo et al (2016)	Millot & Anthony (1958)	Origin(s)	Insertion(s)	Articulation mode	Function	Mass (g)	Bundle lenght (cm)	ACSA (cm²)
Lateral face	*Abductor profundus 10*	*Abductor profundus*	Adducteur profond	Scapulocoracoid: proximal portion of internal posterior surface	Mesomere 1 along the ventral edge	Poly-articular	Adduction and protraction	0,219	6,00	0,034
	Abductor profundus 11			Scapulocoracoid: proximal portion of internal posterior surface	Mesomere 1 along the ventral edge	Mono-articular	Adduction and protraction	0,267	3,00	0,084
	Abductor profundus 12			Scapulocoracoid: proximal portion of internal posterior surface	Mesomere 1 along the ventral edge	Mono-articular	Adduction and protraction	0,605	6,00	0,095
	Abductor profundus 13			Scapulocoracoid: proximal portion of internal posterior surface	Mesomere 1 along the ventral edge	Mono-articular	Adduction and protraction	0,414	4,50	0,087
	Abductor profundus 14			Scapulocoracoid: proximal portion of internal posterior surface	Mesomere 1 along the ventral edge	Mono-articular	Adduction and protraction	0,451	4,20	0,101
	Abductor profundus 15			Scapulocoracoid: proximal portion of internal posterior surface	Mesomere 1: proximal edge (lateral face)	Mono-articular	Adduction and protraction	0,247	4,50	0,052
	Abductor profundus 16			Scapulocoracoid: proximal portion of internal posterior surface	Mesomere 1: proximal edge (lateral face)	Mono-articular	Adduction and protraction	0,027	4,00	0,006
	Abductor profundus 17			Scapulocoracoid: proximal portion of internal posterior surface	Mesomere 1: proximal edge (lateral face)	Mono-articular	Adduction and protraction	0,140	4,20	0,031

Table 2.2 (suite)

	Muscle	Diogo et al (2016)	Millot & Anthony (1958)	Origin(s)	Insertion(s)	Articulation mode	Function	Mass (g)	Bundle lenght (cm)	ACSA (cm²)
Lateral face	*Abductor profundus 18*	*Abductor profundus*	Adducteur profond	Scapulocoracoid: proximal portion of internal posterior surface	Mesomere 1: proximal edge (lateral face)	Mono-articular	Adduction and protraction	0,101	4,00	0,024
	Abductor profundus 19			Scapulocoracoid: proximal portion of internal posterior surface	Mesomere 1: proximal edge (lateral face)	Mono-articular	Adduction and protraction	0,014	3,70	0,003
	Abductor profundus 20			Scapulocoracoid: proximal portion of internal posterior surface	Mesomere 1: proximal edge (lateral face)	Mono-articular	Adduction and protraction	0,383	4,00	0,090
	Abductor profundus 21			Scapulocoracoid: proximal portion of internal posterior surface	Mesomere 1: proximal edge (lateral face)	Mono-articular	Adduction and protraction	0,689	4,00	0,163
	Abductor profundus 22			Scapulocoracoid: proximal portion of internal posterior surface	Mesomere 1: proximal edge (lateral face)	Mono-articular	Adduction and protraction	0,046	4,00	0,011
	Abductor profundus 23			Scapulocoracoid: proximal portion of internal posterior surface	Mesomere 1: proximal edge (lateral face)	Mono-articular	Adduction and protraction	0,254	3,60	0,066
	Abductor profundus 24			Scapulocoracoid: proximal portion of internal posterior surface	Mesomere 1: proximal edge (lateral face)	Mono-articular	Adduction and protraction	0,035	3,10	0,011
	Abductor profundus 25			Scapulocoracoid: proximal portion of internal posterior surface	Mesomere 1: proximal edge (lateral face)	Mono-articular	Adduction and protraction	0,129	3,70	0,033

Table 2.2 (suite)

	Muscle	Diogo et al (2016)	Millot & Anthony (1958)	Origin(s)	Insertion(s)	Articulation mode	Function	Mass (g)	Bundle lenght (cm)	ACSA (cm²)
Lateral face	*Abductor profundus 26*	*Abductor profundus*	Adducteur profond	Scapulocoracoid: proximal portion of internal posterior surface	Mesomere 1: proximal edge (lateral face)	Mono-articular	Adduction and protraction	0,247	3,80	0,061
	Abductor profundus 27			Scapulocoracoid: proximal portion of internal posterior surface	Mesomere 1: proximal edge (lateral face)	Mono-articular	Adduction and protraction	0,089	3,10	0,027
	Abductor profundus 28			Scapulocoracoid: proximal portion of internal posterior surface	Mesomere 1: proximal edge (lateral face)	Mono-articular	Adduction and protraction	0,194	4,00	0,046
	Abductor profundus 29			Scapulocoracoid: proximal portion of internal posterior surface	Mesomere 1: proximal edge (lateral face)	Mono-articular	Adduction and protraction	0,226	4,50	0,047
	Abductor profundus 30			Scapulocoracoid: proximal portion of internal posterior surface	Mesomere 1: proximal edge (lateral face)	Mono-articular	Adduction and protraction	2,886	3,00	0,907
	Abductor profundus 31			Scapulocoracoid: proximal portion of internal posterior surface	Mesomere 1: proximal edge (lateral face)	Mono-articular	Adduction and protraction	1,173	3,25	0,340
Medial face	*Adductor profondus 1*	*Adductor profundus*	Abducteur profond	Cleithrum: medio-caudal edge of the superior portion	Mesomeres 1-3 along the dorsal edge (medial face)	Poly-articular	Abduction and retraction	0,869	8,30	0,099
	Adductor profondus 2			Cleithrum: medio-caudal edge of the superior portion	Mesomeres 1-3 along the dorsal edge (medial face)	Poly-articular	Abduction and retraction	2,323	10,50	0,209
	Adductor profondus 3			Cleithrum: medio-caudal edge of the superior portion	Mesomeres 1-3 along the dorsal edge (medial face)	Poly-articular	Abduction and retraction	3,253	12,60	0,244

Table 2.2 (suite)

	Muscle	Diogo et al (2016)	Millot & Anthony (1958)	Origin(s)	Insertion(s)	Articulation mode	Function	Mass (g)	Bundle lenght (cm)	ACSA (cm²)
Medial face	*Adductor profondus 4*	*Adductor profundus*	Abducteur profond	Cleithrum: medio-caudal edge of the superior portion	Mesomeres 1-3 along the dorsal edge (medial face)	Poly-articular	Abduction and retraction	1,798	8,00	0,212
	Adductor profondus 5			Cleithrum: medio-caudal edge of the superior portion	Mesomeres 1-2 along the dorsal edge (medial face)	Poly-articular	Abduction and retraction	0,694	5,50	0,119
	Adductor profondus 6			Cleithrum: medio-caudal edge of the superior portion	Mesomeres 1-2 along the dorsal edge (medial face)	Poly-articular	Abduction and retraction	0,134	3,50	0,036
	Adductor profondus 7			Scapulocoracoid: proximal portion of the ventral surface	Mesomeres 2-3 along the ventral edge (medial face)	Poly-articular	Adduction and retraction	1,948	10,50	0,175
	Adductor profondus 8			Scapulocoracoid: proximal portion of the ventral surface	Mesomeres 2-3 along the ventral edge (medial face)	Poly-articular	Adduction and retraction	2,460	12,50	0,186
	Adductor profondus 9			Scapulocoracoid: proximal portion of the ventral surface	Mesomeres 2-3 along the ventral edge (medial face)	Poly-articular	Adduction and retraction	2,028	13,00	0,147
	Adductor profondus 10			Scapulocoracoid: proximal portion of the ventral surface	Mesomeres 2-3 along the ventral edge (medial face)	Poly-articular	Adduction and retraction	1,228	14,50	0,080

Abductor profundi 3-5: originate on the ventral side of the scapulocoracoid. They follow the ventral edge of mesomeres 1 to 3 and insert on the lateral side of the fin via a long tendon. They permit the adduction and protraction of the fin.

Abductor profundi 6-7: originate on the ventral side of the scapulocoracoid. They follow the dorsal edge of mesomeres 1 to 3 and insert on the lateral side of the fin via a long tendon. They permit the abduction and protraction of the fin.

Abductor profundi 8-9: originate on the ventral side of the scapulocoracoid, near the edge of the extracleithrum. They follow the ventral edge of mesomeres 1 and 2 and insert on the lateral side of the fin via a long tendon. They permit the adduction and protraction of mesomeres 1 and 2.

Abductor profundi 10-14: originate on the ventral side of the scapulocoracoid, near the edge of the extracleithrum on the lateral side of the girdle. They insert on the lateral side of the mesomere 1 via a long tendon and follow the ventral edge of this mesomere. They permit the adduction and protraction of the mesomere 1.

Abductor profundi 15-31: originate on the ventral side of the fin, on the articular process of the scapulocoracoid. They insert on the proximal edge of the mesomere 1 via a short tendon, on the lateral side of the fin. They permit the adduction and protraction of the mesomere 1.

Adductor profundus

The *adductor profundus* muscle is formed by ten poly-articular muscle bundles that run under the surface of the *abductor superficialis* muscle (Fig. 2.4 B).

Adductor profundi 1-6: originate from the medio-caudal edge of the superior portion of the cleithrum (Table 2.2). They follow the dorsal edge of mesomeres 1 to 3 and insert via a long tendon to the medial side of the fin. They permit the abduction and retraction of the fin.

Adductor profundi 7-10: originate on the ventral side of the scapulocoracoid (Table 2.2). They follow the ventral edge of mesomeres 2 and 3, and insert via a long tendon on the medial side of the fin. They permit the adduction and retraction of the fin.

Deep layer (Table 2.3)

Here, we refer to *pronator* and *supinator* muscles as the muscles of the deep layer that insert respectively on the lateral and medial sides of the pectoral fin (see Diogo et al., 2016; Miyake et al., 2016) (Fig. 2.5). However, the exact role of each muscle can be different from what the name suggests, as indicated in the Table 2.3.

The deep layer is composed of eight antagonistic pairs of *pronator* and *supinator* muscles that cover the entire endoskeletal axis of the pectoral fin and the proximal portion of dermal fin rays and a post-axial muscle (*pterygialis caudalis*) (Fig. 2.5). In the deep layer, most of the muscles are mono-articular.

Pronator muscles

The *pronator* muscles group is formed by eight pronator muscles at the lateral side of the pectoral fin that run obliquely across the ventral margin of the fin (Fig. 2.5 A). The pronator 1b is the only pronator bundles that originates and inserts on the medial side of the fin.

The *pronator 1-4* muscles are mono-articular. Their numbers correspond to the mesomere they insert upon (or the previous pre-axial radial), and they originate from the previous element (scapulocoracoid or mesomere). They permit the pronation of the associated element and of the fin.

The *pronators 5-8* insert on the proximal portion of the fin rays, and originate on the mesomere 3 (*pron. 5* and *7*), the mesomere 4 (*pron. 6*) and mesomere 2 (*pron. 8*). They permit the lateral flexion of the fin rays and the pronation (*pron. 5, 6a*) and supination of the fin (*pron. 6b, 6c, 7, 8*).

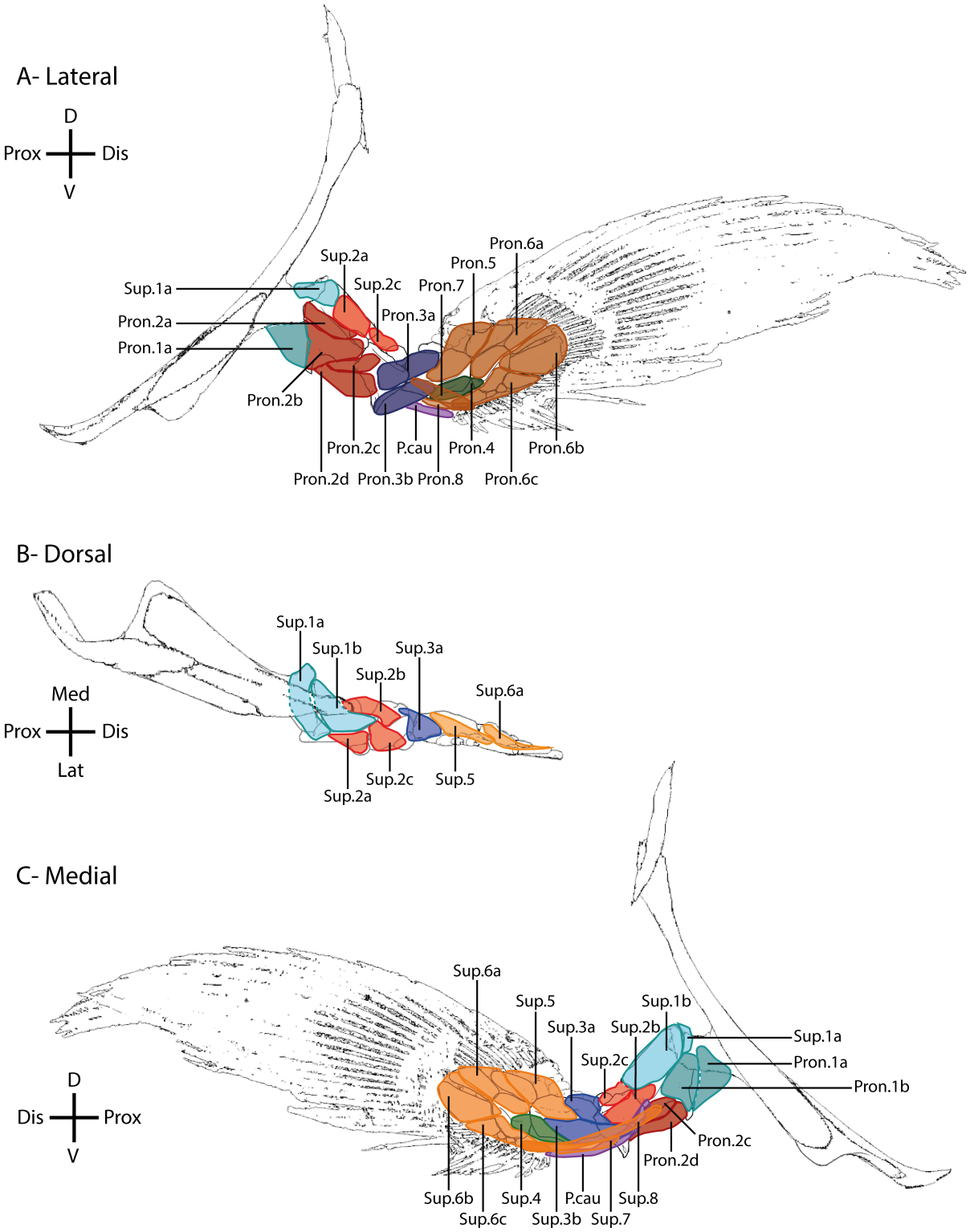

Figure 2.5: Deep muscle layer of the pectoral fin of the coelacanth *Latimeria chalumnae* in lateral (A), dorsal (B) and medial (C) views. P.caud: *pterygialis caudalis*; Pron: *pronator*; Sup: *supinator*; D: dorsal; Dis: distal; Lat: lateral; Med, medial; Prox: proximal; V: ventral.

Table 2.3: Muscles of the deep layer of the pectoral fin of the coelacanth *Latimeria chalumnae*.

	Muscle	Diogo et al (2016)	Millot & Anthony (1958)	Origin(s)	Insertion(s)	Articulation mode	Function	Mass (g)	Bundle lenght (cm)	ACSA (cm²)
Lateral face	*Pronator 1a*	*Supinator 1*	Supinateur 1	Scapulocoracoid: glenoid process (medial side)	Mesomere 1: proximal portion of the ventral ridge (lateral side)	Mono-articular	Pronation	6,000	5,00	1,132
	Pronator 1b			Scapulocoracoid: proximal part of the inferior portion of the glenoid process (medial side)	Mesomere 1: ventro-medial face	Mono-articular	Pronation	5,411	3,50	1,458
	Pronator 2a			Mesomere 1: proximal portion of ventral edge (lateral side)	Pre-axial radial 1 (lateral side)	Mono-articular	Pronation	0,312	3,00	0,098
	Pronator 2b			Mesomere 1: ventral edge and ventral ridge (lateral side)	Pre-axial radial 1 (lateral side)	Mono-articular	Pronation	2,739	2,65	0,975
	Pronator 2c	*Supinator 2*	Supinateur 2	Mesomere 1: distal portion of ventral edge (medial side)	Mesomere 2: proximal portion of the dorsal edge	Mono-articular	Pronation	3,018	3,00	0,949
	Pronator 2d			Mesomere 1: distal portion of ventral edge (medial side)	Mesomere 2: proximal portion of the ventro-lateral ridge	Poly-articular	Pronation	2,286	6,00	0,359
	Pronator 3a			Mesomere 2: proximal portion of the ventro-lateral ridge	*Pre-axial radial 2;* Mesomere 3: proximal portion of the dorsal edge (lateral face)	Mono-articular	Pronation	2,971	3,25	0,862
	Pronator 3b	*Supinator 3*	Supinateur 3	Mesomere 2: distal part of the ventro-lateral ridge	Mesomere 3: ventral side of the lateral ridge	Mono-articular	Pronation	2,200	3,50	0,593
	Pronator 4			Mesomere 3: ventral ridge	Mesomere 4: proximal portion of lateral ridge	Mono-articular	Pronation	0,718	2,50	0,271

Table 2.3 (suite)

	Muscle	Diogo et al (2016)	Millot & Anthony (1958)	Origin(s)	Insertion(s)	Articulation mode	Function	Mass (g)	Bundle lenght (cm)	ACSA (cm²)
Lateral face	*Pronator 5*	*Supinator 3*	Supinateur 3	Mesomere 3: ventral ridge (lateral side)	Proximal portion of fin rays 1-6	Mono-articular	Lateral flexion of fin rays and pronation	3,454	4,50	0,724
	Pronator 6a	*Supinator 4*	Supinateur 4	Mesomere 4: lateral edge	Proximal portion of fin rays 6-12	Mono-articular	Lateral flexion of fin rays and pronation	2,568	3,50	0,692
	Pronator 6b			Mesomere 4: distal portion of lateral edge	Proximal portion of fin rays 13-21	Mono-articular	Lateral flexion of fin rays and supination	1,356	2,75	0,465
	Pronator 6c			Mesomere 4: lateral edge	Proximal portion of fin rays 21-33	Mono-articular	Lateral flexion of fin rays and supination	1,957	1,75	1,055
	Pronator 7	*Pterygialis caudalis*	Supinateur 5	Mesomere 3: ventral edge	Proximal portion of fin rays 28-33	Poly-articular	Lateral flexion of fin rays and supination	0,164	3,80	0,041
	Pronator 8			Mesomere 2: distal portion of the dorso-lateral edge	Proximal portion of fin rays 28-33	Poly-articular	Lateral flexion of fin rays and supination	0,978	5,50	0,168
Medial face	*Supinator 1a*	*Pronator 1*	Pronateur 1	Scapulocoracoid: superior portion of the glenoid process	Mesomere 1: proximal portion of the ventral ridge (lateral side)	Mono-articular	Supination	1,880	1,50	1,182
	Supinator 1b			Scapulocoracoid: superior portion of the glenoid process	Mesomere 1: distal portion of dorso-medial face	Mono-articular	Supination	5,140	3,50	1,385
	Supinator 2a		Pronateur 2	Mesomere 1: proximal portion of the dorsal ridge (lateral side)	Pre-axial radial 1 (lateral side)	Mono-articular	Supination	1,244	1,50	0,782
	Supinator 2b	*Pronator 2*		Mesomere 1: distal portion of the medial edge	Mesomere 2: dorso-medial edge	Mono-articular	Supination	2,689	3,00	0,846
	Supinator 2c			Mesomere 1: distal portion of the dorsal ridge (lateral side)	Pre-axial radial 2: Proximal portion	Poly-articular	Supination	0,591	2,50	0,223

Table 2.3 (suite)

	Muscle	Diogo et al (2016)	Millot & Anthony (1958)	Origin(s)	Insertion(s)	Articulation mode	Function	Mass (g)	Bundle lenght (cm)	ACSA (cm²)
Medial face	*Supinator 3a*	*Pronator 2*	Pronateur 3	Mesomere 2: distal portion of the dorso-medial ridge	Pre-axial radial 2; proximal element of pre-axial accessory element	Mono-articular	Supination	1,875	2,00	0,884
	Supinator 3b	*Pronator 3*		Mesomere 2: distal portion of ventro-medial ridge	Mesomere 3: distal portion of the medial ridge	Mono-articular	Supination	1,699	4,00	0,401
	Supinator 4			Mesomere 3: distal portion of the ventral ridge (medial side)	Mesomere 4: proximal portion of the ventral edge (medial side)	Mono-articular	Supination	0,663	2,75	0,227
	Supinator 5			Mesomere 3: distal portion of the dorsal ridge (medial side)	Proximal portion of fin rays 1-7	Mono-articular	Medial flexion of fin rays and supination	1,667	2,25	0,699
	Supinator 6a	*Pronator 4*	Pronateur 4	Mesomere 4: dorsal edge (medial side)	Proximal portion of fin rays 7-12	Mono-articular	Medial flexion of fin rays and supination	0,873	2,75	0,299
	Supinator 6b			Mesomere 4: distal portion of the ventral edge (medial side)	Proximal portion of fin rays 13-23	Mono-articular	Medial flexion of fin rays and pronation	0,924	2,75	0,317
	Supinator 6c			Mesomere 4: ventral edge (medial side)	Proximal portion of fin rays 23-33	Mono-articular	Medial flexion of fin rays and pronation	0,749	1,75	0,404
	Supinator 7	*Pterygialis caudalis*	Pronateur 5	Mesomere 2: distal portion of medial edge	Proximal portion of fin rays 28-33	Poly-articular	Medial flexion of fin rays and pronation	0,364	4,50	0,076
	Supinator 8			Mesomere 1: ventro-letral edge	Proximal portion of fin rays 28-33	Poly-articular	Medial flexion of fin rays and pronation	0,700	6,50	0,102
	Pterygialis caudalis		*Undescribed*	Mesomere 1: distal portion of the medial edge	Proximal portion of fin ray 33	Poly-articular	Adduction	0,691	8,00	0,0815

Supinator muscles

The *supinator* muscles group is formed by eight *supinator* muscles on the medial side of the pectoral fin (Fig. 2.5 B). The organization of these muscles is quiet similar to that of the pronator muscles. The *supinator 1a, 2a, 2c* insert on the lateral side of the fin.

The *supinators 1-4* are mono-articular muscles. These muscles permit the supination of the associated elements and of the fin.

The *supinators 5-8* insert on the proximal portion of the fin rays at the medial side of the fin. They are symmetrical to the *pronator 5-8* and permit their antagonistic movement (Table 2.3).

Pterygialis caudalis

The *pterygialis caudalis* follows the post-axial edge of the pectoral fin. It originates on the medial side of mesomere 1 and inserts at the base of fin ray 33. It permits the adduction of the fin.

Pelvic musculature anatomy

Eighty-three muscle bundles, organized into 12 functional groups, were identified for the pelvic fin of *L. chalumnae*. Moreover, most of these muscle bundles are separated in several muscles sub-bundles (Sup. Table 2.1). The resting position of the pelvic fin was considered as the fin positioned along the ventral side of the body, with the leading edge directed laterally. *Abductor* muscles are on the ventral side of the fin, and *adductor* muscles are located on the dorsal side of the fin. Compared to the pectoral fin, most muscles of the pelvic fin are poly-articular and originate from the pelvic girdle and insert at the base of the fin rays. For the pelvic fin in its resting position, movements are defined as follow:

-Protraction: the pre-axial edge of the fin has a forward movement

-Retraction: the pre-axial edge of the fin has a backward movement

-Abduction: the ventral side of the fin has a downward movement

-Adduction: the dorsal side of the fin has an upward movement

-Pronation: the ventral face of the fin has a medial pivoting movement around the axis of the fin

-Supination: the ventral face of the fin has a lateral pivoting movement around the axis of the fin.

As for the pectoral fin, the pelvic fin, having an important mobility, is not maintained in this reference position during swimming. The movements of the fin defined here thus refer to the resting position of the fin (Fig. 2.2). Since the pectoral and pelvic fins are oriented in different plans, the movements of the two fins are defined differently. Thus the protraction movement of the pectoral fin corresponds to an abduction movement of the pelvic fin, and an abduction movement of the pectoral fin corresponds to a protraction movement of the pelvic fin.

Superficial layer (Table 2.4)

Since the muscle organization is simpler compare to that of the pectoral fin, we provide here a general description of the origin and insertion of the muscles of the superficial layer. The detailed origins and insertions of each muscles in the superficial layer are provided in Table 2.4.

The superficial layer of the pelvic fin is formed by four muscle masses: the *adductor superficialis pelvicus* on the dorsal side and the *abductor superficialis pelvicus* on the ventral side of the fin, as well as the *pterygialis cranialis* on the pre-axial side and the *pterygialis caudalis* on the post-axial side of the fin (Fig. 2.6). All the muscles of the superficial layer are poly-articular.

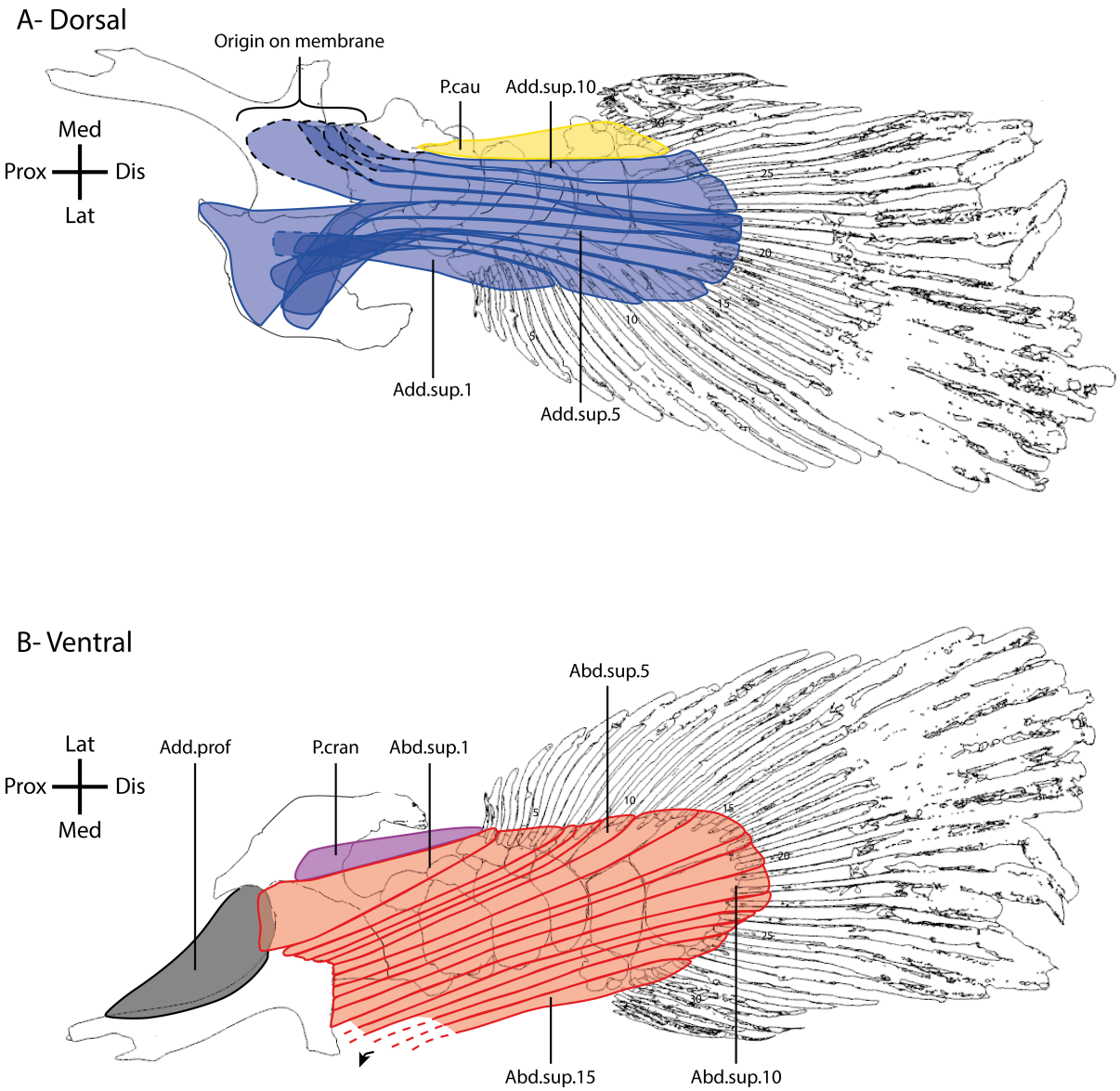

Figure 2.6: Superficial muscle layer of the pelvic fin of the coelacanth *Latimeria chalumnae* in dorsal (A) and ventral (B) views. Abd.prof: *abductor profundus*, Abd.sup: *abductor superficialis*; Add.sup: *adductor superficialis*, P.cau: *pterygialis caudalis*, P.cran: *pterygialis cranialis*. Origin on membrane indicates the membrane that separates the pelvic muscles from the abdominal muscles.

Table 2.4: Muscles of the Superficial layer of the pelvic fin of the coelacanth *Latimeria chalumnae*.

	Muscle	Diogo *et al* (2016)	Millot & Anthony (1958)	Origin(s)	Insertion(s)	Articulation mode	Function	Mass (g)	ACSA (cm²)
Ventral face	*Pterygialis cranialis*	*Pterygialis cranialis*	Abducteur de la nageoire	Pelvic girdle: Anterior side of the base of the lateral process, ventral side	*Ventral face: Proximal portion of the dermal ray 1; *Pre-axial radial 2, lateral edge	Poly-articular	Protraction	2,280	0,341
	Abductor superficialis pelvicus 1	*Abductor superficialis*	Abaisseur superficiel	Aponeurosis on *Adductor profundus*	*Pre-axial radials 1-2, *Ventral face: Proximal portion of dermal rays 1-2	Poly-articular	Protraction and abduction	3,970	0,468
	Abductor superficialis pelvicus 2			Pelvic girdle: Lateral side of the base of the anterior process	Ventral face: Proximal portion of dermal rays 3-7	Poly-articular	Abduction	4,350	0,363
	Abductor superficialis pelvicus 3			Pelvic girdle: base of the medial process, ventral face	Ventral face: Proximal portion of the dermal ray 8	Poly-articular	Abduction	0,640	0,068
	Abductor superficialis pelvicus 4			Pelvic girdle: base at the posterior edge of the medial process	Ventral face: Proximal portion of the dermal ray 9	Poly-articular	Abduction	0,520	0,060
	Abductor superficialis pelvicus 5			Pelvic girdle: posterior edge of the the medial process	Ventral face: Proximal portion of dermal rays 10-11	Poly-articular	Abduction	0,620	0,065
	Abductor superficialis pelvicus 6			Pelvic girdle: posterior edge of the the medial process	Ventral face: Proximal portion of dermal rays 11-14	Poly-articular	Abduction	1,140	0,111
	Abductor superficialis pelvicus 7			Pelvic girdle: posterior edge of the the medial process	Ventral face: Proximal portion of dermal rays 14-17	Poly-articular	Abduction	1,470	0,127
	Abductor superficialis pelvicus 8			Pelvic girdle: posterior edge of the the medial process	Ventral face: Proximal portion of dermal rays 17-18	Poly-articular	Abduction	1,550	0,137
	Abductor superficialis pelvicus 9			Pelvic girdle: posterior edge of the the medial process	Ventral face: Proximal portion of dermal rays 19-20	Poly-articular	Abduction	0,700	0,062

Table 2.4 (suite)

	Muscle	Diogo *et al* (2016)	Millot & Anthony (1958)	Origin(s)	Insertion(s)	Articulation mode	Function	Mass (g)	ACSA (cm²)
Ventral face	*Abductor superficialis pelvicus 10*	*Abductor superficialis*	Abaisseur superficiel	Pelvic girdle: posterior edge of the the medial process, on the ligament that linked the two medal processes	Ventral face: Proximal portion of dermal rays 20-21	Poly-articular	Abduction	0,660	0,062
	Abductor superficialis pelvicus 11			aponeurosis between the two fins (dorsal to *Abd.sup.pelv.10)*	Ventral face: Proximal portion of the dermal ray 22	Poly-articular	Abduction	0,540	0,067
	Abductor superficialis pelvicus 12			aponeurosis between the two fins (dorsal to *Abd.sup.pelv.11)*	Ventral face: Proximal portion of the dermal ray 23	Poly-articular	Abduction	0,560	0,064
	Abductor superficialis pelvicus 13			aponeurosis between the two fins (dorsal to *Abd.sup.pelv.12)*	Ventral face: Proximal portion of dermal rays 23 and 24	Poly-articular	Abduction	0,440	0,055
	Abductor superficialis pelvicus 14			aponeurosis between the two fins (dorsal to *Abd.sup.pelv.13)*	Ventral face: Proximal portion of dermal rays 25 and 26	Poly-articular	Abduction	1,810	0,211
	Abductor superficialis pelvicus 15			aponeurosis between the two fins (dorsal to *Abd.sup.pelv.14)*	Ventral face: Proximal portion of dermal rays 26 to 30	Poly-articular	Retraction and abduction	4,000	0,563
Dorsal face	*Pterygialis caudalis*	*Pterygialis caudalis*	Adducteur de la nageoire	Pelvic girdle: Postero-superior process, ventral side	Dorsal face: Proximal portion of dermal rays 28-30	Poly-articular	Adduction	1,000	0,201
	Adductor superficialis pelvicus 1	*Adductor superficialis*	Elévateur superficiel, faisceau secondaire	Pelvic girdle: Base of lateral process, ventral side	Dorsal face: *Pre-axial radials 1-2, *Proximal portion of dermal rays 1-8	Poly-articular	Protraction and adduction	1,800	0,215
	Adductor superficialis pelvicus 2		Elévateur superficiel, faisceau principal	Pelvic girdle: Posterior edge of lateral process, dorsal and ventral side	Dorsal face: Proximal portion of dermal rays 8-11	Poly-articular	Adduction	0,738	0,084

Table 2.4 (suite)

	Muscle	Diogo *et al* (2016)	Millot & Anthony (1958)	Origin(s)	Insertion(s)	Articulation mode	Function	Mass (g)	ACSA (cm²)
Dorsal face	*Adductor superficialis pelvicus 3*	*Adductor superficialis*	Elévateur superficiel, faisceau principal	Pelvic girdle: Posterior edge of the lateral process, dorsal side	Dorsal face: Proximal portion of dermal rays 12-15	Poly-articular	Adduction	0,910	0,095
	Adductor superficialis pelvicus 4			Pelvic girdle: Lateral process, dorsal side	Dorsal face: Proximal portion of dermal rays 15-18	Poly-articular	Adduction	1,370	0,145
	Adductor superficialis pelvicus 5			Pelvic girdle: Lateral process, dorsal side	Dorsal face: Proximal portion of dermal rays 18-20	Poly-articular	Adduction	1,400	0,139
	Adductor superficialis pelvicus 6			Pelvic girdle: Antero-lateral edge of the lateral process, dorsal side	Dorsal face: Proximal portion of the dermal ray 21	Poly-articular	Adduction	1,180	0,115
	Adductor superficialis pelvicus 7			*Membrane between pelvic muscles and abdominal muscles; *Pelvic girdle: Lateral process, dorsal side	Dorsal face: Proximal portion of the dermal ray 22	Poly-articular	Adduction	3,330	0,291
	Adductor superficialis pelvicus 8			Membrane between pelvic muscles and abdominal muscles	Dorsal face: *Dorsal ridge of the mesomere 3; *Proximal portion of dermal rays 21-23	Poly-articular	Adduction	1,460	0,147
	Adductor superficialis pelvicus 9			Membrane between pelvic muscles and abdominal muscles	Dorsal face: *Dorsal ridge of the mesomere 2; *Proximal portion of dermal rays 23-25	Poly-articular	Adduction	0,540	0,088
	Adductor superficialis pelvicus 10			Membrane between pelvic muscles and abdominal muscles	Dorsal face: Proximal portion of dermal rays 26-27	Poly-articular	Adduction	0,350	0,066

Adductor superficialis pelvicus

The *adductor superficialis pelvicus* is composed of ten dorsal muscle bundles which are oriented proximally to distally and numbered from the pre-axial to post-axial side of the pelvic fin (Fig. 2.6 A). These muscle bundles originate on (i) the lateral process of the pelvic girdle (*add. sup. pelvicus 1-7*), onto both the dorsal and the ventral side, and (ii) on the fascia that separates the pelvic fin muscles from the abdominal muscles (*add. sup. pelvicus 7-10*; Table 2.4). They insert at the base of fin rays 1 to 27 on the dorsal side of the fin via short aponeurosis. Due to their origin onto the curved concave lateral process of the pelvic girdle, these muscle bundles cross each other (Fig. 2.6 A). The *add. sup. pelvicus 8* and *9* also insert respectively on the dorsal ridge of the mesomere 3 and mesomere 2 by a strong fibrous connective tissue band. The *add. sup. pelvicus 1* also inserts on the pre-axial radials 1 and 2. The *add. sup. pelvicus 2-6* have a gutter-like shape and surround the *adductor profundus pelvicus* of the middle layer as follows. The *add. sup. pelvicus 2* surrounds *adductor profundus pelvicus 1-2*, the *add. sup. pelvicus 3* surrounds *add. prof. pelvicus 3-4*, the *add. sup. pelvicus 4* surrounds the *add. prof. pelvicus 5-6-7-9*, the *add. sup. pelvicus 5* surrounds the *add. prof. pelvicus 8-10* and the *add. sup. pelvicus 6* surrounds the *add. prof. pelvicus 11-12*. All *add. sup. pelvicus* bundles permit the adduction of the fin rays. The *add. sup. pelvicus 1* also permits the protraction of the fin.

Pterygialis caudalis

The *pterygialis caudalis* originates from the ventral side of the postero-superior process of the pelvic girdle and inserts at the base of the pelvic fin rays 28-30 (Fig. 2.6 A). Based on its origin and insertion, the role of the *pterygialis caudalis* is to adduct the pelvic fin.

Abductor superficialis pelvicus

The *abductor superficialis pelvicus* is composed of 15 ventral muscle bundles. As for the dorsal muscles, these muscles are numbered from pre-axial to post-axial, and are oriented from proximal to distal (Fig. 2.6 B). They originate: (i) anteriorly on the lateral process of the pelvic girdle, on the *adductor profundus pelvicus*, via an aponeurosis, (ii) on the ventral side of the pelvic girdle, (iii) on the medial process of the pelvic girdle, and (iv) on the aponeurosis between the two pelvic fins from ventral to dorsal (Table 2.4). The *abd. sup. 15* has the most dorsal origin on this aponeurosis. They insert on the ventral side of the fin, at the base of fin rays 1-30. The *abd. sup. pelvicus 1* also inserts on the latero-ventral side of pre-axials 1 and 2. These bundles permit the abduction of the fin. The *abd. sup. pelvicus 1* also permits the protraction of the fin, and the *abd. sup. pelvicus 15* the retraction of the fin, based on their origin and insertion.

Pterygialis cranialis

The *pterygialis cranialis* is a pre-axial muscle, that originates on the ventral side of the lateral process of the pelvic girdle and inserts on the lateral side of the pre-axial radial 2 and at the base of fin ray 1 (Fig. 2.6 B). Based on its origin and insertion, the role of the *pterygialis cranialis* is to protract the pelvic fin.

Middle layer (Table 2.5)

The middle layer is formed by two muscle masses: the a*dductor profundus pelvicus* on the dorsal side and the *abductor profundus pelvicus* on the ventral side of the pelvic fin (Fig. 2.7). As for the superficial layer, the muscle bundles are poly-articular. The exact origin and insertion of the muscle bundles of the middle layer are listed in Table 2.5, and detailed origins and insertions of each sub-bundle of the different muscles is listed in Supplementary Table 2.1.

Adductor profundus pelvicus

On the dorsal side of the pelvic fin, the middle layer is subdivided into 12 *adductor profundus pelvicus* muscle bundles. They originate (i) from the anterior process of the pelvic girdle, (ii) on the fascia that separates the pelvic fin muscles from the abdominal muscles and (iii) on the anterior part of the lateral process (Fig. 2.7 A). These muscles overlap and intersect each other, and insert at the base of fin rays 6-21, and on the mesomeres 1 to 4 (Table 2.5). Most of these bundles are separated into several sub-bundles (indicated by capital letters), that are also separated in different fascicules (indicated by lowercase letters) (Table 2.5; Sup. Fig. 2.1; Sup. Table 2.1). Unlike the bundles of the superficial layer, these muscle bundles insert onto the fin rays and mesomeres through long tendons (Fig. 2.7 A). The role of the *add. prof. pelvicus* muscle bundles is mainly the adduction of the pelvic fin, but also the flexion of the mesomere 1 (*add. prof. pelvicus 8A*), of the mesomere 2 (*add. prof. pelvicus 10A*), of the mesomere 3 (*add. prof. pelvicus 4A-8B-9-10B*), and of the mesomere 4 (*add. prof. pelvicus 7C-8C-11*).

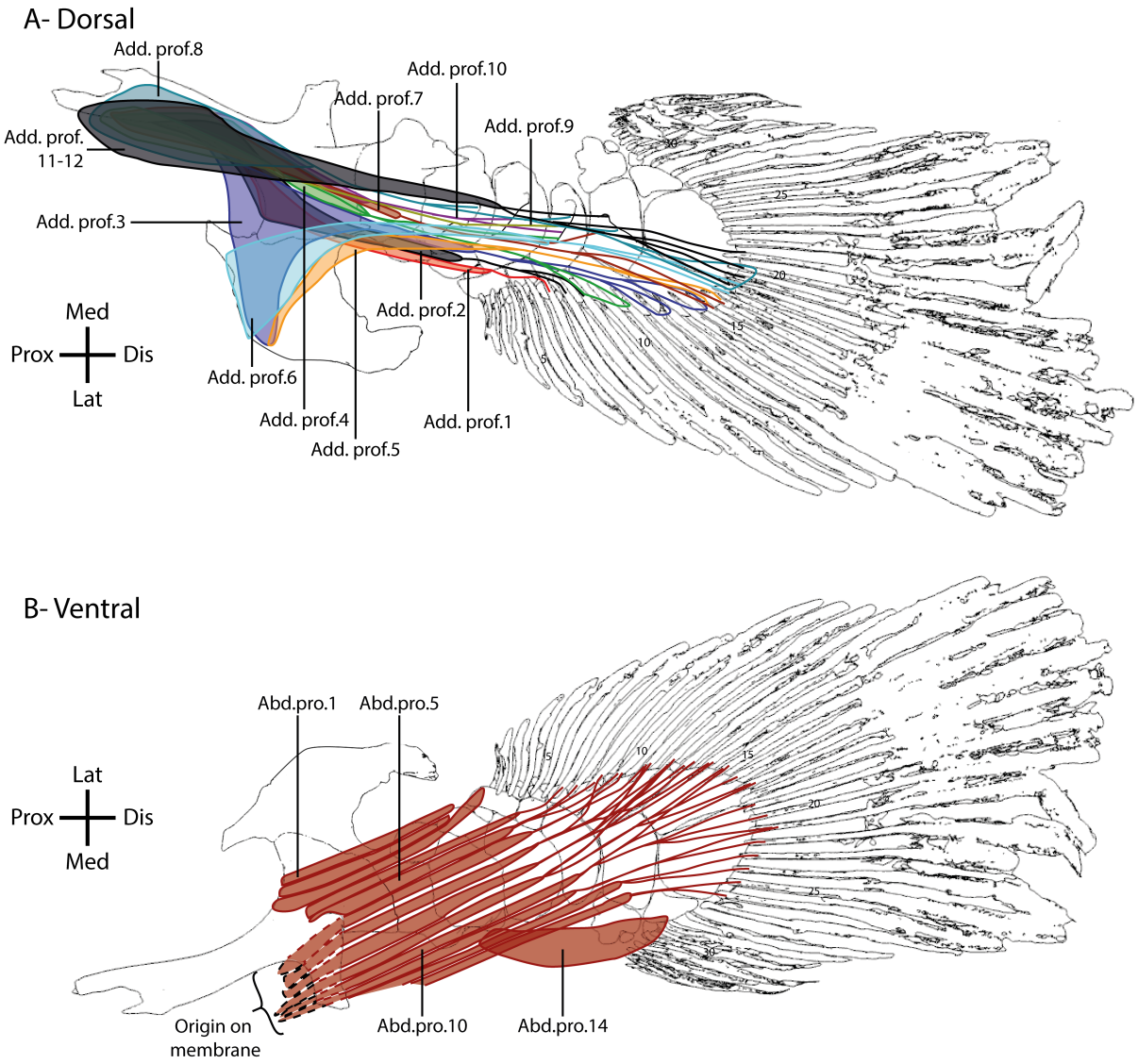

Figure 2.7: Middle muscle layer of the pelvic fin of the coelacanth *Latimeria chalumnae* in dorsal (A) and ventral (B) views. Abd.prof.: *abductor profundus*, Add.prof.: *adductor profundus*. Origin on membrane indicates the membrane that separates the pelvic muscles from the abdominal muscles.

Table 2.5: Muscles of the middle layer of the pelvic fin of the coelacanth *Latimeria chalumnae*.

	Muscle	Diogo *et al* (2016)	Millot & Anthony (1958)	Origin(s)	Insertion(s)	Articulation mode	Function	Mass (g)	ACSA (cm²)
Ventral face	*Abductor profundus pelvicus 1*	*Abductor profundus*	Abaisseur profond	Pelvic girdle: anterior edge of the base of the lateral process (ventral side), adjacent to the anterior process	Ventral face: Antero-lateral edge of the pre-axial radial 2	Poly-articular	Protraction	0,160	0,039
	Abductor profundus pelvicus 2			Pelvic girdle: anterior edge of the base of the lateral process (ventral side), adjacent to the anterior process	ventral face: Lateral edge of the pre-axial radial 1	Poly-articular	Protraction	0,210	0,051
	Abductor profundus pelvicus 3			Pelvic girdle: anterior edge of the base of the lateral process (ventral side), adjacent to the anterior process	Ventral face: Pre-axial radial 1	Poly-articular	Protraction	0,150	0,046
	Abductor profundus pelvicus 4			Pelvic girdle: base of the posterior side of the medial process, ventral side	Ventral face: Proximal portion of the dermal ray 7	Poly-articular	Abduction	0,220	0,027
	Abductor profundus pelvicus 5			Pelvic girdle: base of the posterior side of the medial process, dorsal and ventral side	Ventral face: Proximal portion of dermal rays 8-10	Poly-articular	Abduction	0,820	0,129
	Abductor profundus pelvicus 6			*Membrane between pelvic muscles and abdominal muscles; Pelvic girdle: *base of the posterior side of the medial process (ventral side); *dorsal side of the medial process	Ventral face: Proximal portion of dermal rays 10-11	Poly-articular	Abduction	1,340	0,267

Table 2.5 (suite)

	Muscle	Diogo *et al* (2016)	Millot & Anthony (1958)	Origin(s)	Insertion(s)	Articulation mode	Function	Mass (g)	ACSA (cm²)
Ventral face	*Abductor profundus pelvicus 7*	*Abductor profundus*	Abaisseur profond	Pelvic girdle: dorsal side of the medial process	Proximal portion of the dermal ray 9 and dermal rays 11 to 14	Poly-articular	Abduction	1,154	0,290
	Abductor profundus pelvicus 8			*Pelvic girdle: dorsal side of the medial process; *Membrane between pelvic muscles and abdominal muscles	Proximal portion of dermal rays 11, 12 and 14	Poly-articular	Abduction	0,950	0,207
	Abductor profundus pelvicus 9			*Pelvic girdle: dorsal side of the medial process; *Membrane between pelvic muscles and abdominal muscles	Ventral face: Proximal portion of dermal rays 12-13 and 15-17	Poly-articular	Abduction	1,801	0,303
	Abductor profundus pelvicus 10			*Pelvic girdle: dorsal side of the medial process; *Membrane between pelvic muscles and abdominal muscles	Ventral face: Proximal portion of dermal rays 15, 17 and 19-21	Poly-articular	Abduction	3,960	0,532
	Abductor profundus pelvicus 11			*Pelvic girdle: dorsal side of the medial process; *Membrane between pelvic muscles and abdominal muscles	Ventral face: Proximal portion of dermal rays 21-22	Poly-articular	Abduction	2,060	0,200
	Abductor profundus pelvicus 12			Membrane between pelvic muscles and abdominal muscles	Ventral face: Proximal portion of dermal rays 23-24	Poly-articular	Abduction	1,630	0,215
	Abductor profundus pelvicus 13			Aponeurosis between the two pelvic fins	Ventral face: Proximal portion of dermal rays 25-26	Poly-articular	Abduction	0,700	0,120

Table 2.5 (suite)

	Muscle	Diogo *et al* (2016)	Millot & Anthony (1958)	Origin(s)	Insertion(s)	Articulation mode	Function	Mass (g)	ACSA (cm²)
Ventral face	*Abductor profundus pelvicus 14*	*Abductor profundus*	Abaisseur profond	*Edge of the medial bud of Mesomere 1; *aponeurosis between the two fins	Ventral face: Proximal portion of dermal rays 30-33	Poly-articular	Abduction and Retraction	3,182	0,556
Dorsal face	*Adductor profundus pelvicus pelvicus 1*	*Adductor profundus*	Elévateur profond	Pelvic girdle: lateral edge of the base of the anterior stick, dorsal side	Dorsal face: Proximal portion of the dermal ray 7	Poly-articular	Adduction	0,280	0,033
	Adductor profundus pelvicus pelvicus 2			Pelvic girdle: Lateral edge of the anterior stick (ventral and dorsal side)	Dorsal face: Proximal portion of dermal rays 8 and 9	Poly-articular	Adduction	1,670	0,177
	Adductor profundus pelvicus pelvicus 3			Pelvic girdle: *Lateral process (dorsal side); *Lateral edge of the base of the anterior stick (ventral side)	Dorsal face: Proximal portion of dermal rays 12 to 15	Poly-articular	Adduction	1,275	0,133
	Adductor profundus pelvicus 4A			Pelvic girdle: Lateral edge of the base of the anterior stick, dorsal side	Dorsal face: Dorsal ridge of the mesomere 3	Poly-articular	Dorsal flexion of mesomere 3	0,711	0,128
	Adductor profundus pelvicus 4B			Pelvic girdle: Lateral edge of the base of the anterior stick, dorsal side	Dorsal face: Proximal portion of dermal rays 9 to 11 and dermal ray 13	Poly-articular	Adduction	0,955	0,159
	Adductor profundus pelvicus 5			Pelvic girdle: Antero-lateral edge of the lateral process (dorsal side)	Dorsal face: Proximal portion of dermal rays 15 and 16	Poly-articular	Adduction	0,220	0,037
	Adductor profundus pelvicus 6			Pelvic girdle: Anterior edge of the lateral process (dorsal side)	Dorsal face: Proximal portion of dermal rays 17 and 18	Poly-articular	Adduction	1,570	0,260
	Adductor profundus pelvicus 7A			Pelvic girdle: Lateral edge of the anterior stick (ventral and dorsal side)	Dorsal face: Proximal portion of dermal rays 15 and 16	Poly-articular	Adduction	1,100	0,175

Table 2.5 (suite)

	Muscle	Diogo *et al* (2016)	Millot & Anthony (1958)	Origin(s)	Insertion(s)	Articulation mode	Function	Mass (g)	ACSA (cm²)
Dorsal face	*Adductor profundus pelvicus 7B*	*Adductor profundus*	Elévateur profond	Pelvic girdle: Lateral edge of the anterior stick (ventral and dorsal side)	Dorsal face: Dorsal ridge of the mesomere 4	Poly-articular	Dorsal flexion of mesomere 4	0,720	0,166
	Adductor profundus pelvicus 8A			Pelvic girdle: Medial edge of the base of the anterior stick (dorsal side)	Dorsal face: Dorsal ridge of mesomeres 1	Mono-articular	Dorsal flexion of mesomere 1	0,450	0,106
	Adductor profundus pelvicus 8B			*Membrane between pelvic muscles and abdominal muscles; *Pelvic girdle: Medial edge of the anterior stick, anterior to *Add.prof.pelv.8a* (dorsal side)	Dorsal face: Dorsal ridge of mesomere 3	Poly-articular	Dorsal flexion of mesomere 3	1,390	0,299
	Adductor profundus pelvicus 8C			*Membrane between pelvic muscles and abdominal muscles; *Pelvic girdle: Anterior side of the anterior process, dorsal and ventral side	Dorsal face: Dorsal ridge of the mesomere 4	Poly-articular	Dorsal flexion of mesomere 4	2,410	0,392
	Adductor profundus pelvicus 8D			*Pelvic girdle: Anterior edge of the lateral process, dorsal side; *Pelvic girdle: Anterior side of the anterior process, dorsal and ventral side	Dorsal face: Proximal portion of dermal rays 17 to 20	Poly-articular	Adduction	3,520	0,494
	Adductor profundus pelvicus 9			Pelvic girdle: lateral edge of the anterior part of the anterior stick, ventral and dorsal side	Dorsal face: Dorsal ridge of the mesomere 3	Poly-articular	Dorsal flexion of mesomere 3	0,670	0,179

Table 2.5 (suite)

	Muscle	Diogo *et al* (2016)	Millot & Anthony (1958)	Origin(s)	Insertion(s)	Articulation mode	Function	Mass (g)	ACSA (cm²)
Dorsal face	*Adductor profundus pelvicus 10A*	*Adductor profundus*	Elévateur profond	Pelvic girdle: Anterior process, dorsal side	Dorsal ridge of the mesomere 2	Poly-articular	Dorsal flexion of mesomere 2	0,420	0,104
	Adductor profundus pelvicus 10B			Pelvic girdle: Anterior process, dorsal side	Dorsal face: Dorsal ridge of the mesomere 3	Poly-articular	Dorsal flexion of mesomere 3	0,890	0,198
	Adductor profundus pelvicus 11			* Membrane between pelvic muscles and abdominal muscles; *Medial edge of the anterior stick	Dorsal face: Mesomere 4	Poly-articular	Dorsal flexion of mesomere 4	2,430	0,523
	Adductor profundus pelvicus 12			*Pelvic girdle: Anterior edge of the lateral process, dorsal side; *Lateral edge of the anterior stidk; *Membrane between pelvic muscles and abdominal muscles	Dorsal face: Proximal portion of dermal rays 18 to 21	Poly-articular	Adduction	2,940	0,411

Abductor profundus pelvicus

There are 14 *abductor profondus pelvicus* muscle bundles on the ventral side of the pelvic fin, that originate (i) from the base of the lateral process (along the anterior edge), (ii) on the medial process, (iii) far anterior to the medial process, on the aponeurosis between the two pelvic girdles (dorsal to the *abd. sup. pelvicus* 15), and (iv) on the fascia that separates the pelvic muscles from the abdominal muscles (Fig. 2.7 B). *Abd. prof. pelvicus 1-3* insert on the pre-axial radial 1-2 and are protractor of the fin, *abd. prof. pelvicus 4-14* insert on the fin rays 7-30 and are abductor of the fin (Table 2.5). The *abd. prof. pelvicus 14* is also a retractor of the fin. As for the *add. prof. pelvicus* these muscle bundles insert on the fin rays through long tendons and are separated in several sub-bundles (Sup. Table 2.1).

Deep layer (Table 2.6)

The deep layer is formed by *pronator* and *flexor* muscles on the dorsal side, and *supinator* muscles on the ventral side of the pelvic fin. These muscles allow the rotation of the fin, based on their origins and insertions (Fig. 2.8). Except for the *flexor* muscles, the terminology used is based on Diogo et al. (2016). However, the function of the different *pronator* and *supinator* muscles is different from that suggested in previous studies. The detailed origins and insertions of each muscle of the deep layer are summarized in Table 2.6.

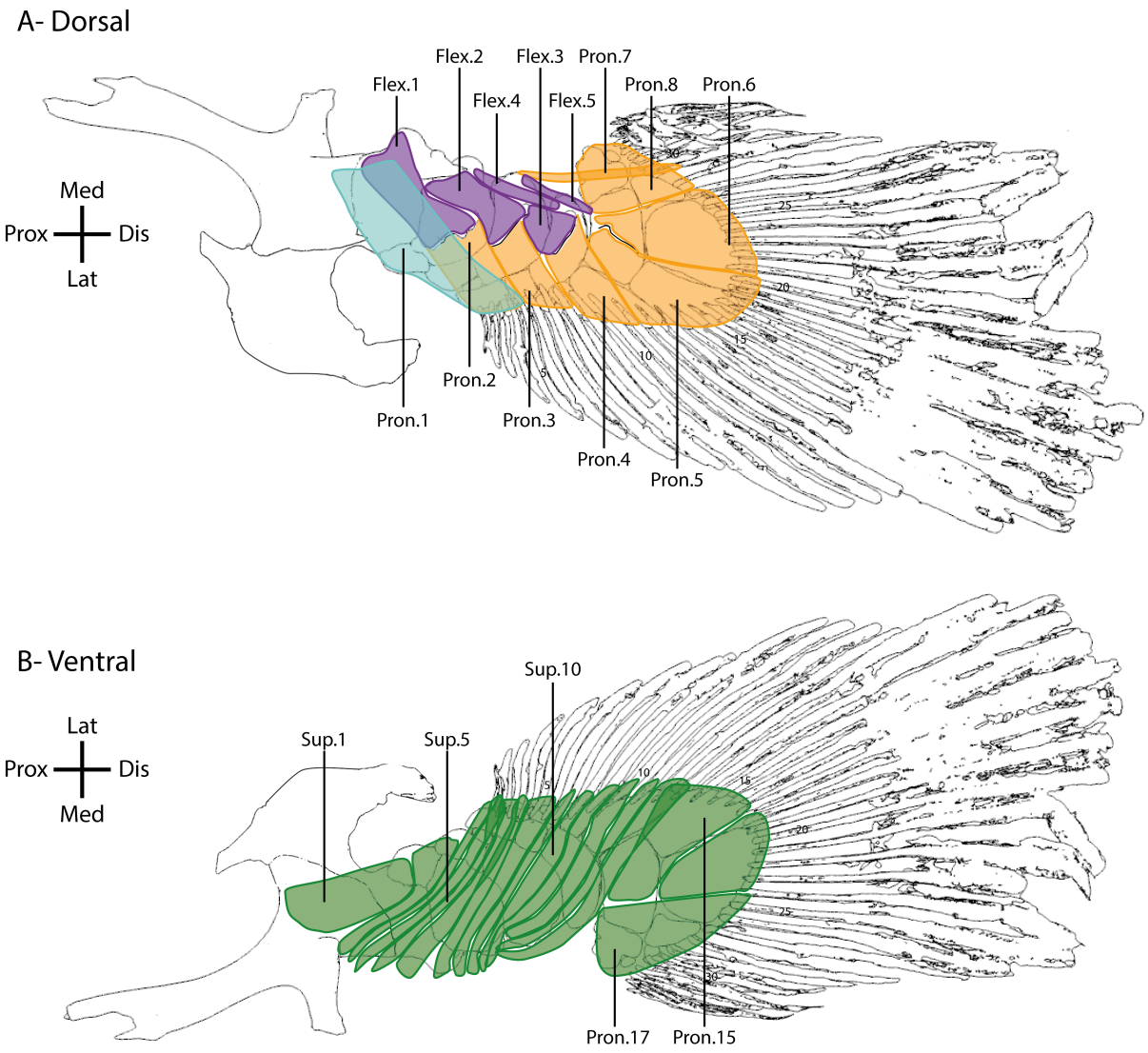

Figure 2.8: Deep muscle layer of the pelvic fin of the coelacanth *Latimeria chalumnae* in dorsal (A) and ventral (B) views. Flex.: *flexor*; Pron: *pronator*; Sup: *supinator*.

Table 2.6: Muscles of the middle layer of the pelvic fin of the coelacanth *Latimeria chalumnae*.

	Muscle	Diogo *et al* (2016)	Millot & Anthony (1958)	Origin(s)	Insertion(s)	Articulation mode	Function	Mass (g)	ACSA (cm²)
Ventral face	*Supinator 1*	*Supinator 1*	Supinateur	Pelvic girdle: between lateral and medial processes (ventral face) and at the posterior edge of the base of the medial process (ventral face)	Ventral face: Anterior side of the pre-axial radial 0	Poly-articular	Pronation	0,540	0,138
	Supinator 2			Pelvic girdle: medial side of the girdle	Ventral face: Posterior side of the pre-axial radial 0 and anterior side of the pre-axial radial 1	Poly-articular	Pronation	1,310	0,272
	Supinator 3			Membrane between pelvic muscles and abdominal muscles	Ventral face: *Pre-axial radial 1; *Base of the dermal ray 1	Poly-articular	Pronation	1,344	0,219
	Supinator 4			Membrane between pelvic muscles and abdominal muscles	Ventral face: Base of the dermal ray 2	Poly-articular	Pronation	1,392	0,146
	Supinator 5			*Membrane between pelvic muscles and abdominal muscles; *Medial edge of the girdle; *Proximo-medial edge of the mesomere 1	Ventral face: *Pre-axial radial 2; *Base of dermal rays 1 and 2	Poly-articular	Pronation	1,509	0,287
	Supinator 6	*Supinator 2-4*		*Membrane between pelvic muscles and abdominal muscles; *Proximo-medial edge of the mesomere 1	Ventral face: Base of dermal rays 2, 3 and 5	Poly-articular	Pronation	1,873	0,283
	Supinator 7			Medial edge of the mesomere 1	Ventral face: Base of dermal rays 3-4	Poly-articular	Pronation	0,464	0,111

Table 2.6 (suite)

	Muscle	Diogo *et al* (2016)	Millot & Anthony (1958)	Origin(s)	Insertion(s)	Articulation mode	Function	Mass (g)	ACSA (cm²)
Ventral face	*Supinator 8*	*Supinator 2-4*	Supinateur	*Membrane between pelvic muscles and abdominal muscles; *Postero-superior process; *Medial edge of the mesomere 1	Ventral face: Base of dermal rays 4-6	Poly-articular	Pronation	1,377	0,216
	Supinator 9			*Membrane between pelvic muscles and abdominal muscles; *Aponeurosis between the two fins; *Proximo-medial edge of the mesomere 2	Ventral face: Base of the dermal ray 7	Poly-articular	Pronation	1,676	0,267
	Supinator 10			*Aponeurosis between the two fins; *Dorso-medial edge of the mesomere 1; *Proximo-medial edge of the mesomere 2	Ventral face: Base of the dermal ray 8	Poly-articular	Pronation	0,997	0,199
	Supinator 11			*Aponeurosis between the two fins; *Medial edge of the mesomere 2	Ventral face: Base of the dermal ray 9	Poly-articular	Pronation	0,578	0,133
	Supinator 12			*Aponeurosis between the two fins; *Medial edge of the mesomere 2; *Mesomere 3	Ventral face: Base of the dermal ray 10	Poly-articular	Pronation	0,756	0,161

Table 2.6 (suite)

	Muscle	Diogo *et al* (2016)	Millot & Anthony (1958)	Origin(s)	Insertion(s)	Articulation mode	Function	Mass (g)	ACSA (cm²)
Ventral face	*Supinator 13*	*Supinator 2-4*	Supinateur	*Medial bud of mesomere 1; *Medial edge of mesomere 2; *Medial edge of mesomere 3	Ventral face: Base of the dermal ray 11	Poly-articular	Pronation	0,933	0,203
	Supinator 14			*Medial bud of the mesomere 1; *Medial edge of the mesomere 2; *Medial edge of the mesomere 3	Ventral face: Base of dermal rays 12-13	Poly-articular	Pronation	1,228	0,243
	Supinator 15		*Undescribed*	Mesomere 4	Ventral face: Base of dermal rays 12-17	Mono-articular	Pronation	0,700	0,425
	Supinator 16			Proximo-medial edge of the distal radial	Ventral face: Base of dermal rays 18-24	Mono-articular	Abduction	0,642	0,261
	Supinator 17			*Medial edge of the Mesomere 4; *Proximal edge of the post-axial radial	Ventral face: Base of dermal rays 24-33	Mono-articular	Supination	1,164	0,598
Dorsal face	*Pronator 1*	*Pronator 1*	Pronateur 1-3	Pelvic girdle, between the anterior stick and the postero-superior process, dorsal side	Dorsal face: *Pre-axial radials 0-2; *Proximal portion of dermal rays 1 to 5	Poly-articular	Supination	3,490	0,962
	Pronator 2			Mesomere 1, dorsal ridge	Dorsal face: Proximal portion of dermal rays 1 to 5	Poly-articular	Supination	0,966	0,375
	Pronator 3	*Pronator 2*		Mesomere 2, dorsal ridge	Dorsal face: Proximal portion of dermal rays 6 to 8	Mono-articular	Supination	0,680	0,256
	Pronator 4	*Pronator 3*		Mesomere 3, dorsal ridge	Dorsal face: Proximal portion of dermal rays 9 to 11	Mono-articular	Supination	0,681	0,202

Table 2.6 (suite)

	Muscle	Diogo *et al* (2016)	Millot & Anthony (1958)	Origin(s)	Insertion(s)	Articulation mode	Function	Mass (g)	ACSA (cm²)
Dorsal face	*Pronator 5*	*Pronator 4*	Pronateur 4	Mesomere 4, lateral edge of the dorsal ridge	Dorsal face: Proximal portion of dermal rays 12 to 20	Mono-articular	Supination and dorsal flexion of fin rays	0,617	0,241
	Pronator 6		Pronateur 5	Mesomere 4, medial edge of the dorsal ridge	Dorsal face: Proximal portion of dermal rays 20 to 27	Mono-articular	Dorsal flexion of fin rays and pronation	1,671	0,634
	Pronator 7	*Undescribed*		Mesomere 2, medial bud	Dorsal face: Proximal portion of the dermal ray 29	Poly-articular	Dorsal flexion of fin rays	0,156	0,046
	Pronator 8			Mesomere 4 proximo-medial edge and proximal edge of post-axial radial	Dorsal face: Proximal portion of dermal rays 28 to 32	Mono-articular	Pronation	1,066	0,503
	Flexor 1		*Undescribed*	Pelvic girdle: postero-superior process (dorsal side)	Mesomere 1, proximal side of the dorsal ridge	Mono-articular	Dorsal flexion of the mesomere 1	1,570	0,423
	Flexor 2			Pelvic girdle: postero-superior process (ventral side) and mesomere 1 (dorsal side)	Mesomere 2, proximal side of the dorsal ridge	Mono-articular	Dorsal flexion of the mesomere 2	1,058	0,370
	Flexor 3			Mesomere 2, distal side of dorsal ridge	Mesomere 3, proximo-lateral side of the dorsal ridge	Mono-articular	Dorsal flexion of the mesomere 3	0,116	0,109
	Flexor 4			Mesomere 1, distal edge of the medial bud	Mesomere 3, proximo-medial side of the dorsal ridge	Poly-articular	Dorsal flexion of the mesomere 3	0,340	0,139
	Flexor 5			Mesomere 2, distal edge of the medial bud	Mesomere 4, proximo-medial edge	Poly-articular	Dorsal flexion of the mesomere 4	0,437	0,187

Pronator muscles

The *pronator* muscles are formed by eight muscles (Table 2.6), each muscle is itself separated into several muscle bundles (Fig. 2.8 A; Sup. Fig. 2.2; Sup. Table 2.1). The *pronators* are numbered from 1 to 8. The *pronator 1* originates from the pelvic girdle and inserts on the pre-axial radials 0-2 and fin rays 1-5. *Pronators 2-4* originate respectively from the dorsal ridge of the mesomere 1, mesomere 2 and mesomere 3 and insert on fin rays 1 to 11. The *pronator 5* and *pronator 6* originate both on the dorsal ridge of the mesomere 4, but the *pronator 5* from the lateral side of this ridge, and the *pronator 6* from the medial side of the ridge. The *pronator 5* inserts on fin rays 12-19 and the *pronator 6* inserts on the fin rays from the post-axial side of the fin (20-27). The *pronator 7* originates from the medial process of the mesomere 2 and inserts at the base of fin ray 29, and the *pronator 8* originates from the proximal edge of the mesomere 4 and inserts on fin rays 28 to 32. Whereas the muscles are called "pronator", *pronators 1*-4 are supinators of the pelvic fin. The *pronator 5* is involved in the flexion of the pre-axial radial 4 and fin rays 12-20 and the supination of the fin. The *pronator 6* is involved in the flexion of the distal radial and fin rays 20-27 and the pronation of the fin. The *pronator 7* is involved in the flexion of fin ray 29 and *pronator 8* in the pronation of the fin. Most of these *pronator* muscles are mono-articular (Table 2.6).

Flexor muscles

Flexor muscles originate and insert on two different mesomeres. *Flexors 1-3* originate respectively on the pelvic girdle, the mesomere 1, and the mesomere 2, and insert on the following elements (Table 2.6; Fig. 2.8 A). These muscles are mono-articular. The *flexors 4-5* are bi-articular, they originate respectively on mesomeres 1 and 2, and insert on mesomeres 3 and 4. *Flexor* muscles permit the flexion of mesomeres 1-4.

Supinator muscles

The ventral side of the pelvic fin is formed by 17 *supinator* muscles (Table 2.6; Fig. 2.8 B). Except for the *supinator 1*, all these *supinator* muscles are subdivided in several bundles (Sup. Table 2.1). The *supinator 1* originates on the ventral side of the pelvic girdle and inserts on the anterior side of the pre-axial radial 0. The *supinators 2-14* have multiples origins and insertions since the smallest bundles of a muscle are covered by the longest bundles (Sup. Table 2.1). They insert from the pre-axial radial 0 to the fin ray 12. The *supinators 15-17* are also formed by several bundles, but they are smaller and originate from the mesomere 4 and the distal radial. Moreover, the different bundles are adjacent and insert on fin rays 12 to 33, similar in their

arrangement to the *pronators 5-6* (Fig. 2.8 B). The *supinators 1-15* permit the pronation of the fin, the *supinator 16* permits the abduction of the fin, and *supinator 17* permits the supination of the fin.

Muscle architecture

Muscle mass

The pectoral fin musculature of specimen CCC14 weighs 165.8 g (0.43% body mass). The ratio between muscles of the lateral and medial sides of the pectoral fin is different. Muscles of the lateral face weigh 93.9 g, whereas muscles of the medial face weigh 71.9 g. Moreover, the distribution of the muscle mass is unequal among the different layers of the lateral side: the deep layer is the heaviest (36.1g), then the superficial layer (30.5 g), and finally the middle layer (27.3 g). On the medial side, the distribution of the muscles mass is more unequal, the superficial layer having the heaviest mass (33.4 g) then the deep layer (21.7 g), and the middle layer (16.7 g) (Table 2.7).

Table 2.7: Muscular properties of the different muscles layers of the pectoral and the pelvic fins of the coelacanth *Latimeria chalumnae*.

Pectoral fin	Layer	Mass (g)	ACSA (cm²)	**Pelvic fin**	Layer	Mass (g)	ACSA (cm²)
Lateral face	Superficial	30,52	8,79	Ventral face	Superficial	25,25	2,82
	Middle	27,25	4,23		Middle	18,34	2,98
	Deep	36,13	9,84		Deep	18,48	4,16
	Total	**93,90**	**22,87**		**Total**	**62,07**	**9,97**
Medial face	Superficial	33,43	4,83	Dorsal face	Superficial	14,08	1,59
	Middle	16,74	1,51		Middle	23,62	3,98
	Deep	21,75	7,91		Deep	12,85	4,45
	Total	**71,91**	**14,25**		**Total**	**50,55**	**10,01**

The pelvic fin musculature of specimen CCC27 weights 112.6g (0.30% body mass). Similar to the pectoral fin of CCC14, the two sides (ventral and dorsal, corresponding respectively to the lateral and medial sides of the pectoral fin) differ in the distribution of the muscle mass. The ventral face musculature (62.1 g) is more important than that of the dorsal side (50.5 g). The distribution of the muscle masses along the three layers is also unequal, but more so on the dorsal side compared to the ventral side. On the dorsal side, the middle layer contributes around half of the total (23.6 g), whereas on the ventral side, the distribution of the mass is more similar across layers with the superficial layer being only slightly heavier than the other layers (25.3 g; Table 7).

Anatomical cross-section area

The Anatomical cross-sectional area (ACSA) of the pectoral fin is 37.2 cm², but its distribution between the two sides of the fin is unequal. The ACSA of the lateral and medial side is 23.0 cm² and 14.2 cm² respectively. The distribution of the ACSA on the different layers for lateral and medial sides of the fin is similar to the distribution of the muscle masses, the deep layer having an ACSA that is higher than that of the superficial and the middle layers (9.8 cm², 7.8 cm² and 4.2 cm² for the lateral side; 7.9 cm²; 4.8 cm² and 1.5 cm² for the medial side). Of the 86 muscle bundles of the pectoral fin, 30 bundles are only involved in the articulation between the pectoral girdle and the first mesomere (Tabs 2.1-2.3). The total mass of these bundles is 57.8 g (35% total pectoral muscles mass), corresponding to an ACSA of 12.7 cm² (34% total pectoral ACSA).

The ACSA of the pelvic fin is 20.0 cm², and the distribution is similar for the dorsal and ventral sides (10.0 cm² and 10.0 cm²). The distribution of the ACSA across the different muscle layers shows that on the ventral side, the superficial and middle layers are similar (2.9 and 3.0 cm² respectively), whereas on the dorsal side, they are different (1.6 and 4.0 cm²). The deep layer of the ventral and dorsal sides is the most strongly developed (4.2 and 4.5 cm² respectively).

Joint mobility

Pectoral fin mobility

The pectoral fin of *L. chalumnae* shows a large degree of mobility in the three planes, defined as abduction/adduction, protraction/retraction, and pronation/supination movements. The range of mobility is higher for the joint between the pectoral girdle and the first mesomere (mean: 102° for abduction/adduction, 93° for protraction/retraction and 90° for pronation/supination) (Fig. 2.9). Mobility generally decreases along the metapterygial axis, and the distal joint is the least mobile in all planes (30° for abduction/adduction, 55° for protraction/retraction and 41° for pronation/supination for CCC19, ligament damaged for CCC14). The pectoral fins (CCC14, CCC19) show a similar joint mobility along the metapterygial axis. The large difference of mobility (Fig. 2.9) observed for the abduction/adduction of mesomere 1 with the girdle and mesomere 4 with the mesomere 3, and the pronation/supination of the mesomere 2 with the mesomere 1 are possibly due to damaged ligaments on the CCC19 specimen.

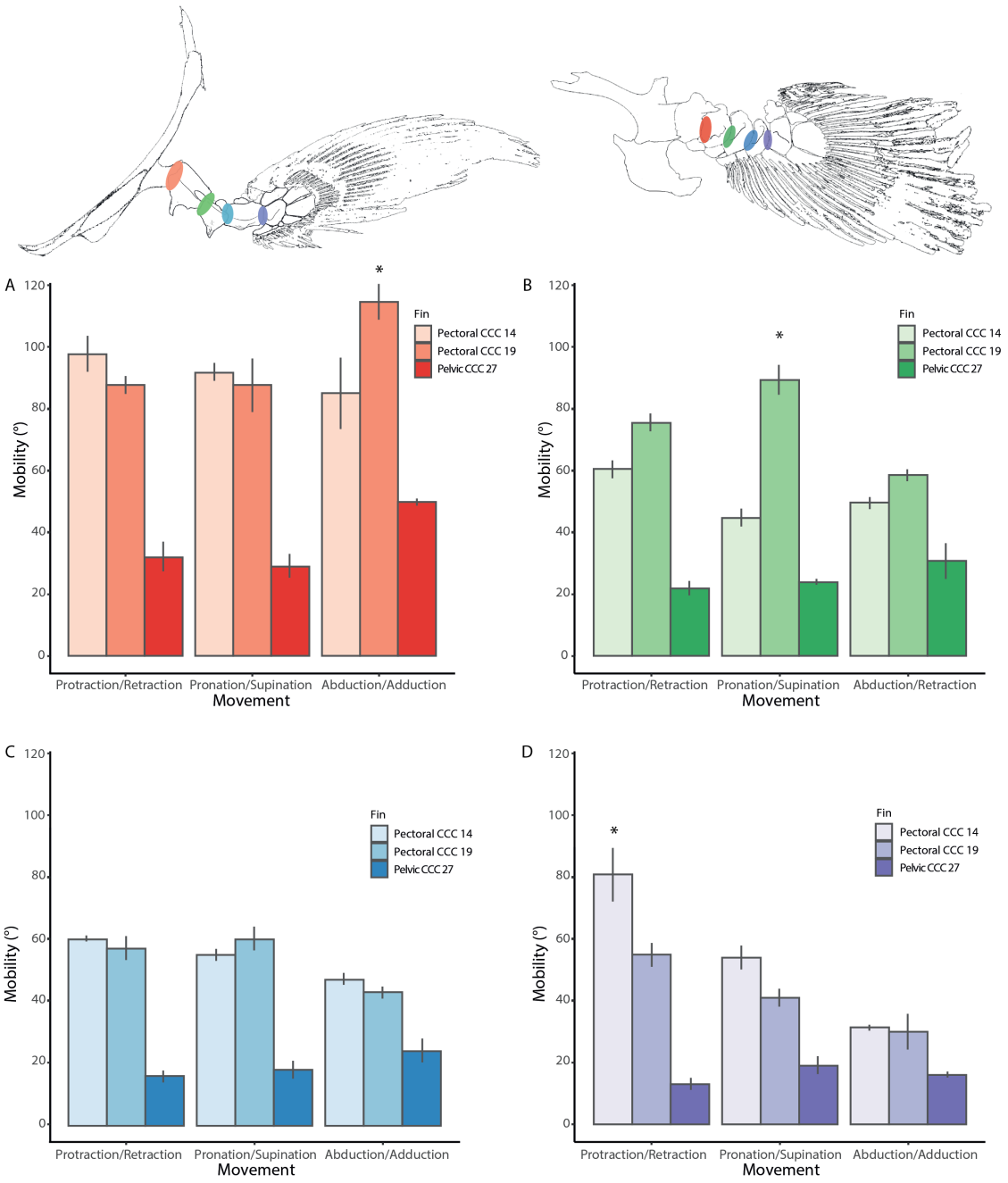

Figure 2.9: Range of mobility of the joints in the three planes along the metapterygial axis. A: Joint mobility between the girdle and the mesomere 1, B: Joint mobility between the mesomere 1 and the mesomere 2; C: Joint mobility between the mesomere 2 and the mesomere 3; D: Joint mobility between the mesomere 3 and the mesomere 4. The * indicates a large difference of mobility between the two different pectoral fins. This difference either suggests a greater inter-individual variability of mobility, or more probably is due to a damaged ligament.

Pelvic fin mobility

Similar to the pectoral fin, the joint between the pelvic girdle and the first mesomere is the most mobile with an important range of motion for the abduction/adduction movement (50°). Antero-posterior and rotational movements have a reduced range of motion (respectively 32° and 29°).

The measurements also show that the mobility decreases along the metapterygial axis, and that the distal joint is less mobile than the more proximal joints (Fig. 2.9). Overall, the mobility of the pelvic fin is less important than that of the pectoral fin.

Discussion

The muscular anatomy of the paired fins of *Latimeria chalumnae*

In accordance with previous descriptions (Millot and Anthony, 1958; Diogo et al., 2016; Miyake et al., 2016) our results show that the muscular anatomy of the pectoral and pelvic fins of the African coelacanth are arranged in three layers: superficial, middle and deep. However, both the pectoral and pelvic fins show a more complex muscular organization in terms of number of muscle bundles than previously described. Indeed, we observed 86 muscle bundles for the pectoral fin and 83 muscle bundles for the pelvic fin, whereas Millot and Anthony (1958) described only 40 muscle bundles for each fins. The more recent study of Miyake et al. (2016) described 48 muscles bundles for the pectoral fin, while that of Diogo et al. (2016) described a new *elevator lateralis* muscle at the dorsal side of the pelvic fin, originating on the abaxial musculature and inserting on the first mesomere. This muscle was subsequently reported in other studies (Molnar et al., 2018, 2020). However, this muscle was never observed in our dissections, neither in the description of Millot and Anthony (1958). Moreover, the presence of a fascia that separates the pelvic muscles from the abdominal cavity does not let supposed that such a muscle could be present in *Latimeria*.

The organization of the muscles along the metapterygial axis differs between the pectoral and pelvic fins. The pectoral fin shows an important number of mono-articular muscles on the lateral and medial sides of the fin (Figs 2.3-2.5) connecting adjacent elements, especially in the superficial and deep layers. Whereas the anatomy of the muscles on the lateral and medial sides of the fin appears symmetrical, the distribution of the mass is different between the two sides. Indeed, the lateral side of the pectoral fin contains more muscle mass than the medial side (93.9 g *vs* 71.9 g; representing respectively 57% and 43% of the total pectoral mass). In the pelvic fin the anatomy appears more asymmetrical (Figs 2.6-2.8). In the middle layer, the muscles of the dorsal side only insert on the pre-axial fin rays (fin rays 7-21) and only cover the lateral part of the dorsal side of the fin. In contrast, on the ventral side, the muscles insert on the pre-axial radial elements, and on fin rays 7-33, and cover the entire ventral side of the fin. Moreover, in the deep layer, muscles are short and *pronators* join the mesomeres and the fin

rays on the dorsal side. There are additional five *flexor* muscles that connect the mesomeres. On the ventral side, however, most of the muscles are longer and originate dorsally on the membrane between the two fins. On the pelvic fin, the majority of muscles are poly-articular and insert directly on the fin rays. As for the pectoral fin, the distribution of the muscle mass is asymmetric. The ventral side of the fin has a more important mass than the dorsal side (63.1 g *vs* 50.5 g; representing respectively 56% and 44% of the total pelvic muscle mass). In the pectoral fin the more muscular side is involved in fin protraction, and in the pelvic fin, since the two fins have different orientations, it is then the equivalent side, involved in the fin abduction, that has the most muscular mass. However, whereas for the pectoral fin the ACSA on the lateral side of the fin is higher (Table 2.7), for the pelvic fin the ACSA on the ventral and dorsal sides is similar.

A smaller pelvic fin compared to the pectoral fin is common in actinopterygians and non-tetrapod sarcopterygians (Coates, 1995; Coates and Ruta, 2007; Shubin et al., 2014). The coelacanth presents a similar muscular anatomy, since the pelvic fin is smaller in size and mass than the pectoral fin, and that the muscle mass of the pectoral fin (166g) is higher than that of the pelvic fin (113g). However, the total masses of the pectoral and pelvic fins correspond only to 0.86% and 0.60% of the total body mass. The muscle architecture also differs between the pectoral and the pelvic fin. The ACSA of the pectoral fin is greater than that of the pelvic fins (Table 2.7). Since the ACSA is a proxy of the force that can be developed by muscles (Close, 1972), it appears that the pectoral fin can generate more force and is thus likely more involved in generating propulsion or in the stabilization of the coelacanth. This is in accordance with observations of Fricke and Hissmann (1992), who suggested that the pectoral fin is important in locomotion. In teleosts, the pectoral fins have an active role for a variety of manoeuvring behaviours and for low-speed swimming (Gibb et al., 1994; Drucker and Lauder, 2003; Standen and Lauder, 2005; Don et al., 2013). In teleosts, the pelvic fins help control the body position during manoeuvres and control stability (Lauder and Drucker, 2004; Standen, 2008; Don et al., 2013). As in teleosts, the respective role of the pectoral and pelvic fins is likely different in the coelacanth, with the pectoral fins presumably having a more active role in contrast to the pelvic fins that likely have a function in body stabilization and manoeuvres (Fricke and Hissmann, 1992).

Whereas the two sides of the pelvic fin show an equal ACSA and should be able to develop the same force, in the pectoral fin the distribution is unequal. Indeed, the lateral side of the fin has a

higher ACSA than the medial side (Table 2.7). This suggests that the lateral side of the pectoral fin (resulting in fin protraction) is stronger than the medial side (responsible for retraction). In the cod (*Gadus morhua*)and the saithe (*Gadus virens*), it has been shown that the abductor muscle mass of the pectoral fin is the same as the adductor muscle mass, whereas for the mackerel (*Scomber scombrus*), the abductor muscle mass is twice that of the adductor muscle mass (Geerlink, 1987). It appears that in the cod and the saithe the pectoral fins have a more important role in the backward movements of the pectoral fin for braking than in the mackerel. During locomotion of *Latimeria*, Fricke and Hissmann (1992) showed that the lateral side of the pectoral fin (*ventral face* in their paper) pushes the water against the direction of the motion suggesting that the muscles of this side are mainly involved in braking whereas the muscles from the medial side may be more important in generating propulsion.

The pelvic girdle of *L. chalumnae* has a superficial ossification around the anterior process and the medial process, associated with an internal trabecular system (Mansuit et al., 2020b). It has been suggested that this ossification may reinforce these parts of the pelvic girdle to resist to the force developed by the muscles that insert there. The anterior process is long and thin, and even if the medial process is slightly more robust, the insertion area of the muscles is small such that high stresses may indeed be imposed on these processes. Based on our data it appears that the ACSA of the muscles inserting there is greater on the anterior (2.8 cm^2) and medial processes (2.6 cm^2) compare to other parts of the girdle (Sup. Table 2.2). The robust part of the girdle with the articular head also is submitted to significant muscle forces (2.5 cm^2). This part is not ossified, neither associated with a trabecular system. However the robustness of this part of the girdle might explain that there is no needing of such reinforcement to support the force developed by the muscles. The high value of ACSA of the muscle bundles inserting on the ossified part of the girdle supports the hypothesis of reinforcement of these parts to support the forces generated by the muscles during contraction. The ACSA of the muscle bundles on the lateral process is also important (2.0 cm^2), but since the surface of the lateral process is larger than the anterior or medial processes, the force produced by bundles is also distributed across a larger surface, likely reducing stress concentrations. The role of muscles in the ossification of bones during the development has been demonstrated for chickens and mice (Nowlan et al., 2008, 2010), with muscle presence and its activity being essential in the ossification of the bones. When the muscle mass is reduced, or the muscular activity is reduced, the ossification of the bone is reduced (Nowlan et al., 2008).

As all sarcopterygian fishes, the coelacanth *L. chalumnae* has lobed paired fins (e.g. Millot and Anthony, 1958), different in their anatomy from the fins of most actinopterygians. Different authors have pointed out that actinopterygians and sarcopterygians differ in the origin and insertion of fin muscles. In actinopterygians, muscles extend from the girdle to the fin rays, passing over radials (e.g. Lauder and Drucker, 2004; Diogo and Abdala, 2007; Diogo et al., 2009; Wilhelm et al., 2015). In sarcopterygians, muscles present a more complex organization and insert on the endoskeletal elements of the appendages, in order to move the other skeletal elements of the fin or limb, and only the coelacanth possesses muscles that insert also on the fin rays (Boisvert et al., 2013). In tetrapods, there is a functional regionalization of the metapterygial axis in stylo-, zeugo- and autopod, associated with the complex muscular organization of the limbs (Ashley-Ross, 1994; King and Hale, 2014). Associated with this functional regionalization of the limbs, tetrapods have an important proportion of mono-articular muscles and they have lost the *abductor* and *adductor* muscles (Miyake et al., 2016). The functional regionalization found in the tetrapod limbs (stylo-, zeugo- and autopode) is not present in the paired fins of non-sarcopterygian fishes (Janvier, 1996; King and Hale, 2014) and there is no regionalization of muscles along the metapterygial axis. In sarcopterygian fishes, since there is no substrate locomotion only based on the appendages, there is no need for a such functional regionalization of the fin. Yet, the muscles of the pectoral and pelvic fins of *Latimeria* differ in their organisation with more muscles inserting on the metapterygial axis of the pectoral fin than on the pelvic fin (e.g. *abductor/adductor superficialis; supinator*) (Figs 2.2, 2.4, 2.5, 2.7). On the pelvic fin of *L. chalumnae*, most muscles extend from the pelvic girdle to the fin rays. Only in the deep muscle layer can be observed some inter-mesomere muscles or muscles that originate from mesomeres and insert on the fin rays (*flexor* and *pronator* muscles). This muscles organization is similar to the muscles arrangement in actinopterygians, with muscles that originate on the girdle and insert at the base of the fin rays (Adriaens et al., 1993; Lauder and Drucker, 2004; Molnar et al., 2017). By contrast, in the pectoral fin, monoarticular inter-mesomere muscles allow the lateral or medial flexion of the different mesomeres. Thus, it can be considered that the pelvic fin has a more plesiomorphic organization of the muscles than the pectoral fin. Without a strict functional regionalization of the muscles, there is an anatomical regionalization of the muscles on the pectoral fin that might be drive the subsequent. Indeed, there is an important number of mono-articular muscles that are involved only for the mobility of the “shoulder” (i.e. the mobility of mesomere 1 on the pectoral girdle) of *L. chalumnae* (30 muscle bundles that corresponds to 35% of the pectoral muscle mass). The important number of muscles associated with this joint might be associated with the large stroke amplitude of the pectoral fin and the

diversity and complexity of fin movements observed during swimming (Fricke and Hissmann, 1992; Décamps et al., 2017). In tetrapods, rotational movements around the joint between the pelvic girdle and the femur are permitted by the coordinated activity of muscles associated with these elements (Wentink, 1976; Ashley-Ross, 1995; Aiello et al., 2014). The large number of muscles associated with the first mesomere of the pectoral fin of *L. chalumnae* could underlie a similar functional mechanism allowing for the mobility of the pectoral fin.

Joint mobility along the metapterygial axis of the fins

Data on the joint mobility demonstrated that the most proximal joint of the pectoral and pelvic fins (shoulder and hip) has the highest degree of mobility, and that the following joints along the metapterygial axis are less mobile. However, whereas the mobility of the pelvic fin follows the same general decreasing trends in mobility along its metapterygial axis as the pectoral fin, it is less mobile (Fig. 2.9). This difference of mobility was firstly documented *in vivo* during locomotion (Fricke and Hissmann, 1992), and was suggested to be due to the wide attachment of the pelvic fin to the body. The pectoral and pelvic fins have a similar organization of the endoskeleton except for the presence of the pre-axial radial 0 on the pelvic fin (Millot and Anthony, 1958; Mansuit et al., 2020b). It has been suggested previously that this element could reduce the mobility of this fin, and our measurements of the degree of mobility of this joint support this hypothesis. Moreover, the morphology of the mesomeres and pre-axial radial elements is different in the pectoral and pelvic fins (Fig. 2.1). The shape of the pelvic mesomeres may constrain the mobility of the elements, as the size of pelvic pre-axial radials is proportionally larger than those of the pectoral fin, and may consequently limit the lateral mobility of the elements.

Measurements made *in vivo* and during the firsts dissections confirm the mobility of the pectoral fin of *L. chalumnae*, since the pectoral fin is able to rotate a full 180° (Millot and Anthony, 1958; Fricke and Hissmann, 1992). However, this alleged 'rotation' is more important than the "shoulder joint" allows, and is thus the consequence of the mobility of the different joint of the metapterygial axis. Similarly, the pectoral fin can be moved in the dorso-ventral and antero-posterior directions up to 120° *in vivo* (Fricke and Hissmann, 1992), an excursion angle that is greater than the mobility of the "shoulder joint" for respectively the abduction/adduction and the protraction/retraction movements. Here as well it is the combination of the mobility at successive joints that allows the large stroke amplitude of the pectoral fin. More detailed kinematic analyses of fin movements in 3D are clearly needed to be able to link joint mobility to overall fin movements.

The African lungfish *Protopterus annectens* also has an important mobility of the pelvic fin *in vivo*, possibly superior to that of the pelvic fin of *L. chalumnae* (King et al., 2011; Aiello et al., 2014). The joint mobility of the first mesomere with the body shows a more important mobility compare to the coelacanth along the antero-dorsal and dorso-ventral axis. The long-axis rotational mobility was not calculated, neither the mobility of the different joints along the metapterygial axis, but *in vivo* footage shows that the large mobility at the hip joint is present for the different joint all along the entire metapterygial axis during 'walking' locomotion. This suggests that the joints between mesomeres of the paired fins of *P. annectens* are not constrained as observed for the pelvic fin of *L. chalumnae* (King et al., 2011; Aiello et al., 2014). The large mobility of the joints along the fins is useful for the 'walking' locomotion of the lungfish *P. annectens* in its aquatic environment (King et al., 2011). Different from the African lungfish, the coelacanth only uses its fins for the swimming. In cetaceans, the appendages are modified into flippers and mainly useful for the manoeuvering and turning (e.g. Felts, 1966; Fish and Battle, 1995). In these animals the shoulder joint presents a large mobility in the three directions, whereas the elbow and wrist joint have a restricted mobility that turns the limb into a paddle-like structure. This large mobility at the shoulder and restricted mobility within the limb permits the production of thrust for locomotion and manoeuvering (Felts, 1966). Even if the joint mobility of the fins of the coelacanth is not as restricted as for example the elbow and wrist of cetaceans, the relatively rigid fins might allow thrust production, necessary for locomotion and manoeuvring.

Conclusion

As previously described, our dissections of the pectoral and pelvic fins of the African coelacanth *L. chalumnae* showed that the muscles are organized in three different muscles layers, but with a more complex organization than previously known. The pectoral and pelvic fins show a different organization of the muscle bundles. The pectoral muscles are mostly mono-articular and insert on the different elements of the endoskeletal metapterygial axis of the fin, whereas almost all pelvic muscles are poly-articular and run from the pelvic girdle to the fin rays. Thus, the pelvic fin shows a more plesiomorphic configuration of the muscles, similar to that of actinopterygians, whereas the pectoral fin shows a muscular anatomy closer to that of lungfishes and tetrapods. The muscular properties of the pelvic fin allow to show that the partial ossification of the pelvic girdle of the fin is associated with muscles stronger than on the other part of the girdle. This ossification might permit to resist to the muscular constraints on

the girdle.

Muscular properties show a difference of contribution of the pectoral and pelvic fins, since the pectoral fin has a more important ACSA and can develop more strength than the pelvic fin. A stronger pectoral fin can show a more important contribution of the fin in the locomotion than the pelvic fin, and it is in agreement with the observations of the locomotion of the coelacanth. Indeed, the pectoral fin seems more active than the pelvic fin for the locomotion and the manoeuvring.

Finally, the joint mobilities of the two fins are really different, with a pelvic fin less mobile than the pectoral fin. It is supposed that the morphology of the mesomeres and the pre-axial radial of the pelvic fin constrain the joints of the fin. Moreover, the presence of the supernumerary element pre-axial radial 0 at the base of the pelvic fin limit also the mobility of the hip, whereas on the pectoral fin, the shoulder presents a large mobility in all the directions.

Acknowledgements

We thank C. Bens and A. Verguin of the Collections de Pièces anatomiques en Fluides of the MNHN de Paris. The MNHN gives access to the collections in the framework of the RECOLNAT national Research Infrastructure. This work was supported by a grant from Agence Nationale de la Recherche in the LabEx ANR-10-LABX-0003-BCDiv, program 'Investissements d'avenir' no ANR-11-IDEX-0004-02.

Authors contribution

AHu and RM performed the dissections and measurements for the pectoral and pelvic fins respectively. AHu and RM interpreted the results and wrote the manuscript. AHe and MH designed the research and revised the manuscript.

Bibliography

Adriaens, D., Decleyre, D., and Verraes, W. (1993). Morphology of the pectoral girdle in *Pomatoschistus lozanoi* De Buen, 1923 (Gobiidae), in relation to pectoral fin adduction. *Belgian journal of zoology*, 123(2):135–157.

Agassiz, L. (1839). *Recherches sur les poissons fossiles - Tome II, Contenant l'Histoire de l'Ordre des Ganoïdes*. Petitpierre, Neuchâtel.

Ahlberg, P. E. (1992). Coelacanth fins and evolution. *Nature*, 358:459.

Aiello, B. R., King, H. M., and Hale, M. E. (2014). Functional subdivision of fin protractor and retractor muscles underlies pelvic fin walking in the African lungfish *Protopterus annectens*. *Journal of Experimental Biology*, 217(19):3474–3482.

Amaral, D. B. and Schneider, I. (2018). Fins into limbs : Recent insights from sarcopterygian fish. *Genesis*, 56:e23052.

Amemiya, C. T., Alfoldi, J., Lee, A. P., Fan, S., Philippe, H., MacCallum, I., Braasch, I., Manousaki, T., Schneider, I., Rohner, N., Organ, C., Chalopin, D., Smith, J. J., Robinson, M., Dorrington, R. A., Gerdol, M., Aken, B., Biscotti, M. A., Barucca, M., Baurain, D., Berlin, A. M., Blatch, G. L., Buonocore, F., Burmester, T., Campbell, M. S., Canapa, A., Cannon, J. P., Christoffels, A., De Moro, G., Edkins, A. L., Fan, L., Fausto, A. M., Feiner, N., Forconi, M., Gamieldien, J., Gnerre, S., Gnirke, A., Goldstone, J. V., Haerty, W., Hahn, M. E., Hesse, U., Hoffmann, S., Johnson, J., Karchner, S. I., Kuraku, S., Lara, M., Levin, J. Z., Litman, G. W., Mauceli, E., Miyake, T., Mueller, M. G., Nelson, D. R., Nitsche, A., Olmo, E., Ota, T., Pallavicini, A., Panji, S., Picone, B., Ponting, C. P., Prohaska, S. J., Przybylski, D., Saha, N. R., Ravi, V., Ribeiro, F. J., Sauka-Spengler, T., Scapigliati, G., Searle, S. M., Sharpe, T., Simakov, O., Stadler, P. F., Stegeman, J. J., Sumiyama, K., Tabbaa, D., Tafer, H., Turner-Maier, J., Van Heusden, P., White, S., Williams, L., Yandell, M., Brinkmann, H., Volff, J. N., Tabin, C. J., Shubin, N. H., Schartl, M., Jaffe, D. B., Postlethwait, J. H., Venkatesh, B., Di Palma, F., Lander, E. S., Meyer, A., and Lindblad-Toh, K. (2013). The African coelacanth genome provides insights into tetrapod evolution. *Nature*, 496(7445):311–316.

Ashley-Ross, M. A. (1994). Hindlimb Kinematics During Terrestrial Locomotion in a Salamander (*Dicamptodon Tenebrosus*). *The Journal of experimental biology*, 193:255–83.

Ashley-Ross, M. A. (1995). Patterns of hind limb motor output during walking in the salamander *Dicamptodon tenebrosus*, with comparisons to other tetrapods. *Journal of Comparative Physiology A*, 177(3):273–285.

Boisvert, C. A., Joss, J. M., and Ahlberg, P. E. (2013). Comparative pelvic development of the axolotl (*Ambystoma mexicanum*) and the Australian lungfish (*Neoceratodus forsteri*): conservation and innovation across the fish-tetrapod transition. *EvoDevo*, 4(3):1–19.

Close, R. I. (1972). Dynamic Mammalian Properties of Skeletal Muscles. *Physiological Reviews*, 52(1):129–197.

Coates, M. I. (1994). The origin of vertebrate limbs. *Development*, Supplement:169–180.

Coates, M. I. (1995). Fish fins or tetrapod limbs - a simple twist of fate ? *Current Biology*, 5(8):844–848.

Coates, M. I., Jeffery, J. E., and Ruta, M. (2002). Fins to limbs: What the fossils say. *Evolution & Development*, 4(5):390–401.

Coates, M. I. and Ruta, M. (2007). Skeletal Changes in the Transition from Fins to Limbs. In Hall, B. K., editor, *Fins Into Limbs: Evolution, Development, and Transformation*, chapter Chapter 2, pages 15–38. Chicago, the univer edition.

Dabrowski, K. (1978). The density and chemical composition of fish muscle. *Experientia*, 34(10):1263–1265.

Décamps, T., Herrel, A., Ballesta, L., Holon, F., Rauby, T., Gentil, Y., Gentil, C., Dutel, H., Debruyne, R., Charrassin, J. B., Eveillard, G., Clément, G., and Herbin, M. (2017). The third dimension: a novel set-up for filming coelacanths in their natural environment. *Methods in Ecology and Evolution*, 8(3):322–328.

Diogo, R. and Abdala, V. (2007). Comparative Anatomy, Homologies and Evolution of the Pectoral Muscles of Bony Fish and Tetrapods: A New Insight. *Journal of Morphology*, 268:504–517.

Diogo, R., Abdala, V., Aziz, M. A., Lonergan, N., and Wood, B. A. (2009). From fish to modern humans - Comparative anatomy, homologies and evolution of the pectoral and forelimb musculature. *Journal of Anatomy*, 214(5):694–716.

Diogo, R., Johnston, P., Molnar, J. L., and Esteve-Altava, B. (2016). Characteristic tetrapod musculoskeletal limb phenotype emerged more than 400 MYA in basal lobe-finned fishes. *Scientific Reports*, 6:1–9.

Don, E. K., Currie, P. D., and Cole, N. J. (2013). The evolutionary history of the development of the pelvic fin/hindlimb. *Journal of Anatomy*, 222:114–133.

Drucker, E. G. and Lauder, G. V. (2002). Wake dynamics and locomotor function in fishes: Interpreting evolutionary patterns in pectoral fin design. *Integrative and Comparative Biology*, 42(5):997–1008.

Drucker, E. G. and Lauder, G. V. (2003). Function of pectoral fins in rainbow trout: behavioral repertoire and hydrodynamic forces. *The Journal of Experimental Biology*, 206:813–826.

Erdmann, M. V., Caldwell, R. L., and Moosa, M. K. (1998). Indonesian 'king of the sea' discovered. *Nature*, 395(6700):335.

Felts, W. J. L. (1966). Some Functional and Structural Characteristics of Cetacean Flippers and Flukes. In Norris, K. S., editor, *Whales, Dolphins, and Porpoises*, chapter 14, pages 255–276. The Regents of the University of California, Berkeley and Los Angeles.

Fish, F. E. and Battle, J. M. (1995). Hydrodynamic Design of the Humpback Whale Flipper. *Journal of Morphology*, 225:51–60.

Forey, P. L. (1998). *History of the Coelacanth Fishes*. Thomson Science, London, chapman & edition.

Fricke, H. and Hissmann, K. (1992). Locomotion, fin coordination and body form of the living coelacanth *Latimeria chalumnae*. *Environmental Biology of Fishes*, 34(4):329–356.

Fricke, H., Reinicke, O., Hofer, H., and Nachtigall, W. (1987). Locomotion of the coelacanth *Latimeria chalumnae* in its natural environment. *Nature*, 329:331–333.

Fricke, H., Schauer, J., Hissmann, K., Kasang, L., and Plante, R. (1991). Coelacanth *Latimeria chalumnae* aggregates in caves : first observations on their resting habitat and social behavior. *Environmental Biology of Fishes*, 30:281–285.

Friedman, M., Coates, M. I., and Anderson, P. (2007). First discovery of a primitive coelacanth fin fills a major gap in the evolution of lobed fins and limbs. *Evolution & Development*, 9(4):329–337.

Geerlink, P. (1987). The role of the pectoral fins in braking of mackerel, cod and saithe. *Netherlands Journal of Zoology*, 37(1):81–104.

Gibb, A. C., Jayne, B. C., and Lauder, G. V. (1994). Kinematics of Pectoral Fin Locomotion in the Bluegill Sunfish *Lepomis Macrochirus*. *The Journal of experimental biology*, 189(1):133–61.

Hissmann, K., Fricke, H., Schauer, J., Ribbink, A. J., Roberts, M., Sink, K., and Heemstra, P. C. (2006). The South African coelacanths - An account of what is known after three submersible expeditions. *South African Journal of Science*, 102(9-10):491–500.

Janvier, P. (1996). *Early vertebrates*. Oxford University Press, Oxford.

Johanson, Z., Joss, J., Boisvert, C. A., Ericsson, R., Sutija, M., and Ahlberg, P. E. (2007). Fish Fingers : Digit Homologues in Sarcopterygian Fish Fins. *Journal of Experimental Zoology Part B: Molecular and Developmental Evolution*, 308:757–768.

Kardong, K. V. (2018). *Vertebrates: Comparative Anatomy, Function, Evolution - Eight Edition*. McGraw-Hill Education, New York.

King, H. M. and Hale, M. E. (2014). Musculoskeletal morphology of the pelvis and pelvic fins in the lungfish *Protopterus annectens*. *Journal of Morphology*, 275(4):431–441.

King, H. M., Shubin, N. H., Coates, M. I., and Hale, M. E. (2011). Behavioral evidence for the evolution of walking and bounding before terrestriality in sarcopterygian fishes. *PNAS*, 108(52):21146–21151.

Lauder, G. V. and Drucker, E. G. (2004). Morphology and experimental hydrodynamics of fish fin control surfaces. *IEEE Journal of Oceanic Engineering*, 29(3):556–571.

Loeb, G. and Gans, C. (1986). *Electromyography for experimentalists*. Chicago, the univer edition.

Mansuit, R., Clément, G., Herrel, A., Dutel, H., Tafforeau, P., Santin, M. D., and Herbin, M. (2020a). Development and growth of the pectoral girdle and fin skeleton in the extant coelacanth *Latimeria chalumnae*. *Journal of Anatomy*, 236(3):493–509.

Mansuit, R., Clément, G., Herrel, A., Dutel, H., Tafforeau, P., Santin, M. D., and Herbin, M. (2020b). Development and growth of the pelvic fin in the extant coelacanth *Latimeria chalumnae*. *The Anatomical Record*.

Millot, J. and Anthony, J. (1958). *Anatomie de Latimeria chalumnae - Tome I: Squelette, Muscles et Formations de soutien*. CNRS, Paris, cnrs edition.

Miyake, T., Kumamoto, M., Iwata, M., Sato, R., Okabe, M., Koie, H., Kumai, N., Fujii, K., Matsuzaki, K., Nakamura, C., Yamauchi, S., Yoshida, K., Yoshimura, K., Komoda, A., Uyeno, T., and Abe, Y. (2016). The pectoral fin muscles of the coelacanth *Latimeria chalumnae*: Functional and evolutionary implications for the fin-to-limb transition and subsequent evolution of tetrapods. *The Anatomical Record*, 299(9):1203–1223.

Molnar, J. L., Diogo, R., Hutchinson, J. R., and Pierce, S. E. (2018). Reconstructing pectoral appendicular muscle anatomy in fossil fish and tetrapods over the fins-to-limbs transition. *Biological Reviews*, 93:1077–1107.

Molnar, J. L., Diogo, R., Hutchinson, J. R., and Pierce, S. E. (2020). Evolution of Hindlimb Muscle Anatomy Across the Tetrapod Water-to-Land Transition, Including Comparisons With Forelimb Anatomy. *Anatomical Record*, 303(2):218–234.

Molnar, J. L., Johnston, P. S., Esteve-Altava, B., and Diogo, R. (2017). Musculoskeletal anatomy of the pelvic fin of *Polypterus*: implications for phylogenetic distribution and homology of pre- and postaxial pelvic appendicular muscles. *Journal of Anatomy*, 230:532–541.

Moon, B. R. (1999). Testing an inference of function from structure: Snake vertebrae do the twist. *Journal of Morphology*, 241(3):217–225.

Nelson, J. S., Grande, T. C., and Wilson, M. V. (2016). *Fishes of the World - Fifth Edition*. John Wiley & Sons, Hoboken, New Jersey.

Nowlan, N. C., Bourdon, C., Dumas, G., Tajbakhsh, S., Prendergast, P. J., and Murphy, P. (2010). Developing bones are differentially affected by compromised skeletal muscle formation. *Bone*, 46(5):1275–1285.

Nowlan, N. C., Murphy, P., and Prendergast, P. J. (2008). A dynamic pattern of mechanical stimulation promotes ossification in avian embryonic long bones. *Journal of Biomechanics*, 41(2):249–258.

Nulens, R., Scott, L., and Herbin, M. (2011). An updated inventory of all known specimens of the coelacanth, *Latimeria* spp. *Smithiana Publications in Aquatic Biodiversity*, 3:1–52.

Shubin, N. H. and Alberch, P. (1986). A Morphogenetic Approach to the Origin and Basic Organization of the Tetrapod Limb. *Evolutionary Biology*, 20:319–387.

Shubin, N. H., Daeschler, E. B., and Jenkins, F. A. (2014). Pelvic girdle and fin of *Tiktaalik roseae*. *Proceedings of the National Academy of Sciences*, 111(3):893–899.

Standen, E. M. (2008). Pelvic fin locomotor function in fishes: Three-dimensional kinematics in rainbow trout (*Oncorhynchus mykiss*). *Journal of Experimental Biology*, 211(18):2931–2942.

Standen, E. M. and Lauder, G. V. (2005). Dorsal and anal fin function in bluegill sunfish *Lepomis macrochirus*: three-dimensional kinematics during propulsion and maneuvering. *Journal of Experimental Biology*, 208(14):2753–2763.

Wentink, G. (1976). The action of the hind limb musculature of the dog in walking. *Acta anatomica*, 96:70–80.

Wilhelm, B. C., Du, T. Y., Standen, E. M., and Larsson, H. C. (2015). *Polypterus* and the evolution of fish pectoral musculature. *Journal of Anatomy*, 226(6):511–522.

Zhu, M. and Yu, X. (2009). Stem sarcopterygians have primitive polybasal fin articulation. *Biology Letters*, 5(3):372–375.

Supplementary informations

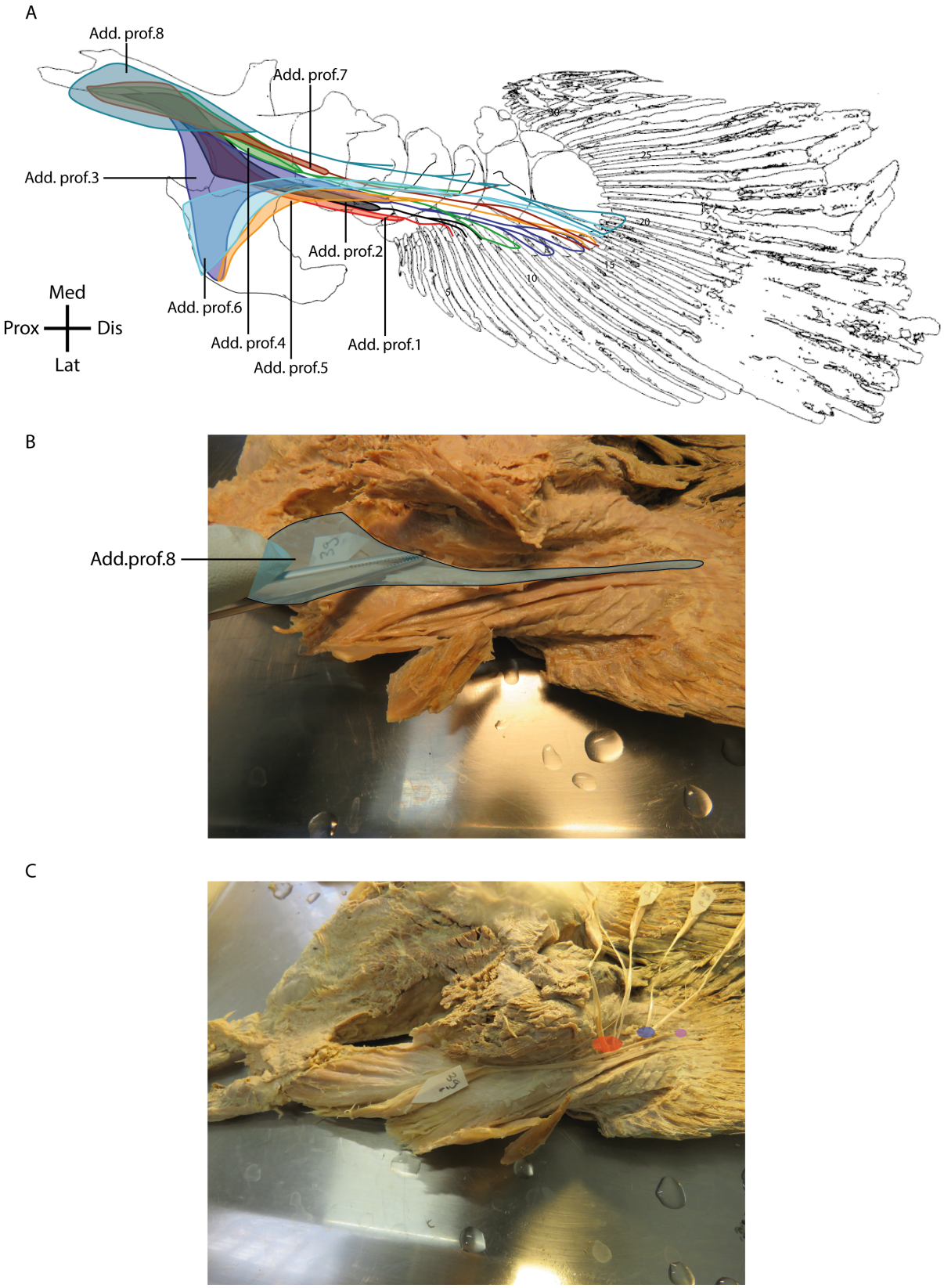

Supplementary Figure 2.1: Muscular anatomy of the pelvic fin of *Latimeria chalumnae* with focus on the *adductor profundus 8* muscle bundle to illustrate the sub-bundles and fascicles. A: Schematic illustration of the muscular organization of the dorsal middle layer of the pelvic fin, Add.prof.9-12 are not illustrated here. B: Zoom on the *adductor profundus 8* in situ (numbered 39 during the dissections). C: The different sub-bundles and fascicles of the Add.prof.8 are shown in situ, red point = insertion of the sub-bundle Add.prof.8B on the mesomere 3; Blue point = insertion of the sub-bundle Add.prof.8C on the mesomere 4; Purple point = insertion of the sub-bundle Add.prof.8D on the fin rays (39i corresponds to a sub-bundle of the Add.prof.8D). The Add.prof.8A and some fascicules of the sub-bundles of Add.prof.8C and 8D were removed before the photo was taken. Add.prof.: *Adductor profundus*.

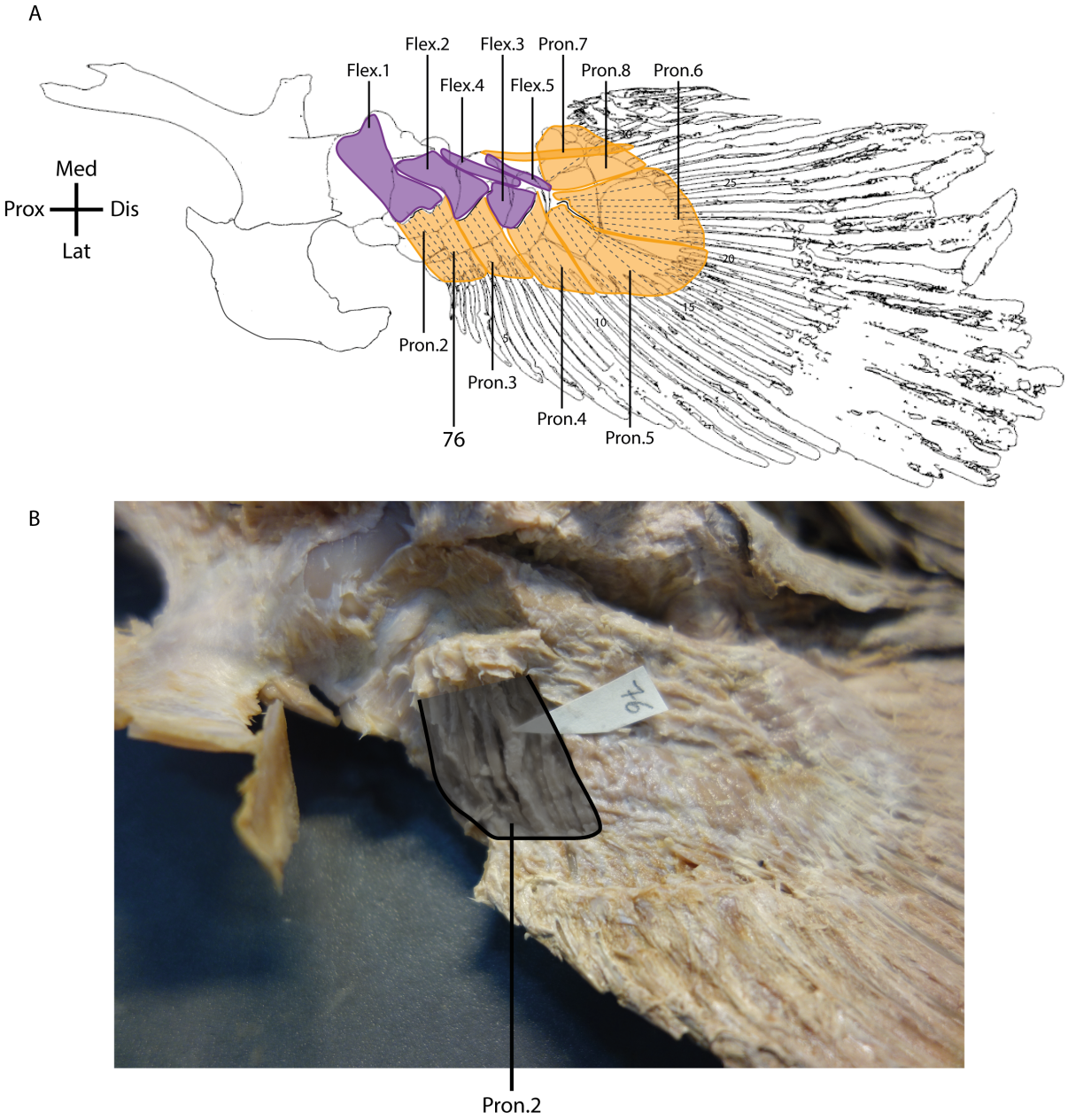

Supplementary Figure 2.2: A, Deep muscle layer of the pelvic fin of *Latimeria chalumnae* in dorsal view illustrating the organization of the bundles of different pronator muscles. B, Zoom on the *pronator 2 in situ*. 76 corresponds to the *pronator 2e* muscle bundle. Flex: *flexor*; Pron: *pronator*.

Supplementary Table 2.1: Details of the sub-division of the different muscle bundles of the pelvic fin of the extant coelacanth *Latimeria chalumnae* and the properties.

Muscle (Millot & Anthony, 1958)	Muscle	Subdivision	Origin(s)	Insertion(s)	Articulation mode	Mass (g)	Bundle Total lenght (cm)	Bundle lenght (cm)	Mean Fiber lenght (cm)	ACSA (cm²)
"Adducteur de la nageoire"	*Pterygialis caudalis*	*Pterygialis caudalis*	Pelvic girdle: Postero-superior process, ventral side	Dorsal side: Proximal portion of dermal rays 28-30	Poly-articular	1	6.4	4.7	2.76	0.201
"Elévateur superficiel, faisceau secondaire"	*Adductor superficialis pelvicus 1*	*Adductor superficialis pelvicus 1*	Pelvic girdle: Base of lateral process, ventral side	Dorsal side: *Pre-axial radials 1-2, *Proximal portion of dermal rays 1-8	Poly-articular	1.8	7.9	7.9	3.39	0.215
"Elévateur superficiel, faisceau principal"	*Adductor superficialis pelvicus 2*	*Adductor superficialis pelvicus 2a*	Pelvic girdle: Posterior edge of lateral process, dorsal and ventral side	Dorsal side: Proximal portion of dermal rays 8-11	Poly-articular	0.71	9.5	8.8	2.47	0.076
		Adductor superficialis pelvicus 2b	Under the Adductor superficialis pelvicus 2a	Dorsal side: Proximal portion of dermal ray 9	Poly-articular	0.028	5.2	3.3	2.22	0.008
	Adductor superficialis pelvicus 3	*Adductor superficialis pelvicus 3*	Pelvic girdle: Posterior edge of the lateral process, dorsal side	Dorsal side: Proximal portion of dermal rays 12-15	Poly-articular	0.91	10.4	9	2.27	0.095
	Adductor superficialis pelvicus 4	*Adductor superficialis pelvicus 4*	Pelvic girdle: Lateral process, dorsal side	Dorsal side: Proximal portion of dermal rays 15-18	Poly-articular	1.37	10.7	8.9	2.67	0.145
	Adductor superficialis pelvicus 5	*Adductor superficialis pelvicus 5*	Pelvic girdle: Antero-lateral edge of the lateral process, dorsal side	Dorsal side: Proximal portion of dermal rays 18-20	Poly-articular	1.4	11.8	9.5	2.85	0.139
	Adductor superficialis pelvicus 6	*Adductor superficialis pelvicus 6*	Pelvic girdle: Antero-lateral edge of the lateral process, dorsal side	Dorsal side: Proximal portion of the dermal ray 21	Poly-articular	1.18	11.8	9.7	2.92	0.115

Supplementary Table 2.1 (suite)

Muscle (Millot & Anthony, 1958)	Muscle	Subdivision	Origin(s)	Insertion(s)	Articulation mode	Mass (g)	Bundle Total lenght (cm)	Bundle lenght (cm)	Mean Fiber lenght (cm)	ACSA (cm²)
"Elévateur superficiel, faisceau principal"	*Adductor superficialis pelvicus 7*	*Adductor superficialis pelvicus 7*	*Membrane between pelvic muscles and abdominal muscles; *Pelvic girdle: posterior edge of the lateral process, dorsal side	Dorsal side: Proximal portion of the dermal ray 22	Poly-articular	3.33	13.5	10.8	3.99	0.291
	Adductor superficialis pelvicus 8	*Adductor superficialis pelvicus 8*	Membrane between pelvic muscles and abdominal muscles	Dorsal side: *Dorsal ridge of the mesomere 3; *Proximal portion of dermal rays 21-23	Poly-articular	1.46	12.4	9.4	3.46	0.147
	Adductor superficialis pelvicus 9	*Adductor superficialis pelvicus 9*	Membrane between pelvic muscles and abdominal muscles	Dorsal side: *Dorsal ridge of the mesomere 2; *Proximal portion of dermal rays 23-25	Poly-articular	0.54	9.2	5.8	4.04	0.088
	Adductor superficialis pelvicus 10	*Adductor superficialis pelvicus 10a*	Membrane between pelvic muscles and abdominal muscles	Dorsal side: Proximal portion of the dermal ray 26	Poly-articular	0.2	7.5	5.5	4.33	0.034
	Adductor superficialis pelvicus 10	*Adductor superficialis pelvicus 10b*	Membrane between pelvic muscles and abdominal muscles	Dorsal side: Proximal portion of the dermal ray 27	Poly-articular	0.15	6.5	4.5	2.22	0.031
"Elévateur profond"	*Adductor profundus pelvicus 1*	*Adductor profundus pelvicus 1*	Pelvic girdle: lateral edge of the base of the anterior process, dorsal side	Dorsal side: Proximal portion of the dermal ray 7	Poly-articular	0.28	10.5	8.1	3.738	0.033

Supplementary Table 2.1 (suite)

Muscle (Millot & Anthony, 1958)	Muscle	Subdivision	Origin(s)	Insertion(s)	Articulation mode	Mass (g)	Bundle Total lenght (cm)	Bundle lenght (cm)	Mean Fiber lenght (cm)	ACSA (cm²)
"Elévateur profond"	*Adductor profundus pelvicus 2*	*Adductor profundus pelvicus 2*	Pelvic girdle: *Lateral process (dorsal side); *Lateral edge of the anterior process (ventral and dorsal side)	Dorsal side: Proximal portion of dermal rays 8-9	Poly-articular	1.67	13.8	8.9	6.067	0.177
	Adductor profundus pelvicus 3	*Adductor profundus pelvicus 3a*	Pelvic girdle: *Lateral process (dorsal side); *Lateral edge of the base of the anterior process (ventral side)	Dorsal side: Proximal portion of dermal rays 14-15	Poly-articular	0.962	15.9	10.1	5.283	0.090
		Adductor profundus pelvicus 3b	Pelvic girdle: Lateral edge of the base of the anterior process (ventral side)	Dorsal side: Proximal portion of dermal rays 12-13	Poly-articular	0.313	11.5	6.9	5.189	0.043
	Adductor profundus pelvicus 4A	*Adductor profundus pelvicus 4a*	Pelvic girdle: Lateral edge of the base of the anterior process, dorsal side	Dorsal side: Dorsal ridge of the mesomere 3	Poly-articular	0.342	10.3	5	3.375	0.065
		Adductor profundus pelvicus 4b	Pelvic girdle: Lateral edge of the base of the anterior process, dorsal side	Dorsal side: Dorsal ridge of the mesomere 3	Poly-articular	0.369	12	5.5	3.661	0.063
	Adductor profundus pelvicus 4B	*Adductor profundus pelvicus 4c*	Pelvic girdle: Lateral edge of the base of the anterior process, dorsal side	Dorsal side: Proximal portion of dermal rays 9-11	Poly-articular	0.579	15	5.2	4.528	0.105

Supplementary Table 2.1 (suite)

Muscle (Millot & Anthony, 1958)	Muscle	Subdivision	Origin(s)	Insertion(s)	Articulation mode	Mass (g)	Bundle Total lenght (cm)	Bundle lenght (cm)	Mean Fiber lenght (cm)	ACSA (cm²)
"Elévateur profond"	*Adductor profundus pelvicus 4B*	*Adductor profundus pelvicus 4d*	Pelvic girdle: Lateral edge of the base of the anterior process, dorsal side	Dorsal side: Proximal portion of the dermal ray 13	Poly-articular	0.376	16.2	6.6	4.939	0.054
	Adductor profundus pelvicus 5	*Adductor profundus pelvicus 5a*	Pelvic girdle: Antero-lateral edge of the lateral process (dorsal side)	Dorsal side: Proximal portion of dermal rays 15-16	Poly-articular	0.08	11.2	6.9	3.769	0.011
		Adductor profundus pelvicus 5b	Pelvic girdle: Antero-lateral edge of the lateral process (dorsal side)	Dorsal side: base of the postero-superior process	Poly-articular	0.03	4	3	2.204	0.009
		Adductor profundus pelvicus 5c	Pelvic girdle: Antero-lateral edge of the lateral process (dorsal side)	Dorsal side: Proximal portion of dermal rays 15-16	Poly-articular	0.11	6.1	6.1	4.83	0.017
	Adductor profundus pelvicus 6	*Adductor profundus pelvicus 6a*	Pelvic girdle: Anterior edge of the lateral process (dorsal side)	Dorsal side: Proximal portion of dermal rays 17-18	Poly-articular	0.47	12.5	6.1	4.581	0.073
		Adductor profundus pelvicus 6b	Pelvic girdle: Anterior edge of the lateral process (dorsal side)	Dorsal side: Proximal portion of dermal rays 17-18	Poly-articular	0.22	11.2	5.1	4.827	0.041
		Adductor profundus pelvicus 6c	Pelvic girdle: Anterior edge of the lateral process (dorsal side)	Dorsal side: Proximal portion of dermal rays 17-18	Poly-articular	0.24	13.9	5.1	5.06	0.044
		Adductor profundus pelvicus 6d	Pelvic girdle: Anterior edge of the lateral process (dorsal side)	Dorsal side: Proximal portion of dermal rays 17-18	Poly-articular	0.38	9.7	5.1	5.018	0.070

Supplementary Table 2.1 (suite)

Muscle (Millot & Anthony, 1958)	Muscle	Subdivision	Origin(s)	Insertion(s)	Articulation mode	Mass (g)	Bundle Total lenght (cm)	Bundle lenght (cm)	Mean Fiber lenght (cm)	ACSA (cm²)
"Elévateur profond"	*Adductor profundus pelvicus 6*	*Adductor profundus pelvicus 6e*	Pelvic girdle: Anterior edge of the lateral process (dorsal side)	Dorsal side: Proximal portion of the dermal ray 17	Poly-articular	0.26	7.9	7.6	4.921	0.032
	Adductor profundus pelvicus 7A	*Adductor profundus pelvicus 7a*	On the Adductor profundus pelvicus 7c (ventral side of the fin)	Dorsal side: Proximal portion of the dermal ray 16	Poly-articular	0.12	14.7	7.4	5.131	0.015
		Adductor profundus pelvicus 7b	On the Adductor profundus pelvicus 7d (ventral side of the fin)	Dorsal side: Proximal portion of the dermal ray 15	Poly-articular	0.14	14.3	7.3	4.583	0.018
		Adductor profundus pelvicus 7c	Pelvic girdle: Lateral edge of the anterior process (ventral side)	Dorsal side: Proximal portion of the dermal ray 16	Poly-articular	0.27	12.1	4.8	4.617	0.053
		Adductor profundus pelvicus 7d	Pelvic girdle: Lateral edge of the anterior process (ventral side)	Dorsal side: Proximal portion of the dermal ray 15	Poly-articular	0.15	10.8	5	4.304	0.028
	Adductor profundus pelvicus 7A	*Adductor profundus pelvicus 7g*	Pelvic girdle: Lateral edge of the anterior process (ventral side)	Dorsal side: Proximal portion of the dermal ray 15	Poly-articular	0.42	12.1	6.6	4.049	0.060
	Adductor profundus pelvicus 7B	*Adductor profundus pelvicus 7e*	Pelvic girdle: Lateral edge of the anterior process (dorsal side)	Dorsal side: Dorsal ridge of the mesomere 4	Poly-articular	0.17	14.1	3.5	3.234	0.046
		Adductor profundus pelvicus 7f	Pelvic girdle: Lateral edge of the anterior process (ventral side)	Dorsal side: Dorsal ridge of the mesomere 4	Poly-articular	0.23	8.6	4.1	3.7	0.053

Supplementary Table 2.1 (suite)

Muscle (Millot & Anthony, 1958)	Muscle	Subdivision	Origin(s)	Insertion(s)	Articulation mode	Mass (g)	Bundle Total lenght (cm)	Bundle lenght (cm)	Mean Fiber lenght (cm)	ACSA (cm²)
"Elévateur profond"	*Adductor profundus pelvicus 7B*	*Adductor profundus pelvicus 7h*	Pelvic girdle: Anterior end of the lateral edge of the anterior process (ventral and dorsal side)	Dorsal side: Dorsal ridge of the mesomere 4	Poly-articular	0.32	10.7	4.5	3.287	0.067
	Adductor profundus pelvicus 8A	*Adductor profundus pelvicus 8a*	Pelvic girdle: Medial edge of the base of the anterior stick (dorsal side)	Dorsal side: Dorsal ridge of mesomeres 1	Mono-articular	0.45	6.7	4	2.549	0.106
	Adductor profundus pelvicus 8B	*Adductor profundus pelvicus 8b*	Pelvic girdle: Medial edge of the anterior stick, just anterior to *Add. prof. pelv. 8a* (dorsal side)	Dorsal side: Dorsal ridge of mesomere 3	Poly-articular	0.88	11.2	4.5	2.778	0.184
	Adductor profundus pelvicus 8B	*Adductor profundus pelvicus 8c*	Membrane between pelvic muscles and abdominal muscles and medial edge of the anterior stick (anterior to *Add. prof. pelv. 8b)*	Dorsal side: Dorsal ridge of mesomere 3	Poly-articular	0.18	10.8	4.9	3.18	0.035
		Adductor profundus pelvicus 8d	Membrane between pelvic muscles and abdominal muscles and medial edge of the anterior stick (cover by *Add. prof. pelv. 8c*)	Dorsal side: Dorsal ridge of mesomere 3	Poly-articular	0.33	11.4	3.9	2.939	0.080

Supplementary Table 2.1 (suite)

Muscle (Millot & Anthony, 1958)	Muscle	Subdivision	Origin(s)	Insertion(s)	Articulation mode	Mass (g)	Bundle Total lenght (cm)	Bundle lenght (cm)	Mean Fiber lenght (cm)	ACSA (cm²)
"Elévateur profond"	*Adductor profundus pelvicus 8C*	*Adductor profundus pelvicus 8e*	Membrane between pelvic muscles and abdominal muscles and medial edge of the anterior part of the anterior stick (dorsal side)	Dorsal side: Dorsal ridge of mesomere 4	Poly-articular	0.34	12.7	4.8	3.952	0.067
		Adductor profundus pelvicus 8h	Pelvic girdle: Anterior side of the anterior process (dorsal and ventral side)	Dorsal side: Dorsal ridge of mesomere 4	Poly-articular	2.07	14.8	6	3.576	0.325
	Adductor profundus pelvicus 8D	*Adductor profundus pelvicus 8f*	Pelvic girdle: Anterior edge of the lateral process (dorsal side)	Dorsal side: Proximal portion of dermal rays 17-20	Poly-articular	1.74	15.1	7.4	5.12	0.222
		Adductor profundus pelvicus 8g	Pelvic girdle: Anterior side of the anterior process (dorsal side)	Dorsal side: Proximal portion of the dermal ray 20	Poly-articular	0.38	7.6	3.4	2.902	0.105
	Adductor profundus pelvicus 8D	*Adductor profundus pelvicus 8i*	Pelvic girdle: Anterior side of the anterior process (ventral side)	Dorsal side: Proximal portion of dermal rays 17-20	Poly-articular	1.4	16.5	7.9	4.702	0.167
	Adductor profundus pelvicus 9	Adductor profundus pelvicus 9a	Pelvic girdle: lateral edge of the anterior part of the anterior stick (dorsal side)	Dorsal side: Dorsal ridge of the mesomere 3	Poly-articular	0.35	12	3.9	2.795	0.085

Supplementary Table 2.1 (suite)

Muscle (Millot & Anthony, 1958)	Muscle	Subdivision	Origin(s)	Insertion(s)	Articulation mode	Mass (g)	Bundle Total lenght (cm)	Bundle lenght (cm)	Mean Fiber lenght (cm)	ACSA (cm²)
"Elévateur profond"	*Adductor profundus pelvicus 9*	*Adductor profundus pelvicus 9b*	Pelvic girdle: lateral edge of the anterior part of the anterior stick (dorsal and ventral side)	Dorsal side: Dorsal ridge of the mesomere 3	Poly-articular	0.32	11.8	3.2	2.877	0.094
	Adductor profundus pelvicus 10A	Adductor profundus pelvicus 10a	Pelvic girdle: Anterior process (dorsal side)	Dorsal ridge of the mesomere 2	Poly-articular	0.42	8.7	3.8	2.418	0.104
	Adductor profundus pelvicus 10B	Adductor profundus pelvicus 10b	Pelvic girdle: Anterior process (dorsal side)	Dorsal side: Dorsal ridge of the mesomere 3	Poly-articular	0.19	9.6	4.4	2.522	0.041
		Adductor profundus pelvicus 10c	Pelvic girdle: Anterior process (dorsal side)	Dorsal side: Dorsal ridge of the mesomere 3	Poly-articular	0.7	11	4.2	2.804	0.157
	Adductor profundus pelvicus 11	*Adductor profundus pelvicus 11a*	Membrane between pelvic muscles and abdominal muscles	Dorsal side: Mesomere 4	Poly-articular	0.73	8.2	5.3	3.217	0.130
		Adductor profundus pelvicus 11b	Membrane between pelvic muscles and abdominal muscles, attached to the medial edge of the anterior stick by a membrane	Dorsal side: Mesomere 4	Poly-articular	0.32	9.7	5.5	2.671	0.055
		Adductor profundus pelvicus 11c	Membrane between pelvic muscles and abdominal muscles, attached to the medial edge of the anterior stick by a membrane	Dorsal side: Mesomere 4	Poly-articular	0.67	10.3	4.5	3.186	0.140

Table 2.1 (suite)

Muscle (Millot & Anthony, 1958)	Muscle	Subdivision	Origin(s)	Insertion(s)	Articulation mode	Mass (g)	Bundle Total lenght (cm)	Bundle lenght (cm)	Mean Fiber lenght (cm)	ACSA (cm²)
"Elévateur profond"	*Adductor profundus pelvicus 11*	*Adductor profundus pelvicus 11d*	Membrane between pelvic muscles and abdominal muscles, above the anterior stick of the girdle	Dorsal side: Mesomere 4	Poly-articular	0.13	10.7	3.6	3.506	0.034
		Adductor profundus pelvicus 11e	Membrane between pelvic muscles and abdominal muscles, above the anterior stick of the girdle	Dorsal side: Mesomere 4	Poly-articular	0.3	9.6	3.6	3.451	0.079
		Adductor profundus pelvicus 11f	Membrane between pelvic muscles and abdominal muscles, above the anterior stick of the girdle	Dorsal side: Mesomere 4	Poly-articular	0.19	10	3	2.839	0.060
		Adductor profundus pelvicus 11g	Membrane between pelvic muscles and abdominal muscles, above the anterior stick of the girdle	Dorsal side: Mesomere 4	Poly-articular	0.09	10.5	3.3	2.836	0.026
	Adductor profundus pelvicus 12	*Adductor profundus pelvicus 12a*	Membrane between pelvic muscles and abdominal muscles, above the anterior stick of the girdle	Dorsal side: Proximal portion of dermal rays 19-21	Poly-articular	0.13	9.6	5.6	4.182	0.022

Supplementary Table 2.1 (suite)

Muscle (Millot & Anthony, 1958)	Muscle	Subdivision	Origin(s)	Insertion(s)	Articulation mode	Mass (g)	Bundle Total lenght (cm)	Bundle lenght (cm)	Mean Fiber lenght (cm)	ACSA (cm²)
"Elévateur profond"	*Adductor profundus pelvicus 12*	*Adductor profundus pelvicus 12b*	Membrane between pelvic muscles and abdominal muscles, above the anterior stick of the girdle	Dorsal side: Proximal portion of dermal rays 18-19 and 20-21	Poly-articular	0.12	6.8	5.6	4.182	0.020
		Adductor profundus pelvicus 12c	Membrane between pelvic muscles and abdominal muscles, above the anterior stick of the girdle	Dorsal side: Proximal portion of dermal rays 18-19 and 20-21	Poly-articular	0.15	13.5	5	4.304	0.028
		Adductor profundus pelvicus 12d	Membrane between pelvic muscles and abdominal muscles, above the anterior stick of the girdle	Dorsal side: Proximal portion of dermal rays 19-20	Poly-articular	0.16	11.5	5.2	3.812	0.029
		Adductor profundus pelvicus 12e	Pelvic girdle: Anterior edge of the lateral process (dorsal side) and lateral edge of the anterior stick (ventral side)	Dorsal side: Proximal portion of dermal rays 19-20	Poly-articular	2.38	15	7.2	4.231	0.312
Pronateur 1-3	*Pronator 1*	*Pronator 1a*	Pelvic girdle, between the anterior stick and the postero-superior process (dorsal side)	Dorsal side: Pre-axial radials 0	Mono-articular	0.54	4.5	4.5	1.5	0.113

Supplementary Table 2.1 (suite)

Muscle (Millot & Anthony, 1958)	Muscle	Subdivision	Origin(s)	Insertion(s)	Articulation mode	Mass (g)	Bundle Total lenght (cm)	Bundle lenght (cm)	Mean Fiber lenght (cm)	ACSA (cm²)
Pronateur 1-3	*Pronator 1*	*Pronator 1b*	Pelvic girdle, between the anterior stick and the postero-superior process (dorsal side)	Dorsal side: Pre-axial radials 1	Poly-articular	0.35	4.9	4.9	1.941	0.067
		Pronator 1c	Pelvic girdle, between the anterior stick and the postero-superior process (dorsal side)	Dorsal side: Pre-axial radials 0-1	Mono-articular	0.27	2.6	2.6	1.236	0.098
		Pronator 1d	Pelvic girdle, between the anterior stick and the postero-superior process (dorsal side)	Dorsal side: Proximal portion of dermal ray 1	Poly-articular	0.36	6.9	4.9	1.544	0.069
		Pronator 1e	Pelvic girdle, between the anterior stick and the postero-superior process (dorsal side)	Dorsal side: Proximal portion of dermal ray 2	Poly-articular	0.04	4.8	1.5	1.229	0.025
		Pronator 1f	Pelvic girdle, between the anterior stick and the postero-superior process (dorsal side)	Dorsal side: Proximal portion of dermal ray 3	Poly-articular	0.14	5.7	1.9	1.24	0.070
		Pronator 1g	Pelvic girdle, between the anterior stick and the postero-superior process (dorsal side)	Dorsal side: Proximal portion of dermal ray 4	Poly-articular	0.29	7.5	2.5	1.616	0.109

Supplementary Table 2.1 (suite)

Muscle (Millot & Anthony, 1958)	Muscle	Subdivision	Origin(s)	Insertion(s)	Articulation mode	Mass (g)	Bundle Total lenght (cm)	Bundle lenght (cm)	Mean Fiber lenght (cm)	ACSA (cm²)
Pronateur 1-3	*Pronator 1*	*Pronator 1h*	Pelvic girdle, between the anterior stick and the postero-superior process (dorsal side)	Dorsal side: Pre-axial radials 2	Poly-articular	0.15	4.4	3.7	1.596	0.038
		Pronator 1i	Pelvic girdle, between the anterior stick and the postero-superior process (dorsal side)	Dorsal side: *Ridge on the mesomere 1; *Proximal portion of dermal rays 1-5	Poly-articular	0.52	6.8	4	1.636	0.123
		Pronator 1j	Pelvic girdle, between the anterior stick and the postero-superior process (dorsal side)	Dorsal side: *Ridge on the mesomere 1; *Proximal portion of dermal rays 1 and 4-5	Poly-articular	0.52	7.7	3.3	2.298	0.149
		Pronator 1k	Pelvic girdle, between the anterior stick and the postero-superior process (dorsal side)	Dorsal side: *Ridge on the mesomere 1; *Proximal portion of the dermal ray 3	Poly-articular	0.35	5.1	3.3	2.306	0.100
	Pronator 2	*Pronator 2a*	Mesomere 1, lateral extremity of the dorsal ridge	Dorsal side: Proximal portion of dermal ray 1	Poly-articular	0.138	1.8	1.8	0.996	0.072
		Pronator 2b	Mesomere 1, dorsal ridge, medial to Pronator 2a	Dorsal side: Proximal portion of dermal ray 2	Poly-articular	0.1	2	2	1.325	0.047
		Pronator 2c	Mesomere 1, dorsal ridge, medial to Pronator 2b	Dorsal side: Proximal portion of dermal ray 3	Poly-articular	0.15	2.3	2.3	1.477	0.062

Supplementary Table 2.1 (suite)

Muscle (Millot & Anthony, 1958)	Muscle	Subdivision	Origin(s)	Insertion(s)	Articulation mode	Mass (g)	Bundle Total lenght (cm)	Bundle lenght (cm)	Mean Fiber lenght (cm)	ACSA (cm²)
Pronateur 1-3	*Pronator 2*	*Pronator 2d*	Mesomere 1, dorsal ridge, medial to Pronator 2c	Dorsal side: Proximal portion of dermal ray 3	Poly-articular	0.13	2.7	2.7	1.465	0.045
		Pronator 2e	Mesomere 1, dorsal ridge, medial to Pronator 2d	Dorsal side: Proximal portion of dermal ray 4	Poly-articular	0.13	3.1	3.1	1.184	0.040
		Pronator 2f	Mesomere 1, dorsal ridge, medial to Pronator 2e	Dorsal side: Proximal portion of dermal ray 5	Poly-articular	0.09	2.6	2.6	1.178	0.033
		Pronator 2g	Mesomere 1, medial extremity of the dorsal ridge, medial to Pronator 2f	Dorsal side: Proximal portion of dermal ray 5	Poly-articular	0.228	2.8	2.8	1.184	0.077
	Pronator 3	*Pronator 3a*	Mesomere 2, lateral extremity of the dorsal ridge	Dorsal side: Proximal portion of the dermal ray 6	Mono-articular	0.195	2.1	2.1	1.09	0.088
		Pronator 3b	Mesomere 2, dorsal ridge, medial to Pronator 3a	Dorsal side: Proximal portion of the dermal ray 7	Mono-articular	0.069	2.5	2.5	1.053	0.026
		Pronator 3c	Mesomere 2, dorsal ridge, medial to Pronator 3b	Dorsal side: Proximal portion of the dermal ray 7	Mono-articular	0.21	2.8	2.8	1.144	0.071
		Pronator 3d	Mesomere 2, medial extremity of the dorsal ridge, medial to Pronator 3c	Dorsal side: Proximal portion of the dermal ray 8	Mono-articular	0.206	2.7	2.7	1.051	0.072
	Pronator 4	*Pronator 4a*	Mesomere 3, lateral extremity of the dorsal ridge	Dorsal side: Proximal portion of the dermal ray 9	Mono-articular	0.186	3	3	0.98	0.058

Supplementary Table 2.1 (suite)

Muscle (Millot & Anthony, 1958)	Muscle	Subdivision	Origin(s)	Insertion(s)	Articulation mode	Mass (g)	Bundle Total lenght (cm)	Bundle lenght (cm)	Mean Fiber lenght (cm)	ACSA (cm²)
Pronateur 1-3	*Pronator 4*	*Pronator 4b*	Mesomere 3, dorsal ridge, medial to Pronator 4a	Dorsal side: Proximal portion of the dermal ray 9	Mono-articular	0.06	2.5	2.5	0.818	0.023
		Pronator 4c	Mesomere 3, dorsal ridge, medial to Pronator 4b	Dorsal side: Proximal portion of the dermal ray 10	Mono-articular	0.225	3.1	3.1	0.905	0.068
		Pronator 4d	Mesomere 3, medial extremity of the dorsal ridge, medial to Pronator 4c	Dorsal side: Proximal portion of the dermal ray 11	Mono-articular	0.21	3.8	3.8	0.767	0.052
Pronateur 4	*Pronator 5*	*Pronator 5a*	Mesomere 4, proximal extremity of the lateral edge of the dorsal ridge	Dorsal side: Proximal portion of the dermal ray 12	Mono-articular	0.171	2.6	2.6	0.558	0.062
		Pronator 5b	Mesomere 4, lateral edge of the dorsal ridge, just distal to Pronator 5a	Dorsal side: Proximal portion of the dermal ray 13	Mono-articular	0.101	2.5	2.5	0.535	0.038
		Pronator 5c	Mesomere 4, lateral edge of the dorsal ridge, just distal to Pronator 5b	Dorsal side: Proximal portion of dermal rays 14-15	Mono-articular	0.09	2.6	2.6	0.494	0.033
		Pronator 5d	Mesomere 4, lateral edge of the dorsal ridge, just distal to Pronator 5c	Dorsal side: Proximal portion of dermal rays 15-17	Mono-articular	0.129	2.2	2.2	0.554	0.055
		Pronator 5e	Mesomere 4, lateral edge of the dorsal ridge, just distal to Pronator 5d	Dorsal side: Proximal portion of the dermal ray 17	Mono-articular	0.039	2.2	2.2	0.373	0.017

Supplementary Table 2.1 (suite)

Muscle (Millot & Anthony, 1958)	Muscle	Subdivision	Origin(s)	Insertion(s)	Articulation mode	Mass (g)	Bundle Total lenght (cm)	Bundle lenght (cm)	Mean Fiber lenght (cm)	ACSA (cm²)
Pronateur 4	*Pronator 5*	*Pronator 5f*	Mesomere 4, distal extremity of the lateral edge of the dorsal ridge, just distal to Pronator 5e	Dorsal side: Proximal portion of dermal rays 18-20	Mono-articular	0.087	2.3	2.3	0.575	0.036
Pronateur 5	*Pronator 6*	*Pronator 6a*	Mesomere 4, distal extremity of the medial edge of the dorsal ridge	Dorsal side: Proximal portion of the dermal ray 20	Mono-articular	0.099	2.3	2.3	0.805	0.041
		Pronator 6b	Mesomere 4, medial edge of the dorsal ridge, just proximal to Pronator 6a	Dorsal side: Proximal portion of the dermal ray 21	Mono-articular	0.146	2.8	2.8	0.923	0.049
		Pronator 6c	Mesomere 4, medial edge of the dorsal ridge, just proximal to Pronator 6b	Dorsal side: Proximal portion of dermal rays 22-23	Mono-articular	0.213	2.6	2.6	0.949	0.077
		Pronator 6d	Mesomere 4, medial edge of the dorsal ridge, just proximal to Pronator 6c	Dorsal side: Proximal portion of the dermal ray 23	Mono-articular	0.042	2.3	2.3	1.102	0.017
		Pronator 6e	Mesomere 4, medial edge of the dorsal ridge, just proximal to Pronator 6d	Dorsal side: Proximal portion of the dermal ray 23	Mono-articular	0.155	3	3	1.068	0.049
		Pronator 6f	Mesomere 4, medial edge of the dorsal ridge, just proximal to Pronator 6e	Dorsal side: Proximal portion of the dermal ray 24	Mono-articular	0.12	2.7	2.7	1.311	0.042

Supplementary Table 2.1 (suite)

Muscle (Millot & Anthony, 1958)	Muscle	Subdivision	Origin(s)	Insertion(s)	Articulation mode	Mass (g)	Bundle Total lenght (cm)	Bundle lenght (cm)	Mean Fiber lenght (cm)	ACSA (cm²)
Pronateur 5	*Pronator 6*	*Pronator 6g*	Mesomere 4, medial edge of the dorsal ridge, just proximal to Pronator 6f	Dorsal side: Proximal portion of dermal rays 24-25	Mono-articular	0.526	2.4	2.4	1.375	0.207
		Pronator 6h	Mesomere 4, proximal extremity of the medial edge of the dorsal ridge, just proximal to Pronator 6g	Dorsal side: Proximal portion of dermal rays 26-27	Mono-articular	0.37	2.3	2.3	1.296	0.152
	Pronator 7	*Pronator 7*	Mesomere 2, medial bud	Dorsal side: Proximal portion of the dermal ray 29	Poly-articular	0.156	3.2	3.2	1.629	0.046
	Pronator 8	*Pronator 8a*	Mesomere 4 proximo-medial edge	Dorsal side: Proximal portion of dermal rays 28-29	Mono-articular	0.501	2.5	2.5	1.052	0.189
		Pronator 8b	Proximal edge of post-axial radial	Dorsal side: Proximal portion of dermal rays 30-32	Mono-articular	0.565	1.7	1.7	1.011	0.314
Undescribed	Flexor 1	Flexor 1	Pelvic girdle: postero-superior process (dorsal side)	Mesomere 1, proximal side of the dorsal ridge	Mono-articular	1.57	3.5	3.5	2.267	0.423
	Flexor 2	Flexor 2	Pelvic girdle: postero-superior process (ventral side) and mesomere 1 (dorsal side)	Mesomere 2, proximal side of the dorsal ridge	Mono-articular	1.058	2.7	2.7	1.704	0.370
	Flexor 3	Flexor 3	Mesomere 2, distal side of dorsal ridge	Mesomere 3, proximo-lateral side of the dorsal ridge	Mono-articular	0.116	1	1	0.527	0.109

Supplementary Table 2.1 (suite)

Muscle (Millot & Anthony, 1958)	Muscle	Subdivision	Origin(s)	Insertion(s)	Articulation mode	Mass (g)	Bundle Total lenght (cm)	Bundle lenght (cm)	Mean Fiber lenght (cm)	ACSA (cm²)
Undescribed	Flexor 4	Flexor 4	Mesomere 1, distal edge of the medial bud	Mesomere 3, proximo-medial side of the dorsal ridge	Poly-articular	0.34	2.3	2.3	1.468	0.139
	Flexor 5	Flexor 5	Mesomere 2, distal edge of the medial bud	Mesomere 4, proximo-medial edge	Poly-articular	0.437	2.2	2.2	1.136	0.187
"Abducteur de la nageoire"	*Pterygialis cranialis*	*Pterygialis cranialis*	Pelvic girdle: Anterior side of the base of the lateral process, ventral side	*Ventral side: Proximal portion of the dermal ray 1; *Pre-axial radial 2, lateral edge	Poly-articular	2.28	6.3	6.3	3.598	0.341
"Abaisseur superficiel"	*Abductor superficialis pelvicus 1*	*Abductor superficialis pelvicus 1*	Aponeurosis on *Adductor profundus pelvicus*	*Pre-axial radials 1-2, *Ventral side: Proximal portion of dermal rays 1-2	Poly-articular	3.97	8	8	4.243	0.468
"Abaisseur superficiel"	*Abductor superficialis pelvicus 2*	*Abductor superficialis pelvicus 2*	*Pelvic girdle: Lateral side of the base of the anterior process; *Aponeurosis on the *Adductor profundus pelvicus*	Ventral side: Proximal portion of dermal rays 3-7	Poly-articular	4.35	11.3	11.3	5.243	0.363
	Abductor superficialis pelvicus 3	*Abductor superficialis pelvicus 3*	*Pelvic girdle: base of the medial process, ventral side; *Aponeurosis on the Adductor profundus pelvicus	Ventral side: Proximal portion of the dermal ray 8	Poly-articular	0.64	8.9	8.9	2.848	0.068
	Abductor superficialis pelvicus 4	*Abductor superficialis pelvicus 4*	Pelvic girdle: base at the posterior edge of the medial process	Ventral side: Proximal portion of the dermal ray 9	Poly-articular	0.52	8.2	8.2	2.642	0.060

Supplementary Table 2.1 (suite)

Muscle (Millot & Anthony, 1958)	Muscle	Subdivision	Origin(s)	Insertion(s)	Articulation mode	Mass (g)	Bundle Total lenght (cm)	Bundle lenght (cm)	Mean Fiber lenght (cm)	ACSA (cm²)
"Abaisseur superficiel"	*Abductor superficialis pelvicus 5*	*Abductor superficialis pelvicus 5*	Pelvic girdle: posterior edge of the the medial process	Ventral side: Proximal portion of dermal rays 10-11	Poly-articular	0.62	9	9	2.915	0.065
	Abductor superficialis pelvicus 6	*Abductor superficialis pelvicus 6*	Pelvic girdle: posterior edge of the the medial process	Ventral side: Proximal portion of dermal rays 11-14	Poly-articular	1.14	9.7	9.7	3.003	0.111
	Abductor superficialis pelvicus 7	*Abductor superficialis pelvicus 7*	Pelvic girdle: posterior edge of the the medial process	Ventral side: Proximal portion of dermal rays 14-17	Poly-articular	1.47	10.9	10.9	4.935	0.127
	Abductor superficialis pelvicus 8	*Abductor superficialis pelvicus 8*	Pelvic girdle: posterior edge of the the medial process	Ventral side: Proximal portion of dermal rays 17-18	Poly-articular	1.55	10.7	10.7	5.379	0.137
	Abductor superficialis pelvicus 9	*Abductor superficialis pelvicus 9*	Pelvic girdle: posterior edge of the the medial process	Ventral side: Proximal portion of dermal rays 19-20	Poly-articular	0.7	10.6	10.6	5.446	0.062
	Abductor superficialis pelvicus 10	*Abductor superficialis pelvicus 10*	Pelvic girdle: posterior edge of the the medial process, on the ligament that linked the two medal processes	Ventral side: Proximal portion of dermal rays 20-21	Poly-articular	0.66	10.1	10.1	5.601	0.062
	Abductor superficialis pelvicus 11	*Abductor superficialis pelvicus 11*	aponeurosis between the two fins	Ventral side: Proximal portion of the dermal ray 22	Poly-articular	0.54	7.6	7.6	5.734	0.067
	Abductor superficialis pelvicus 12	*Abductor superficialis pelvicus 12*	aponeurosis between the two fins	Ventral side: Proximal portion of the dermal ray 23	Poly-articular	0.56	8.2	8.2	5.361	0.064

Supplementary Table 2.1 (suite)

Muscle (Millot & Anthony, 1958)	Muscle	Subdivision	Origin(s)	Insertion(s)	Articulation mode	Mass (g)	Bundle Total lenght (cm)	Bundle lenght (cm)	Mean Fiber lenght (cm)	ACSA (cm²)
"Abaisseur superficiel"	*Abductor superficialis pelvicus 13*	*Abductor superficialis pelvicus 13*	aponeurosis between the two fins	Ventral side: Proximal portion of dermal rays 23 and 24	Poly-articular	0.44	7.5	7.5	5.135	0.055
	Abductor superficialis pelvicus 14	*Abductor superficialis pelvicus 14*	aponeurosis between the two fins	Ventral side: Proximal portion of dermal rays 25 and 26	Poly-articular	1.81	8.1	8.1	5.468	0.211
	Abductor superficialis pelvicus 15	*Abductor superficialis pelvicus 15*	aponeurosis between the two fins	Ventral side: Proximal portion of dermal rays 26 to 30	Poly-articular	4	6.7	6.7	4.736	0.563
"Abaisseur profond"	*Abductor profundus pelvicus 1*	*Abductor profundus pelvicus 1*	Pelvic girdle: anterior edge of the lateral process, ventral side	Ventral side: Antero-lateral edge of the pre-axial radial 2	Poly-articular	0.16	3.9	3.9	2.858	0.039
	Abductor profundus pelvicus 2	*Abductor profundus pelvicus 2*	Pelvic girdle: anterior edge of the base of the lateral process, ventral side	ventral side: Lateral edge of the pre-axial radial 1	Poly-articular	0.21	5.3	3.9	1.672	0.051
	Abductor profundus pelvicus 3	*Abductor profundus pelvicus 3*	Pelvic girdle: anterior edge of the base of the lateral process, ventral side	Ventral side: Pre-axial radial 1	Poly-articular	0.15	4	3.1	1.813	0.046
	Abductor profundus pelvicus 4	*Abductor profundus pelvicus 4*	Pelvic girdle: base of the posterior side of the medial process, ventral side	Ventral side: Proximal portion of the dermal ray 7	Poly-articular	0.22	9.6	7.7	4.639	0.027
	Abductor profundus pelvicus 5	*Abductor profundus pelvicus 5a*	Pelvic girdle: the posterior side of the medial process, dorsal side	Ventral side: Proximal portion of dermal rays 8-9	Poly-articular	0.36	10	8.9	4.483	0.038

Supplementary Table 2.1 (suite)

Muscle (Millot & Anthony, 1958)	Muscle	Subdivision	Origin(s)	Insertion(s)	Articulation mode	Mass (g)	Bundle Total lenght (cm)	Bundle lenght (cm)	Mean Fiber lenght (cm)	ACSA (cm²)
"Abaisseur profond"	*Abductor profundus pelvicus 5*	*Abductor profundus pelvicus 5b*	Pelvic girdle: the posterior side of the medial process, dorsal side	Ventral side: Proximal portion of the dermal ray 8	Poly-articular	0.22	8.6	6.7	4.702	0.031
		Abductor profundus pelvicus 5c	On the Abductor profundus pelvicus 5a	Ventral side: Proximal portion of the dermal ray 10	Poly-articular	0.11	6.3	4.4	2.409	0.024
		Abductor profundus pelvicus 5d	Pelvic girdle: the posterior side of the medial process, dorsal side	On the Abductor profundus pelvicus 5a	Poly-articular	0.08	2.8	2.8	2.301	0.027
		Abductor profundus pelvicus 5e	Pelvic girdle: base of the posterior side of the medial process, ventral side	Ventral side: Proximal portion of dermal rays 8-10	Poly-articular	0.05	5.3	5.3	4.918	0.009
	Abductor profundus pelvicus 6	*Abductor profundus pelvicus 6a*	Pelvic girdle: dorsal side of the medial process	Ventral side: Proximal portion of the dermal ray 11	Poly-articular	0.15	6.9	5.1	4.565	0.028
		Abductor profundus pelvicus 6b	Pelvic girdle: base of the posterior side of the medial process (ventral side)	Ventral side: Proximal portion of the dermal ray 10	Poly-articular	0.25	9.7	5.9	5.077	0.040
		Abductor profundus pelvicus 6c	On the Abductor profundus pelvicus 6a	Ventral side: Proximal portion of the dermal ray 11	Poly-articular	0.1	6.3	3.5	2.65	0.027
		Abductor profundus pelvicus 6d	Pelvic girdle: dorsal side of the medial process	On the Abductor profundus pelvicus 6a	Poly-articular	0.07	2.4	2.4	2.046	0.028

Supplementary Table 2.1 (suite)

Muscle (Millot & Anthony, 1958)	Muscle	Subdivision	Origin(s)	Insertion(s)	Articulation mode	Mass (g)	Bundle Total lenght (cm)	Bundle lenght (cm)	Mean Fiber lenght (cm)	ACSA (cm²)
"Abaisseur superficiel"	*Abductor profundus pelvicus 6*	*Abductor profundus pelvicus 6e*	Pelvic girdle: dorsal side of the medial process	Ventral side: Proximal portion of the dermal ray 11	Poly-articular	0.53	9.1	4.7	3.947	0.106
		Abductor profundus pelvicus 6f	Membrane between pelvic muscles and abdominal muscles	On the aponeurosis above supinator muscles	Poly-articular	0.1	6.9	6.3	2.886	0.015
		Abductor profundus pelvicus 6g	Membrane between pelvic muscles and abdominal muscles	On the aponeurosis above supinator muscles	Poly-articular	0.14	5.7	5.7	2.789	0.023
	Abductor profundus pelvicus 7	*Abductor profundus pelvicus 7a*	On the Abductor profundus pelvicus 7b	Ventral side: Proximal portion of the dermal ray 12	Poly-articular	0.08	7.1	4	2.937	0.019
		Abductor profundus pelvicus 7b	Pelvic girdle: dorsal side of the medial process	Ventral side: Proximal portion of the dermal ray 11	Poly-articular	0.11	9.1	5.3	4.218	0.020
		Abductor profundus pelvicus 7c	Pelvic girdle: dorsal side of the medial process	Ventral side: Proximal portion of dermal rays 13-14	Poly-articular	0.22	7.1	4.9	4.001	0.042
		Abductor profundus pelvicus 7d	Pelvic girdle: dorsal side of the medial process	Ventral side: Proximal portion of the dermal ray 12	Poly-articular	0.11	9.8	3.1	2.784	0.033
		Abductor profundus pelvicus 7e	Pelvic girdle: dorsal side of the medial process	Ventral side: Proximal portion of dermal rays 11-12	Poly-articular	0.16	9.5	2.4	2.309	0.063
		Abductor profundus pelvicus 7f	Pelvic girdle: dorsal side of the medial process	Ventral side: Proximal portion of dermal rays 13-14	Poly-articular	0.17	10.3	3.9	2.757	0.041

Supplementary Table 2.1 (suite)

Muscle (Millot & Anthony, 1958)	Muscle	Subdivision	Origin(s)	Insertion(s)	Articulation mode	Mass (g)	Bundle Total lenght (cm)	Bundle lenght (cm)	Mean Fiber lenght (cm)	ACSA (cm²)
"Abaisseur superficiel"	*Abductor profundus pelvicus 7*	*Abductor profundus pelvicus 7g*	Pelvic girdle: dorsal side of the medial process	Ventral side: Proximal portion of the dermal ray 9	Poly-articular	0.26	8.3	4	3.038	0.061
		Abductor profundus pelvicus 7h	On the aponeurosis above supinator muscles	On the aponeurosis above supinator muscles	Poly-articular	0.044	4.8	3.9	0.676	0.011
	Abductor profundus pelvicus 8	*Abductor profundus pelvicus 8a*	*Pelvic girdle: dorsal side of the medial process; *Membrane between pelvic muscles and abdominal muscles	Proximal portion of the dermal ray 11	Poly-articular	0.48	10.2	4.4	4.341	0.103
		Abductor profundus pelvicus 8b	*Pelvic girdle: dorsal side of the medial process; *Membrane between pelvic muscles and abdominal muscles	Proximal portion of the dermal ray 14	Poly-articular	0.38	10.8	5	3.26	0.072
		Abductor profundus pelvicus 8c	*Pelvic girdle: dorsal side of the medial process; *Membrane between pelvic muscles and abdominal muscles	Proximal portion of the dermal ray 12	Poly-articular	0.09	10.5	2.6	2.02	0.033

Supplementary Table 2.1 (suite)

Muscle (Millot & Anthony, 1958)	Muscle	Subdivision	Origin(s)	Insertion(s)	Articulation mode	Mass (g)	Bundle Total lenght (cm)	Bundle lenght (cm)	Mean Fiber lenght (cm)	ACSA (cm²)
"Abaisseur superficiel"	*Abductor profundus pelvicus 9*	*Abductor profundus pelvicus 9a*	*Pelvic girdle: dorsal side of the medial process; *Membrane between pelvic muscles and abdominal muscles	Ventral side: Proximal portion of dermal rays 15-17	Poly-articular	0.58	11.3	5.9	3.261	0.093
		Abductor profundus pelvicus 9b	*Pelvic girdle: dorsal side of the medial process; *Membrane between pelvic muscles and abdominal muscles	Ventral side: Proximal portion of dermal rays 12-13	Poly-articular	0.47	10.9	5.3	3.397	0.084
		Abductor profundus pelvicus 9c	Membrane between pelvic muscles and abdominal muscles	On the aponeurosis above supinator muscles	Poly-articular	0.751	70.9	5.6	3.059	0.127
	Abductor profundus pelvicus 10	*Abductor profundus pelvicus 10a*	*Pelvic girdle: dorsal side of the medial process; *Membrane between pelvic muscles and abdominal muscles	Ventral side: Proximal portion of the dermal ray 20	Poly-articular	0.55	11.5	7.9	5.022	0.066
		Abductor profundus pelvicus 10b	*Pelvic girdle: dorsal side of the medial process; *Membrane between pelvic muscles and abdominal muscles	Ventral side: Proximal portion of dermal rays 19-20	Poly-articular	0.21	8.7	7	5.993	0.028

Supplementary Table 2.1 (suite)

Muscle (Millot & Anthony, 1958)	Muscle	Subdivision	Origin(s)	Insertion(s)	Articulation mode	Mass (g)	Bundle Total lenght (cm)	Bundle lenght (cm)	Mean Fiber lenght (cm)	ACSA (cm²)
"Abaisseur superficiel"	*Abductor profundus pelvicus 10*	*Abductor profundus pelvicus 10c*	*Pelvic girdle: dorsal side of the medial process; *Membrane between pelvic muscles and abdominal muscles	Ventral side: Proximal portion of the dermal ray 15	Poly-articular	0.63	12.5	7	4.562	0.085
		Abductor profundus pelvicus 10d	*Pelvic girdle: dorsal side of the medial process; *Membrane between pelvic muscles and abdominal muscles	Ventral side: Proximal portion of the dermal ray 17	Poly-articular	0.85	11.5	6	3.299	0.134
		Abductor profundus pelvicus 10e	On the Abductor profundus pelvicus 10f	Ventral side: Proximal portion of the dermal ray 20	Poly-articular	0.15	6.3	4.7	4.146	0.030
		Abductor profundus pelvicus 10f	*Pelvic girdle: dorsal side of the medial process; *Membrane between pelvic muscles and abdominal muscles	Ventral side: Proximal portion of the dermal ray 21	Poly-articular	1.37	10.6	8	3.359	0.162
		Abductor profundus pelvicus 10g	On the aponeurosis above supinator muscles	On the Abductor profundus pelvicus 10f and Proximal portion of the dermal ray 21	Poly-articular	0.2	11.8	6.9	5.863	0.027

Supplementary Table 2.1 (suite)

Muscle (Millot & Anthony, 1958)	Muscle	Subdivision	Origin(s)	Insertion(s)	Articulation mode	Mass (g)	Bundle Total lenght (cm)	Bundle lenght (cm)	Mean Fiber lenght (cm)	ACSA (cm²)
"Abaisseur superficiel"	*Abductor profundus pelvicus 11*	*Abductor profundus pelvicus 11*	*Pelvic girdle: dorsal side of the medial process; *Membrane between pelvic muscles and abdominal muscles	Ventral side: Proximal portion of dermal rays 21-22	Poly-articular	2.06	12.6	9.7	5.786	0.200
	Abductor profundus pelvicus 12	*Abductor profundus pelvicus 12a*	Membrane between pelvic muscles and abdominal muscles	Ventral side: Proximal portion of the dermal ray 23	Poly-articular	1	11.7	8.2	6.509	0.115
		Abductor profundus pelvicus 12b	On the aponeurosis above supinator muscles	On the Abductor profundus pelvicus 12a	Poly-articular	0.09	5.2	5.2	4.426	0.016
		Abductor profundus pelvicus 12c	* Membrane between pelvic muscles and abdominal muscles; *aponeurosis between the two fins	Ventral side: Proximal portion of dermal rays 23-24	Poly-articular	0.54	8	6.1	5.458	0.084
	Abductor profundus pelvicus 13	*Abductor profundus pelvicus 13*	Aponeurosis between the two pelvic fins	Ventral side: Proximal portion of dermal rays 25-26	Poly-articular	0.7	7.3	5.5	4.74	0.120
	Abductor profundus pelvicus 14	*Abductor profundus pelvicus 14*	*Edge of the medial bud of Mesomere 1; *aponeurosis between the two fins	Ventral side: Proximal portion of dermal rays 30-33	Poly-articular	3.182	5.4	5.4	1.469	0.556

Supplementary Table 2.1 (suite)

Muscle (Millot & Anthony, 1958)	Muscle	Subdivision	Origin(s)	Insertion(s)	Articulation mode	Mass (g)	Bundle Total lenght (cm)	Bundle lenght (cm)	Mean Fiber lenght (cm)	ACSA (cm²)
Supinator 1	*Supinator 1*	*Supinator 1*	Pelvic girdle: between lateral and medial processes (ventral side) and at the posterior edge of the base of the medial process (ventral side)	Ventral side: Anterior side of the pre-axial radial 0	Poly-articular	0.54	3.7	3.7	1.435	0.138
	Supinator 2	*Supinator 2a*	Pelvic girdle: medial side of the girdle	Ventral side: Pre-axial radial 0	Mono-articular	0.69	4.2	4.2	1.544	0.155
		Supinator 2b	Pelvic girdle: medial side of the girdle	Ventral side: Posterior side of the pre-axial radial 0 and anterior side of the pre-axial radial 1	Poly-articular	0.62	5	5	1.191	0.117
	Supinator 3	*Supinator 3a*	Membrane between pelvic muscles and abdominal muscles	Ventral side: Proximal portion of the dermal ray 1	Poly-articular	0.966	6.8	6.8	2.035	0.134
		Supinator 3b	Membrane between pelvic muscles and abdominal muscles	Ventral side: Pre-axial radial 1	Poly-articular	0.378	4.2	4.2	1.161	0.085
	Supinator 4	*Supinator 4*	Membrane between pelvic muscles and abdominal muscles	Ventral side: Proximal portion of the dermal ray 2	Poly-articular	1.392	9	9	3.037	0.146

Supplementary Table 2.1 (suite)

Muscle (Millot & Anthony, 1958)	Muscle	Subdivision	Origin(s)	Insertion(s)	Articulation mode	Mass (g)	Bundle Total lenght (cm)	Bundle lenght (cm)	Mean Fiber lenght (cm)	ACSA (cm²)
Supinator 1	*Supinator 5*	*Supinator 5a*	Membrane between pelvic muscles and abdominal muscles	Ventral side: Proximal portion of the fin ray 2	Poly-articular	0.406	8	3.3	2.17	0.116
		Supinator 5b	*Membrane between pelvic muscles and abdominal muscles; *Medial edge of the girdle	Ventral side: *Pre-axial radial 2; *Base of fin rays 1-2	Poly-articular	0.929	9	7.4	2.73	0.118
	Supinator 5	*Supinator 5c*	Proximo-medial edge of the mesomere 1	Ventral side: Proximal portion of the fin ray 1	Poly-articular	0.174	3.1	3.1	1.437	0.053
Supinator 2	*Supinator 6*	Supinator 6a	Membrane between pelvic muscles and abdominal muscles	Ventral side: Proximal portion of the fin ray 3	Poly-articular	0.824	8.5	6.3	3.999	0.123
		Supinator 6b	Membrane between pelvic muscles and abdominal muscles	Ventral side: Proximal portion of the fin ray 5	Poly-articular	0.745	8.5	5.8	3.775	0.121
		Supinator 6c	Proximo-medial edge of the mesomere 1	Ventral side: Proximal portion of the fin ray 2	Poly-articular	0.304	7.5	7.5	3.904	0.038
	Supinator 7	Supinator 7a	Proximo-medial edge of the mesomere 1	Ventral side: Proximal portion of the fin ray 3	Poly-articular	0.155	6.1	4.9	3.957	0.030
		Supinator 7b	Medial edge of the mesomere 1	Ventral side: Proximal portion of fin rays 3-4	Poly-articular	0.309	4	3.6	1.541	0.081

Supplementary Table 2.1 (suite)

Muscle (Millot & Anthony, 1958)	Muscle	Subdivision	Origin(s)	Insertion(s)	Articulation mode	Mass (g)	Bundle Total lenght (cm)	Bundle lenght (cm)	Mean Fiber lenght (cm)	ACSA (cm²)
Supinator 2	*Supinator 8*	Supinator 8a	*Membrane between pelvic muscles and abdominal muscles; *Medial edge of the mesomere 1	Ventral side: Proximal portion of fin rays 4-5	Poly-articular	0.404	6.5	6.5	2.035	0.059
		Supinator 8b	Vental side of the postero-superior process	Ventral side: Proximal portion of the fin ray 5	Poly-articular	0.622	8.2	6.5	3.927	0.090
		Supinator 8c	Medial edge of the mesomere 1	Ventral side: Proximal portion of the fin ray 6	Poly-articular	0.351	4.9	4.9	1.97	0.068
	Supinator 9	Supinator 9a	*Membrane between pelvic muscles and abdominal muscles; * Medial edge of the mesomere 1	Ventral side: Proximal portion of the fin ray 7	Poly-articular	0.988	9.5	7.4	4.118	0.126
		Supinator 9b	Aponeurosis between the two fins	Ventral side: Proximal portion of the fin ray 7	Poly-articular	0.377	7.3	5.1	4.128	0.070
		Supinator 9c	Proximo-medial edge of the mesomere 2	Ventral side: Proximal portion of the fin ray 7	Poly-articular	0.311	4.1	4.1	1.807	0.072
Supinator 3	*Supinator 10*	Supinator 10a	*Aponeurosis between the two fins; *Dorso-medial edge of the mesomere 1	Ventral side: Proximal portion of the fin ray 8	Poly-articular	0.766	7.5	5.1	3.415	0.142
		Supinator 10b	Proximo-medial edge of the mesomere 2	Ventral side: Proximal portion of the fin ray 8	Poly-articular	0.231	4.2	3.8	1.764	0.057
	Supinator 11	Supinator 11a	*Aponeurosis between the two fins; *Medial edge of the mesomere 2	Ventral side: Proximal portion of the fin ray 9	Poly-articular	0.285	6.3	3.5	2.984	0.077

Supplementary Table 2.1 (suite)

Muscle (Millot & Anthony, 1958)	Muscle	Subdivision	Origin(s)	Insertion(s)	Articulation mode	Mass (g)	Bundle Total lenght (cm)	Bundle lenght (cm)	Mean Fiber lenght (cm)	ACSA (cm²)
Supinator 3	*Supinator 11*	Supinator 11b	Medial edge of the mesomere 2	Ventral side: Proximal portion of the fin ray 9	Poly-articular	0.293	5.6	4.9	1.966	0.056
Supinator 4	*Supinator 12*	Supinator 12a	Aponeurosis between the two fins	Ventral side: Proximal portion of the fin ray 10	Poly-articular	0.475	7.9	4.6	3.607	0.097
		Supinator 12b	Medial edge of the mesomere 2	Ventral side: Proximal portion of the fin ray 10	Poly-articular	0.147	5.1	4.9	2.551	0.028
		Supinator 12c	Medial edge of the mesomere 3	Ventral side: Proximal portion of the fin ray 10	Poly-articular	0.134	3.6	3.6	1.469	0.035
	Supinator 13	Supinator 13a	*Medial bud of mesomere 1; *Medial edge of mesomere 2	Ventral side: Proximal portion of the fin ray 11	Poly-articular	0.66	7.8	4.5	3.518	0.138
		Supinator 13b	Medial edge of the mesomere 3	Ventral side: Proximal portion of the fin ray 11	Poly-articular	0.273	4	4	1.448	0.064
	Supinator 14	Supinator 14a	*Medial bud of the mesomere 1; *Medial edge of the mesomere 2	Ventral side: Proximal portion of the fin ray 12	Poly-articular	0.63	7.7	5.2	3.4	0.114
		Supinator 14b	Medial bud of the mesomere 1	Ventral side: Proximal portion of the fin ray 13	Poly-articular	0.387	6.9	5	2.841	0.073
		Supinator 14c	Medial edge of the mesomere 3	Ventral side: Proximal portion of the fin ray 12	Poly-articular	0.211	4.8	3.6	1.375	0.055
Undescribed	*Supinator 15*	Supinator 15a	Mesomere 4	Ventral side: Proximal portion of the fin ray 12	Mono-articular	0.66	2.5	2.5	0.758	0.249
		Supinator 15b	Mesomere 4	Ventral side: Proximal portion of fin rays 13-17	Mono-articular	0.634	3.4	3.4	0.764	0.176
	Supinator 16	Supinator 16a	Proximo-medial edge of the distal radial	Ventral side: Proximal portion of fin rays 18-19	Mono-articular	0.201	2.7	2.7	0.49	0.070

Supplementary Table 2.1 (suite)

Muscle (Millot & Anthony, 1958)	Muscle	Subdivision	Origin(s)	Insertion(s)	Articulation mode	Mass (g)	Bundle Total lenght (cm)	Bundle lenght (cm)	Mean Fiber lenght (cm)	ACSA (cm^2)
Undescribed	*Supinator 16*	Supinator 16b	Proximo-medial edge of the distal radial	Ventral side: Proximal portion of fin rays 20-21	Mono-articular	0.17	2.4	2.4	0.765	0.067
		Supinator 16c	Proximo-medial edge of the distal radial	Ventral side: Proximal portion of fin rays 22-23	Mono-articular	0.097	2	2	0.864	0.046
		Supinator 16d	Proximo-medial edge of the distal radial	Ventral side: Proximal portion of fin rays 23-24	Mono-articular	0.174	2.1	2.1	0.927	0.078
	Supinator 17	Supinator 17a	Medial edge of the Mesomere 4	Ventral side: Proximal portion of the fin ray 24	Mono-articular	0.166	2.9	2.9	0.896	0.054
		Supinator 17b	Medial edge of the Mesomere 4	Ventral side: Proximal portion of fin rays 25-28	Mono-articular	0.683	1.8	1.8	1.051	0.358
		Supinator 17c	Proximal edge of the post-axial radial	Ventral side: Proximal portion of fin rays 29-33	Mono-articular	0.315	1.6	1.6	1.243	0.186

CHAPTER III

Evolution of the functional muscular anatomy of pectoral and pelvic appendages across the water-to-land transition

---

Context of the Chapter III

The aim of this thesis is to focus on the evolution of the muscle architecture in the context of the fin-to-limb transition, thanks to our interpretations on the endoskeletal and muscular anatomy of the paired fins of the coelacanth, and inferences on its locomotion. In the previous chapter, we saw that the muscular anatomy and muscle architecture of the pectoral and pelvic fins permit to investigate the locomotion of the coelacanth. It is supposed that during the fin-to-limb transition, there was a locomotor shift from pectoral to pelvic appendages (e.g. Coates et al., 2002), based on the skeletal morphology in the fossil record. If the evolution of the muscle anatomy has been approached during the fin-to-limb transition (Diogo et al., 2016; Molnar et al., 2018, 2020), the evolution of the muscle architecture has never been studying so far. Yet, its study permits to investigate the evolution of the force generation of the limbs during the fin-to-limb transition, and so to infer the evolution of locomotor behaviour, what we investigated in the **Chapter III**. Data obtained from the dissections of the paired fins of *Latimeria* were used in this study. The other specimens used in the study were chosen since they represent taxa that are phylogenetically (tetrapods) or ecologically (actinopterygians) of interest to understand the main evolutionary trends during the fin-to-limb transition, and because they were available for dissections.

Among living sarcopterygian fishes, lungfishes are a peculiar interest since they represent the sister-taxa of tetrapods, and they would be appropriated to be included int he study. We could have access to the African lungfish *Protopterus* for dissections, that is used in studies on the locomotion and the water-to-land transition (King et al., 2011). However, its paired fins are highly modified, as well as its muscular anatomy. In *Protopterus*, the pelvic fin musculature is only formed by one retractor and one protractor muscles at the base of fin, and the rest of the fin is formed by circumradialis muscles (Aiello et al., 2014; King and Hale, 2014). The pectoral fin of *Protopterus* shows a more complex muscular anatomy between the pectoral girdle and the first mesomere, but the rest of the fin is also formed by circumradialis muscles (Wilhelm, 2015). Similarly the paired fins of the South American lungfish *Lepidosiren* are also highly modified. Since the comparison of their muscular anatomy with those of other "fishes" and tetrapods as proposed by Diogo et al. (2016) is not easy to approach, we decided to not include them in the study. The paired fins of the Australian lungfish *Neoceratodus* show an anatomy closer to that of the coelacanth, but specimens were unfortunately not available, and this key taxon is thus not included in this current study.

This chapter is a preliminary study, which will be add with more specimens before being submitted to publication.

Bibliography

Aiello, B. R., King, H. M., and Hale, M. E. (2014). Functional subdivision of fin protractor and retractor muscles underlies pelvic fin walking in the African lungfish *Protopterus annectens*. *Journal of Experimental Biology*, 217(19):3474–3482.

Coates, M. I., Jeffery, J. E., and Ruta, M. (2002). Fins to limbs: What the fossils say. *Evolution & Development*, 4(5):390–401.

Diogo, R., Johnston, P., Molnar, J. L., and Esteve-Altava, B. (2016). Characteristic tetrapod musculoskeletal limb phenotype emerged more than 400 MYA in basal lobe-finned fishes. *Scientific Reports*, 6:1–9.

King, H. M. and Hale, M. E. (2014). Musculoskeletal morphology of the pelvis and pelvic fins in the lungfish *Protopterus annectens*. *Journal of Morphology*, 275(4):431–441.

King, H. M., Shubin, N. H., Coates, M. I., and Hale, M. E. (2011). Behavioral evidence for the evolution of walking and bounding before terrestriality in sarcopterygian fishes. *PNAS*, 108(52):21146–21151.

Molnar, J. L., Diogo, R., Hutchinson, J. R., and Pierce, S. E. (2018). Reconstructing pectoral appendicular muscle anatomy in fossil fish and tetrapods over the fins-to-limbs transition. *Biological Reviews*, 93:1077–1107.

Molnar, J. L., Diogo, R., Hutchinson, J. R., and Pierce, S. E. (2020). Evolution of Hindlimb Muscle Anatomy Across the Tetrapod Water-to-Land Transition, Including Comparisons With Forelimb Anatomy. *Anatomical Record*, 303(2):218–234.

Wilhelm, B. C. (2015). *The pectoral anatomy of Polypterus and Protopterus, and the evolution of pectoral musculature in fishes*. PhD thesis, McGill University, Montreal, Quebec.

Evolution of the functional muscular anatomy of pectoral and pelvic appendages across the water-to-land transition

Mansuit Rohan[1,2], Herbin Marc[2], Huby Alessia[3], Clément Gaël[1], Herrel Anthony[2]

[1]UMR 7207 Centre de Recherche en Paléontologie, Paris, MNHN – Sorbonne Université – CNRS, Département Origines & Evolution, Muséum national d'Histoire naturelle, 8 rue Buffon, 75005 Paris, France

[2]UMR 7179 MECADEV, MNHN – CNRS, Département Adaptations du Vivant, Muséum national d'Histoire naturelle, 55 rue Buffon, 75005 Paris, France

[3]Laboratory of Functional and Evolutionary Morphology, FOCUS Research Unit, Department of Biology, Ecology and Evolution, University of Liège, Liège, Belgium

Introduction

The water-to-land transition of vertebrates is associated with a number of morphological transformations of the body associated with changes in the environment and its physical characteristics (Brazeau and Ahlberg, 2006; Daeschler et al., 2006). Two of the most marked anatomical features are the presence of limbs with digits in tetrapods in contrast to fins and lepidotrichia in fishes (e.g. Coates et al., 2002; Ahlberg et al., 2005; Pierce et al., 2012) and the enlargement of the pelvic girdle associated with an attachment of the ilium to the sacral vertebrae, ultimately permitting the weight-bearing function of the hindlimb (Coates et al., 2002; Cole et al., 2011; Boisvert et al., 2013). The evolution of the tetrapod limb has been actively studied for more than half a century. Most studies have focused on skeletal adaptations observable on fossil material (Andrews and Westoll, 1970; Coates et al., 2002; Boisvert, 2005; Daeschler et al., 2006; Shubin et al., 2006; Boisvert et al., 2008; Pierce et al., 2012). Additionally, developmental (e.g. Shubin and Alberch, 1986; Joss and Longhurst, 2001; Cole et al., 2011; Boisvert et al., 2013) and genetic studies (e.g. Coates, 1995; Johanson et al., 2007; Zhang et al., 2010; Nakamura et al., 2016) have shed light on the evolution of the tetrapod limb. The evolution of limbs from fins was also marked by a new mode of locomotion (Ahlberg et al., 2005; Cole et al., 2011; Pierce et al., 2012). In fishes, locomotion is dependent on lateral undulations of the body and the use of the pectoral fins. In most tetrapods, lateral undulations are still important but there is dominance of the pelvic appendages in generating propulsion (Coates et al., 2002; Boisvert, 2005; Cole et al., 2011; Boisvert et al., 2013). The evolution from "front to back propulsion" has been studied in early tetrapodomorphs fossils (e.g. Carroll et al., 2005; Clack, 2012; Boisvert et al., 2013), yet has never been explored using living analogs.

In order to understand the processes involved in the changes of locomotion in extant vertebrates, it is necessary to not only understand the bony skeleton but also the associated muscle anatomy as ultimately muscles are generating the forces permitting the locomotion. Unfortunately, soft tissues are rarely preserved in the fossil record and it is consequently near impossible to study the evolution of the muscle anatomy during the fin-to-limb transition which occurred during the Palaeozoic. Reconstruction of the muscle anatomy of the appendages of early tetrapods have been proposed in several studies (e.g. Romer, 1924; Andrews and Westoll, 1970; Ahlberg, 1989). Recently, a comparison of the muscular anatomy between extant tetrapods, the coelacanth *Latimeria*, and the lungfish *Neoceratodus* homologies between most of the appendicular muscles of these sarcopterygian fishes and those of tetrapods were proposed (Diogo et al., 2016; Molnar et al., 2018, 2020). Despite the importance of understanding

the homology between different representative vertebrae taxa, these studies remain largely descriptive (Přikryl et al., 2009; King and Hale, 2014; Ercoli et al., 2015; Wilhelm et al., 2015; Miyake et al., 2016; Freitas et al., 2017; Molnar et al., 2017; Siomava and Diogo, 2018) and do not permit to quantitatively test the evolution of hind limb drive associated with the transition. Only few studies present quantitative information such as the muscle mass and muscle length (Herrel et al., 2005; Payne et al., 2005; Thorsen and Hale, 2005; Smith et al., 2006; Allen et al., 2010, 2015; Dickson and Pierce, 2019) which are crucial to interpret the ecological and locomotor changes that may have occurred during the water-to-land transition.

In vertebrates, osteichthyans are divided in actinopterygians and sarcopterygians, two clades partly defined on the anatomy of the pectoral and pelvic appendages (e.g. Janvier, 1996). Actinopterygians (ray-finned fishes) have dermal paired fin rays that insert directly at the level of the pectoral and pelvic girdles by means of several radial elements connected to three basal cartilages (poly-basal articulation), and covered by small muscles located within the body wall. Sarcopterygians (lobe-finned fishes) have paired appendages with an endoskeletal metapterygial axis formed by the alignment of several endoskeletal elements between the pectoral and pelvic girdles and the fin rays/digit. This metapterygial axis is covered by large muscles located outside the body wall. The metapterygial axis is connected to the girdle by only one proximal element (mono-basal articulation, Rosen et al., 1981; Janvier, 1996). Living sarcopterygians include the coelacanth, lungfish and tetrapods. The first mesomere of the pectoral and pelvic fin corresponds respectively to the humerus and femur of tetrapods (Johanson et al., 2007).

Here, we quantify the muscle architecture of pectoral and pelvic appendages in extant vertebrates to test the hypothesis that a switch to a hind limb driven locomotion as observed in the fossil record of early tetrapodomorphs is associated with changes in the limb muscles and their architecture. We further test whether relative appendage size is impacted by the fin-to-limb or the water-to-land transition by testing quantifying muscle architecture for terrestrial and aquatic representatives of several vertebrates groups. Finally, we tested whether changes in locomotor mode (aquatic versus terrestrial) impacted muscle architecture and the investment in different muscle groups of the fore and hind limb.

Material & Methods

Study specimens

The pectoral and pelvic appendages of nine species of different vertebrate taxa were dissected in this chapter. The taxa available for dissections and used for this study include three actinopterygians (the bichir *Polypterus senegalus*, the sturgeon *Acipenser stellatus* and the European bass *Dicentrarchus labrax*), the African coelacanth *Latimeria chalumnae*, and five tetrapods (the mudpuppy *Necturus maculosus*, the tegu lizard *Salvator merianae*, the crocodilian *Alligator mississippiensis*, the grison *Galictis vittata* and the otter *Lontra longicauda*) (Fig. 3.1). Specimens were obtained through the collections of the Museum national d'Histoire naturelle (Paris, France), the Institut Pasteur, Cayenne, The Aquarium tropical de la POrte Dorée (Paris, France), and the research collection of Anthony Herrel. The pectoral and pelvic fins of *Latimeria* were dissected in two different specimens of similar size and mass: MNHN-ZA-AC-2012-11 (CCC 14) and MNHN-AC-ZA-2012-21 (CCC 27) (Nulens et al., 2011). Data on the muscle architecture for the fins of *Latimeria* are derived from a previous study (Huby *et al*, in prep). Data for the muscular anatomy of the fore and hind limbs of two otters and four grisons specimens were obtained from a previous study (Anne-Claire Fabre, Anthony Herrel, unpublished results). For all other species, only one specimen per species were dissected for now. For *Polypterus* and *Dicentrarchus*, the left and right fins were dissected, whereas for all other species, only one pectoral and one pelvic appendages were dissected. Since the total body mass of the *Alligator* was unknown, we estimated it based on the femur length using the linear regression provided by Allen et al. (2010). The means of the different values off body-mass, muscle mass, muscle length and fibre length are provide for each taxon.

Species were chosen to provide a sample that includes several taxa across the vertebrate tree of life and spanning bother the fin-to-limb transition. Moreover, we included both aquatic and terrestrial representatives of different clades where possible. *Necturus* is a fully aquatic animal with musculature adapted for aquatic locomotion (Neill 1963; Craig et al 2016), *Alligator* and *Lontra* are amphibious and *Salvator* and *Galictis* are terrestrial.

The muscles were classified in groups, using the homologies between fin and limb muscles proposed by Diogo et al. (2016) and Molnar et al. (2018, 2020). Four intrinsic muscles groups are considered here: the *abductor superficialis*, *abductor profundus*, *adductor superficialis* and *adductor profundus* groups. Concerning the pelvic limb of tetrapods, the *caudofemoralis* is

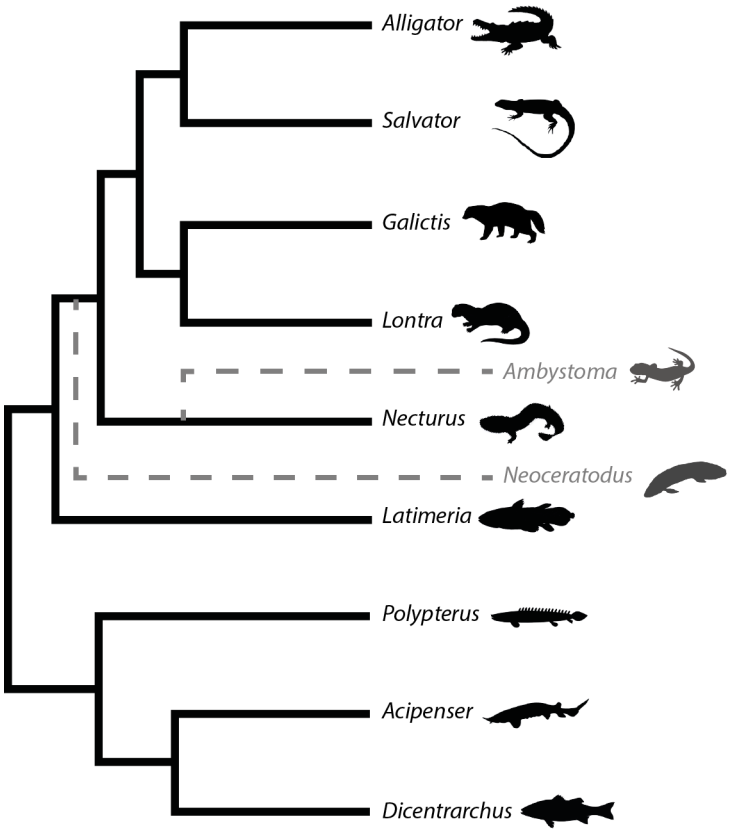

Figure 3.1: Phylogeny of the species used in this study. Species in grey show species that should be included in the study before publication.

also included in our study since it inserts on the femur bone. Homologies between the muscles of the pectoral and pelvic appendages in each the different species included in this study are shown in Annex Tables 3.1-3.2.

Muscles data

Muscles were dissected, identified, removed, measured with a ruler, weighed to the nearest 0.0001g or 0.001g using an electronic balance (Mettler AE100; Ohaus Scout pro) and then placed in a 70% aqueous solution of ethanol to preserved them until the end of the dissection. For some of the large specimens (*Alligator*, *Acipenser* and *Salvator*), the fibre length was measured directly on the muscle with a ruler, because muscle fibres were clearly visible with the naked eye. In order to measure fibre length, muscles were cut parallel to their long axis which allowed a clear identification of the fibres. For all other specimens, muscles were blotted dry after weighing and placed for a minimum of 24 hours in a 30% solution of nitric acid to dissolve all connective tissue (Loeb and Gans, 1986). The nitric acid was removed and replaced by a 50% aqueous glycerol solution (Antón, 1999; Herrel et al., 2008). For each muscle, the length of 10 randomly selected fibres was measured using the software Fiji (version ImageJ 1.52p,

Java 1.8.0_172) and mean fibre length was then calculated. The recorded parameters (muscle mass, muscle length and mean fibre length) allow us to determine the following variables.

The anatomical and physiological cross-section areas (ACSA, PCSA*) of each muscle were calculated. During our dissections, we did not measure the pennation angle of the muscle fibres. For shallow angles the cosinus of this angle is close to 1 and as such this should not impact our estimates of the force generating capacity of the muscles to a large degree. The ACSA is based on the standard muscular density (ρ), the muscle mass (m) and the muscle length (L_{muscle}), using the following equation:

$$ACSA[cm^2] = m[g]/(\rho[g.cm^{-3}] * L_{muscle}[cm])$$

The PCSA* is based on the muscle mass (m), the standard muscular density (ρ) and the mean fibre length (L_f) using the following equation:

$$PCSA^*[cm^2] = m[g]/(\rho[g.cm^{-3}] * L_f[cm])$$

The value of the muscular density of ray-finned fishes is ρ=1.05 g.cm^{-3} (Wainwright, 1988) and that of tetrapods is ρ=1.06 g.cm^{-3} (Mendez and Keys, 1960). Since the muscular density of *Latimeria chalumnae* is unknown, we choose to calculate ACSA and PCSA using the tetrapod muscular density value, due to the closer relationship of coelacanth with tetrapods. When a muscle is formed by several bundles, we first calculated the different muscle architecture variables for each bundle and then summed these values for mass and cross-sectional area to obtain the information for the whole muscle. The ACSA and PCSA are both proxies for maximal force that can be generated by a muscle, but while the ACSA underestimated it, the PCSA* as measured here can overestimated it.

Joints mobility

We measured the joint mobility after the complete dissection of the appendages with ligaments and joint capsules intact. To do so, we introduced two parallel needles in each of the two elements that compose a joint. Then the elements were moved maximally in given a plane to estimate the degree of freedom of the joint for abduction/adduction, protraction/retraction (or flexion/extension) and pronation/supination. For both appendages, pronation/supination quantifies the possibility for long-axis rotation. The protraction/retraction quantifies the mobility along the antero-posterior axis of the body, for the proximal joints (shoulder and hip), that

corresponds to the flexion/extension of the joint for the second joint (elbow and knee). The abduction/adduction shows the range of mobility along the dorso-ventral axis of the body for the proximal joints and the lateral/medial mobility of the joint for the second joint (that corresponds to the pre-axial/post-axial mobility of the joint for *Latimeria*). For each movement type, five measures were taken after the joint was returned to its resting position. The angles formed by the needles were determined on pictures of the joint at its maximal excursion using the software Fiji (version ImageJ 1.52p, Java 1.8.0_172). For each joint the mean of the five measures was retained. The joint mobility was measured for the shoulder and elbow for the pectoral appendage and the hip and knee for the pelvic appendage (or related joint in the pectoral and pelvic fin of *Latimeria*). To measure the abduction/adduction of the elbow and knee of tetrapods, it was necessary to extend the joint to the maximum, otherwise supination/pronation mobility would be included in the abduction/adduction mobility measurement.

We were able to obtain joint mobility data only for *Latimeria*, *Alligator*, and *Salvator*. Since only a few taxa are included, these results presented must be considered preliminary work. Further taxa will be added before publication.

Statistical analyses

Analyses were performed using the software R v.4.0.2 (R Core Team, 2020). Since the different taxa used in this study present a large variation of size and body mass, the measures of interest (muscle mass, ACSA, PCSA*) were $\log_{10}$-transformed to fulfil the assumption of normality and homoscedasticity. The $\log_{10}$-transformed data were then regressed against the $\log_{10}$-transformed body mass for each taxon, to remove the effect of size in our analyses. Univariate analyses of covariance (ANCOVA) were performed to test the three different hypotheses.

To test the evolution of the total muscle masses of the appendages compared to the total body mass (TBM), we performed the ANCOVA on the log10-transformed total mass of limbs with the TBM as a co-variate to test for difference between the two types of appendages (fish or tetrapod).

To test the shift in locomotory dominance from pectoral to pelvic appendages, we performed the ANCOVA on the log10-transformed pelvic muscle mass, ACSA and PCSA with the log10-transformed pectoral muscle mass, ACSA and PCSA as a co-variate to test the differences

between the two types of appendages.

To test the evolution of the different muscle groups within each appendage we only considered the *abductor* and *adductor superficialis/profundus* groups present both in fins and limbs. Thereby, we removed *caudofemoralis*, since this muscle is not present in all taxa and its origin remains uncertain (abaxial origin, according to Diogo et al. (2016)). We thus recalculated the total pelvic mass, ACSA and PCSA, without the *caudofemoralis*. We performed the ANCOVA on the log10-transformed group masses, ACSA and PCSA with the total mass, ACSA and PCSA of the pectoral and pelvic fins as co-variates to test the differences between the two types of appendages. For this analysis, we removed *Polypterus* and *Acipenser* from the dataset, since the *adductor profundus* muscle group is missing in the pectoral fin, and the *abductor profundus* and *adductor profundus* muscle groups are missing for the pelvic fin.

Results

Muscle anatomy

- *Muscular anatomy of the fins in actinopterygians*

The muscular anatomy of appendages is simpler in actinopterygians than sarcopterygians. As highlighted in previous studies (e.g. Diogo and Abdala, 2007, 2010; Wilhelm et al., 2015; Diogo et al., 2016; Molnar et al., 2020), it can be roughly described as formed by four muscles masses: the *abductor superficialis* and *profundus* on the external side of the fin, and the *adductor superficialis* and *profundus* on the internal side of the fin. In the teleost *Dicentrarchus*, the muscle masses are divided into several muscles for the different muscle groups. In *Polypterus* and *Acipenser*, the *adductor profundus* is not present in the pectoral fin, and the pelvic fin is only formed by the *abductor* and *adductor superficialis* muscle groups (Annex Table 3.2). All muscles originate from the pectoral or pelvic girdles and insert at the base of the fin rays. There are no extrinsic muscles of the fin.

- *Muscular anatomy of the fins in Latimeria*

In the coelacanth, the muscular anatomy is also formed by relatively few muscle groups, but the organisation is more complex, with a large number of *abductor* and *adductor superficialis* and *profundus* muscle bundles and sub-divisions. Moreover, there is a third muscle layer con-

sidered as part of *profundus* and formed by the *pronator* and *supinator* muscles. There are also some inter-mesomere muscles in the pelvic fin, the *flexor* muscles. As in *Polypterus* the pre-axial and post-axial muscles of the pelvic fin (*pterygialis cranialis, caudalis*) are present in *Latimeria*. Whereas most of the muscle bundles of the pelvic fin insert on the fin rays (79%) similar to actinopterygians, an important number of muscles insert on the endoskeletal elements of the pectoral fin (only 37% of muscles bundles insert on the fin rays) (see Huby *et al*., in prep; Chap II for more details). Whereas recent descriptions of the muscular anatomy of the pelvic fin of *Latimeria* mention a *levator lateralis* that originates on the axial skeleton (Diogo et al., 2016), we did not observe such a muscle during our dissections. On the contrary, we observed that the pelvic muscles are separated from the hypaxial muscles by a thick aponeurosis.

- *Muscular anatomy of the limbs in tetrapods*

In tetrapods, there is a large number of well-differentiated muscles compared to fishes. One major muscle of the pelvic limb is the *caudofemoralis* that takes up more than 25% of the total pelvic muscle mass in *Alligator* and *Salvator*. This muscle is the only one that is extrinsic to the girdle and limbs and has no homologous muscle on the pelvic fin of actinopterygians and coelacanths. It originates on caudal vertebrae and inserts on the proximal part of the femur and is the principal retractor of the femur.

Muscles data

- *Evolution of limb muscle mass*

The ANCOVA shows a significant effect of the total body-mass ($F(1, 5) = 637.66$; p-value < 0.001) and appendage-type (i.e. fin versus limb; $F(1, 5) = 91.87$; p-value < 0.001), but no interaction between body mass and appendage-type ($F(1, 5) = 0.810$; p-value $= 0.41$). Tetrapods have proportionally heavier appendages than fish (Fig. 3.2).

- *Pelvic vs pectoral appendages*

The ANCOVA shows a significant effect of the pectoral muscles mass ($F(1, 5) = 528.72$; $P < 0.001$) and of the appendage-type ($F(1, 5) = 9.80$; $P = 0.026$) on the pelvic muscle mass, but no interaction ($F(1, 5) = 3.80$; $P = 0.11$). A subsequent ANCOVA showed a significant effect of the pectoral muscle ACSA ($F(1, 5) = 1151.96$; $P < 0.001$) and appendage-type (F (1,

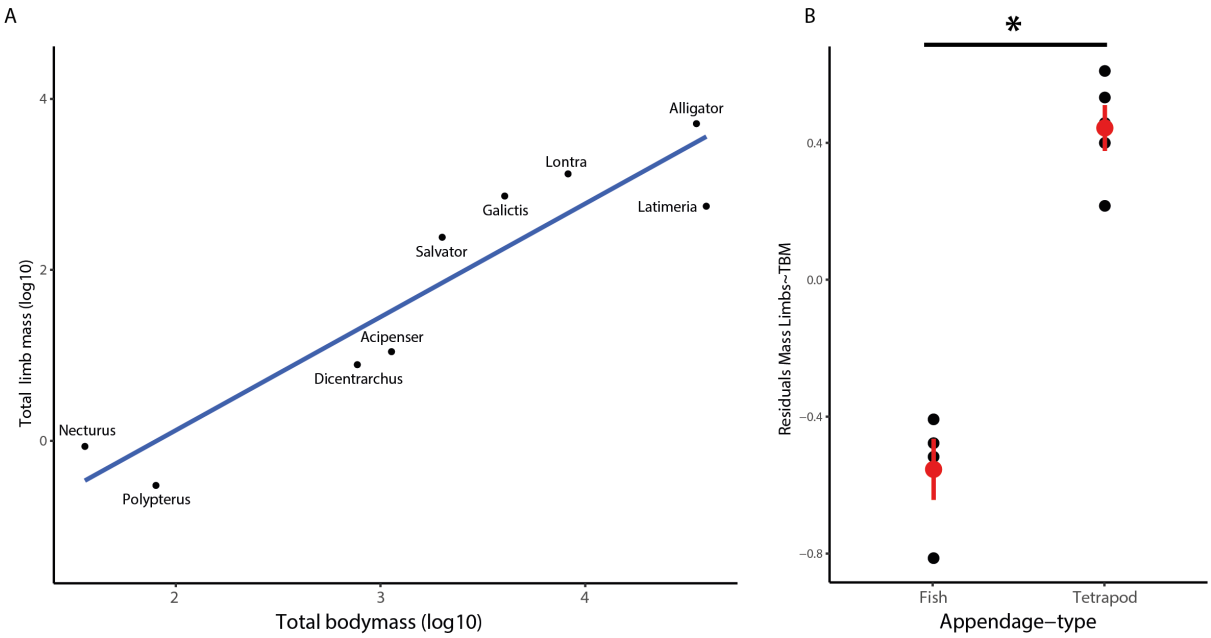

Figure 3.2: A) Regression between the $\log_{10}$-total muscle mass of the limb and the $\log_{10}$-total body mass for the different species. B) Plot of the residuals for the two types of appendages. Tetrapods limbs are relatively heavier than the fish fins. * indicates a significant effect of the appendage-type.

5) = 38.20; P = 0.0016), but no interaction (F (1, 5) = 6.56; P = 0.051). The ANCOVA on the pelvic muscle PCSA further showed a significant effect of the pectoral muscles PCSA (F (1, 5) = 526.13; P < 0.001) and appendage-type (F (1, 5) = 11.35; P = 0.02), but no interaction (F (1, 5) = 1.39; P = 0.29). In summary, independently of variation in body mass, the mass, ACSA, PCSA of the pelvic appendage in tetrapods is greater that in fishes (Fig. 3.3). Moreover, whereas in fish the pectoral fins are heavier and have a greater ACSA and PCSA than the related pelvic fins, in tetrapods hind limbs are in general heavier than forelimbs, with a more important ACSA and PCSA (Annex Fig. 3.1).

- *Muscle groups*

The ANCOVA on the different pectoral or pelvic muscle group masses shows a significant effect of the total pectoral/pelvic muscle mass and of the appendage-type (Table 3.1). Only for the *abductor profundus* group of the pelvic appendage was no difference between appendage-type detected (F (1, 3) = 7.38; P= 0.073). For all muscle groups of both the pectoral and pelvic fins interactions between the total pectoral/pelvic mass and appendage-type were non significant with the exception of the *adductor superficialis* of the pelvic appendage (F (1, 3) = 22.13; P= 0.018). In tetrapods, the *abductor superficialis* and *adductor superficialis* groups of the pectoral and pelvic limbs have a proportionally greater mass than in fishes, whereas the mass of the

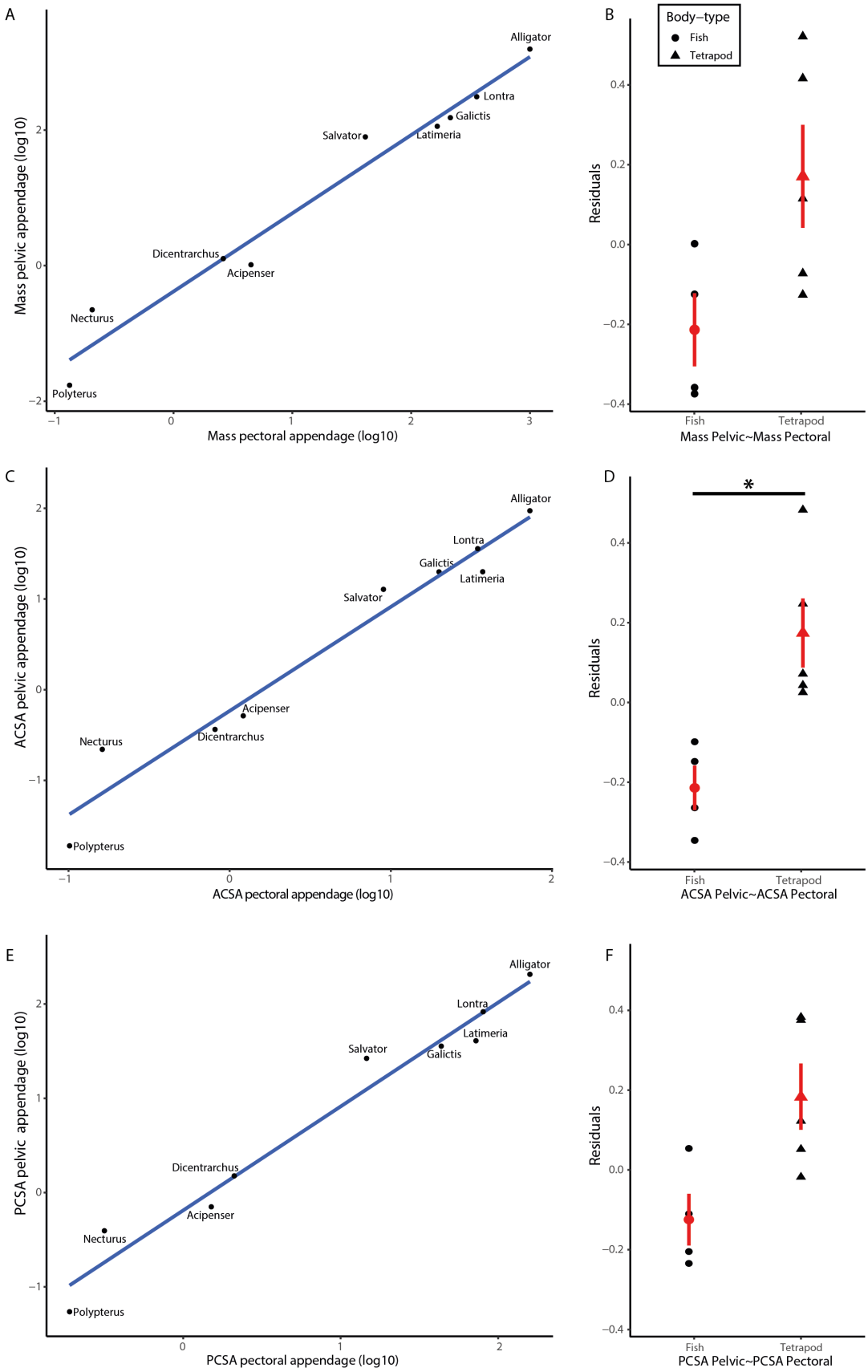

Figure 3.3: Comparison of the muscular properties (mass, ACSA, PCSA) of the pectoral and pelvic appendages. (A, C, E) Regression of the $\log_{10}$-pelvic mass, ACSA and PCSA against the $\log_{10}$-pectoral mass, ACSA and PCSA. (B, D, F) Plots of the residuals of the ANCOVA analyses of the relation between pectoral and pelvic appendages. * indicates a significant effect of the appendage-type.

adductor profundus is less important in tetrapods compared to fish (Fig. 3.4). The mass of the *abductor profundus* group develops in different ways in the pectoral and pelvic appendages, however. In tetrapods, the *abductor profundus* of the pectoral appendage is lighter in fish relative to that of the total pectoral limb. Yet, for the pelvic appendage, the two types of appendages (fin or limb) are similar in terms of the *abductor profundus* group mass.

The ANCOVA on the different pectoral and pelvic muscle groups ACSA shows in general a significant effect of the total pectoral/pelvic ACSA and of the appendage-type (Table 3.1). Only the *adductor profundus* group of the pelvic appendage shows no significant difference for the total pelvic ACSA ($F(1, 3) = 8.36$; $P = 0.063$) and the appendage-type ($F(1, 3) = 0.99$; $P = 0.39$). For most of the muscle groups, there is no interaction between the total pectoral/pelvic ACSA and the appendage-type, except for the *adductor superficialis* group of the pectoral appendage ($F(1, 3) = 14.76$; $P = 0.031$). In tetrapods, the ACSA of *abductor superficialis* and *adductor superficialis* groups relatively to the total ACSA is greater, whereas the relative ACSA of *abductor profundus* group is lower both for the pectoral and pelvic appendages, relatively to the total ACSA produced by the appendage (Fig. 3.4). The ACSA of the *adductor profundus* shows different results in pectoral and pelvic appendages. In tetrapods the ACSA of the *adductor profundus* group of the pectoral appendage relatively to the total ACSA of the pectoral appendage is less important than in fishes. For the pelvic appendage, the ACSA of the *adductor profundus* group is not different between fish and tetrapods.

The ANCOVA on the different pectoral and pelvic muscle group PCSA shows in general a significant effect of the total pectoral/pelvic muscle and the appendage-type (Table 3.1). The *adductor profundus* group of the pelvic appendage is the only group that shows no significant effect of the total pelvic PCSA ($F(1, 3) = 5.91$; $P = 0.093$) and appendage-type ($F(1, 3) = 0.44$; $P = 0.55$). For none of the muscle groups was the interaction between the total appendage PCSA and the appendage-type significant. In tetrapods, the PCSA of *abductor superficialis* and *adductor superficialis* groups is more important than in fish, whereas the PCSA of the *abductor profundus* group relatively to the total PCSA of the appendages is less important for both the pectoral and pelvic appendages (Fig. 3.4). The PCSA of the *adductor profundus* group of the pectoral appendage is less important in tetrapods than in fish. For the pelvic appendage the PCSA of the *adductor profundus* group is not different between fishes and tetrapods.

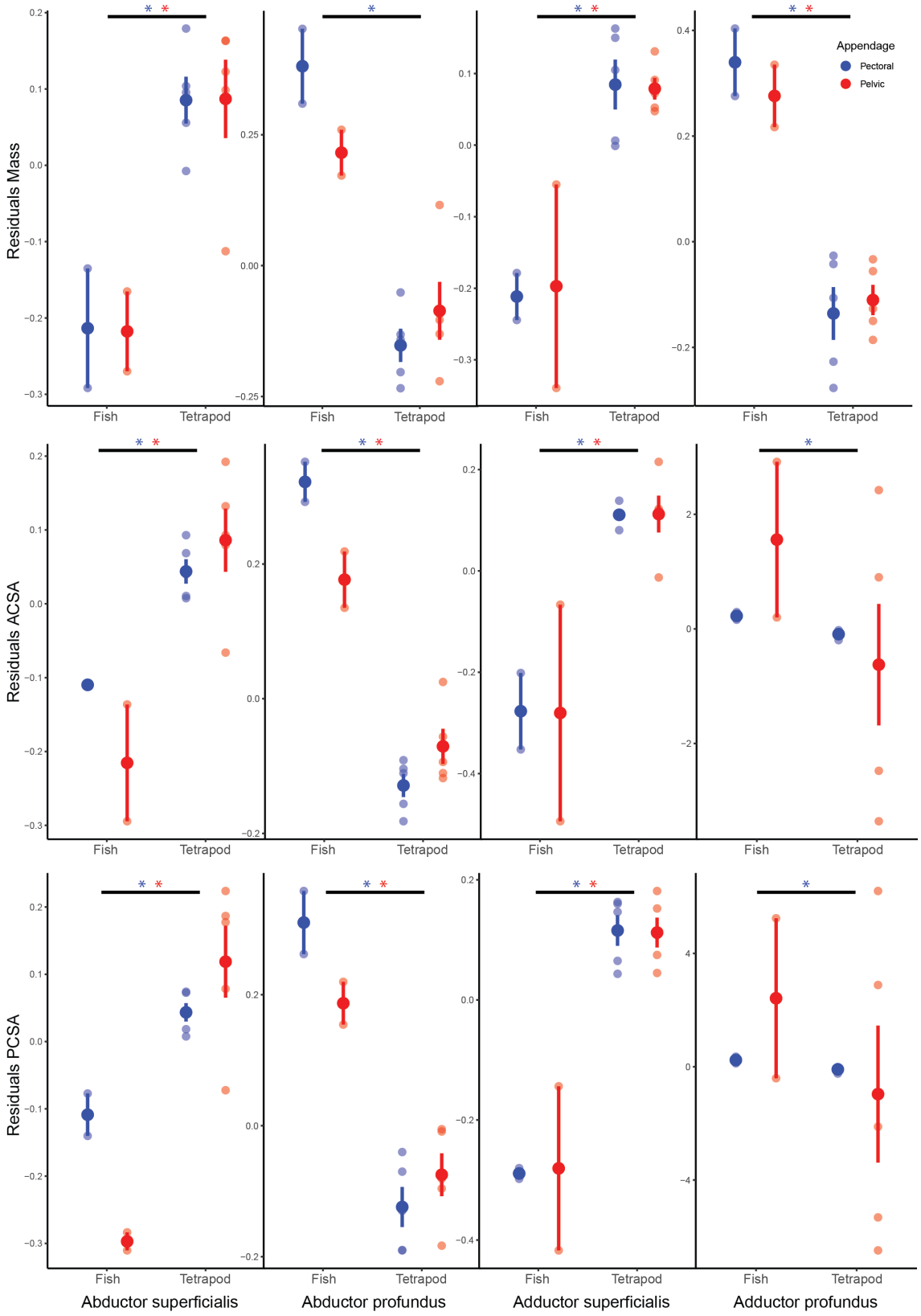

Figure 3.4: Plot of the residuals of the ANCOVA analyses for muscle mass, ACSA, and PCSA for the different muscle groups. In fish deep muscles groups are heavier and have a more important ACSA and PCSA, whereas in tetrapods the superficial muscle groups are heavier and stronger. * indicates a significant effect of the appendage type.

Table 3.1: Results of ANCOVA analyses for the different muscles groups. Grey boxes show non significant effect.

		Pectoral appendage			Pelvic Appendage		
		Mass	ACSA	PCSA	Mass	ACSA	PCSA
Abductor superficialis	Total appendage	F= 1625.243 P= 3.36e-05	F= 3356.827 P= 1.13e-05	F= 7957.070 P= 3.11e-06	F= 1180.076 P= 5.42e-05	F= 729.197 P= 1.1e-04	F= 547.916 P= 1.71e-04
	Appendage-type	F= 21.303 P= 0.019	F= 20.928 P= 0.020	F= 51.877 P= 0.006	F= 12.333 P= 0.039	F= 12.787 P= 0.037	F= 19.641 P= 0.021
	Interaction	F= 1.459 P= 0.314	F= 0.063 P= 0.818	F= 5.372 P= 0.103	F= 0.617 P= 0.324	F= 0.377 P= 0.583	F= 0.432 P= 0.558
Abductor profundus	Total appendage	F= 1972.665 P= 2.51e-05	F= 5439.380 P= 5.19e-06	F= 1977.441 P= 2.5e-05	F= 540.062 P= 1.75e-04	F= 1956.128 P= 2.54e-06	F= 984.743 P= 7.11e-05
	Appendage-type	F= 83.853 P= 0.003	F= 247.597 P=5.85e-04	F= 76.898 P= 0.003	F= 7.375 P= 0.073	F= 31.640 P= 0.011	F= 16.791 P= 0.026
	Interaction	F= 0.817 P= 0.433	F= 0.137 P= 0.736	F= 2.913 P= 0.186	F= 0.034 P= 0.865	F= 0.72 P= 0.806	F= 0.048 P= 0.841
Adductor superficialis	Total appendage	F= 1959.684 P= 2.54e-05	F= 9741.45 P= 2.29e-06	F= 1617.887 P= 3.38e-05	F= 6232.460 P= 4.48e-06	F= 542.625 P= 1.73e-04	F= 1205.170 P= 5.26e-05
	Appendage-type	F= 22.558 P= 0.018	F= 379.550 P= 2.95e-04	F= 64.923 P= 0.004	F= 75.960 P= 0.003	F= 27.651 P= 0.013	F= 58.460 P= 0.005
	Interaction	F= 1.025 P= 0.386	F= 14.760 P= 0.031	F= 0.024 P= 0.887	F= 22.130 P= 0.018	F= 8.283 P= 0.064	F= 6.79 P= 0.080
Adductor profundus	Total appendage	F= 1155.431 P= 5.6e-05	F= 2851.681 P= 1.45e-05	F= 806.628 P= 9.58e-05	F= 3482.642 P= 1.07e-05	F= 8.359 P= 0.063	F= 5.912 P= 0.093
	Appendage-type	F= 33.864 P= 0.010	F= 64.168 P= 0.004	F= 17.533 P= 0.025	F= 77.294 P= 0.003	F= 0.992 P= 0.393	F= 0.444 P= 0.553
	Interaction	F= 1.998 P= 0.253	F= 7.832 P= 0.068	F= 4.962 P= 0.119	F= 0.474 P= 0.541	F= 0.420 P= 0.563	F= 0.415 P= 0.565

Mobility

The shoulder joint of *Latimeria* has an important mobility in the three different planes with the maximum range of mobility observed for abduction/adduction (101°). In tetrapods the shoulder joint is less mobile than in *Latimeria*. *Alligator* further showed a greater mobility than *Salvator* for the abduction/adduction and protraction/retraction. The long-axis rotation of the shoulder is rather low in tetrapods (Table 3.2).

The hip joint of *Latimeria* is less mobile than the shoulder joint. The maximum range of mobility was observed for the abduction/adduction movement (50°). The protraction/retraction as well long-axis rotation is more limited (32 and 29°) due to the pre-axial radial 0 element of the pelvic fin (see Huby *et al*, in prep; Chap II). For *Salvator* the hip has a greater mobility in the three planes compared to *Latimeria* with the maximum range of mobility observed for protraction/retraction (69°).

Table 3.2: Mobility of the different joints

		Abduction/Adduction	Protraction/Retraction	Pronation/Supination
Shoulder	*Latimeria*	102° (± 17°)	93° (± 7°)	90° (± 7°)
	Salvator	74° (± 10°)	54° (± 3°)	46° (± 2°)
	Alligator	80° (± 4°)	89° (± 9°)	33° (± 4°)
Hip	*Latimeria*	50° (± 1°)	32° (± 5°)	29° (± 4°)
	Salvator	59° (± 4°)	69° (± 3°)	33° (± 2°)
	Alligator	*na*	*na*	*na*
		Abduction/Adduction	Flexion/Extension	Pronation/Supination
Elbow	*Latimeria*	54° (± 5°)	69° (± 9°)	68° (± 23°)
	Salvator	14° (± 3°)	70° (± 3°)	51° (± 3°)
	Alligator	0°	99° (± 2°)	36° (± 1°)
Knee	*Latimeria*	22° (± 1°)	31° (± 6°)	24° (± 3°)
	Salvator	0°	68° (± 4°)	31° (± 4°)
	Alligator	0°	63° (± 3°)	13° (± 2°)

The second joint of the pectoral fin of *Latimeria*, corresponding to the elbow joint in tetrapods (Miyake et al., 2016), is less mobile than the shoulder jointand shows a maximum range of mobility in flexion/extension and for long-axis rotation (respectively 69° and 68° vs 55° for abduction/adduction). In tetrapods the abduction/adduction mobility of the elbow is very constrained since there is no mobility for *Alligator* and only a mobility of 14° for *Salvator*. The mobility of flexion/extension of the elbow is important (*Alligator*: 99°, *Salvator*: 70°). The long-axis rotation is less important for tetrapods compared to that observed in *Latimeria* (respectively 36° and 51°, versus 68° for *Latimeria*).

The second joint of the pelvic fin of *Latimeria* corresponding to the knee joint in tetrapods, is less mobile than the related joint of the pectoral fin and shows a maximum range of mobility of 31° for the flexion/extension movement. The rotational movement as well as the abduction/adduction movement of the knee is limited (respectively 24° and 22°). In *Alligator* and *Salvator*, the knee permits no abduction/adduction movement. The maximum range of mobility was observed for the flexion/extension with a slightly higher mobility for *Salvator* (68° vs 63° for *Alligator*). In *Salvator*, the rotational movement of the knee is also less important than for related joint in the pectoral limb (31° vs 51° for the elbow), and is very limited in *Alligator* (13°).

Discussion

Increase of the size of appendages

The dramatic enlargement of the appendicular skeleton relative to the body size during the evolutionary history of tetrapodomorphs has been interpreted as an innovation associated with the fin-to-limb transition (Andrews and Westoll, 1970).When taking into account variation in body mass the comparison of the respective muscle masses of the appendages corroborates this hypothesis. Here, the term "fish" is used to designate vertebrate species with fins - actinopterygians, coelacanth and lungfish - independent from their phylogenetic position. In fish, the muscle mass of appendages is less important than in tetrapods (Fig. 3.2). According to Andrews and Westoll (1970), the size difference between fins and limbs is probably due to their different functions. In fishes, the locomotion and propulsion are mainly produced by the caudal fin and lateral undulation of the body, and not by the paired fins (Bainbridge, 1963; Lighthill, 1971; Webb, 1982; Lauder, 2000; Coates et al., 2002; Boisvert, 2005; Don et al., 2013). In terrestrial tetrapods, limbs support and move the body against gravity and permit locomotion by walking, running, climbing, or jumping. However, early tetrapods (i.e., first animals with limbs and digits) such as *Acanthostega* or *Ichthyostega* were not terrestrial animals but lived in aquatic environment (Coates and Clack, 1995) and probably could not use their limbs for fully terrestrial locomotion (Pierce et al., 2012). Finned animals such as the Devonian elpistostegalian *Tiktaalik* lived in shallow-water and subaerial habitats and their fins are thought to be limb-like fins allowing body mass support (Daeschler et al., 2006; Shubin et al., 2006; Hohn-Schulte et al., 2013). It has been demonstrated that the endoskeleton of the pectoral fin of *Polypterus* becomes longer and more robust in terrestrial environments due to the increase use of the pectoral fin for locomotion and to lift the anterior part of the body above the substrate (Standen et al., 2014; Du and Standen, 2020). Terrestrial walking requires greater forces to move the ap-

pendages, compared to swimming (Du and Standen, 2017). In benthic anglerfishes that 'walk' on the substrate instead of swimming, the pectoral fins are more robust and have larger and stronger muscles relative to their body size, compared to the pelagic anglerfishes that swim (Dickson and Pierce, 2019). These more robust and stronger fins are essential to support the larger pushing forces against the substrate that are necessary for the locomotion. Thus, larger muscles, allow to produce greater forces needed to support the body and to move on land.

Shift from pectoral to pelvic appendage dominance

The fin-to-limb transition has been suggested to be marked by a shift from pectoral to pelvic dominance in size and importance during locomotion (Coates et al., 2002; Boisvert, 2005; Don et al., 2013). The muscular anatomy of fins and limbs tends to confirm this hypothesis, since the muscular mass of the pelvic fin is smaller than in the pectoral fin, whereas the muscular mass of hind limb is more important than in the forelimb (Fig. 3.3; Annex Fig. 3.1). The total appendage cross-sectional area follows the same trend. Since The CSA is a good proxy for maximum force produced by a muscle, the hind limb muscles of tetrapods are much stronger than those of the pelvic fins of fishes, and also stronger than the forelimbs. For crocodylians including *Alligator* it has suggested that stronger hind limb muscles are indicative of a more important body weight support on the pelvic limbs compared to the pectoral limbs (Allen et al., 2010). Heavier and stronger hind versus forelimb muscles have been demonstrated in different groups of tetrapodsincluding *Anolis* lizards, the crocodylians *Alligator* and *Crocodylus*, and the horse (e.g. Payne et al., 2005; Herrel et al., 2008; Allen et al., 2010, 2015). In fish, the propulsive force for fast swimming, fast turning and acceleration is mostly generated by the caudal fin and the axial muscles (Bainbridge, 1963; Lighthill, 1971; Webb, 1982; Lauder, 2000; Coates et al., 2002; Boisvert, 2005; Don et al., 2013). The pectoral fins are important for propulsion at low-speed and are actively recruited for different types of maneuvers including deceleration, turning or station holding (e.g. Wilga and Lauder, 1999; Lauder, 2000; Drucker and Lauder, 2003). Pelvic fins, which are smaller and less powerful than the pectoral fins, have a different function than the hind limbs in tetrapods. In fish the pelvic fins play a role in steady swimming and maneuvering (Webb, 1982; Don et al., 2013; Standen, 2008). It is interesting to note that in tetrapods with a sprawling limb posture (salamanders, lizards, crocodiles), one of the most important muscles of the pelvic limb in term of mass and intrinsic force is the *caudofemoralis* muscle, an extrinsic muscle that is the major limb retractor (Reilly and Elias, 1998; Blob and Biewener, 2001; Russel et al., 2001; Molnar et al., 2014; McInroe et al., 2016; Pierce et al., 2020). This muscle originates from the ventral abaxial musculature, but its homology with mus-

cles in sarcopterygian fish remains debated.

In early tetrapodomorph fishes such as the Devonian *Eusthenopteron* or *Panderichthys*, pelvic appendages are smaller than the pectoral ones and locomotor forces were likely mainly produced by body flexion and caudal fin movements with the pectoral fin generating mainly forces during braking or maneuvering as in actinopterygian fishes (Andrews and Westoll, 1970; Boisvert, 2005; Shubin et al., 2014). In the Devonian *Tiktaalik*, one of the closest fossil relatives to tetrapods, the relatively large pectoral and pelvic appendages are of similar size (Shubin et al., 2014). Consequently, this species has been suggested to be a functionally transitional stage between the "front-wheel drive" and caudal propulsion of fishes and the "rear-wheel drive" of tetrapods. However, the pelvic girdle of *Tiktaalik* is not fused to the vertebrae, and it has been suggested that the pelvic fins did not allow weight bearing (Shubin et al., 2014), whereas the pectoral fins present features that likely permitted a limbed-like support of the body away from the substrate (Daeschler et al., 2006; Shubin et al., 2006). Thus, the ancestrally larger muscular mass present in the anterior appendages might have been used initially for body support and to lift the head of the substrate for feeding (Van Wassenbergh et al., 2006) or vigilance, rather than allowing terrestrial locomotion. The shift of mass and intrinsic force from the anterior to posterior appendages in early tetrapodomorphs seems to occur before the shift from "front-wheel drive" to "rear-wheel drive" in locomotion. In amphibious tetrapods such as crocodiles or salamanders that have strong pectoral and pelvic limbs, propulsive forces are produced by the undulation of the trunk and the tail in water whereas the appendages permit the stabilization of the body (Fish, 1984a; Frolich and Biewener, 1992; D'Août and Aerts, 1997; Seebacher et al., 2003). The undulation of the body during terrestrial locomotion remains however important in tetrapods since its permits to increase the stride length (Ritter, 1992; Reilly and Elias, 1998). Since aquatic propulsion by means of tail movements is more efficient and less energetically expensive than the limb-based propulsion by paddling (Fish, 1984b, 1996), early tetrapods with an aquatic life-style such as *Acanthostega* or *Ichthyostega* likely used the tail undulations to produced propulsive force. The limbs of early tetrapods are, in contrast thought to be used to move through vegetation (Coates and Clack, 1995) and/or for the stabilization of the body.

Distribution of muscle groups in fins and limbs

The distribution of appendicular muscles groups is different in fish and tetrapods. The *abductor* and *adductor superficialis* groups are heavier and stronger in tetrapods than in fish, both in the pectoral and pelvic appendages. Similarly, the deep muscle groups are proportionally

less heavy (except for the *abductor profundus* group in the pelvic appendage) and less forceful (except for the *adductor profundus* in the pelvic appendage) in tetrapods. Thus, during the fin-to-limb transition, there was a shift in the distribution of the muscle groups with a reduction of the deep muscle groups in tetrapods and the development of the superficial muscle groups in term of mass and strength. In our analyses we considered only four different muscle groups, *i.e. abductor/adductor superficialis/profundus* groups, since these are present in both sarcopterygians and actinopterygians (Diogo et al., 2016). However, as discussed above, the *caudofemoralis* muscle of the pelvic limb of tetrapods, excluded from the analyses because it has no homologous muscle in the pelvic fin of fishes, has an important contribution to the motion of the hind limb and represents a large part of the total pelvic muscle mass. However, taking into account the *caudofemoralis* in our analyses did not qualitatively change the results (see Annex Table 3.3).

Homologies between tetrapod and fish muscles show that most of the tetrapod appendicular muscles belong to the superficial groups (Diogo et al., 2016; Molnar et al., 2018, 2020). However, the distribution of the mass and intrinsic force of appendicular muscles groups is different in fish with the deep groups being more important than the superficial groups, especially for the pectoral fin (see Annex Tables 3.4-3.5). *Polypterus* and *Acipenser* were removed from the analysis since some of the muscle groups were absent and as such it is hard to derive general trends for the muscular anatomy of fins. In our dissections, we only found one *adductor* muscle group in the pectoral fin of *Polypterus*, but it has been shown that this muscle can be separated into a superficial and a deep layer (Wilhelm et al., 2015). In the sturgeon *Acipenser*, the pectoral fins are not oriented vertically as typically observed in actinopterygians, but in a horizontal orientation. In contrast to most actinopterygians the pectoral fins in *Acipenser* do not permit the production of thrust for propulsion or maneuvres, yet aid in body orientation by re-orienting the posterior part of the fin (Wilga and Lauder, 1999). This could explain the absence of some muscle groups in fin of these animals.

The distribution of muscle groups on the pectoral muscular anatomy of fishes of the Labroidei is similar to that of fishes of our study with superficial muscles that are less developed in mass than deep muscles groups (Thorsen and Westneat, 2005). It has been proposed for Labroidei that the disparity in muscle masses of the pectoral fin may be attributed to specialized locomotor behaviours and the production of the thrust for propulsion during swimming. In anglerfishes, pelagic species have deep muscles groups that are more developed and stronger than the

superficial muscles groups (Dickson and Pierce, 2019) despite the fact that they are 'walking' species. Thus, the distribution of the muscular properties in the appendages might not be dependent of the type of locomotion (i.e. walking versus swimming) but rather on phylogenetical heritage. However, more data on a greater diversity of species are needed to explore these questions further.

Joint mobility

The articular surface of the pectoral and pelvic girdles with their respective limbs, called glenoid surface and acetabulum, have a different morphology in *Latimeria* compared to tetrapods. In the coelacanth, the glenoid surface and the acetabulum are convex, and posteriorly oriented (Millot and Anthony, 1958; Mansuit et al., 2020a,b). In tetrapods, both the glenoid surface and the acetabulum are concave, with a posterolateral orientation for the glenoid surface, and a lateral orientation for the acetabulum (e.g. Coates and Ruta, 2007; Boisvert et al., 2013). The change in morphology from a convex to concave articular surface appeared early in the tetrapodomorph clade, since it is already present in Rhizodontida, the most basal group of tetrapodomorphs and in osteolepiforms such as *Eusthenopteron* (e.g. Andrews and Westoll, 1970; Johanson and Ahlberg, 2001; Coates and Ruta, 2007). The different morphology of the articular surfaces, associated with the orientation change, impacts the mobility of the limbs. Our results suggest that the pectoral fin of *Latimeria* has a more important mobility at the shoulder in the three planes compared to tetrapods (Table 3.2). We suggest that a convex articular surface may limit the mobility of the appendages. However, in *Latimeria* the mobility of the hip joint is more limited than that of the pectoral fin due to the pre-axial radial 0 element (Chap. II; Huby *et al*, *in prep*). As for *Latimeria*, the acetabulum of lungfish such as *Neoceratodus* is convex (Coates and Ruta, 2007). The study of the mobility of its pelvic fins will be important to compare its mobility with that of *Latimeria*. We suggest that the mobility of the pelvic fin in *Neoceratodus* will be greater since there is no pre-axial radial 0 and the acetabulum is convex. Similar to the mobility of the pectoral fin of the coelacanth, we also predict that the mobility of the pectoral fin in lungfish is greater than that observed in tetrapods since the glenoid is convex. It is possible that the "reorientation" of the articular surfaces of the girdles also impact the mobility of the appendages, but since this reorientation on a more lateral side occurred in early tetrapods (Coates and Ruta, 2007; Boisvert et al., 2013), it is not possible to test the change of mobility independently of the type of articular surface (convex *vs* concave).

Whereas in *Latimeria* the joint mobility in the three planes is similar both for the elbow and

the knee, this is not the case in tetrapods. Indeed, the abduction/adduction is absent, or very limited (14° for the elbow of *Salvator*), and the flexion/extension capacity of the two joints is far greater than their rotational mobility (Table 3.2). The elbow joint is formed by the humerus which articulates with both the radius and the ulna. Consequently, this articulation can be regarded a hinge with limited lateral movement in amniotes tetrapods (Sigurdsen and Bolt, 2009; Evans and de Lahunta, 2013). In amniotes, the oleocranon fossa of the humerus that receives the intercotylar or anconeal process, associated with thick ligaments, limits the lateral mobility of the elbow (i.e. abduction/adduction) (e.g. Evans and de Lahunta, 2013). However, in extant lissamphibians, the elbow joint works rather as a ball-and-socket joint rather than a hinge, and the lateral mobility of this joint is thus more important than in amniotes (Sigurdsen and Bolt, 2009). In the coelacanth the "elbow joint" cannot be regarded as a hinge, but is rather a ball-and-socket joint formed by the first and second mesomeres. This explains the greater mobility in *Latimeria* than in tetrapods. Similarly, the knee joint of tetrapods works as a hinge, with no lateral mobility permitted (Rewcastle, 1980, 1983). This reduced mobility is due to the different ligaments involved in the joint and the patella (Rewcastle, 1980; Evans and de Lahunta, 2013), when the joint is fully extended. However, both the tegu lizard and the alligator have a sprawling posture and do not have elbow and knee fully extended. In this sprawling posture the joints can have abduction/adduction movements due to the gliding and rolling motion of the bones involved in the joints (Landsmeer, 1983; Dye, 1987). The "knee joint" of *Latimeria* presents a small abduction/adduction mobility, less important than for the corresponding joint in the pectoral fin. This difference in mobility is attributed to the arc-shaped morphology of the mesomeres, as well as the presence of large pre-axial radial elements that limit the latero-medial mobility of the joint (see Chapter II).

The mobility of the joints was also studied in the early tetrapod *Ichthyostega* (Pierce et al., 2012). The study showed that the shoulder mobility of *Ichthyostega* is more limited compared to different tetrapods used in the study. However for the hip, only the rotational mobility is restricted in *Ichthyostega* compared to tetrapods. The abduction/adduction mobility of the elbow seems more restricted in *Ichthyostega*, compared to other tetrapods, except for the seal and the otter, in which this movement is highly restricted. The mobility in the two other planes is similar in *Ichthyostega* and tetrapods. For the knee, *Ichthyostega* presents a less important mobility for the flexion/extension, but a similar mobility in the two other planes compared to the tetrapods examined. However, these results have to be interpreted with caution. Indeed, the joint mobility was calculated based on virtual models, and the role of the ligaments that may restrict

the joint mobility was not taken into account. Consequently, the mobility may be overestimated compared to the data presented in this study. Moreover, since our mobility measurement was made on formaldehyde-fixed specimens (which may stiffen the ligaments and joints) our results might underestimate the real mobility of the different joints.

Conclusion

Despite being a preliminary study, the present work shows promising results on the evolution of the muscular anatomy and function of the appendages during the fin-to-limb transition. The general increase of the total muscular mass of the limbs relative to the body size observed in tetrapods supports observations on the skeletal elements in the fossil record. These larger and heavier appendages are also stronger, associated with a different role of the fins and limbs. Indeed, in fishes, the propulsion is mainly produced by the lateral undulation of the body, whereas the fins are more used as control structures. In terrestrial tetrapods, the limbs and their muscles need to produce more force to support the body weight and generate propulsive forces, associated with a more robust endoskeleton.

The suggested shift in locomotion from an anterior to posterior driven system, as suggested by changes in the skeletal anatomy during the fin-to-limb transition is also corroborated by the muscle architecture data. Indeed, whereas in fishes, pectoral fins have heavier and stronger muscles than the pelvic fins; in tetrapods, the hind limbs are relatively heavier and stronger. However, even if the hind limbs produce the main propulsive force, the forelimbs always have an important role in body support and locomotion. Finally, we show that there is a shift in the distribution of the muscle groups during the fin-to-limb transition. In terrestrial tetrapods, it is mainly the superficial muscles groups that contribute to the over muscular mass and force production of the limbs. This shift in the distribution of the muscular properties in appendages seems to be due to a phylogenetic heritage, rather than to a specific functional role of the muscle groups.

The study of the evolution of joint mobility in sarcopterygians shows that the shoulder in the coelacanth is more mobile that of tetrapods, possibly linked with its convex glenoid articulation. The hip of the coelacanth, that also presents a convex articular surface, has a lower mobility than that of tetrapods, however. This difference in mobility is attributed to the presence of the pre-axial radial 0 element positioned against the pelvic girdle and reducing limb movements. To test if a higher mobility is associated with a convex articular surface it is necessary to examine lungfish, the only other sarcopterygians with convex glenoid and acetabulum articulation. Our data also show that the elbow and knee in tetrapods have limited mobility for the abduc-

tion/adduction (lateral mobility of the joints), linked with the ligaments and the joint morphology. However, in natural position, lateral mobility is possible associated with the gliding and rolling movements of the bones involved in the joint. It is necessary to complete our dataset on joint mobility since only three species are included for now.

Acknowledgements

We thank C. Bens and A. Verguin of the Collections de Pièces anatomiques en Fluides of the MNHN de Paris for access to the specimens for dissections. We thank the Aquarium de la Porte Dorée for providing the *Alligator* for dissection, B. De Thoisy for the *Galicitis* and *Lontra* specimens and Anne-Claire Fabre for allowing us to use the data on *Galictis* muscles used in the chapter. We are grateful to Christine Böhmer, Maxime Taverne and Colline Brassard for their help with the statistical analyses. The MNHN gives access to the collections in the framework of the RECOLNAT national Research Infrastructure. This work was supported by a grant from Agence Nationale de la Recherche in the LabEx ANR-10-LABX-0003-BCDiv, program 'Investissements d'avenir' no ANR-11-IDEX-0004-02.

Bibliography

Ahlberg, P. E. (1989). Paired fin skeletons and relationships of the fossil group Porolepiformes (Osteichthyes: Sarcopterygii). *Zoological Journal of the Linnean Society*, 96(2):119–166.

Ahlberg, P. E., Clack, J. A., and Blom, H. (2005). The axial skeleton of the Devonian tetrapod *Ichthyostega*. *Nature*, 437(7055):137–140.

Allen, V. R., Elsey, R. M., Jones, N., Wright, J., and Hutchinson, J. R. (2010). Functional specialization and ontogenetic scaling of limb anatomy in *Alligator mississippiensis*. *Journal of Anatomy*, 216:423–445.

Allen, V. R., Molnar, J. L., Parker, W., Pollard, A., Nolan, G., and Hutchinson, J. R. (2015). Comparative architectural properties of limb muscles in Crocodylidae and Alligatoridae and their relevance to divergent use of asymmetrical gaits in extant Crocodylia. *Journal of Anatomy*, 225:569–582.

Andrews, S. M. and Westoll (1970). The Postcranial Skeleton of *Eusthenopteron foordi* Whiteaves. *Earth and Environmental Science Transactions of the Royal Society of Edinburgh*, 68(9):207–329.

Antón, S. C. (1999). Macaque Masseter Muscle: Internal Architecture, Fiber Length and Cross-Sectional Area. *International Journal of Primatology*, 20(3):441–462.

Bainbridge, R. (1963). Caudal Fin and Body Movement in the Propulsion of some Fish. *Journal of Experimental Biology*, 40(1):23–56.

Blob, R. W. and Biewener, A. A. (2001). Mechanics of limb bone loading during terrestrial locomotion in the green iguana (*Iguana iguana*) and American alligator (*Alligator mississippiensis*). *The Journal of Experimental Biology*, 204(6):1099–1122.

Boisvert, C. A. (2005). The pelvic fin and girdle of *Panderichthys* and the origin of tetrapod locomotion. *Nature*, 438(7071):1145–1147.

Boisvert, C. A., Joss, J. M., and Ahlberg, P. E. (2013). Comparative pelvic development of the axolotl (*Ambystoma mexicanum*) and the Australian lungfish (*Neoceratodus forsteri*): conservation and innovation across the fish-tetrapod transition. *EvoDevo*, 4(3):1–19.

Boisvert, C. A., Mark-Kurik, E., and Ahlberg, P. E. (2008). The pectoral fin of *Panderichthys* and the origin of digits. *Nature*, 456(7222):636–638.

Brazeau, M. D. and Ahlberg, P. E. (2006). Tetrapod-like middle ear architecture in a Devonian fish. *Nature*, 439(7074):318–321.

Carroll, R. L., Irwin, J., and Green, D. M. (2005). Thermal physiology and the origin of terrestriality in vertebrates. *Zoological Journal of the Linnean Society*, 143(3):345–358.

Clack, J. A. (2012). *Gaining Ground, Second Edition: The Origin and Evolution of Tetrapods*. Indiana University Press, Bloomington.

Coates, M. I. (1995). Fish fins or tetrapod limbs - a simple twist of fate ? *Current Biology*, 5(8):844–848.

Coates, M. I. and Clack, J. A. (1995). ROMER's gap: tetrapod origins and terrestriality. *Bulletin du Museum national d'Histoire naturelle. Section C, Sciences de la Terre, paléontologie, géologie, minéralogie*, 17(1-4):373–388.

Coates, M. I., Jeffery, J. E., and Ruta, M. (2002). Fins to limbs: What the fossils say. *Evolution & Development*, 4(5):390–401.

Coates, M. I. and Ruta, M. (2007). Skeletal Changes in the Transition from Fins to Limbs. In Hall, B. K., editor, *Fins Into Limbs: Evolution, Development, and Transformation*, chapter Chapter 2, pages 15–38. Chicago, the univer edition.

Cole, N. J., Hall, T. E., Don, E. K., Berger, S., Boisvert, C. A., Neyt, C., Ericsson, R., Joss, J., Gurevich, D. B., and Currie, P. D. (2011). Development and evolution of the muscles of the pelvic fin. *PLoS Biology*, 9(10):16–18.

Daeschler, E. B., Shubin, N. H., and Jenkins Jr., F. A. (2006). A Devonian tetrapod-like fish and the evolution of the tetrapod body plan. *Nature*, 440:757–763.

D'Août, K. and Aerts, P. (1997). Kinematics and efficiency of steady swimming in adult axolotls (Ambystoma mexicanum). *Journal of Experimental Biology*, 200(13):1863–1871.

Dickson, B. V. and Pierce, S. E. (2019). How (and why) fins turn into limbs: insights from anglerfish. *Earth and Environmental Science Transactions of the Royal Society of Edinburgh*, 109:87–103.

Diogo, R. and Abdala, V. (2007). Comparative Anatomy, Homologies and Evolution of the Pectoral Muscles of Bony Fish and Tetrapods: A New Insight. *Journal of Morphology*, 268:504–517.

Diogo, R. and Abdala, V. (2010). *Muscles of Vertebrates: Comparative Anatomy, Evolution, Homologies and Development*. Crc press edition.

Diogo, R., Johnston, P., Molnar, J. L., and Esteve-Altava, B. (2016). Characteristic tetrapod musculoskeletal limb phenotype emerged more than 400 MYA in basal lobe-finned fishes. *Scientific Reports*, 6:1–9.

Don, E. K., Currie, P. D., and Cole, N. J. (2013). The evolutionary history of the development of the pelvic fin/hindlimb. *Journal of Anatomy*, 222:114–133.

Drucker, E. G. and Lauder, G. V. (2003). Function of pectoral fins in rainbow trout: behavioral repertoire and hydrodynamic forces. *The Journal of Experimental Biology*, 206:813–826.

Du, T. Y. and Standen, E. M. (2017). Phenotypic plasticity of muscle fiber type in the pectoral fins of *Polypterus senegalus* reared in a terrestrial environment. *The Journal of Experimental Biology*, 220(19):3406–3410.

Du, T. Y. and Standen, E. M. (2020). Terrestrial acclimation and exercise lead to bone functional response in *Polypterus* pectoral fins. *Journal of Experimental Biology*.

Dye, S. (1987). An Evolutionary Perspective of the Knee. *Journal of Bone and Joint Surgery*, 69(7):976–983.

Ercoli, M. D., Álvarez, A., Stefanini, M. I., Busker, F., and Morales, M. M. (2015). Muscular Anatomy of the Forelimbs of the Lesser Grison (*Galictis cuja*), and a Functional and Phylogenetic Overview of Mustelidae and Other Caniformia. *Journal of Mammalian Evolution*, 22:57–91.

Evans, H. E. and de Lahunta, A. (2013). *Miller's Anatomy of the Dog - Fourth Edition*. Elsevier Inc., St. Louis, Missouri.

Fish, F. E. (1984a). Kinematics of Undulatory Swimming in the American Alligator. *Copeia*, 1984(4):839–843.

Fish, F. E. (1984b). Mechanics, power output and efficiency of the swimming muskrat (*Ondatra zibethicus*). *Journal of Experimental Biology*, 110:183–201.

Fish, F. E. (1996). Transitions from drag-based to lift-based propulsion in mammalian swimming. *American Zoologist*, 36(6):628–641.

Freitas, L. M., Pereira, D. K. S., Pereira, K. F., dos Santos, O. P., and Lima, F. C. (2017). Muscular anatomy of the pectoral girdle and forelimb of *Iguana i. iguana* (Squamata: Iguanidae). *Bioscience Journal*, 33(5):1284–1294.

Frolich, B. Y. L. M. and Biewener, A. A. (1992). Kinematic and Electromyographic Analysis of the functional role of the body axis during Terrestrial and Aquatic Locomotion in the Salamander *Ambystoma Tigrinum*. *Journal of Experimental Biology*, 162(1):107–130.

Herrel, A., Van Wassenbergh, S., Wouters, S., Adriaens, D., and Aerts, P. (2005). A functional morphological approach to the scaling of the feeding system in the African catfish, *Clarias gariepinus*. *Journal of Experimental Biology*, 208(11):2091–2102.

Herrel, A., Vanhooydonck, B., Porck, J., and Irschick, D. J. (2008). Anatomical Basis of Differences in Locomotor Behavior in *Anolis* Lizards : A Comparison Between Two Ecomorphs. *Bulletin of the Museum of Comparative Zoology*, 159(4):213–238.

Hohn-Schulte, B., Preuschoft, H., Witzel, U., and Distler-Hoffmann, C. (2013). Biomechanics and functional preconditions for terrestrial lifestyle in basal tetrapods, with special consideration of *Tiktaalik roseae*. *Historical Biology*, 25(2):167–181.

Janvier, P. (1996). *Early vertebrates*. Oxford University Press, Oxford.

Johanson, Z. and Ahlberg, P. E. (2001). Devonian rhizodontids and tristichopterids (Sarcopterygii; Tetrapodomorpha) from East Gondwana. *Transactions of the Royal Society of Edinburgh, Earth Sciences*, 92:43–74.

Johanson, Z., Joss, J., Boisvert, C. A., Ericsson, R., Sutija, M., and Ahlberg, P. E. (2007). Fish Fingers : Digit Homologues in Sarcopterygian Fish Fins. *Journal of Experimental Zoology Part B: Molecular and Developmental Evolution*, 308:757–768.

Joss, J. and Longhurst, T. (2001). Lungfish paired fins. In Ahlberg, P. E., editor, *Major Events in Early Vertebrate Evolution*, chapter 21, pages 370–376. London, taylor & f edition.

King, H. M. and Hale, M. E. (2014). Musculoskeletal morphology of the pelvis and pelvic fins in the lungfish *Protopterus annectens*. *Journal of Morphology*, 275(4):431–441.

Landsmeer, J. M. (1983). The mechanism of forearm rotation in *Varanus exanthematicus*. *Journal of Morphology*, 175(2):119–130.

Lauder, G. V. (2000). Function of the caudal fin during locomotion in fishes: kinematics, flow visualization, and evolutionary patterns. *American Zoologist*, 40:101–122.

Lighthill, M. J. (1971). Large-amplitude elongated-body theory of fish locomotion. *Proceedings of the Royal Society of London. Series B. Biological Sciences*, 179:125–138.

Loeb, G. and Gans, C. (1986). *Electromyography for experimentalists*. Chicago, the univer edition.

Mansuit, R., Clément, G., Herrel, A., Dutel, H., Tafforeau, P., Santin, M. D., and Herbin, M. (2020a). Development and growth of the pectoral girdle and fin skeleton in the extant coelacanth *Latimeria chalumnae*. *Journal of Anatomy*, 236(3):493–509.

Mansuit, R., Clément, G., Herrel, A., Dutel, H., Tafforeau, P., Santin, M. D., and Herbin, M. (2020b). Development and growth of the pelvic fin in the extant coelacanth *Latimeria chalumnae*. *The Anatomical Record*.

McInroe, B., Astley, H. C., Gong, C., Kawano, S. M., Schiebel, P. E., Rieser, J. M., Choset, H., Blob, R. W., and Goldman, D. I. (2016). Tail use improves performance on soft substrates in models of early vertebrate land locomotors. *Science*, 353(6295):154–158.

Mendez, J. and Keys, A. (1960). Density and composition of mammalian muscle. *Metabolism: Clinical and Experimental*, 9:184–188.

Millot, J. and Anthony, J. (1958). *Anatomie de Latimeria chalumnae - Tome I: Squelette, Muscles et Formations de soutien*. CNRS, Paris, cnrs edition.

Miyake, T., Kumamoto, M., Iwata, M., Sato, R., Okabe, M., Koie, H., Kumai, N., Fujii, K., Matsuzaki, K., Nakamura, C., Yamauchi, S., Yoshida, K., Yoshimura, K., Komoda, A., Uyeno, T.,

and Abe, Y. (2016). The pectoral fin muscles of the coelacanth *Latimeria chalumnae*: Functional and evolutionary implications for the fin-to-limb transition and subsequent evolution of tetrapods. *The Anatomical Record*, 299(9):1203–1223.

Molnar, J. L., Diogo, R., Hutchinson, J. R., and Pierce, S. E. (2018). Reconstructing pectoral appendicular muscle anatomy in fossil fish and tetrapods over the fins-to-limbs transition. *Biological Reviews*, 93:1077–1107.

Molnar, J. L., Diogo, R., Hutchinson, J. R., and Pierce, S. E. (2020). Evolution of Hindlimb Muscle Anatomy Across the Tetrapod Water-to-Land Transition, Including Comparisons With Forelimb Anatomy. *Anatomical Record*, 303(2):218–234.

Molnar, J. L., Johnston, P. S., Esteve-Altava, B., and Diogo, R. (2017). Musculoskeletal anatomy of the pelvic fin of *Polypterus*: implications for phylogenetic distribution and homology of pre- and postaxial pelvic appendicular muscles. *Journal of Anatomy*, 230:532–541.

Molnar, J. L., Pierce, S. E., and Hutchinson, J. R. (2014). An experimental and morphometric test of the relationship between vertebral morphology and joint stiffness in Nile crocodiles (*Crocodylus niloticus*). *Journal of Experimental Biology*, 217(5):758–768.

Nakamura, T., Gehrke, A. R., Lemberg, J., Szymaszek, J., and Shubin, N. H. (2016). Digits and fin rays share common developmental histories. *Nature*, 537(7619):225–228.

Nulens, R., Scott, L., and Herbin, M. (2011). An updated inventory of all known specimens of the coelacanth, *Latimeria* spp. *Smithiana Publications in Aquatic Biodiversity*, 3:1–52.

Payne, R. C., Hutchinson, J. R., Robilliard, J. J., Smith, N. C., and Wilson, A. M. (2005). Functional specialisation of pelvic limb anatomy in horses (*Equus caballus*). *Journal of Anatomy*, 206(6):557–574.

Pierce, S. E., Clack, J. A., and Hutchinson, J. R. (2012). Three-dimensional limb joint mobility in the early tetrapod *Ichthyostega*. *Nature*, 486(7404):523–526.

Pierce, S. E., Lamas, L. P., Pelligand, L., Schilling, N., and Hutchinson, J. R. (2020). Patterns of limb and epaxial muscle activity during walking in the fire salamander, *Salamandra salamandra*. *Integrative Organismal Biology*.

Přikryl, T., Aerts, P., Havelková, P., Herrel, A., and Roček, Z. (2009). Pelvic and thigh musculature in frogs (Anura) and origin of anuran jumping locomotion. *Journal of Anatomy*, 214:100–139.

R Core Team (2020). A Language and Environment for Statistical Computing (Version 4.0.2). *Vienna: R Foundation for Statistical Computing*.

Reilly, S. M. and Elias, J. A. (1998). Locomotion in *Alligator mississippiensis*: Kinematic effects of speed and posture and their relevance to the sprawling-to-erect paradigm. *Journal of Experimental Biology*, 201(18):2559–2574.

Rewcastle, S. C. (1980). Form and function in lacertilian knee and mesotarsal joints; a contribution to the analysis of sprawling locomotion. *Journal of Zoology*, 191(2):147–170.

Rewcastle, S. C. (1983). Fundamental Adaptations in the Lacertilian Hind Limb: A Partial Analysis of the Sprawling Limb Posture and Gait. *Copeia*, 1983(2):476.

Ritter, D. (1992). Lateral bending during lizard locomotion. *Journal of experimental biology*, 173:1–10.

Romer, A. S. (1924). Pectoral limb musculature and shoulder-girdle structure in fish and tetrapods. *The Anatomical Record*, 27(2):119–143.

Rosen, D. E., Forey, P. L., Gardiner, B. G., and Patterson, C. (1981). Lungfishes, tetrapods, paleontology, and plesiomorphy. *Bulletin of the American Museum of Natural History*, 167(4):159–276.

Russel, A. P., Bergmann, P. J., and Barbadillo, L. J. (2001). Maximal Caudal Autotomy in *Podarcis hispanica* (Lacertidae): The Caudofemoralis Muscle Is Not Sundered. *Copeia*, 2001(1):154–163.

Seebacher, F., Elsworth, P. G., and Franklin, C. E. (2003). Ontogenetic changes of swimming kinematics in a semi-aquatic reptile (*Crocodylus porosus*). *Australian Journal of Zoology*, 51(1):15–24.

Shubin, N. H. and Alberch, P. (1986). A Morphogenetic Approach to the Origin and Basic Organization of the Tetrapod Limb. *Evolutionary Biology*, 20:319–387.

Shubin, N. H., Daeschler, E. B., and Jenkins, F. A. (2014). Pelvic girdle and fin of *Tiktaalik roseae*. *Proceedings of the National Academy of Sciences*, 111(3):893–899.

Shubin, N. H., Daeschler, E. B., and Jenkins, F. A. J. (2006). The pectoral fin of *Tiktaalik roseae* and the origin of the tetrapod limb. *Nature*, 440.

Sigurdsen, T. and Bolt, J. R. (2009). The lissamphibian humerus and elbow joint, and the origins of modern amphibians. *Journal of Morphology*, 270(12):1443–1453.

Siomava, N. and Diogo, R. (2018). Comparative anatomy of zebrafish paired and median fin muscles: basis for functional, developmental, and macroevolutionary studies. *Journal of Anatomy*, 232(2):186–199.

Smith, N. C., Wilson, A. M., Jespers, K. J., and Payne, R. C. (2006). Muscle architecture and functional anatomy of the pelvic limb of the ostrich (*Struthio camelus*). *Journal of Anatomy*, 209(6):765–779.

Standen, E. M. (2008). Pelvic fin locomotor function in fishes: Three-dimensional kinematics in rainbow trout (*Oncorhynchus mykiss*). *Journal of Experimental Biology*, 211(18):2931–2942.

Standen, E. M., Du, T. Y., and Larsson, H. C. E. (2014). Developmental plasticity and the origin of tetrapods. *Nature*, 513(7516):54–58.

Thorsen, D. H. and Hale, M. E. (2005). Development of zebrafish (*Danio rerio*) pectoral fin musculature. *Journal of Morphology*, 266(2):241–255.

Thorsen, D. H. and Westneat, M. W. (2005). Diversity of pectoral fin structure and function in fishes with labriform propulsion. *Journal of Morphology*, 263(2):133–150.

Van Wassenbergh, S., Herrel, A., Adriaens, D., Huysentruyt, F., Devaere, S., and Aerts, P. (2006). A catfish that can strike its prey on land. *Nature*, 440:881.

Wainwright, P. C. (1988). Morphology and ecology: functional basis of feeding constraints in Caribbean labrid fishes. *Ecology*, 69(3):635–645.

Webb, P. W. (1982). Locomotor Patterns in the Evolution of Actinopterygian Fishes. *American Zoologist*, 22:329–342.

Wilga, C. D. and Lauder, G. V. (1999). Locomotion in sturgeon: function of the pectoral fins. *The Journal of experimental biology*, 202(Pt 18):2413–2432.

Wilhelm, B. C., Du, T. Y., Standen, E. M., and Larsson, H. C. (2015). *Polypterus* and the evolution of fish pectoral musculature. *Journal of Anatomy*, 226(6):511–522.

Zhang, J., Wagh, P., Guay, D., Sanchez-Pulido, L., Padhi, B. K., Korzh, V., Andrade-Navarro, M. A., and Akimenko, M. A. (2010). Loss of fish actinotrichia proteins and the fin-to-limb transition. *Nature*, 466(7303):234–237.

Supplementary informations

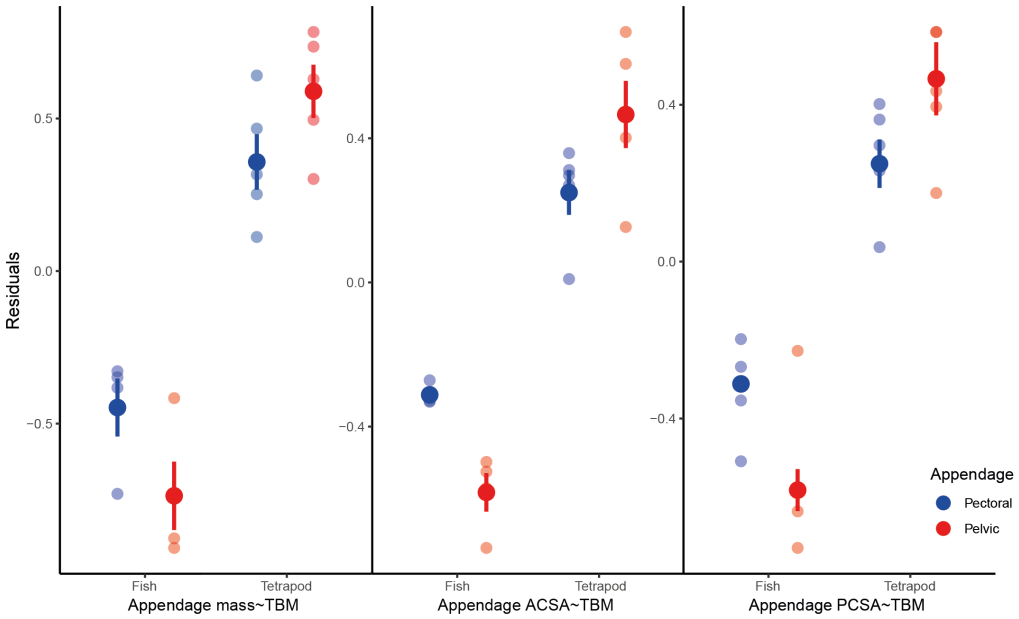

Annex Figure 3.1: Plot of the residuals of the ANCOVA analyses for muscle mass, ACSA, and PCSA of the relation between the pectoral and pelvic appendages with the total body mass.

Annex Table 3.1: Hypotheses of homology between pectoral appendicular muscles of extant taxa, based on Diogo et al. (2016).

Muscle group	*Polypterus sengalus*	*Dicentrarchus labrax*	*Acipenser stellatus*	*Latimeria chalumnae*	*Necturus maculosus*	*Salvator merianae*
Abductor superficialis	*Abductor superficialis* *Zonopterygialis medialis*	*Abductor superficialis*	*Abductor*	*Abductor superficialis 1-8*	*Pectoralis*	*Pectoralis*
					Coracobrachialis	*Coracobrachialis (brevis/longus)*
					Humeroantebrachialis	*Brachialis*
					Flexor antebrachii et carpi radialis	*Flexor carpi radialis*
						Pronator teres
					Flexor digitorum communis	*Flexor digitorum longus (pars ulnaris/radialis)*
					Flexor antebrachii et carpi ulnaris	*Flexor carpi ulnaris*
						Epitrochleanconeus
Abductor profundus	*Abductor profundus*	*Abductor profundus* *Arrector ventralis*	*Arrector ventralis*	*Abductor profundus 1-31*	*Coracoradialis*	*Biceps brachii*
					Supracoracoideus	*Supracoracoideus*
						Coracohumeralis anterior
					FAM +FAL + CCL + PP1	*Flexor digitorum longus (pars profundus)*
					Pronator quadratus	*Pronator quadratus*
						Pronator accessorius
Adductor superficialis	*Adductor* *Coracometapterygialis 1-2*	*Adductor superficialis* *Adductor medialis*	*Adductor*	*Adductor superficialis 1-7* *Supinator 1-8*	*Latissimus dorsi*	*Latissimus dorsi*
					Deltoideus scapularis	*Deltoideus scapularis*
					Triceps brachii (coracoideus/humeralis)	*Triceps brachii*
					Extensor digitorum	*Extensor digitorum longus*
					Extensor antebrachii et carpi ulnaris	*Extensor carpi ulnaris*
					Extensor carpi radialis longus	*Extensor carpi radialis*
						-
						-
					-	*Supinator longus*
Adductor profundus	-	*Adductor profundus* *Adductor radialis* *Arrector dorsalis*	-	*Adductor profundus 1-10* *Supinator 1-8* *Pterygialis caudalis*	*Procoracohumeralis*	*Deltoideus clavicularis*
						-
						Scapulohumeralis anterior
					Subcoracoscapularis	*Subscapularis*
						Subcoracoideus
						-
					Abductor et extensor digiti 1	*Supinator manus*

Annex Table 3.1 (suite)

Muscle group	*Alligator mississippiensis*	*Galictis vittata*	*Lontra longicauda*
Abductor superficialis	*Pectoralis*	*Pectoralis major*	*Pectoralis major*
		Pectoralis minor	*Pectoralis minor*
		Pectoralis superficialis	-
	Coracobrachialis brevis (dorsalis/ventralis)	*Coracobrachialis*	-
	Brachialis	*Brachialis*	*Brachialis*
	Pronator teres	*Flexor carpi radialis*	*Flexor carpi radialis*
		Pronator teres	*Pronator teres*
	Flexor digitorum longus pars humeralis	*Flexor digitorum profundus*	*Flexor digitorum profundus*
		Palmaris longus	*Palmaris profundus*
	Flexor carpi ulnaris	*Flexor carpi ulnaris (humeral/ulnar head)*	*Flexor carpi ulnaris (humeral/ulnar head)*
	-	-	-
Abductor profundus	*Biceps brachii*	*Biceps brachii*	*Biceps brachii*
	Supracoracoideus (longus/intermedium/brevis)	*Supraspinatus*	*Supraspinatus*
		Infraspinatus	*Infraspinatus*
	-	-	-
	Flexor digitorum longus pars ulnaris	-	-
	Pronator quadratus	*Pronator quadratus*	*Pronator quadratus*
	-	-	-
Adductor superficialis	*Latissismus dorsi*	*Latissimus dorsi*	*Latissimus dorsi*
	Deltoideus scapularis	*Spinodeltoideus*	*Spinodeltoideus*
		Teres minor	-
	Scapulo-humeralis caudalis	-	-
	Triceps brachii	*Triceps brachii*	*Triceps brachii*
	Extensor capi ulnaris longus	*Extensor digitorum communis*	*Extensor digitorum communis*
		Extensor digitorum lateralis	*Extensor digitorum lateralis*
	Flexor ulnaris longus	*Extensor carpi ulnaris*	*Extensor carpi ulnaris*
		Anconeus	*Anconeus*
	Extensor carpi radialis longus	*Extensor carpi radialis (brevis/longus)*	*Extensor carpi radialis longus*
	-	*Brachioradialis*	*Brachioradialis*
	Abductor radialis	-	-
	Supinator	*Supinator*	*Supinator*
Adductor profundus	*Deltoideus clavicularis*	*Clavobrachialis*	*Cleidobrachialis*
		Acromiodeltoideus	*Acromiodeltoideus*
	Humeroradialis	-	-
	-	-	-
	Subscapularis	*Subscapularis*	*Subscapularis*
	-	-	-
	Teres major	*Teres major*	*Teres major*
	Extensor carpi radialis brevis (pars radialis/ulnaris)	*Extensor brevis pollicis*	*Extensor brevis pollicis*

Annex Table 3.2: Hypotheses of homology between pelvic appendicular muscles of extant taxa, based on Diogo et al. (2016).

Muscle group	*Polypterus sengalus*	*Dicentrarchus labrax*	*Acipenser stellatus*	*Latimeria chalumnae*	*Necturus maculosus*	*Salvator merianae*
Abaxial	-	-	-	-	*Caudofemoralis*	*Caudofemoralis (brevis/longus)*
Abductor superficialis	*Abductor*	*Abductor superficialis*	*Abductor*	*Abductor superficialis 1-15*	*Pubotibialis*	*Pubotibialis (dorsal/ventral)*
					Puboischiotibialis	*Puboischiotibialis*
					Ischioflexorius	*Flexor tibialis internus 1-3*
						Flexor tibialis externus
					Flexor digitorum communis	*Femorotibial gastrocnemius*
						Femoral gastrocnemius (superficialis/profundus)
	Pterygialis cranialis			*Pterygialis cranialis*		*Flexor digitorum longus femoralis*
Abductor profundus	-	*Abductor profundus*	-	*Abductor profundus 1-14*	*Pubofemoralis*	*Adductor femoris*
					Ischiofemoralis	*Ischiotrochantericus*
					Puboischifemoralis externus	*Puboischiofemoralis externus (4 heads)*
				Supinator 1-17	*FAM + FAL + CCL*	*Flexor digitorum longus fibularis*
					Pronator profundus	*Pronator profundus*
					Interosseus cruris	*Interosseus cruris*
						Popliteus
Adductor superficialis	*Adductor*	*Adductor superficialis*	*Adductor*	*Adductor superficialis 1-10*	*Iliotibialis (anterior/posterior)*	*Iliotibialis*
						Femorotibialis (lateralis/medialis)
						Ambiens
					Iliofibularis	*Iliofibularis*
		Extensor proprius			*Extensor cruris tibialis*	*Tibialis anterior*
					Extensor tarsi tibialis	
					Extensor cruris et tarsi fibularis	*Peroneus brevis*
						Peroneus longus
						-
	Pterygialis caudalis	*Pre-axial muscle*		*Pterygialis caudalis*	*Extensor digitorum longus*	*Extensor digitorum longus*
Adductor profundus	-	*Adductor profundus*	-	*Adductor profundus 1-12*	*Puboischiofemoralis internus*	*Puboischiofemoralis internus 1-3*
				Pronator 1-8	*Iliofemoralis*	*Iliofemoralis*
				Flexor 1-5		

Annex Table 3.2 (suite)

Muscle group	*Alligator mississippiensis*	*Galictis vittata*	*Lontra longicauda*
Abaxial	*Caudofemoralis (brevis/longus)*	-	*Caudofemoralis*
Abductor superficialis	-	*Adductor longus*	*Adductor longus*
		Pectineus	*Pectineus*
	Puboischitibialis	*Gracilis*	*Gracilis*
	Flexor tibialis internus 1-3	*Semimembranosus*	*Semimembranosus*
		Biceps femoris	*Biceps femoris*
	Flexor tibialis externus	*Semitendinosus*	*Semitendinosus*
	Gastrocnemius internus	*Gastrocnemius caput mediale*	*Gastrocnemius caput mediale*
	Gastrocnemius plantaris	-	-
	Gastrocnemius externus	*Gastrocnemius caput laterale*	*Gastrocnemius caput laterale*
		Plantaris	*Plantaris*
		Soleus	*Soleus*
	Flexor digitorum longus	*Flexor digitorum longus*	*Flexor digitorum longus*
	-	*Flexor digitorum hallucis*	*Flexor digitorum hallucis*
	Flexor hallucis longus	-	-
Abductor profundus	*Adductor femoris 1-2*	*Adductor femoris (magnus/brevis)*	*Adductor femoris (magnus/brevis)*
	Ischiotrochantericus	*Obturator internus*	*Obturator internus*
		Gemellus superior	*Gemellus superior*
		Gemellus inferior	*Gemellus inferior*
	Puboischiofemoralis externus 1-3	*Quadratus femoris*	*Quadratus femoris*
		Obturator externus	-
	-	-	-
	Pronator profundus	*Tibialis posterior*	*Tibialis posterior*
	Interosseus cruris	-	-
		Popliteus	*Popliteus*
Adductor superficialis	*Iliotibialis (1-3)*	*Gluteus maximus*	*Gluteus maximus*
		Rectus femoris	*Rectus femoris*
	Femorotibialis (externus/internus)	*Vastus (lateralis/intermedius/medialis)*	*Vastus (lateralis/intermedius/medialis)*
	Ambiens	*Sartorius*	*Sartorius*
	Iliofibularis	*Tenuissimus*	*Tenuissimus*
	Tibialis anterior	*Tibialis anterior*	*Tibialis anterior*
	Fibularis brevis	*Peroneus brevis*	*Peroneus brevis*
	Fibularis longus	*Peroneus longus*	*Peroneus longus*
	-	*Peroneus tertius*	*Peroneus tertius*
	Extensor digitorum longus	*Extensor digitorum longus*	*Extensor digitorum longus*
	-	-	*Extensor hallucis*
	Extensor digitorum fibularis brevis	-	-
Adductor profundus	*Puboischiofemoralis internus 1-2*	*Iliacus*	*Iliopsoas complex*
		Psoas major	
	Iliofemoralis	*Gluteus medius*	*Gluteus medius*
		Gluteus minimus	*Gluteus minimus*
		-	*Capsularis*
		Pyriformis	*Pyriformis*
		Tensor fasciae latae	*Tensor fasciae latae*

Annex Table 3.3: Results of the ANCOVA analyses for the different muscles groups considering the *caudofemoralis*. Grey boxes show non-significant effects.

		Pectoral appendage			Pelvic Appendage		
		Mass	ACSA	PCSA	Mass	ACSA	PCSA
Abductor superficialis	Total appendage	F= 1628.682 P= 3.35e-05	F= 3364.190 P= 1.13e-05	F= 7978.078 P= 3.09e-06	F= 326.760 P= 3.69e-04	F= 411.104 P= 2.62e-04	F= 355.596 P= 3.26e-04
	Appendage-type	F= 21.245 P= 0.0192	F= 20.740 P= 0.020	F= 52.126 P= 0.006	F= 2.065 P= 0.246	F= 5.957 P= 0.092	F=10.619 P= 0.047
	Interaction	F= 1.479 P= 0.311	F= 0.050 P= 0.838	F= 5.429 P= 0.102	F= 0.617 P= 0.490	F= 0.096 P= 0.777	F= 0.404 P= 0.570
Abductor profundus	Total appendage	F= 1951.822 P= 2.55e-05	F= 5295.264 P= 5.72e-06	F= 1967.723 P= 2.52e-05	F= 2327.240 P= 1.96e-05	F= 12896.572 P= 1.51e-06	F= 982.20 P= 7.14e-05
	Appendage-type	F= 82.614 P= 0.003	F= 240.858 P= 5.81e-04	F= 76.436 P= 0.003	F= 45.983 P= 0.007	F= 255.907 P= 5.31e-04	F= 21.39 P= 0.019
	Interaction	F= 0.866 P= 0.421	F= 0.154 P= 0.721	F= 2.863 P= 0.189	F= 0.572 P= 0.504	F= 1.699 P= 0.283	F= 0.147 P= 0.727
Adductor superficialis	Total appendage	F= 1959.918 P= 2.54e-05	F= 9664.830 P= 2.32e-06	F= 1623.311 P= 3.36e-05	F= 1765.783 P= 2.97e-05	F= 1061.170 P= 6.78e-05	F= 2444.49 P= 1.82e-05
	Appendage-type	F= 22.591 P= 0.018	F= 379.300 P= 2.96e-04	F= 64.922 P= 0.004	F= 13.252 P= 0.036	F= 45.000 P= 0.007	F= 100.360 P= 0.002
	Interaction	F= 1.033 P= 0.384	F= 14.090 P= 0.033	F= 0.021 P= 0.895	F= 4.661 P= 0.120	F= 14.240 P= 0.033	F= 11.990 P= 0.041
Adductor profundus	Total appendage	F= 1134.072 P= 5.76e-05	F= 2656.369 P= 1.61e-05	F= 828.078 P= 9.21e-05	F= 3745.935 P= 9.61e-06	F= 8.652 P= 0.060	F= 6.018 P= 0.091
	Appendage-type	F= 33.749 P= 0.010	F= 60.790 P= 0.004	F= 17.813 P= 0.024	F= 112.074 P=0.002	F= 1.117 P= 0.368	F= 0.512 P= 0.526
	Interaction	F= 2.122 P= 0.241	F= 7.969 P= 0.067	F=4.664 P= 0.120	F= 1.523 P= 0.305	F= 0.443 P= 0.554	F= 0.432 P= 0.558

Annex Table 3.4: Muscles of the pectoral and pelvic fins of the African coelacanth *Latimeria chalumnae* and ACSA and PCSA.

Pectoral fin lateral face			ρ= 1,06 g.cm-3 (Tetrapod)		ρ = 1,05 g.cm-3 (Fish)	
Muscle	Mass (g)	Bundle lenght (cm)	ACSA (cm²)	PCSA (cm²)	ACSA (cm²)	PCSA (cm²)
Abductor superficialis 1	9.000	4.25	1.998	5.418	2.017	5.470
Abductor superficialis 2	3.653	5.00	0.689	1.217	0.696	1.228
Abductor superficialis 3	4.042	2.25	1.695	2.984	1.711	3.012
Abductor superficialis 4	3.980	3.50	1.073	2.131	1.083	2.151
Abductor superficialis 5	2.899	2.00	1.367	2.197	1.380	2.218
Abductor superficialis 6	2.423	2.75	0.831	1.482	0.839	1.497
Abductor superficialis 7	1.786	3.00	0.562	1.091	0.567	1.102
Abductor superficialis 8	2.732	4.50	0.573	1.451	0.578	1.465
Abductor profundus 1	2.327	4.30	0.511	0.676	0.515	0.682
Abductor profundus 2	1.545	4.00	0.364	1.046	0.368	1.056
Abductor profundus 3	1.568	14.00	0.106	0.245	0.107	0.247
Abductor profundus 4	7.000	18.00	0.367	0.802	0.370	0.809
Abductor profundus 5	1.495	10.00	0.141	0.250	0.142	0.252
Abductor profundus 6	0.327	11.00	0.028	0.063	0.028	0.064
Abductor profundus 7	1.482	11.00	0.127	0.213	0.128	0.215
Abductor profundus 8	1.642	10.50	0.148	0.279	0.149	0.281
Abductor profundus 9	1.032	8.00	0.122	0.217	0.123	0.219
Abductor profundus 10	0.219	6.00	0.034	0.061	0.035	0.061
Abductor profundus 11	0.267	3.00	0.084	0.116	0.085	0.117
Abductor profundus 12	0.605	6.00	0.095	0.155	0.096	0.156
Abductor profundus 13	0.414	4.50	0.087	0.124	0.088	0.125
Abductor profundus 14	0.451	4.20	0.101	0.138	0.102	0.139
Abductor profundus 15	0.247	4.50	0.052	0.071	0.052	0.072
Abductor profundus 16	0.027	4.00	0.006	0.009	0.006	0.009
Abductor profundus 17	0.140	4.20	0.031	0.038	0.032	0.038
Abductor profundus 18	0.101	4.00	0.024	0.032	0.024	0.033
Abductor profundus 19	0.014	3.70	0.003	0.004	0.004	0.004
Abductor profundus 20	0.383	4.00	0.090	0.108	0.091	0.109
Abductor profundus 21	0.689	4.00	0.163	0.222	0.164	0.224
Abductor profundus 22	0.046	4.00	0.011	0.013	0.011	0.014
Abductor profundus 23	0.254	3.60	0.066	0.098	0.067	0.099
Abductor profundus 24	0.035	3.10	0.011	0.012	0.011	0.013
Abductor profundus 25	0.129	3.70	0.033	0.045	0.033	0.046
Abductor profundus 26	0.247	3.80	0.061	0.091	0.062	0.092
Abductor profundus 27	0.089	3.10	0.027	0.028	0.027	0.028
Abductor profundus 28	0.194	4.00	0.046	0.074	0.046	0.075
Abductor profundus 29	0.226	4.50	0.047	0.070	0.048	0.071
Abductor profundus 30	2.886	3.00	0.907	1.030	0.916	1.040
Abductor profundus 31	1.173	3.25	0.340	0.374	0.344	0.377
Pronator 1a	6.000	5.00	1.132	2.095	1.143	2.115
Pronator 1b	5.411	3.50	1.458	2.537	1.472	2.561
Pronator 2a	0.312	3.00	0.098	0.255	0.099	0.257
Pronator 2b	2.739	2.65	0.975	1.397	0.984	1.410
Pronator 2c	3.018	3.00	0.949	1.030	0.363	1.040
Pronator 2d	2.286	6.00	0.359	1.341	0.958	1.354
Pronator 3a	2.971	3.25	0.862	1.020	0.871	1.030
Pronator 3b	2.200	3.50	0.593	0.682	0.599	0.688
Pronator 4	0.718	2.50	0.271	0.558	0.274	0.564
Pronator 5	3.454	4.50	0.724	1.901	0.731	1.919
Pronator 6a	2.568	3.50	0.692	3.621	0.699	3.656
Pronator 6b	1.356	2.75	0.465	1.679	0.470	1.695
Pronator 6c	1.957	1.75	1.055	1.583	1.065	1.598
Pronator 7	0.164	3.80	0.041	0.268	0.169	0.270
Pronator 8	0.978	5.50	0.168	0.065	0.041	0.066

Annex Table 3.4 (suite): Muscles of the pectoral and pelvic fins of the African coelacanth *Latimeria chalumnae* and ACSA and PCSA.

Pelvic fin medial Face			ρ= 1,06 g.cm-3 (Tetrapod)		ρ = 1,05 g.cm-3 (Fish)	
Muscle	Mass (g)	Bundle lenght (cm)	ACSA (cm²)	PCSA (cm²)	ACSA (cm²)	PCSA (cm²)
Adductor superficialis 1	14.000	8.00	1.651	2.181	1.667	2.201
Adductor superficialis 2	7.000	10.00	0.660	2.223	0.667	2.245
Adductor superficialis 3	2.612	10.00	0.246	0.771	0.249	0.779
Adductor superficialis 4	2.838	4.50	0.595	1.065	0.601	1.075
Adductor superficialis 5	2.477	10.50	0.223	0.870	0.225	0.878
Adductor superficialis 6	2.238	3.50	0.603	1.338	0.609	1.351
Adductor superficialis 7	2.265	2.50	0.855	1.757	0.863	1.774
Adductor profondus 1	0.869	8.30	0.099	0.152	0.100	0.154
Adductor profondus 2	2.323	10.50	0.209	0.369	0.211	0.373
Adductor profondus 3	3.253	12.60	0.244	0.666	0.246	0.673
Adductor profondus 4	1.798	8.00	0.212	0.528	0.214	0.533
Adductor profondus 5	0.694	5.50	0.119	0.385	0.120	0.389
Adductor profondus 6	0.134	3.50	0.036	0.047	0.036	0.048
Adductor profondus 7	1.948	10.50	0.175	0.254	0.177	0.257
Adductor profondus 8	2.460	12.50	0.186	0.256	0.187	0.259
Adductor profondus 9	2.028	13.00	0.147	0.220	0.149	0.222
Adductor profondus 10	1.228	14.50	0.080	0.137	0.081	0.138
Supinator 1a	1.880	1.50	1.182	1.601	1.194	1.616
Supinator 1b	5.140	3.50	1.385	2.135	1.399	2.156
Supinator 2a	1.244	1.50	0.782	1.043	0.790	1.053
Supinator 2b	2.689	3.00	0.846	1.374	0.854	1.387
Supinator 2c	0.591	2.50	0.223	0.303	0.225	0.306
Supinator 3a	1.875	2.00	0.884	1.274	0.893	1.287
Supinator 3b	1.699	4.00	0.401	0.931	0.405	0.940
Supinator 4	0.663	2.75	0.227	0.605	0.230	0.611
Supinator 5	1.667	2.25	0.699	1.319	0.706	1.332
Supinator 6a	0.873	2.75	0.299	1.206	0.302	1.217
Supinator 6b	0.924	2.75	0.317	0.834	0.320	0.842
Supinator 6c	0.749	1.75	0.404	0.918	0.407	0.927
Supinator 7	0.364	4.50	0.076	0.293	0.077	0.295
Supinator 8	0.700	6.50	0.102	0.219	0.103	0.221
Pterygialis caudalis	0.691	8.00	0.081	0.231	0.082	0.233

Annex Table 3.4 (suite): Muscles of the pectoral and pelvic fins of the African coelacanth *Latimeria chalumnae* and ACSA and PCSA.

Pelvic fin dorsal face		ρ= 1,06 g.cm-3 (Tetrapod)		ρ = 1,05 g.cm-3 (Fish)	
Muscle	Mass (g)	ACSA (cm²)	PCSA (cm²)	ACSA (cm²)	PCSA (cm²)
Pterygialis caudalis	1.000	0.201	0.342	0.203	0.345
Adductor superficialis pelvicus 1	1.800	0.215	0.501	0.217	0.505
Adductor superficialis pelvicus 2	0.738	0.084	0.283	0.085	0.286
Adductor superficialis pelvicus 3	0.910	0.095	0.378	0.096	0.381
Adductor superficialis pelvicus 4	1.370	0.145	0.483	0.147	0.488
Adductor superficialis pelvicus 5	1.400	0.139	0.463	0.140	0.467
Adductor superficialis pelvicus 6	1.180	0.115	0.381	0.116	0.385
Adductor superficialis pelvicus 7	3.330	0.291	0.787	0.294	0.794
Adductor superficialis pelvicus 8	1.460	0.147	0.398	0.148	0.402
Adductor superficialis pelvicus 9	0.540	0.088	0.126	0.089	0.127
Adductor superficialis pelvicus 10	0.350	0.066	0.107	0.066	0.108
Adductor profundus pelvicus 1	0.280	0.033	0.071	0.033	0.071
Adductor profundus pelvicus 2	1.670	0.177	0.260	0.179	0.262
Adductor profundus pelvicus 3	1.275	0.133	0.229	0.134	0.231
Adductor profundus pelvicus 4a	0.711	0.128	0.191	0.129	0.193
Adductor profundus pelvicus 4b	0.955	0.159	0.192	0.160	0.194
Adductor profundus pelvicus 5	0.220	0.037	0.054	0.038	0.055
Adductor profundus pelvicus 6	1.570	0.260	0.306	0.263	0.309
Adductor profundus pelvicus 7a	1.100	0.175	0.237	0.176	0.239
Adductor profundus pelvicus 7b	0.720	0.166	0.200	0.167	0.202
Adductor profundus pelvicus 8a	0.450	0.106	0.167	0.107	0.168
Adductor profundus pelvicus 8b	1.390	0.299	0.458	0.302	0.463
Adductor profundus pelvicus 8c	2.410	0.392	0.627	0.396	0.633
Adductor profundus pelvicus 8d	3.520	0.494	0.725	0.499	0.732
Adductor profundus pelvicus 9	0.670	0.179	0.223	0.181	0.225
Adductor profundus pelvicus 10a	0.420	0.104	0.164	0.105	0.165
Adductor profundus pelvicus 10b	0.890	0.198	0.307	0.200	0.310
Adductor profundus pelvicus 11	2.430	0.523	0.736	0.528	0.743
Adductor profundus pelvicus 12	2.940	0.411	0.660	0.415	0.666
Pronator 1	3.490	0.962	1.987	0.971	2.006
Pronator 2	0.966	0.375	0.739	0.379	0.746
Pronator 3	0.680	0.256	0.589	0.259	0.594
Pronator 4	0.681	0.202	0.741	0.204	0.748
Pronator 5	0.617	0.241	1.100	0.243	1.111
Pronator 6	1.671	0.634	1.366	0.640	1.379
Pronator 7	0.156	0.046	0.090	0.046	0.091
Pronator 8	1.066	0.503	0.976	0.507	0.986
Flexor 1	1.570	0.423	0.653	0.427	0.660
Flexor 2	1.058	0.370	0.586	0.373	0.591
Flexor 3	0.116	0.109	0.208	0.110	0.210
Flexor 4	0.340	0.139	0.218	0.141	0.221
Flexor 5	0.437	0.187	0.363	0.189	0.366

Annex Table 3.4 (suite): Muscles of the pectoral and pelvic fins of the African coelacanth *Latimeria chalumnae* and ACSA and PCSA.

Pelvic fin ventral face		ρ= 1,06 g.cm-3 (Tetrapod)		ρ = 1,05 gcm-3 (Fish)	
Muscle	Mass (g)	ACSA (cm²)	PCSA (cm²)	ACSA (cm²)	PCSA (cm²)
Pterygialis cranialis	2.280	0.341	0.598	0.345	0.604
Abductor superficialis pelvicus 1	3.970	0.468	0.883	0.473	0.891
Abductor superficialis pelvicus 2	4.350	0.363	0.783	0.367	0.790
Abductor superficialis pelvicus 3	0.640	0.068	0.212	0.068	0.214
Abductor superficialis pelvicus 4	0.520	0.060	0.186	0.060	0.187
Abductor superficialis pelvicus 5	0.620	0.065	0.201	0.066	0.203
Abductor superficialis pelvicus 6	1.140	0.111	0.358	0.112	0.362
Abductor superficialis pelvicus 7	1.470	0.127	0.281	0.128	0.284
Abductor superficialis pelvicus 8	1.550	0.137	0.272	0.138	0.274
Abductor superficialis pelvicus 9	0.700	0.062	0.121	0.063	0.122
Abductor superficialis pelvicus 10	0.660	0.062	0.111	0.062	0.112
Abductor superficialis pelvicus 11	0.540	0.067	0.089	0.068	0.090
Abductor superficialis pelvicus 12	0.560	0.064	0.099	0.065	0.099
Abductor superficialis pelvicus 13	0.440	0.055	0.081	0.056	0.082
Abductor superficialis pelvicus 14	1.810	0.211	0.312	0.213	0.315
Abductor superficialis pelvicus 15	4.000	0.563	0.797	0.569	0.804
Abductor profundus pelvicus 1	0.160	0.039	0.053	0.039	0.053
Abductor profundus pelvicus 2	0.210	0.051	0.118	0.051	0.120
Abductor profundus pelvicus 3	0.150	0.046	0.078	0.046	0.079
Abductor profundus pelvicus 4	0.220	0.027	0.045	0.027	0.045
Abductor profundus pelvicus 5	0.820	0.129	0.205	0.130	0.207
Abductor profundus pelvicus 6	1.340	0.267	0.352	0.269	0.355
Abductor profundus pelvicus 7	1.154	0.290	0.405	0.293	0.409
Abductor profundus pelvicus 8	0.950	0.207	0.256	0.209	0.259
Abductor profundus pelvicus 9	1.801	0.303	0.530	0.306	0.535
Abductor profundus pelvicus 10	3.960	0.532	0.961	0.537	0.970
Abductor profundus pelvicus 11	2.060	0.200	0.336	0.202	0.339
Abductor profundus pelvicus 12	1.630	0.215	0.257	0.217	0.260
Abductor profundus pelvicus 13	0.700	0.120	0.139	0.121	0.141
Abductor profundus pelvicus 14	3.182	0.556	2.043	0.561	2.063
Supinator 1	0.540	0.138	0.355	0.139	0.358
Supinator 2	1.310	0.272	0.913	0.275	0.921
Supinator 3	1.344	0.219	0.755	0.221	0.762
Supinator 4	1.392	0.146	0.432	0.147	0.437
Supinator 5	1.509	0.287	0.612	0.290	0.618
Supinator 6	1.873	0.283	0.454	0.286	0.458
Supinator 7	0.464	0.111	0.226	0.112	0.228
Supinator 8	1.377	0.216	0.505	0.219	0.510
Supinator 9	1.676	0.267	0.475	0.270	0.479
Supinator 10	0.997	0.199	0.335	0.201	0.338
Supinator 11	0.578	0.133	0.231	0.134	0.233
Supinator 12	0.756	0.161	0.265	0.162	0.267
Supinator 13	0.933	0.203	0.355	0.205	0.358
Supinator 14	1.228	0.243	0.448	0.245	0.452
Supinator 15	0.700	0.425	1.604	0.429	1.620
Supinator 16	0.642	0.261	0.880	0.263	0.888
Supinator 17	1.164	0.598	1.027	0.603	1.037

Annex Table 3.5: Muscles of the pectoral and pelvic appendages of the species used in the study.

Acipenser Total Body mass: 1131g

Pectoral fin

Muscle	Longueur (cm)	Masse (g)	Fibres (cm)	ACSA (cm²)	PCSA (cm²)
Adductor	3.5	1.6358	2.72	0.4451	0.5728
Abductor	3.6	1.1287	2.3	0.2986	0.4674
Arrector ventralis	3.5	1.7245	3.5	0.4693	0.4693
		4.489		**1.2130**	**1.5094**

Pelvic fin

Muscle	Longueur (cm)	Masse (g)	Fibres (cm)	ACSA (cm²)	PCSA (cm²)
Abductor	3.9	0.4257	1.26	0.1040	0.3218
Adductor	1.4	0.6052	1.5	0.4117	0.3843
		1.0309		**0.5157**	**0.7060**

Polypterus Total Body mass: 80g

Pectoral fin Left

Muscle	Longueur (cm)	Masse (g)	Fibre (cm)	ACSA (cm²)	PCSA (cm²)
Abductor superficialis	0.8	0.0091	0.518	0.011	0.017
Abductor profundus	1.4	0.0453	0.693	0.031	0.062
Coracometapterygialis 1	0.7	0.0075	0.569	0.010	0.013
Coracometapterygialis 2	0.8	0.0063	0.356	0.008	0.017
Zonopterygialis medialis	0.6	0.0044	0.236	0.007	0.018
Adductor	1.3	0.054	0.765	0.040	0.067
		0.1266		**0.106**	**0.193**

Pectoral fin Right

Muscle	Longueur (cm)	Masse (g)	Fibre (cm)	ACSA (cm²)	PCSA (cm²)
Abductor superficialis	1	0.011	0.452	0.010	0.023
Abductor profundus	1.5	0.0461	0.803	0.029	0.055
Coracometapterygialis 1	1.1	0.013	0.474	0.011	0.026
Coracometapterygialis 2	0.5	0.0032	0.335	0.006	0.009
Zonopterygialis medialis	0.6	0.0056	0.382	0.009	0.014
Adductor	1.4	0.0451	0.725	0.031	0.059
		0.124		**0.097**	**0.186**

Pelvic fin Left

Muscle	Longueur (cm)	Masse (g)	Fibre (cm)	ACSA (cm²)	PCSA (cm²)
Abductor	0.9	0.0046	0.330	0.005	0.013
Adductor	1.3	0.0086	0.235	0.006	0.035
Pterygialis cranialis	0.6	0.0022	0.347	0.003	0.006
Pterygialis caudalis	0.7	0.0026	0.374	0.004	0.007
		0.018		**0.018**	**0.061**

Pelvic fin Right

Muscle	Longueur (cm)	Masse (g)	Fibre (cm)	ACSA (cm²)	PCSA (cm²)
Abductor	0.9	0.0046	0.281	0.005	0.016
Adductor	0.8	0.0072	0.365	0.009	0.019
Pterygialis cranialis	0.7	0.0013	0.322	0.002	0.004
Pterygialis caudalis	0.7	0.0033	0.353	0.004	0.009
		0.0164		**0.020**	**0.047**

Annex Table 3.5 (suite): Muscles of the pectoral and pelvic appendages of the species used in the study.

Dicentrarchus Total Boddy mass: 770g

Pectoral fin Left

Muscle	Longueur (cm)	Masse (g)	Fibre (cm)	ACSA (cm²)	PCSA (cm²)
Abductor superficialis	3.5	0.8427	1.3233	0.2293	0.606
Abductor profundus	4.3	0.5924	1.1868	0.1312	0.475
Arrector ventralis	3.4	0.1985	0.9843	0.0556	0.192
Adductor superficialis	2.4	0.1764	1.349	0.0700	0.125
Adductor medialis	2.2	0.1187	1.2529	0.0514	0.090
Adductor radialis	1.5	0.0411	0.8988	0.0261	0.044
Adductor profundus	3.2	0.4354	1.3585	0.1296	0.305
Adductor profundus (2nd)	2.7	0.1238	1.4699	0.0437	0.080
Arrector dorsalis	2.8	0.2022	0.9615	0.0688	0.200
		2.7312		**0.8056**	**2.1180**

Pectoral fin Right

Muscle	Longueur (cm)	Masse (g)	Fibre (cm)	ACSA (cm²)	PCSA (cm²)
Abductor superficialis	3.1	0.6495	1.2057	0.1995	0.513
Abductor profundus α	3	0.4395	1.031	0.1395	0.406
Abductor prorfundus β	3.1	0.0971	1.1101	0.0298	0.083
Arrector ventralis	3.6	0.2881	1.2756	0.0762	0.215
Adductor superficialis	2.8	0.1623	1.1722	0.0552	0.132
Adductor medialis	2.1	0.1183	1.0829	0.0537	0.104
Adductor radialis	1.8	0.0701	0.9161	0.0371	0.073
Adductor profundus	3.2	0.4188	1.2747	0.1246	0.313
Adductor profundus (2nd part)	1.6	0.0756	1.0269	0.0450	0.070
Arrector dorsalis	3.2	0.1913	0.9283	0.0569	0.196
		2.5106		**0.8176**	**2.1055**

Pelvic fin Left

Muscle	Longueur (cm)	Masse (g)	Fibre (cm)	ACSA (cm²)	PCSA (cm²)
Abductor superficilis	3.6	0.1647	1.560	0.0436	0.1005
Abductor profundus (lat)	3.5	0.1731	1.231	0.0471	0.1339
Abductor profundus (med)	3.5	0.2155	0.849	0.0586	0.2416
Pre-axial muscle	2.8	0.1476	0.960	0.0502	0.1464
Extensor proprius	2.7	0.0578	0.748	0.0204	0.0736
Adductor superficialis	3.4	0.1813	0.918	0.0508	0.1882
Adductor profundus	3.5	0.3399	0.510	0.0925	0.6352
		1.2799		**0.3632**	**1.5195**

Pelvic fin Right

Muscle	Longueur (cm)	Masse (g)	Fibre (cm)	ACSA (cm²)	PCSA (cm²)
Abductor superficilis	2.7	0.0958	0.680	0.0338	0.1342
Abductor profundus (lat)	3.1	0.1626	1.209	0.0500	0.1281
Abductor profundus (med)	3.4	0.2361	0.624	0.0661	0.3603
Pre-axial muscle	3.2	0.1443	1.104	0.0429	0.1245
Extensor proprius	2.7	0.0652	0.775	0.0230	0.0802
Adductor superficialis	3.4	0.1989	1.408	0.0557	0.1346
Adductor profundus	3.6	0.3587	0.657	0.0949	0.5200
		1.2616		**0.3664**	**1.4818**

Annex Table 3.5 (suite): Muscles of the pectoral and pelvic appendages of the species used in the study.

Necturus Total Body mass: 36g

Forelimb

Muscle	Longueur (cm)	Masse (g)	Fibres (cm)	ACSA (cm²)	PCSA (cm²)
Latissimus dorsi	1.2	0.0323	0.6357	0.0254	0.0479
Deltoideus scapularis	0.6	0.0039	0.4152	0.0061	0.0089
Triceps coracoideus	0.6	0.0025	0.4153	0.0039	0.0057
Triceps humeralis lateralis	1	0.014	0.5056	0.0132	0.0261
Triceps humeralis medialis	0.8	0.0046	0.5284	0.0054	0.0082
Extensor digitorum	0.9	0.0042	0.3971	0.0044	0.0100
Extensor antebrachii et carpi ulnaris	0.6	0.0028	0.405	0.0044	0.0065
Extensor carpi radialis longus	0.8	0.0047	0.5417	0.0055	0.0082
Procoracohumeralis	0.9	0.0033	0.5441	0.0035	0.0057
Subcoracoscapularis	0.7	0.0053	0.5625	0.0071	0.0089
Abductor et extensor digit 1	0.5	0.001	0.333	0.0019	0.0028
Pectoralis	2	0.0722	0.7627	0.0341	0.0893
Coracobrachialis	1	0.0104	0.6244	0.0098	0.0157
Humeroantebrachialis	1.3	0.0104	0.5478	0.0075	0.0179
Flexor antebrachii et carpi radialis	0.8	0.0042	0.4014	0.0050	0.0099
Flexor digitorum communis	0.9	0.0076	0.4308	0.0080	0.0166
Flexor antebrachii et carpi ulnaris	0.7	0.0018	0.4562	0.0024	0.0037
Supracoracoideus	1.7	0.0188	0.9968	0.0104	0.0178
Coracoradialis	0.8	0.0019	0.473	0.0022	0.0038
FAM+FAL+CCL+PP1	0.4	0.0006	0.2265	0.0014	0.0025
		0.2065		**0.1618**	**0.3162**

Hindlimb

Muscle	Longueur (cm)	Masse (g)	Fibres (cm)	ACSA (cm²)	PCSA (cm²)
Caudofemoralis	2.4	0.0219	1.5075	0.0086	0.0137
Iliotibialis anterior	0.7	0.0055	0.4914	0.0074	0.0106
Iliotibialis posterior	0.8	0.069	0.4307	0.0814	0.1511
Iliofibularis (pars 1)	0.8	0.0018	0.6156	0.0021	0.0028
Iliofibularis (pars 2)	1.3	0.004	1.3	0.0029	0.0029
Extensor cruris tibialis	1	0.0018	0.81775	0.0017	0.0021
Extensor cruris et tarsi fibularis	0.7	0.0046	0.3799	0.0062	0.0114
Extensor digitorum longus	0.9	0.0099	0.4678	0.0104	0.0200
Extensor tarsi tibialis	0.6	0.0022	0.322	0.0035	0.0064
Puboischiofemoralis internus	1.2	0.0069	0.74	0.0054	0.0088
Iliofemoralis	0.8	0.0162	0.4899	0.0191	0.0312
Pubotibialis (pars 1)	1.3	0.0065	0.8161	0.0047	0.0075
Puboischiotibialis	1.1	0.0169	0.6294	0.0145	0.0253
Pubotibialis (pars 2)	1.4	0.0045	0.3927	0.0030	0.0108
Ischioflexorius (partie 1)	1.3	0.0054	0.6418	0.0039	0.0079
Ischioflexorius (partie 2)	1.2	0.0026	0.52685714	0.0020	0.0047
Flexor digitorum communis	1.2	0.0089	0.4488	0.0070	0.0187
Pubofemoralis	1.2	0.0222	0.7	0.0175	0.0299
Ischiofemoralis	1	0.0045	0.7216	0.0042	0.0059
Puboischifemoralis externus	0.6	0.0062	0.4644	0.0097	0.0126
CMCL + FAL + FAM + PP + IOC	0.5	0.0024	0.2387	0.0045	0.0095
		0.2239		**0.2199**	**0.3938**

Annex Table 3.5 (suite): Muscles of the pectoral and pelvic appendages of the species used in the study.

Salvator Total Body mass: 2000g

Forelimb

Muscle	Longueur (cm)	Masse (g)	Fibres (cm)	ACSA (cm²)	PCSA (cm²)
Latissimus dorsi	5	4.8	4.56	0.906	0.993
Deltoideus scapularis	4.2	1.02	2.74	0.229	0.351
Triceps lateralis	3.7	2.859	2.42	0.729	1.115
Triceps longus (scapularis + coracoideus heads)	4.2	2.472	2.02	0.555	1.154
Triceps medialis	3.5	1.182	2	0.319	0.558
Supinator longus	3.6	1.111	1.54	0.291	0.681
Extensor carpi ulnaris	3.2	0.332	2	0.098	0.157
Extensor carpi radialis	4	0.374	2.36	0.088	0.150
Extensor digitorum longus superficialis (1)	3.8	0.342	2.34	0.085	0.138
Extensor digitorum longus superficialis (2)	2.6	0.165	2.04	0.060	0.076
Extensor digitorum longus profundus	3.1	0.461	1.46	0.140	0.298
Deltoideus clavicularis	2.8	0.51	2.46	0.172	0.196
Scapulohumeralis anterior	3	0.704	1.86	0.221	0.357
Subscapularis	2.9	1.491	2.32	0.485	0.606
Subcoracoideus	3.6	1.615	2.06	0.423	0.740
Supinator manus	2	0.154	1.08	0.073	0.135
Pectoralis	8.9	9.19	4.6	0.974	1.885
Pectoralis pars profundus	4.5	0.98	3	0.205	0.308
Coracobrachialis brevis	3.8	0.581	2.18	0.144	0.251
Coracobrachialis longus	4.8	0.7	3.24	0.138	0.204
Brachialis	4.3	0.424	3.08	0.093	0.130
Flexor carpi ulnaris	4	1.658	1.74	0.391	0.899
Flexor digitorum longus (pars ulnaris 2)	3.2	0.408	2.36	0.120	0.163
Flexor digitorum longus (pars radialis)	2.8	0.287	1.86	0.097	0.146
Flexor carpi radialis	5.1	1.365	3.38	0.252	0.381
Flexor digitorum longus pars ulnaris (1)	3.3	0.64	1.62	0.183	0.373
Pronator teres	4.3	0.805	2.1	0.177	0.362
Epitrochleanconus	1.8	0.248	1.22	0.130	0.192
Biceps brachii	4.9	1.439	3.48	0.277	0.390
Supracoracoideus	3.9	0.502	2.16	0.121	0.219
Coracohumeralis anterior	5.5	1.57	4.52	0.269	0.328
Pronator accessorius	2.7	0.168	1.88	0.059	0.084
Pronator quadratus	2.7	0.225	0.58	0.079	0.366
Flexor digitorum longus pars profundus	2.9	0.356	1.38	0.116	0.243
		41.138		**8.699**	**14.626**

Hindlimb

Muscle	Longueur (cm)	Masse (g)	Fibres (cm)	ACSA (cm²)	PCSA (cm²)
Caudofemoralis longus	17.3	17	5	0.927	3.208
Caudofemoralis brevis	5	4.067	2.28	0.767	1.683
Iliofibularis	4.8	3.825	4.3	0.752	0.839
Iliotibialis	5.7	3.26	1.66	0.540	1.853
Femorotibialis lateralis	3.6	1.731	2.02	0.454	0.808
Ambiens	4.2	1.697	2.04	0.381	0.785
Femorotibialis medialis	4	1.649	1.7	0.389	0.915
Peroneus longus	4.3	1.424	1.74	0.312	0.772
Peroneus longus pars profundus	3.8	0.502	1.24	0.125	0.382
Peroneus brevis	4.1	1.529	1.9	0.352	0.759
Tibialis anterior	4.9	1.6	3.38	0.308	0.447
Extensor digitorum longus	5	1.239	3.26	0.234	0.359
Iliofemoralis	2.1	0.395	1.38	0.177	0.270
Puboischiofemoralis internus 1->3	6	7.309	4.14	1.149	1.666
Puboischiotibialis	8.1	5.049	5.56	0.588	0.857
Flexor tibialis externus	5.9	1.298	4.18	0.208	0.293
Flexor tibialis internus 1	4.8	3.178	3.8	0.625	0.789
Flexor tibialis internus 2 (pars superficialis)	5.9	1.311	4.92	0.210	0.251
Flexor tibialis internus 2 (pars profundus)	6.4	1.684	5.36	0.248	0.296
Flexor tibialis internus 3	5.8	0.964	4.42	0.157	0.206
Pubotibialis (ventral head)	6.7	1.652	5.46	0.233	0.285
Pubotibialis (dorsal head)	5.9	0.272	4.7	0.043	0.055
Femorotibial gastrocnemius	4.8	2.766	1.86	0.544	1.403
Femoral gastrocnemius superficialis	4.2	1.798	1.48	0.404	1.146
Femoral gastrocnemius profundus	5.9	2.736	1.32	0.437	1.955
Flexor digitorum longus femoralis 5	3	0.205	2	0.064	0.097
Flexor digitorum longus femoralis 1->4	3.1	0.186	2.02	0.057	0.087
Adductor femoris	6	1.628	4.08	0.256	0.376
Ischitrochantericus	3.8	1.279	1.72	0.318	0.702
Puboischiofemoralis externus a1	1.8	0.156	1.38	0.082	0.107
Puboischiofemoralis externus a2	4.2	2.599	2.58	0.584	0.950
Puboischiofemoralis externus a3	3.6	0.949	2.5	0.249	0.358
Puboischiofemoralis externus b	3.7	0.772	2.7	0.197	0.270
Popliteus	2.8	0.43	1	0.145	0.406
Pronator profundus	3.5	0.452	1.3	0.122	0.328
Interosseus cruris	2.8	0.495	0.84	0.167	0.556
Flexor digitorum longus fibularis 5	3.6	0.35	2.14	0.092	0.154
Flexor digitorum longus fibularis 1->4	3.8	0.847	2	0.210	0.400
Flexor hallucis	1.2	0.07	0.82	0.055	0.081
		80.353		**13.159**	**27.151**

Annex Table 3.5 (suite): Muscles of the pectoral and pelvic appendages of the species used in the study.

Alligator Total Body mass: 34 890 g (estimate mass)

Forelimb

Muscle	Longueur (cm)	Masse (g)	Fibres (cm)	ACSA (cm²)	PCSA (cm²)
Latissimus dorsi	10.7	44	5.4	3.879	7.652
Deltoideus scapularis	10	18	4.3	1.698	3.968
Scapulohumeralis caudalis	9.1	18	5.2	1.866	3.291
Triceps longus lateralis	13.7	44	5.4	3.030	7.687
Triceps longus medialis (=longus caudalis)	13.8	40	4.5	2.734	8.312
Triceps brevis cranialis	12.7	42	8.8	3.120	4.523
Triceps brevis intermedius	12.5	61	4.2	4.604	13.702
Triceps brevis caudalis	11.5	25	3.9	2.051	6.079
Supinator	9	13.2	4.8	1.384	2.584
Extensor carpi radialis longus	9.2	6	3.9	0.615	1.437
Abductor radialis	6.6	5	2.5	0.715	1.857
Extensor carpi ulnaris longus	9.8	6	5.5	0.578	1.022
Flexor ulnaris longus	9.5	8	2.2	0.794	3.369
Teres major	10	17	7.2	1.604	2.227
Deltoideus clavicularis	12.5	51	5.1	3.849	9.397
Humeroradialis	9.2	18	7.5	1.846	2.252
Subscapularis	7.8	29	4.7	3.507	5.821
Extensor carpi radialis brevis (pars radialis)	5.1	1.7	3.4	0.314	0.477
Extensor carpi radialis brevis (pars ulnaris)	10	4	2.3	0.377	1.655
Pectoralis	23	345	15.3	14.151	21.245
Coracobrachialis brevis dorsalis	6.5	6	4.1	0.871	1.381
Coracobrachialis brevis ventralis	9	22	7.2	2.306	2.891
Brachialis	8.1	14	6.0	1.631	2.194
Pronator teres	9.3	11	2.8	1.116	3.733
Flexor carpi ulnaris	8	19	1.7	2.241	10.301
Flexor digitorum longus pars humeri	9.5	17	3.8	1.688	4.198
Biceps brachii	12.3	27	6.6	2.071	3.883
Supracoracoideus longus	9.6	12	7.8	1.179	1.455
Supracoracoideus intermedius	10.6	33	6.2	2.937	5.054
Supracoracoideus brevis	7.7	11	5.6	1.348	1.840
Pronator quadratus	10.2	19	2.0	1.757	9.053
Flexor digitorum longus pars ulnaris	10.5	12	2.5	1.078	4.565
		998.9		**72.939**	**159.103**

Hindlimb

Muscle	Longueur (cm)	Masse (g)	Fibres (cm)	ACSA (cm²)	PCSA (cm²)
Caudofemoralis longus	38	562	16.46	13.952	32.211
Caudofemoralis brevis	13.8	45	8.56	3.076	4.959
Iliotibialis 1	9.2	25	4.92	2.564	4.794
Iliotibialis 2 (+ Ambiens)	10.1	71	3.76	6.632	17.814
Iliotibialis 3	11.9	19	4.26	1.506	4.208
Iliofibularis	12.6	22	11.46	1.647	1.811
Femorotibialis externus	11.8	26	3.98	2.079	6.163
Femorotibialis internus	11.9	81	4.76	6.421	16.054
Tibialis anterior	10.7	20	8.66	1.763	2.179
Extensor digitorum longus	10.8	13	6.92	1.136	1.772
Extensor digitorum longus pars profundus	9.4	4	3.68	0.401	1.025
Extensor digitorum fibularis brevis	10.8	10	8.12	0.874	1.162
Fibularis brevis	7.1	6	2.64	0.797	2.144
Fibularis longus	10.7	12	2.82	1.058	4.014
Puboischiofemoralis internus 1	10	38	5.84	3.585	6.139
Puboischiofemoralis internus 2	14.5	53	7.44	3.448	6.720
Iliofemoralis	11.5	34	4.28	2.789	7.494
Flexor tibialis externus	13.9	72	10.84	4.887	6.266
Pars Flexor tibialis externus	9.2	12	7.7	1.231	1.470
Flexor tibialis internus 1	14	10	12.54	0.674	0.752
Flexor tibialis internus 2	17	45	14.64	2.497	2.900
Flexor tibialis internus 3	15.8	31	7.5	1.851	3.899
Puboischiotibialis	15	23	12.58	1.447	1.725
Gastrocnemius internus	13.3	26	11.16	1.844	2.198
Gastrocnemius plantaris	8.3	12	1.9	1.364	5.958
Gastrocnemius externus	11.2	43	5.24	3.622	7.742
Flexor hallucis longus	12	26	2.98	2.044	8.231
Flexor digitorum longus Pars prox	11.2	7	3.2	0.590	2.064
Flexor digitorum longus Pars distal	4.3	4	3	0.878	1.258
Adductor femoris 1	15	43	14.04	2.704	2.889
Adductor femoris 2	15.7	21	11.24	1.262	1.763
Ischiotrochantericus	8.1	13	2.68	1.514	4.576
Puboischiofemoralis externus 1	11.6	35	6.78	2.846	4.870
Puboischiofemoralis externus 2	12.5	38	6.32	2.868	5.672
Puboischiofemoralis externus 3	10.5	35	4.06	3.145	8.133
Pronator profundus	5.2	6	2.46	1.089	2.301
Interosseus cruris	11.6	25	2.16	2.033	10.919
		1568.0		**94.1**	**206.2**

Annex Table 3.5 (suite): Muscles of the pectoral and pelvic appendages of the species used in the study.

Lontra Mean Total Body mass: 8241g 2 specimens used: M3024 and M3022

Forelimb

Muscle	Longueur (cm)	Masse (g)	Fibres (cm)	ACSA (cm²)	PCSA (cm²)
Latissimus dorsi (superficial layer)	15	13.5	11.25	0.849	1.132
Latissimus dorsi	25.75	59.5	22.5	2.180	2.495
Spinodeltoideus	5	4	5	0.755	0.755
Triceps angular	16.5	10	16.5	0.572	0.572
Triceps accessory head	2.25	0.5	2.25	0.210	0.210
Triceps longum	8.75	30.5	3	3.288	9.591
Triceps laterale	7.75	13.5	7.75	1.643	1.643
Triceps brachii mediale (long and intermediate)	7.25	4	7.25	0.520	0.520
Triceps brachii mediale (short portion)	5.5	3.5	5.5	0.600	0.600
Anconeus	4	1	3.25	0.236	0.290
Extensor carpi radialis longus	6.5	8	6.5	1.161	1.161
Brachioradialis	10.25	5	10.25	0.460	0.460
Extensor digiti communis	5.5	2	2.5	0.343	0.755
Extensor digitorum lateralis	6.25	1	1	0.151	0.943
Extensor carpi ulnaris	5.75	3	1.1	0.492	2.573
Supinator	6.5	3.5	1.3	0.508	2.540
Cleidobrachialis	7.25	5	7.25	0.651	0.651
Acromiodeltoideus	3.5	2	3.5	0.539	0.539
Teres major	7.25	5	7.25	0.651	0.651
Subscapularis	6.5	23	1.75	3.338	12.399
Extensor brevis pollicis	5.5	0.5	3.1	0.086	0.152
Pronator teres	4.25	1.25	1.05	0.277	1.123
Flexor carpi radialis	5	0.75	3.5	0.142	0.202
Flexor carpi ulnaris (humeral head)	5.5	0.5	5.5	0.086	0.086
Flexor carpi ulnaris (ulnar head)	7	6	1.4	0.809	4.043
Palmaris longus	8.75	8	1.5	0.863	5.031
Flexor digitorium profundus	6.25	10.5	1.75	1.585	5.660
Brachialis	6.75	5.5	4.5	0.769	1.153
Pectoralis minor	13	45.5	13	3.302	3.302
Pectoralis major	14.5	46.5	10.5	3.025	4.178
Infraspinatus	7.5	9.5	1.35	1.195	6.639
Supraspinatus	8	17.5	3	2.064	5.503
Pronator quadratus	1.75	0.5	1.15	0.270	0.410
Biceps brachii	6.25	6.5	2.5	0.981	2.453
		356.5		**34.599**	**80.416**

Hindlimb

Muscle	Longueur (cm)	Masse (g)	Fibres (cm)	ACSA (cm²)	PCSA (cm²)
Caudofemoralis	7.5	4.5	7.5	0.566	0.566
Gluteus maximus	5	6	1.75	1.132	3.235
Rectus femoris	7.5	14.5	2.35	1.824	5.821
Tenuissimus (abductor cruris)	17.75	4.5	17.75	0.239	0.239
Sartorius	11.75	17.5	11.75	1.405	1.405
Vastus lateralis	7	15.5	3	2.089	4.874
Vastus medialis	6.75	6.5	1.75	0.908	3.504
Vastus intermedius	5	1	3	0.189	0.314
Peroneus longus	7.25	2	2	0.260	0.943
Peroneus brevis	7.5	2.5	1.5	0.314	1.572
Peroneus tertius	7.75	1.5	1.25	0.183	1.132
Tibialis anterior	8.5	13	8.5	1.443	1.443
Extensor digitorum longus	8.75	7	8.75	0.755	0.755
Extensor hallucis	8.5	0.5	8.5	0.055	0.055
Tensor fascia latae	4.25	6	4.25	1.332	1.332
Gluteus medius	4.5	7.5	2.5	1.572	2.830
Gluteus minimus	4.5	3.5	1.75	0.734	1.887
Capsularis	2	0.5	2	0.236	0.236
Pyriformis	3.25	1.5	2.25	0.435	0.629
Iliopsoas complex	9.5	14	4.25	1.390	3.108
Adductor longus	9	3	9	0.314	0.314
Pectineus	6.75	5.5	6.75	0.769	0.769
Biceps femoris	12	31.5	12	2.476	2.476
Semitendinosus	14	14	14	0.943	0.943
Semimembranosus	10.5	33.5	10.5	3.010	3.010
Gracilis	9.75	11.5	9.75	1.113	1.113
Gastrocnemius caput mediale	9.5	15.5	2.5	1.539	5.849
Gastrocnemius caput laterale	9	10.5	2	1.101	4.953
Plantaris	9.75	10	1.85	0.968	5.099
Soleus	6.25	1.25	6.25	0.189	0.189
Flexor digitorum longus	7	1.5	2.75	0.202	0.515
Flexor hallucis longus	6.75	2.5	1	0.349	2.358
Gemellus superior	2.75	1	1.6	0.343	0.590
Gemellus inferior	3.25	0.75	3.25	0.218	0.218
Quadratus femoris	3.75	2.5	3.75	0.629	0.629
Obturator externus	4.25	5	1.15	1.110	4.102
Obturator internus	4.25	4.5	2.25	0.999	1.887
Adductor femoris (magnus et brevis)	11.75	16	11.75	1.285	1.285
Popliteus	6.5	3	0.65	0.435	4.354
Tibialis posterior	8	7.5	1.15	0.884	6.153
		310		**35.938**	**82.685**

Annex Table 3.5 (suite): Muscles of the pectoral and pelvic appendages of the species used in the study.

Galictis Mean Total Body mass: 4042g 4 specimens M48 M2209 M3017 M3018

Forelimb

Muscle	Longueur (cm)	Masse (g)	Fibres (cm)	ACSA (cm²)	PCSA (cm²)
Latissimus dorsi	17.9	23.19	12.00	1.226	1.824
Spinodeltoideus	4.4	1.00	3.73	0.216	0.252
Teres minor	2.6	0.16	1.75	0.057	0.084
Triceps brachii	11.0	5.64	10.75	0.484	0.495
Triceps brachii caput mediale (short portion)	9.5	5.33	9.50	0.529	0.529
Triceps brachii caput mediale (long and intermediale portion)	7.4	3.48	4.00	0.442	0.821
Triceps brachii caput laterale	6.7	7.78	4.50	1.095	1.631
Triceps brachii caput longum	6.6	9.76	2.43	1.390	3.798
Anconeus	3.5	0.91	2.93	0.248	0.294
Triceps brachii caput accessorium	1.9	0.31	1.05	0.154	0.279
Extensor carpi ulnaris	5.6	1.62	1.23	0.271	1.244
Extensor digitorum communis	5.2	0.97	2.38	0.175	0.383
Extensor digitorum lateralis	5.8	0.63	1.30	0.103	0.459
Extensor carpi radialis longus	6.0	0.97	5.33	0.152	0.172
Extensor carpi radialis brevis	5.6	1.17	4.30	0.197	0.257
Brachioradialis	8.7	2.01	7.96	0.218	0.238
Supinator	3.7	0.56	0.80	0.142	0.660
Clavobrachialis	6.5	3.93	6.28	0.574	0.590
Acromodeltoideus	3.8	1.40	2.00	0.344	0.658
Teres major	6.3	1.85	6.13	0.277	0.285
Subscapularis	5.8	7.45	1.38	1.207	5.111
Extensor brevis pollicis	5.5	1.13	2.18	0.193	0.489
Pectoralis major	8.0	13.15	6.56	1.550	1.890
Pectoralis minor	16.9	21.04	12.21	1.173	1.626
Coracobrachialis	1.3	0.14	1.27	0.102	0.102
Pronator teres	4.9	1.63	1.20	0.314	1.283
Palmaris longus	6.5	2.02	1.28	0.292	1.496
Flexor carpi ulnaris (humeral head)	6.1	1.44	1.43	0.222	0.955
Flexor carpi ulnaris (ulnar head)	6.7	2.26	1.28	0.321	1.672
Flexor carpi radialis	4.7	0.79	1.58	0.158	0.472
Flexor digitorum profundus (4 heads)	6.2	6.04	1.86	0.918	3.057
Brachialis	7.7	2.58	5.55	0.316	0.438
Pectoralis superficialis	26.6	64.70	21.83	2.297	2.797
Biceps brachii	6.4	3.31	3.00	0.486	1.041
Supraspinatus	6.8	8.74	2.40	1.208	3.436
Infraspinatus	5.6	4.27	1.70	0.718	2.367
Pronator quadratus	2.6	0.38	1.30	0.139	0.276
		213.71		**19.910**	**43.462**

Hindlimb

Muscle	Longueur (cm)	Masse (g)	Fibres (cm)	ACSA (cm²)	PCSA (cm²)
Gluteus maximus	4.6	4.37	4.63	0.890	0.890
Rectus femoris	7.5	8.34	2.50	1.045	3.146
Tenuissimus	13.5	0.62	13.50	0.043	0.043
Sartorius	13.9	9.79	13.88	0.665	0.665
Vastus lateralis	72.5	8.08	2.63	0.105	2.902
Vastus medialis	6.4	3.01	3.50	0.442	0.812
Vastus intermedius	6.1	2.21	5.00	0.340	0.417
Peroneus longus	6.2	0.88	2.83	0.134	0.293
Peroneus tertius	4.5	0.41	4.53	0.084	0.084
Peroneus brevis	5.4	1.04	1.35	0.180	0.725
Extensor digitorum longus	7.2	2.09	5.38	0.274	0.366
Tibialis anterior	7.0	4.21	6.95	0.572	0.572
Tensor fascia latae	4.4	2.15	4.38	0.463	0.463
Gluteus medius	4.8	6.09	2.28	1.209	2.523
Pyriformis	3.4	1.53	3.38	0.428	0.428
Gluteus minimus	3.4	0.78	2.58	0.218	0.284
Iliacus	5.8	1.23	5.83	0.199	0.199
Psoas major	7.6	4.05	6.33	0.505	0.604
Adductor longus	8.2	3.44	8.18	0.397	0.397
Pectineus	4.6	4.40	4.63	0.897	0.897
Biceps femoris	8.9	17.44	8.88	1.854	1.854
Semitendinosus	13.5	6.88	13.50	0.481	0.481
Semimenbranosus (2 portions)	9.5	16.70	9.50	1.659	1.659
Gracilis	10.1	7.85	10.13	0.731	0.731
Gastrocnemius caput mediale	6.8	5.65	1.60	0.783	3.328
Gastrocnemius caput laterale (4 portions)	6.4	4.79	1.98	0.709	2.288
Plantaris	7.1	3.05	1.63	0.403	1.768
Soleus	5.8	1.87	3.25	0.306	0.541
Flexor longus digitorum	5.6	0.92	2.25	0.154	0.384
Flexor longus hallucis	5.5	1.38	2.18	0.237	0.597
Gemellus superior	2.4	0.38	1.93	0.150	0.185
Gemellus inferior	2.1	0.46	2.05	0.209	0.209
Obturator internus	2.5	0.85	2.48	0.324	0.324
Quadratus femoris	3.6	1.37	3.58	0.362	0.362
Obturator externus	2.9	1.83	2.50	0.600	0.691
Adductor femoris (magnus et brevis)	6.5	8.15	6.50	1.183	1.183
Popliteus	4.0	0.96	1.03	0.229	0.881
Tibialis posterior	6.1	2.58	1.55	0.403	1.572
		151.76		**19.870**	**35.750**

CHAPTER IV

General conclusions and perspectives

---

1 - General conclusions

The water-to-land transition in vertebrates, and the associated fin-to-limb transition, has been studied extensively, with both contributions from the fossil record and the study of living species considered as phylogenetically representative of the water-to-land transition. In this context, the coelacanth is considered as a crucial taxon for the understanding of this major evolutionary step in the vertebrates history. However, despite its importance, the detailed anatomy of the paired fins and their functional anatomy remain poorly investigated in coelacanths. In this thesis, we explore the skeletal and muscular anatomy of the paired fins of the extant coelacanth *Latimeria chalumnae* from a functional perspective, crucial before any interpretations in the context of the fin-to-limb transition can be made. We further initiate a study on the evolution of the muscular architecture in osteichthyans linked to changes in appendage function.

Development of the paired fins

Our results on the development of the pectoral and pelvic fin skeleton of the African coelacanth (**Chapter I**) showed that the development of the pelvic fins lags behind that of the pectoral fins, as is typical for gnathostomes (e.g. Ballard et al., 1993; Grandel and Schulte-Merker, 1998; Joss and Longhurst, 2001). At the fetus stage (the early embrionic stage known so far for the coelacanths), all mesomeres are formed and radial elements are already segmented from the mesomeres in the pectoral fin, whereas the most distal radial elements of the pelvic fin are not yet formed at this stage. The pre-axial and post-axial radial elements of both pectoral and pelvic fins are formed through the fragmentation of the mesomeres, a process already proposed for the formation of the radial elements in the paired fin of the lungfish *Neoceratodus* (Shubin and Alberch, 1986; Joss and Longhurst, 2001).

As described by Millot and Anthony (1958), the pectoral and pelvic fins are similar in their organization, except for the presence of a supernumerary element at the base of the pelvic fin: the pre-axial radial 0. This element questions one of the synapomorphies of crown-sarcopterygians: the paired fins are connected to the girdle by a mono-basal articulation (Rosen et al., 1981; Janvier, 1996; Clack, 2012). The developmental process driving the formation of the radial elements and the morphology of the mesomeres of the pelvic fin suggest that this supernumerary element could be the serial homologue of the pre-axial radial 1 of the pectoral fin. For the pelvic fin of the African coelacanth, it appears that pre-axial radials are formed by the segmentation of the proximo-lateral part of the mesomeres, and not the distal part. We

suggest that the fragmentation of the arced mesomeres permits the seemingly proximo-lateral fragmentation of the mesomeres to form the pre-axial radial elements. This may then bring the pre-axial radial 0 in contact with the pelvic girdle.

Our micro-tomographic analyses on this unique ontogenetic series has shown the progressive ossification of the anterior part of the pelvic girdle during development. This ossification pattern was already mentioned by Ahlberg (1992), but here we highlight the presence of a trabecular system associated with the ossification at the adult stage. We suggest that both the partial ossification and the trabecular system permit to resist the important stresses developed by the muscles inserted on this anterior part of the girdle. This hypothesis was tested and confirmed by the study of the muscle architecture of the pelvic fin (**Chapter II)**. A similar superficial ossification is present on the articular head and the ventral side of the scapulocoracoid of the pectoral girdle, but only in the juvenile and adult specimens. However, this does not seem to be associated with a trabecular system (Fig. 4.1).

In the long fossil record of coelacanths, the pelvic girdle, when preserved, often presents a posterior open end (Forey, 1998). We suggest here that this may be the most ossified part of the girdle that is preserved during fossilization, and that the most cartilaginous parts of the girdle (corresponding to the posterior articular head and the large lateral process) are missing. As an example, the pelvic girdles of Mesozoic coelacanths *Axelrodichthys araripensis* (Fragoso et al., 2018) or *Mawsonia* (Toriño, 2018) are morphologically similar to the ossified parts of the pelvic girdle of *Latimeria*, suggesting that part of the girdle, i.e. the lateral process and articular head, was cartilaginous during their lifetime and not preserved during the fossilization processes. As for the pelvic girdle, the scapulocoracoid of coelacanths is often a small element in fossils, that lies free from the dermal bone elements of the girdle (e.g Stensiö, 1922; Forey, 1998). Moreover, the cleithrum and extracleithrum elements present dorsal, medial, and lateral grooves on the internal surface of the bones, both in the extant coelacanth and in fossil specimens such as *Rhabdoderma* (Forey, 1981), *Trachymetopon* (Dutel et al., 2015) or *Ticinepomis* (Cavin et al., 2019). In the extant coelacanth, the main cartilaginous part of the scapulocoracoid insert in these grooves. Similar to the pelvic girdle, we suggest that in these fossil specimens, the cartilaginous part of the scapulocoracoid was not preserved. Considering the presence of the grooves on the internal surface of the cleithrum and extracleithrum, it will be possible to estimate the size of the original scapulocoracoid, that should be much more massive than the ossified part let supposed.

Figure 4.1: Transverse section (based on a CT scan) of the adult coelacanth *Latimeria* CCC22 at the level of the scapulocoracoids showing the superficial ossification around the articular process. Not to scale.

Role of the muscular anatomy of *Latimeria* in the understanding of the fin-to-limb transition.

Dissections of the pectoral and pelvic fins of the coelacanth highlighted the complexity of the muscular anatomy and of the different organization of the muscle bundles of the two paired fins (**Chapter II**). Whereas previous dissection studies of the muscular anatomy of the paired fins described around 40 muscle bundles for each fin (Millot and Anthony, 1958; Miyake et al., 2016), we observed in our dissections twice the number of muscle bundles for each fin (86 for

the pectoral fin, 83 for the pelvic fin). On the contrary to Diogo et al. (2016) we did not find an *elevator lateralis* muscle on the pelvic fin of *Latimeria*. Rather, there is a fascia that clearly separates the pelvic muscles from the abdominal cavity. The pectoral fin has an important number of muscle bundles that are mono-articular and that insert on the endoskeletal elements of the metapterygial axis. This type of muscular insertion on endoskeletal elements is similar to the condition known for lungfishes and tetrapods (Boisvert et al., 2013). However, whereas muscles of the limbs are differentiated in tetrapods, the muscle bundles are not well differentiated in the pectoral fin of *Latimeria*. Interestingly, it can be considered that the pelvic fin presents a more plesiomorphic organization of the muscular anatomy, similar to that of actinopterygians (e.g. Adriaens et al., 1993; Molnar et al., 2017) since most of the muscle bundles are poly-articular and run from the pelvic girdle to the fin rays. It thus seems that the pectoral and pelvic fins of the coelacanth present two different steps in the development of the muscular anatomy of the paired appendages. This observation can be interesting in the context of the fin-to-limb transition, and suggests a mosaic evolution for the paired appendages, with a fish-like muscular anatomy and a tetrapod-like muscular anatomy with insertion of shorter muscles on the endoskeletal elements of the fin. However, it is necessary to be cautious with this hypothesis, since the clade of coelacanths has diverged from those of other sarcopterygians at least in the Early Devonian (Friedman, 2007). Thus, the extant coelacanth is the result of a 400-million-year long evolutionary history that marked its morphology and its fins. The two fossil coelacanths known so far with preservation of endoskeletal elements of their paired fins show differences with those of *Latimeria*. The metapterygial axis of the pectoral fin of *Shoshonia*, from the Devonian of US, is longer than that of *Latimeria*, with up to eight mesomeres, and with pre-axial radial elements proportionally much longer than those of *Latimeria* (Friedman et al., 2007). The metapterygial axis of the paired fins of *Laugia groenlandica*, from the Triassic of Greenland, are proportionally smaller than those of *Latimeria*, with three axial mesomeres. Moreover, its right and left pelvic girdles are fused medially. Such differences in the endoskeletal anatomy imply differences in the muscular anatomy.

The muscular architecture of the paired fins of the extant coelacanth shows that the pectoral fin is more powerful than the pelvic fin, congruent with observations of swimming coelacanths. Indeed, the pectoral fins appear to have a more active role than the pelvic fins in the locomotion and manoeuvring of the coelacanth (Fricke and Hissmann, 1992). Having more active pectoral fins compared to pelvic fins is common in fish (Gibb et al., 1994; Standen, 2008). In *Latimeria*, as in teleosts, the pelvic fins appear to only assist the control of the body position and the sta-

bility control (Fricke and Hissmann, 1992; Lauder and Drucker, 2004; Don et al., 2013), and do not seem to have a major role in propulsion.

These anatomical and architectural muscle data were used in a more global study on the evolution of the muscular architecture of the appendages during the fin-to-limb transition. Our exploratory study is based on nine different extant taxa: three actinopterygians, the coelacanth, and five tetrapods (**Chapter III**). Our results show a general increase of the muscular mass and force of the appendages in tetrapods, relative to the body size. This increase in the muscular mass of the appendages during the fin-to-limb transition supports the observations on skeletal elements in the fossil record, and it suggests that the size differences (skeletal or muscular) between fins and limbs are due to their different functions (Andrews and Westoll, 1970). In fishes, the part of the body that mainly produces the propulsion force is the axial musculature that transmits force to the caudal fin and causes the lateral undulation of the body. The paired fins are mainly used for manoeuvring (Bainbridge, 1963; Webb, 1982; Don et al., 2013). In coelacanths, propulsion is also produced by the median anal and 2^{nd} dorsal fins (Fricke and Hissmann, 1992). In another way, limbs of terrestrial tetrapods produce the force to move forward and thus require more robust appendages to support both their body mass and to be able to move on land (Hohn-Schulte et al., 2013; Standen et al., 2014; Dickson and Pierce, 2019). However, it has been shown in urodeles, that are considered as organisms that have retained plesiomorphic stance and gait (Pierce et al., 2020), that terrestrial locomotion involves both limb and axial movements (e.g. Ashley-Ross, 1994; Ashley-Ross et al., 2009; Nyakatura et al., 2014).

Our results also support the hypothesis of a locomotor shift from an anterior to posterior driven system during the fin-to-limb transition (Coates et al., 2002; Boisvert et al., 2013; Don et al., 2013). Indeed, in tetrapods, the pelvic appendage shows a general increase in mass and force production that is more important than that of the pectoral appendage. Stronger hind limbs, in association with a robust pelvic girdle fused with the axial skeleton permit to support the body weight and produce the force necessary for propulsion on land (e.g. Payne et al., 2005; Allen et al., 2010; Don et al., 2013).

We also found that there is a shift of the muscular distribution in the appendages. We used the hypotheses of homologies proposed by Diogo et al. (2016) considering that the muscles of limbs are homologous to four muscles groups present in fishes: *abductor/ adductor su-*

perficialis/profundus. In fishes, the heavier and stronger groups are the deep muscles of the pectoral and pelvic fins, whereas in tetrapods the heavier and stronger muscles groups are the superficial groups. Since pelagic anglerfishes "walking" on the marine substrate have stronger deep muscles than superficial muscles (Dickson and Pierce, 2019), we suggest that the shift in the weight distribution across muscles groups distribution is not dependent on the type of locomotion. It is proposed here that the allocation of mass and force to different muscle groups is rather linked to phylogenetic heritage, but this hypothesis needs to be investigated further.

We also study the joint mobility of the fins and limbs in sarcopterygians. We suggest that the convex articular surface of the glenoid of *Latimeria* permits a greater mobility of the fin than the concave glenoid surface of tetrapods. However, the convex acetabulum of the hip of *Latimeria* has a smaller mobility than the concave acetabulum of tetrapods which is attributed to the supernumerary element pre-axial radial 0, positioned against the pelvic girdle.

Chapter III only presents preliminary results, and several taxa will be added to the study before publication. These supplementary taxa are the caiman, the Nile monitor, a terrestrial salamander, and terrestrial and aquatic turtles. It would be interesting to add to the dataset the Australian lungfish *Neoceratodus forsteri*, as another sarcopterygian fish, as well as 'walking' actinopterygians such as mudskippers or the walking cavefish *Cryptotora thamicola*, but access to such specimens may be difficult. We suggest that the distribution of muscular properties is due to a phylogenetic heritage rather than an effect of the functional role of the muscles for the substrate-based locomotion, since 'walking' anglerfishes do not have a similar distribution of muscles than tetrapods. However, anglerfishes are deep benthic organism and buoyancy may impact the role of the fins allowing them to generate propulsion without weight bearing. In actinopterygians that live in semi-aquatic environments, such as *Cryptotora* or mudskippers, muscles may have a different distribution than that of 'walking' anglerfishes. Moreover, the other specimens will permit to add data on the evolution of joint mobility. Lungfishes will be of particular interest, since they are the only other representatives of living sarcopterygian fishes, which present convex glenoid and acetabulum surfaces. The study of their joint mobility will permit to confirm whether or not convex joint permits a higher mobility of the appendage than concave glenoid and acetabulum surfaces. Joint mobility was measured based on formalin-fixed specimens. The effect of the formalin fixation showed a great impact of the fixation on the range of motion of the human spine, compared to fresh material (Wilke et al., 1996). We thus suggested that the formaldehyde fixation of specimens before the dissections and mobil-

ity measurements may have stiffened the ligaments thus causing us to underestimate the true joint. It will be interesting to test this hypothesis by comparing the joint mobility of fresh and fixed specimens.

2 - Future work

Locomotion and coordination of the fins in *Latimeria*

It was initially suggested that the coelacanth was a bottom-crawler due to its close relationship with tetrapods and the anatomy of the paired appendages. It was only in the 80s that Fricke and its colleagues highlighted that the living coelacanth is a slow swimmer that does not used its fin to "walk" on the substrate (Fricke et al., 1987). Our study on the muscular anatomy of the paired fins of the coelacanth permits to characterize the contribution of the fins during its locomotion, but it still needs to be tested *in vivo*. The study of the so peculiar locomotion of the coelacanth is only possible with observations *in situ*, since coelacanths are not maintained in captivity. Coelacanths are listed as critically endangered and are protected from trade under the CITES convention. Moreover, it was never possible to keep coelacanth alive more than a day after their capture (Uyeno, 1991; Erdmann et al., 1999). First *in situ* data on the locomotion were obtained by submersibles (Fricke and Hissmann, 1992; Hissmann et al., 2006), and their study began to lay the groundwork of the locomotor behaviour of the coelacanth qualitatively. The pectoral and pelvic fins of the coelacanth are active during locomotion and the propulsion seems to be mainly produced by the caudal fin during acceleration, and by the median lobed-fins during slow swimming. Moreover, the pectoral fins seem to have a more active role than the pelvic fins for the different manoeuvres. However, all the data were obtained from submersibles which may cause stress and so may modify the natural behaviour of animals (Décamps et al., 2017).

The coelacanth population of Sodwana Bay (South Africa) living at shallower depths (around 120 meters of depth) provided the unique opportunity for divers to make direct observations on coelacanths during locomotion. A joint research program between SAIAB (Grahamstown), SANBI (Pretoria), the Andromede diving team, and the MNHN (Paris, France) was launched in 2013, and its aim was to gain a better understanding of the biology and ecology of the coelacanths. The "Gombessa" field campaign in the Sodwana Bay area, South Africa, permitted to collect new and unique 3D data on the locomotion of the living coelacanth. The combination of autonomous deep diving, much less stressful for the animals than submersibles, with

technological advances in terms of filming, including the use of high speed and high definition cameras recording multiple synchronized views (Décamps et al., 2017) provided the unique opportunity to study the locomotion of these animals in their natural environment (Fig. 4.2). The high-quality footage will allow to study the *in vivo* kinematics and mobility of each fin of the coelacanth and to characterize their complex coordination patterns. Moreover, these data will allow to quantify the intra-articular movements of the skeletal elements with great precision through superimposition of the fine anatomical data obtained during this thesis on the paired fins with the body envelope of the moving animal. This will allow to quantify the skeletal geometry during the unique mode of swimming of the extant coelacanth. These results could then bee used to infer the mobility and skeletal geometry of the paired fins in extinct sarcopterygians in the context of the fin-to-limb transition.

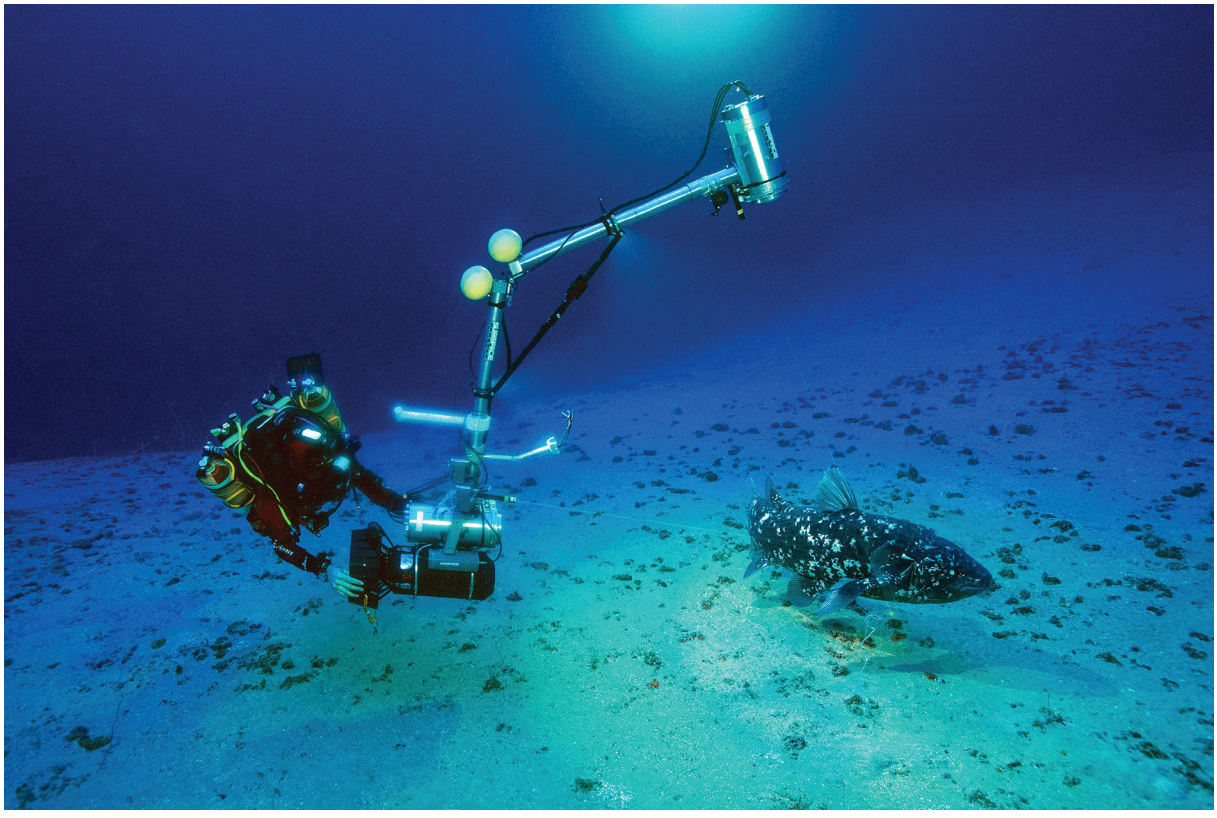

Figure 4.2: *Latimeria chalumnae* filmed with two synchronized cameras during slow locomotion. Photograph taken during the "Gombessa" expedition in 2013, in Sodwana Bay, South Africa. ©Laurent Ballesta, Gombessa expeditions, Andromede Oceanology.

Preliminary studies on the coordination of the lobed fins during locomotion of the coelacanth were undertaken on the basis of these unique videos. The videos were recorded by day, during the resting time of the coelacanth. Thus, coelacanths were not very active and the low speed

locomotion implied mainly the use of the paired and median fins, without lateral undulation of the body, neither the used of the caudal fin for the propulsion. As for the previous observations made by Fricke and colleagues (1992), these first attempts showed that the pectoral fins appear more active with a more important mobility and greater functional role during propulsion and manoeuvring compared to the pelvic fins, consistent with the results of the muscle anatomy and architecture of the two fins (**Chapter II**). These observations also showed that the anal and 2^{nd} dorsal fins seem to produce the main propulsion force for slow swimming. We presume that the muscular anatomy might reflect the role of the median fins in generating propulsion. New detailed dissections of these median fins, as well as of the caudal fin and its caudal lobe, will be crucial to better understand the locomotion of the extant coelacanth *Latimeria*, and the functional morphology of all its fins.

In an evolutionary context, lobed medians fins are specific to coelacanths and they appeared early in their evolutionary history (Ahlberg, 1992; Forey, 1998). The anatomy of these fins is peculiarly similar to that of the pelvic fins, with a metapterygial axis of four mesomeres associated with large pre-axial and post-axial radials elements, with the most proximal pre-axial radial articulated with a large basal plate (Millot and Anthony, 1958; Forey, 1998). Moreover, the muscular anatomy is also organized into three muscle layers, as for the paired fins (Millot and Anthony, 1958). The origin and evolution of the endoskeleton of these fins within the clade Actinistia is still unresolved, but it has been suggested that it appeared from a duplication of the gene expression responsible for the formation of the pelvic appendage (Ahlberg, 1992). The study of the development of these median lobed fins, thanks to the unique imagery data of the different ontogenetic stages, and the detailed redescription of their muscular anatomy might provide new information on this hypothesis in comparison to the pelvic fins.

Consequently, the discovery of new embryos at new development stages would permit to further investigate the development of the coelacanth. New intermediate stages, specifically between the fetus and the pup with yolk sac would be particularly insightful. New fresh material, before any fixation, would permit to sample the RNA, that could be used to study the origin of genes expressed involved in the formation and development of the median lobed-fins. Finally, new accurate tomographic acquisitions on the paired and median fins of the ontogenetic series of coelacantths could permit to study the development of the muscular anatomy of the fins. Such a study, could then be included in a more global study on the development and evolution of the appendage muscles in sarcopterygians.

Contribution of the Early Triassic coelacanth *Laugia groenlandica* to the understanding of the evolution of the paired appendages in coelacanths

The opportunity to visit the collections of the Natural History Museum of Denmark in order to borrow some fossil specimens of *Laugia groenlandica* rendered conventional CT and synchrotron tomography of one of the rare fossil coelacanth taxa known with preservation of the endoskeleton of paired and median fins (Stensiö, 1932) possible. Unfortunately, due to the delay in the different imaging acquisitions we did not yet have the opportunity to diligently work on these paleontological data. An improved knowledge of the appendages of *Laugia* might provide interesting new elements in the understanding of the evolution of the paired appendages

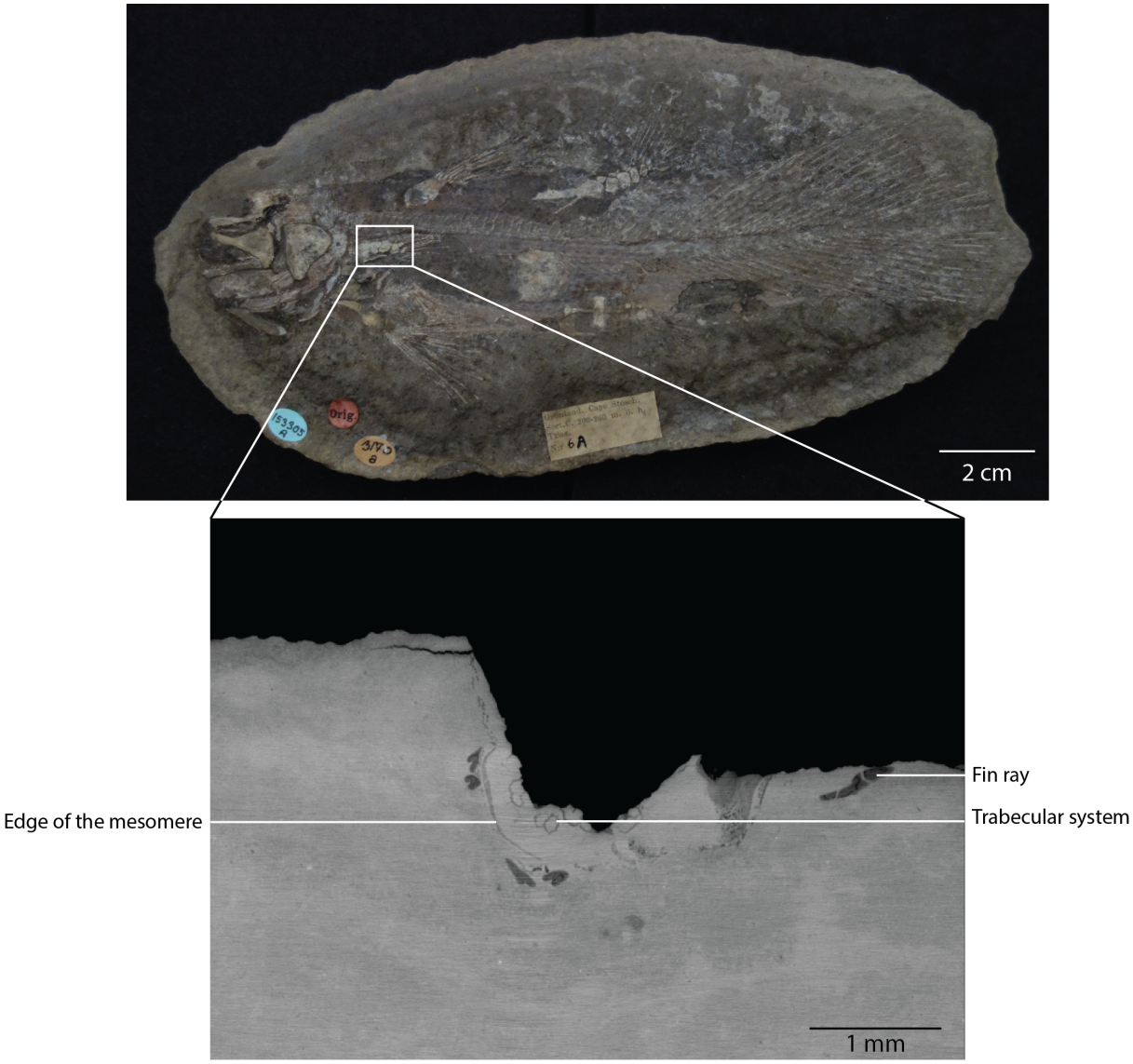

Figure 4.3: *Laugia groenlandica* from the Triassic of Greenland - NHMD 153305, Copenhagen. Top: counterpart of complete specimen. Bottom: ESRF synchrotron virtual transversal section at level of the pectoral fin showing the quality of the resolution, with part of a mesomere and possible presence of a trabecular system.

in coelacanths. The discovery of new fossil coelacanths with preserved fin endoskeletons will also be necessary to investigate the evolution of the paired and median fins in Actinistia further.

A preliminary study with Sophie Sanchez (Uppsala, Sweden) showed that the mesomeres of the pectoral fin of *Laugia groenlandica* appear to present a trabecular system (Fig. 4.3). Since such a trabecular system is not present in the mesomeres of *Latimeria chalumnae*, due to the loss of their ossification during the evolution of coelacanths, the study of this structure in *Laugia* might also provide informative elements on the evolution of the ossification of appendages in coelacanths, as well as on the evolution of the appendage bone microstructures in early sarcopterygians (Sanchez et al., 2012; Kamska et al., 2019).

Bibliography

Adriaens, D., Decleyre, D., and Verraes, W. (1993). Morphology of the pectoral girdle in *Pomatoschistus lozanoi* De Buen, 1923 (Gobiidae), in relation to pectoral fin adduction. *Belgian journal of zoology*, 123(2):135–157.

Ahlberg, P. E. (1992). Coelacanth fins and evolution. *Nature*, 358:459.

Allen, V. R., Elsey, R. M., Jones, N., Wright, J., and Hutchinson, J. R. (2010). Functional specialization and ontogenetic scaling of limb anatomy in *Alligator mississippiensis*. *Journal of Anatomy*, 216:423–445.

Andrews, S. M. and Westoll (1970). The Postcranial Skeleton of *Eusthenopteron foordi* Whiteaves. *Earth and Environmental Science Transactions of the Royal Society of Edinburgh*, 68(9):207–329.

Ashley-Ross, M. A. (1994). Hindlimb Kinematics During Terrestrial Locomotion in a Salamander (*Dicamptodon Tenebrosus*). *The Journal of experimental biology*, 193:255–83.

Ashley-Ross, M. A., Lundin, R., and Johnson, K. L. (2009). Kinematics of level terrestrial and underwater walking in the California newt, *Taricha torosa*. *Journal of Experimental Zoology Part A: Ecological Genetics and Physiology*, 311(4):240–257.

Bainbridge, R. (1963). Caudal Fin and Body Movement in the Propulsion of some Fish. *Journal of Experimental Biology*, 40(1):23–56.

Ballard, W. W., Mellinger, J., and Lechenault, H. (1993). A Series of Normal Stages for Develop-

ment of *Scyliorhinus canicula*, the Lesser Spotted Dogfish (Chondrichthyes: Scyliorhinidae). *The Journal of Experimental Zoology*, 267:318–336.

Boisvert, C. A., Joss, J. M., and Ahlberg, P. E. (2013). Comparative pelvic development of the axolotl (*Ambystoma mexicanum*) and the Australian lungfish (*Neoceratodus forsteri*): conservation and innovation across the fish-tetrapod transition. *EvoDevo*, 4(3):1–19.

Cavin, L., Cupello, C., Yabumoto, Y., Fragoso, L., Deesri, U., and Brito, P. M. (2019). Phylogeny and evolutionary history of mawsoniid coelacanths. *Bulletin of the Kitakyushu Museum of Natural History and Human History*, 17:3–13.

Clack, J. A. (2012). *Gaining Ground, Second Edition: The Origin and Evolution of Tetrapods*. Indiana University Press, Bloomington.

Coates, M. I., Jeffery, J. E., and Ruta, M. (2002). Fins to limbs: What the fossils say. *Evolution & Development*, 4(5):390–401.

Décamps, T., Herrel, A., Ballesta, L., Holon, F., Rauby, T., Gentil, Y., Gentil, C., Dutel, H., Debruyne, R., Charrassin, J. B., Eveillard, G., Clément, G., and Herbin, M. (2017). The third dimension: a novel set-up for filming coelacanths in their natural environment. *Methods in Ecology and Evolution*, 8(3):322–328.

Dickson, B. V. and Pierce, S. E. (2019). How (and why) fins turn into limbs: insights from anglerfish. *Earth and Environmental Science Transactions of the Royal Society of Edinburgh*, 109:87–103.

Diogo, R., Johnston, P., Molnar, J. L., and Esteve-Altava, B. (2016). Characteristic tetrapod musculoskeletal limb phenotype emerged more than 400 MYA in basal lobe-finned fishes. *Scientific Reports*, 6:1–9.

Don, E. K., Currie, P. D., and Cole, N. J. (2013). The evolutionary history of the development of the pelvic fin/hindlimb. *Journal of Anatomy*, 222:114–133.

Dutel, H., Herbin, M., and Clément, G. (2015). First occurrence of a mawsoniid coelacanth in the Early Jurassic of Europe. *Journal of Vertebrate Paleontology*, 35(3):e929581.

Erdmann, M. V., Caldwell, R. L., Jewett, S. L., and Tjakrawidjaja, A. (1999). The second recorded living coelacanth from north Sulawesi. *Environmental Biology of Fishes*, 54(4):445–451.

Forey, P. L. (1981). The coelacanth *Rhabdoderma* in the Carboniferous of the British Isles. *Paleontology*, 24(1):203–229.

Forey, P. L. (1998). *History of the Coelacanth Fishes*. Thomson Science, London, chapman & edition.

Fragoso, L. G. C., Brito, P. M., and Yabumoto, Y. (2018). *Axelrodichthys araripensis* Maisey, 1986 revisited. *Historical Biology*, pages 1–23.

Fricke, H. and Hissmann, K. (1992). Locomotion, fin coordination and body form of the living coelacanth *Latimeria chalumnae*. *Environmental Biology of Fishes*, 34(4):329–356.

Fricke, H., Reinicke, O., Hofer, H., and Nachtigall, W. (1987). Locomotion of the coelacanth *Latimeria chalumnae* in its natural environment. *Nature*, 329:331–333.

Friedman, M. (2007). *Styloichthys* as the oldest coelacanth: Implications for early osteichthyan interrelationships. *Journal of Systematic Palaeontology*, 5(3):289–343.

Friedman, M., Coates, M. I., and Anderson, P. (2007). First discovery of a primitive coelacanth fin fills a major gap in the evolution of lobed fins and limbs. *Evolution & Development*, 9(4):329–337.

Gibb, A. C., Jayne, B. C., and Lauder, G. V. (1994). Kinematics of Pectoral Fin Locomotion in the Bluegill Sunfish *Lepomis Macrochirus*. *The Journal of experimental biology*, 189(1):133–61.

Grandel, H. and Schulte-Merker, S. (1998). The development of the paired fins in the zebrafish (*Danio rerio*). *Mechanisms of Development*, 79(1-2):99–120.

Hissmann, K., Fricke, H., Schauer, J., Ribbink, A. J., Roberts, M., Sink, K., and Heemstra, P. C. (2006). The South African coelacanths - An account of what is known after three submersible expeditions. *South African Journal of Science*, 102(9-10):491–500.

Hohn-Schulte, B., Preuschoft, H., Witzel, U., and Distler-Hoffmann, C. (2013). Biomechanics and functional preconditions for terrestrial lifestyle in basal tetrapods, with special consideration of *Tiktaalik roseae*. *Historical Biology*, 25(2):167–181.

Janvier, P. (1996). *Early vertebrates*. Oxford University Press, Oxford.

Joss, J. and Longhurst, T. (2001). Lungfish paired fins. In Ahlberg, P. E., editor, *Major Events in Early Vertebrate Evolution*, chapter 21, pages 370–376. London, taylor & f edition.

Kamska, V., Daeschler, E. B., Downs, J. P., Ahlberg, P. E., Tafforeau, P., and Sanchez, S. (2019). Long-bone development and life-history traits of the Devonian tristichopterid *Hyneria lindae*. *Earth and Environmental Science Transactions of the Royal Society of Edinburgh*, 109:75–86.

Lauder, G. V. and Drucker, E. G. (2004). Morphology and experimental hydrodynamics of fish fin control surfaces. *IEEE Journal of Oceanic Engineering*, 29(3):556–571.

Millot, J. and Anthony, J. (1958). *Anatomie de Latimeria chalumnae - Tome I: Squelette, Muscles et Formations de soutien*. CNRS, Paris, cnrs edition.

Miyake, T., Kumamoto, M., Iwata, M., Sato, R., Okabe, M., Koie, H., Kumai, N., Fujii, K., Matsuzaki, K., Nakamura, C., Yamauchi, S., Yoshida, K., Yoshimura, K., Komoda, A., Uyeno, T., and Abe, Y. (2016). The pectoral fin muscles of the coelacanth *Latimeria chalumnae*: Functional and evolutionary implications for the fin-to-limb transition and subsequent evolution of tetrapods. *The Anatomical Record*, 299(9):1203–1223.

Molnar, J. L., Johnston, P. S., Esteve-Altava, B., and Diogo, R. (2017). Musculoskeletal anatomy of the pelvic fin of *Polypterus*: implications for phylogenetic distribution and homology of pre- and postaxial pelvic appendicular muscles. *Journal of Anatomy*, 230:532–541.

Nyakatura, J. A., Andrada, E., Curth, S., and Fischer, M. S. (2014). Bridging "Romer's Gap": Limb Mechanics of an Extant Belly-Dragging Lizard Inform Debate on Tetrapod Locomotion During the Early Carboniferous. *Evolutionary Biology*, 41:175–190.

Payne, R. C., Hutchinson, J. R., Robilliard, J. J., Smith, N. C., and Wilson, A. M. (2005). Functional specialisation of pelvic limb anatomy in horses (*Equus caballus*). *Journal of Anatomy*, 206(6):557–574.

Pierce, S. E., Lamas, L. P., Pelligand, L., Schilling, N., and Hutchinson, J. R. (2020). Patterns of limb and epaxial muscle activity during walking in the fire salamander, *Salamandra salamandra*. *Integrative Organismal Biology*.

Rosen, D. E., Forey, P. L., Gardiner, B. G., and Patterson, C. (1981). Lungfishes, tetrapods, paleontology, and plesiomorphy. *Bulletin of the American Museum of Natural History*, 167(4):159–276.

Sanchez, S., Ahlberg, P. E., Trinajstic, K. M., Mirone, A., and Tafforeau, P. (2012). Three-dimensional synchrotron virtual paleohistology: A new insight into the world of fossil bone microstructures. *Microscopy and Microanalysis*, 18:1095–1105.

Shubin, N. H. and Alberch, P. (1986). A Morphogenetic Approach to the Origin and Basic Organization of the Tetrapod Limb. *Evolutionary Biology*, 20:319–387.

Standen, E. M. (2008). Pelvic fin locomotor function in fishes: Three-dimensional kinematics in rainbow trout (*Oncorhynchus mykiss*). *Journal of Experimental Biology*, 211(18):2931–2942.

Standen, E. M., Du, T. Y., and Larsson, H. C. E. (2014). Developmental plasticity and the origin of tetrapods. *Nature*, 513(7516):54–58.

Stensiö, V. E. A. (1922). Über zwei Coelacanthiden aus dem Oberdevon von Wildungen. *Paläontologische Zeitschrift*, 4(2-3):167–210.

Stensiö, V. E. A. (1932). *Triassic Fishes from East Greenland, collected by the Danish Expeditions in 1929-1931*. Meddelelser om Grønland.

Toriño, P. (2018). *El género Mawsonia (Actinistia, Latimerioidei) en la ictiofauna de la Formación Tacuarembó (Jurásico Tardío - Cretácico Temprano, Uruguay): sistemática, osteología y anatomía comparada.* Tesis de maestría en ciencias biológicas, unpublished, Facultad de Ciencas, Universidad de la República.

Uyeno, T. (1991). Observations on locomotion and feeding of released coelacanths, *Latimeria chalumnae*. *Environmental Biology of Fishes*, 32:267–273.

Webb, P. W. (1982). Locomotor Patterns in the Evolution of Actinopterygian Fishes. *American Zoologist*, 22:329–342.

Wilke, H.-J., Krischak, S., and Claes, L. E. (1996). Formalin fixation strongly influences biomechanical properties of the spine. *Journal of Biomechanics*, 29(12):1629–1631.

Abstract

Among the sarcopterygians, the clade of coelacanths (Actinistia) is today only represented by the coelacanth genus *Latimeria*, and is the sister-taxa of the clade lungfish + tetrapods. Due to its phylogenetic position and its ecology, *Latimeria* is considered as a good model to study the fin-to-limb transition. However, it is necessary to have a good understanding of the skeletal and muscular anatomy of its paired fins before to infer its influence in our understanding of the fin-to-limb transition. As for other jawed vertebrates, we show that the development of the pectoral fins occurs earlier than that of the paired fins. The development of the radial elements along the metapterygial axis of the fin occurs by the fragmentation of the associated mesomere, as observed in lungfish. We also highlight the development of a superficial ossification of the anterior part of the pelvic girdle, associated with a trabecular system in the adult. This trabecular system and this ossification permit to resist to the important constraints developed by the muscles inserted on this part of the girdle. The study of the muscular anatomy shows a more complex anatomy than previously known, with that of the pelvic fin that seems more plesiomorphic than that of the pectoral fin. Indeed, the muscles of the pelvic fin run from the girdle to the fin rays, whereas most of the muscles of the pectoral fin insert on the endoskeletal elements, as seen in lungfish and tetrapods. Moreover, the pectoral fin is stronger than the pelvic fin, that indicates a more important role in the locomotion. The joint mobility of the pectoral and pelvic fins was also studied, after complete dissections of the fins. We show that the pectoral fin has a greater mobility than the pelvic fin. This difference of mobility is due to the morphology of the mesomeres of the pelvic fin, with pre-axial radial elements on a more proximo-lateral position than those of the pectoral fin. Finally, we made a preliminary study on the evolution of the muscle architecture during the fin-to-limb transition. It appears that the muscle mass and force are more important in tetrapods than in "fishes", relative to the body size. The limbs need to produce more force than fins, since they are the principal locomotor force generator. In fishes however, the propulsion is mainly produced by the lateral undulation of the body and the caudal fin. Thus the paired fins do not need to produce a large amount of force. The relative increase in mass and force is more important in hind limbs than in forelimbs, what supports the hypothesis of a locomotor shift during the fin-to-limb transition.

Résumé

Les cœlacanthes (Actinistia) forment un clade de sarcoptérygiens seulement représentés de nos jours par le genre *Latimeria*, considéré comme le groupe-frère du clade dipneustes + tétrapodes. De par sa position phylogénétique et son mode de vie, *Latimeria* est considéré comme un bon modèle pour étudier la sortie des eaux des vertébrés et le passage des nageoires aux pattes. Il est cependant nécessaire d'avoir une connaissance approfondie de l'anatomie de son squelette et de ses muscles, avant de pouvoir faire toute interprétation évolutive sur les conditions de la terrestrialisation des vertébrés. L'étude du développement des nageoires paires a montré un développement similaire à celui des autres vertébrés, avec les nageoires pelviennes qui se forment plus tardivement que les nageoires pectorales. Tout comme chez les dipneustes, les éléments radiaux pré-axiaux se mettent en place par la fragmentation du mésomère associé, de façon précoce dans le développement. Nous avons également pu mettre en évidence le développement progressif d'une ossification superficielle de la partie antérieure de la ceinture pelvienne, associée à un système trabéculaire. Le système trabéculaire et l'ossification superficielle permettent de renforcer la ceinture pelvienne cartilagineuse, et ainsi de résister aux importantes contraintes musculaires qui s'exercent sur cette région de la ceinture pelvienne. L'étude de l'anatomie musculaire a permis de mettre en évidence la grande complexité musculaire des nageoires, par rapport à ce qui était déjà connu. La nageoire pelvienne semble de plus avoir une organisation musculaire plus plésiomorphe que la nageoire pectorale, puisque la majorité des muscles pelviens vont de la ceinture pelvienne directement aux rayons des nageoires, de manière similaire à ce qui s'observe chez les actinoptérygiens. En revanche, les muscles de la nageoire pectorale s'insèrent majoritairement sur les éléments endosquelettiques, comme chez les dipneustes et les tétrapodes. De plus, la nageoire pectorale est plus puissante que la nageoire pelvienne, ce qui semble indiquer un rôle plus important pour la locomotion du cœlacanthe. L'étude de la mobilité articulaire des nageoires a montré que la nageoire pectorale a une plus grande mobilité que la nageoire pelvienne. Cette diminution de la mobilité au niveau de la nageoire pelvienne semble être liée à la morphologie particulière de ses mésomères, et de la position proximo-latérale de ses éléments radiaux pré-axiaux. Enfin, nous avons mené une étude préliminaire sur l'évolution de l'architecture musculaire au cours de la terrestrialisation des vertébrés. Il apparait que les pattes ont une masse et une force plus importantes que les nageoires chez les poissons. Ceci serait en lien avec le besoin pour les tétrapodes de produire la force nécessaire au maintien du poids et à la propulsion sur un substrat terrestre. Les poissons en revanche se propulsent principalement par leur nageoire caudale, et ne nécessitent donc pas de nageoires puissantes. Enfin, nous avons montré une augmentation relative de la taille et de la force plus importantes au niveau du membre postérieur qu'au niveau du membre antérieur. Ce résultat supporte l'idée d'un changement locomoteur durant le processus de terrestrialisation des vertébrés vers un mode de propulsion postérieur.